

**Scale-Up of the Solid Polymer Electrolyte Reactor For
Electro-Organic Synthesis**

Robert Stephen Girt

**Thesis submitted to the University of Newcastle upon Tyne
for the Degree of Doctor of Philosophy**

DECEMBER 1997

NEWCASTLE UNIVERSITY LIBRARY

098 50656 4

Thesis L6238



IMAGING SERVICES NORTH

Boston Spa, Wetherby

West Yorkshire, LS23 7BQ

www.bl.uk

CONTAINS
PULLOUT

In the mountains you are worth what you are and not what society has made you; what counts is what you have in your soul and your heart, honesty and determination.

Riccardo Cassin

ABSTRACT

Electro-organic reactions are often complicated by the need to add supporting electrolytes and co-solvents. In many cases these additives take part in side reactions causing low yields and hinder the purification stages. The solid polymer electrolyte (SPE) reactor uses an ion exchange membrane to transfer charged species between the electrodes and so eliminates the need for any additives. In this way improvements in electrochemical processing can be achieved.

The SPE reactor has only been studied for model organic and aqueous based electrochemical reactions. The aims of this project were to develop the reactor for use as a suitable means of synthesising alcohols and acids based on substituted toluenes. This involved selection of suitable electrode material, polymer electrolyte pre-treatment and reactor modelling.

According to published reports the direct electro-oxidation of toluene takes place with maximum yields of 19% with an acetic acid co-solvent and a nitric acid supporting electrolyte. Higher yields are possible with inorganic mediators such as Mn^{3+} and Cr^{6+} . 30% yields of methoxylated products are possible from electrolysis in methanol although many non volatile by-products are formed.

Initial research was spent investigating the oxidation of toluene in sulphuric acid at a lead dioxide rotating disk electrode. It was found that the reaction is mass transfer limited in the potential region below gas evolution. The order of reaction with respect to toluene was 0.5. Electrolysis of toluene on platinum mesh in nitric acid with and without acetic acid was found to produce benzyl alcohol and benzaldehyde with low current efficiencies. Without co-solvent the maximum current efficiency was 10% at 250A/m^2 .

An SPE reactor fabricated from glass with an active electrode area of 5cm^2 was used to perform electrode tests. Highest yields of benzaldehyde were obtained using nickel foam, graphite felt and palladium coated mesh electrodes. The current efficiencies were 52.4%, 20.3% and 10.7% respectively. This work highlighted the need for a good membrane-electrode contact. The oxidation of benzyl alcohol in the same reactor using nickel foam

was accomplished with a current efficiency of 85.4% showing that the difficult step in the oxidation of toluene was the first one to benzyl alcohol.

Pre-treatment of the membrane by swelling in solvents was considered to be an important factor in the performance of the SPE reactor. Several ion exchange membranes were pre-treated in a variety of aqueous and organic solvents including methanol, toluene, DMF, water and sulphuric acid. Nafion®117 was found to increase in size more than the other tested membranes in all solvents except water and sulphuric acid. Many of the pre-treated membranes were tested in an SPE reactor made from steel with an active electrode area of 21cm² for the oxidation of toluene in methanol. The anode-membrane potential was measured as a function of time and current density with Nafion®117 having the lowest values of potential. Selection of the pre-treatment method for future use was determined by assessing the performance in the reactor, contamination of products and chemical hazards. Swelling in aqueous solvents was the chosen procedure.

The steel SPE reactor was operated in continuous mode with recycle for the oxidation of toluene in methanol. Galvanostatic electrolysis took place at several current densities, temperatures and feed concentrations. Two products were identified as α -methoxytoluene and α,α -dimethoxytoluene and these were formed at low current efficiencies between 1.4% and 9%. The main product was thought to be an oligomer of toluene. The gas generated was found to be mainly hydrogen with a small amount of oxygen thought to come from residual water in the pre-treated membrane.

A computer simulation of the SPE reactor for toluene oxidation in methanol was based on two series and one parallel reaction. These were first order in reactant species and followed Tafel type kinetics. Mass transfer of dilute reactants was based on Fickian diffusion. Parameters not available in the literature such as membrane potential and electro-osmotic flow were correlated to applied variables using experimental data and multiple linear regression. The importance of electro-osmotic flow in the SPE reactor was demonstrated by considering its effect on product distribution. The model showed that the oligomerisation of toluene was the dominant reaction making the SPE reactor unsuitable for the oxidation of toluene.

ACKNOWLEDGEMENTS

I would like to thank all those people who have helped me in this project in any way. First my supervisor Professor Keith Scott for his assistance, setting up the project and the collaboration with the University of Dortmund, for reading the draft thesis and correcting many mistakes. My thanks also go to the Engineering and Physical Sciences Research Council for their part in funding the project, to the British Council for funding the collaborative work and to Dr Ian McConvey of Zeneca who helped set up the CASE award sponsorship.

This project would not have had such a successful outcome had it not been for the help of Dr Ralf Gerl. Many thanks go to him for all his hard work during the collaboration and during his holidays in Newcastle. My thanks also extend to those other researchers, Dr Jörisen and Peter Weuta at the University of Dortmund, who were involved in the collaboration and who supplied the MnO_2 coated mesh electrodes. I am also indebted to three other suppliers who donated material for the SPE reactor. They are Solvay S.A. and Eurodia Industrie S.A. who supplied ion exchange membranes and SGL Carbon who supplied the graphite felt.

Thanks also to the technical staff at the University of Newcastle upon Tyne who were involved in the project, ordering materials, fabricating the evacuated box and the rig, modifying the design of the reactor, analysing and preparing chemicals and kicking me at football. They are Erick Horsley, Stewart Latimer, Brian Grover, Dave Norman, Shaky, Ian Strong, Paul Sterling, Chris Edwards, John Marshall, Dave Henderson and Rob Dixon.

Life would have been more unbearable were it not for the friendship of all my colleagues in the Department. I would particularly like to mention Binjie Hu, Dave Hall, Mike Shaw, Wathiq Taama and Tom Jones V. Weekends and holidays mean much to me and more so because of my mountaineering friends - Steve, Mike, Paul, Paul, James, JT, Perry and Adam.

I would also like to thank my girlfriend, Mercedes, for all her love and affection especially during the final stressful months of this project.

These acknowledgements would not be complete without mentioning my parents. I would like to thank them for all their support and encouragement in all that I have done not just these last 3½ years. Without their backing nothing would have been possible.

CONTENTS

CONTENTS	<i>i</i>
LIST OF FIGURES	<i>vi</i>
LIST OF TABLES	<i>ix</i>
NOMENCLATURE	<i>x</i>
Main Symbols	<i>x</i>
Subscript Symbols	<i>xi</i>
Abbreviations	<i>xii</i>
1. INTRODUCTION	<i>1</i>
2. LITERATURE REVIEW	<i>5</i>
2.1 Introduction	<i>5</i>
2.2 Organic Synthesis Using Solid Polymer Electrolytes	<i>5</i>
2.2.1 Reactions Using Solid Polymer Electrolytes	<i>7</i>
2.3 Solid Polymer Electrolyte Membranes	<i>12</i>
2.3.1 Membranes For Fuel Cells	<i>16</i>
2.4 Electro-Organic Synthesis	<i>18</i>
2.4.1 Oxidation Of Toluene	<i>18</i>
2.4.1.1 Direct Electro-Oxidation of Toluene	<i>19</i>
2.4.1.2 Indirect Electro-Oxidation of Toluene	<i>22</i>
2.4.1.3 Methoxylation of Toluene	<i>22</i>
2.5 Summary	<i>24</i>
3. EXPERIMENTAL	<i>26</i>
3.1 Apparatus	<i>26</i>
3.1.1 Reactors	<i>26</i>
3.1.1.1 Undivided Cell	<i>26</i>
3.1.1.2 H - Cell	<i>26</i>
3.1.1.3 Glass SPE reactor	<i>26</i>
3.1.1.4 Steel SPE Reactor	<i>27</i>

3.1.2 Power Supply	28
3.1.2.1 Potentiostat/Galvanostat	28
3.1.2.2 DC Supply	29
3.1.3 Electrodes	29
3.1.3.1 Rotating Disk Electrode	29
3.1.3.2 Reference Electrode	29
3.1.3.3 Anode and Cathode Material	29
3.1.4 Pumps and Flowmeters	29
3.1.5 Experimental Procedures	31
3.1.5.1 Pretreatment of Ion Exchange Membranes	31
3.1.5.2 Electrolysis Experiments	31
3.2 Chemicals	33
3.2.1 Purity And Supplier	33
3.2.2 Ion Exchange Membranes	33
3.2.3 Control of Substances Hazardous to Health (COSHH) Assessments	33
3.3 Product Analysis	34
3.3.1 Gas Chromatography	34
3.3.2 Mass Spectrometry	34
3.3.3 Gas Analysis	34
4. ROTATING DISK ELECTRODE	38
4.1 Introduction	38
4.2 Linear Sweep Voltammetry	38
4.3 Mass Transfer Limiting Current Density	41
4.4 Diffusion Coefficient	42
4.5 Order Of Reaction And Rate Constant	43
4.6 Comparison With The Literature	44
4.7 Conclusions	46
5. EMULSION ELECTROLYSIS	47
5.1 Introduction	47
5.2 With Acetic Acid	47
5.3 The Effect of Acetic Acid Co-Solvent	50
5.4 Summary	52

6. BATCH ELECTROLYSIS	53
6.1 Introduction	53
6.2 Glass SPE Reactor	55
6.2.1 Cyclic Voltammetry	55
6.2.2 Membrane Tests	57
6.2.3 Electrode Tests	58
6.2.4 Oxidation Of Benzyl Alcohol	60
6.3 Steel SPE Reactor	61
6.3.1 Electrode Tests	61
6.4 Summary	62
7. MEMBRANE PRE-TREATMENT	64
7.1 Introduction	64
7.2 Swelling Tests	65
7.3 In-Situ Testing Of Pre-treated Membranes	74
7.4 Final Membrane and Pre-treatment Selection	78
8. FLOW REACTOR	80
8.1 Introduction	80
8.2 Flow Set-up	80
8.2.1 Gas Collection	81
8.3 Flowcell Development	81
8.3.1 Gas Outlet	82
8.3.2 Packed Bed	83
8.3.3 Potential Measurement	83
8.3.4 Temperature Range	85
8.3.5 Current Range	86
8.4 Calculation of Transfer Coefficient	86
8.5 Electrolysis	88
8.6 Results And Data Analysis	90
8.6.1 General Comments	90
8.6.2 Hydrogen Generation	91
8.6.3 Toluene Mass Balance	92

8.6.3.1 By-product Identification	93
8.7 Multiple Linear Regression (MLR)	95
8.7.1 Analysis of MLR	97
8.8 Summary	98
9. MODELLING	100
9.1 Introduction	100
9.2 Reaction Schemes	100
9.2.1 Scheme 1	101
9.2.2 Scheme 2	103
9.3 Mass Balances	105
9.3.1 Anode Mass Balances	105
9.3.2 Other Mass Balances	106
9.4 Galvanostatic Operation	107
9.5 Mass Transfer Coefficient	108
9.6 Transfer Coefficient	109
9.7 Electro-Osmotic Flow	109
9.8 Potentials	110
9.9 Side Reaction	110
9.10 Optimisation	111
9.10.1 MLR Experiments	111
9.10.2 Rate Constants	113
9.11 Comparisons	114
9.11.1 Comparison With MLR Generated Data	114
9.11.2 Comparison With Experimental Data	115
9.12 Effect of Independent Variables	116
9.12.1 Current Density	117
9.12.2 Temperature	117
9.12.3 Feed Concentration	118
9.12.4 Effect Of Feed Rate	119
9.13 Scale-Up	121
9.14 Dependence on Mass Transfer Coefficient	122

9.15 Summary	123
10. CONCLUSIONS	123
REFERENCES	127
APPENDIX 1: PROPERTIES	136
APPENDIX 2: FLOWCELL RESULTS	137
APPENDIX 3: PROGRAM CODE	146
APPENDIX 4: FLOWSHEET	175
APPENDIX 5: REACTOR BLOCK DIAGRAM	176
APPENDIX 6: MLR ASSESSMENTS	177
APPENDIX 7: COMPARISON	181

LIST OF FIGURES

Please note these Figures are in colour

Figure 3-1: The Glass SPE Reactor	27
Figure 3-2: The Steel SPE Reactor	28
Figure 3-3: Pump Calibration Curve	30
Figure 3-4: Calibration of Rotameter	30
Figure 4-1: Background Scans	39
Figure 4-2: Linear Sweep Voltamogram For Toluene in Sulphuric Acid	39
Figure 4-3: Linear Sweep Voltamogram With Various Concentrations	40
Figure 4-4: Linear Sweep Voltamogram At Various Rotation Speeds	40
Figure 4-5: Limiting Current Density	42
Figure 4-6: Determination Of Diffusion Coefficient	43
Figure 4-7: Effect Of Concentration	44
Figure 4-8: Tafel Comparison	45
Figure 4-9: Concentration Dependence Comparison	45
Figure 5-1: Concentration Profile of Benzaldehyde for Conditions Given In Table 5-1	48
Figure 5-2: Current Efficiency Profile for Conditions Given In Table 5-1	48
Figure 5-3: Emulsion Chromatogram	51
Figure 6-1: Schematics Of Transport In SPE Reactors	54
Figure 6-2: Cyclic Voltamograms of the Water-Water System	55
Figure 6-3: Cyclic Voltamograms of the Toluene-Water System	56
Figure 6-4: Cyclic Voltamograms Of Toluene Oxidation	56
Figure 6-5: Deposition Bath	59
Figure 7-1: Swelling in DMF	65
Figure 7-2: Swelling in Toluene at 23°C	66
Figure 7-3: Swelling in Toluene at 100°C	67
Figure 7-4: Pre-treatment in Methanol/Toluene	68
Figure 7-5: Pre-treatment in Methanol	68
Figure 7-6: Pre-treatment in Methanol at 23°C	69
Figure 7-7: Pre-treatment in DMF for 6 Minutes then in Methanol/Toluene	71
Figure 7-8: Pre-treatment in DMF for 3 hours then in Methanol/Toluene	71
Figure 7-9: Pre-treatment in Water	72
Figure 7-10: Pre-treatment in Sulphuric Acid	73
Figure 7-11: Pre-treatment in Various Aqueous Solutions	74
Figure 7-12: Electrolysis Tests with DMF Pre-treated Membranes	75
Figure 7-13: Electrolysis Tests with Membranes Pre-treated in Methanol/Toluene	76

List Of Figures

Figure 7-14: Electrolysis Tests with Membranes Pre-treated in Water	77
Figure 7-15: Electrolysis Tests with Membranes Pre-treated in Various Aqueous Solvents	77
Figure 8-1: Schematic Of Potential Measurement Apparatus	84
Figure 8-2: Potentiostatic Scan for EXP555	86
Figure 8-3: Potentiostatic Scans Of Toluene in Methanol	87
Figure 8-4: iR Compensated Potentiostatic Scans	88
Figure 8-5: Tafel Plot	88
Figure 8-6: Example Result, EXP547	90
Figure 9-1: Electrode Surface At Steady State	102
Figure 9-2: Anode Mass Balance	105
Figure 9-3: Time-Lag in the Recycle Line	107
Figure 9-4: Effect of Current Density on Product Distribution and Potentials	117
Figure 9-5: Effect of Temperature on Product Distribution and Potentials	118
Figure 9-6: Effect of Feed Concentration on Product Distribution and Potentials	119
Figure 9-7: Feed Flow Effect On α -Methoxytoluene Concentration	120
Figure 9-8: Feed Flow Effect On α,α -Dimethoxytoluene	120
Figure 9-9: Scale-up Of The SPE Reactor	121
Figure 9-10: Effect of Mass Transfer Coefficient on Product Distribution	123
Figure 9-11: Effect of Mass Transfer Coefficient on Potentials	123
Figure A6-1: Electro-Osmotic Flow	177
Figure A6-2: Anode Potential	177
Figure A6-3: Membrane Potential	178
Figure A6-4: Cell Potential	178
Figure A6-5: Unreacted Toluene	179
Figure A6-6: α -methoxytoluene Concentration	179
Figure A6-7: α,α -dimethoxytoluene Concentration	180
Figure A7-1: EXP547 - Final Concentrations	181
Figure A7-2: EXP547 - Potentials	181
Figure A7-3: EXP548 - Final Concentrations	182
Figure A7-4: EXP548 - Potentials	182
Figure A7-5: EXP549 - Final Concentrations	183
Figure A7-6: EXP549 - Potentials	183
Figure A7-7: EXP552 - Final Concentrations	184
Figure A7-8: EXP552 - Potentials	184
Figure A7-9: EXP553 - Final Concentrations	185
Figure A7-10: EXP553 - Potentials	185
Figure A7-11: EXP554 - Final Concentrations	186
Figure A7-12: EXP554 - Potentials	186

List Of Figures

<i>Figure A7-13: EXP557 - Final Concentrations</i>	<i>187</i>
<i>Figure A7-14: EXP557 - Potentials</i>	<i>187</i>
<i>Figure A7-15: EXP558 - Final Concentrations</i>	<i>188</i>
<i>Figure A7-16: EXP558 - Potentials</i>	<i>188</i>
<i>Figure A7-17: EXP559 - Final Concentrations</i>	<i>189</i>
<i>Figure A7-18: EXP559 - Potentials</i>	<i>189</i>

LIST OF TABLES

<i>Table 2-1: Summary of Grinberg's SPE Work</i>	8
<i>Table 2-2: Summary of Ogumi et al. 's Papers on SPE Reactions</i>	10
<i>Table 3-1: List of Electrode Suppliers</i>	36
<i>Table 3-2: List of Chemical Suppliers</i>	36
<i>Table 3-3: Summary of Ion Exchange Membranes</i>	37
<i>Table 4-1: Summary of Data from Kinetic Investigations</i>	46
<i>Table 5-1: Emulsion Electrolysis Summary on Platinum</i>	49
<i>Table 6-1: Membrane/ Electrolyte Test Summary on Platinum</i>	57
<i>Table 6-2: Steel SPE Electrode Test Summary</i>	62
<i>Table 7-1: Pre-treatment in Methanol then Toluene</i>	70
<i>Table 8-1: Potential Measurements</i>	84
<i>Table 8-2: Summary of Electrolysis Conditions</i>	89
<i>Table 8-3: Summary Of Gas Analysis</i>	91
<i>Table 8-4: Theoretical Oxygen Generation</i>	92
<i>Table 8-5: Current Efficiency for the SPE Reactor</i>	93
<i>Table 8-6: Elemental Analysis</i>	94
<i>Table 8-7: Data Used in MLR</i>	95
<i>Table 8-8: Empirical Equations from Multiple Linear Regression</i>	96
<i>Table 8-9: Assessment Equations</i>	97
<i>Table 9-1: Reaction Scheme 1 - e-e Mechanism</i>	101
<i>Table 9-2: Reaction Scheme 2: Free Radical Mechanism</i>	104
<i>Table 9-3: MLR Data Set</i>	112
<i>Table 9-4: Mass Balance and Current Efficiency of the MLR Data</i>	113
<i>Table 9-5: Rate Constants At 1.079V Anode Potential</i>	114
<i>Table 9-6: Modelling Results</i>	115
<i>Table 9-7: Mass Balance and Current Efficiency for the Model</i>	115
<i>Table A2-1: EXP547 Readings</i>	137
<i>Table A2-2: EXP548 Readings</i>	138
<i>Table A2-3: EXP549 Readings</i>	139
<i>Table A2-4: EXP552 Readings</i>	140
<i>Table A2-5: EXP553 Readings</i>	141
<i>Table A2-6: EXP554 Readings</i>	142
<i>Table A2-7: EXP557 Readings</i>	143
<i>Table A2-8: EXP558 Readings</i>	144
<i>Table A2-9: EXP559 Readings</i>	145

NOMENCLATURE

Main Symbols

Symbol	Meaning	Units
β	transfer coefficient	
η	overpotential	V
δ	diffusion layer thickness	m
ν	viscosity	Ns/m ²
ω	angular velocity	Hz
ρ	correlation coefficient	
τ	lagtime	min
ε	porosity	
A	electrode area	m ²
A	age	hours
B	constant	
C	concentration	mol/m ³
cov	covariance	
CO_2	carbon dioxide	
d	diameter	m
D	diffusion coefficient	m ² /s
D	dimer	
DMT	α,α -dimethoxytoluene	
e^-	electron	
E	potential	V
η_{aa}	anode overpotential	V
F	Faraday constant	C/mole
f	F/RT	V ⁻¹
g	Runge Kutta constant	
H^+	proton	
H_2O	water	
j	current density	A/m ²
j_d	mass transfer limiting current density	A/m ²
j_k	kinetic current density	A/m ²

j_o	exchange current density	A/m ²
k_f	electrochemical rate constant	dependent upon order
k_L	mass transfer coefficient	m/s
M	methanol	
$MR\bullet$	methoxy radical	
MT	α -methoxytoluene	
\dot{M}	molar flow rate	mol/s
n	electron stoichiometry	
n	number of data points	
N	molar flux rate	mol/m ² .s
p	reaction order	
P	polymer	
r	rate of reaction	mol/m ² .s
Re	Reynolds Number	
s	standard deviation	
S	specific electrode area	m ² /m ³
Sh	Sherwood Number	
T	toluene	
T	temperature	K
t	time	s, min, hours
V	volume	m ³
y	experimental data value	
\bar{y}	mean experimental data value	
z	distance from electrode surface	m

Subscript Symbols

$1, 2, 3, \dots$	label number of reaction step, reactor block or calculation step
A	anode
b	bulk
C	cathode
$CELL$	cell
DMT	α, α -dimethoxytoluene
f	feed

<i>f</i>	fibre
<i>fh</i>	hydraulic fibre
<i>M</i>	membrane
<i>model</i>	model data point
<i>MT</i>	α -methoxytoluene
<i>OS</i>	osmotic
<i>r</i>	recycle
<i>real</i>	experimental data point
<i>s</i>	samples
<i>s</i>	surface
<i>T</i>	toluene
<i>v</i>	variables
<i>W</i>	water

Abbreviations

aem	anion exchange membrane
ce	chronopotentiometry
cem	cation exchange membrane
cpc	controlled potential coulometry
cv	cyclic voltammetry
DC	direct current
DMF	dimethylformamide
dsa	dimensionally stable anode
e	electrochemical step
gc	gas chromatograph
iem	ion exchange membrane
lsv	linear sweep voltammetry
mea	membrane electrode assembly
MLR	multiple linear regression
ms	mass spectrometer
mt	mass transfer step
PEM	polymer electrolyte membrane
PTFE	polytetrafluoroethylene

rde	rotating disk electrode
SCE	standard saturated calomel electrode
SPE	solid polymer electrolyte

1. INTRODUCTION

This thesis reports the investigations and findings of work carried out concerning the oxidation of toluene in the solid polymer electrolyte reactor. The aims of the project were to develop the reactor for use as a suitable means of synthesising alcohols and acids based on substituted toluene compounds. This involved selection of suitable electrode material, polymer electrolyte and reactor configuration. Initial research was based on previous investigations before the final design was completed, tested and simulated.

The products of toluene oxidation are most commonly used as intermediates in the fine chemical, pharmaceutical and dye industries. Toluene is also seen as a replacement feedstock for benzene and future uses are likely to be developed in this direction. Industrially the oxidation of toluene is carried out by the cobalt catalysed liquid phase oxidation with air. This yields mostly benzoic acid with some intermediate benzaldehyde. Other by-products include formic and acetic acids, benzene, benzyl formate and acetate and phthalic acid. Of these only benzene and benzaldehyde are recovered.

The electrochemical oxidation of toluene is carried out with highest yields of benzaldehyde by the indirect method. Transition metal mediators such as cobalt and manganese are used to carry out the oxidation of the methyl group. Again intermediates such as benzyl alcohol, and higher oxidation products like benzoic acid are produced. Supporting electrolytes are most commonly sulphuric acid. The direct method gives yields in batch reactors of only 20% benzaldehyde with nitric acid supporting electrolyte and acetic acid co-solvent. Higher yields have been achieved but only in higher temperature fuel cells.

One of the major problems with electro-organic syntheses is the numbers of additives, side reactions and the cost of separating all these compounds at the purification stage. This is as true with toluene oxidation as with the majority of electro-organic processes. By using a solid polymer electrolyte instead of co-solvents and supporting electrolyte the number of species involved can be reduced. Eliminating species can also reduce the quantity and complexity of the side reactions with a resulting increase in yield and current efficiency.

The heart of the solid polymer electrolyte reactor is the polymer electrolyte. This is often an ion exchange membrane which selectively transfers ions between two electrodes, hence

transferring charge, or electric current. The membrane is sandwiched between two electrodes, which can be pressed onto, or coated onto the polymer. In this way no supporting electrolytes or co-solvents are needed. The organics can be electrolysed directly so long as they are simultaneously in contact with an electrode and membrane. For the oxidation of toluene the reactants required are toluene and an oxygen containing species such as water or methanol.

The precise mechanism of toluene oxidation is not known, nor was it in the scope of this work. However, for the purposes of developing the SPE reactor an understanding of possible steps involved needs to be discussed. Present in the reactor are two electrodes, an ion exchange membrane and two reactants. One reactant is toluene, the other is an oxygen carrying compound. The oxidation is likely to proceed through the electrochemical generation of an intermediate formed from either of the two reactants. This takes place at the surface of one of the electrodes. Any ions that are generated are able to move across the ion selective membrane. Subsequent reactions may be electrochemical in nature. Either these initial reactions or the subsequent reactions generate hydrogen ions as a by-product at the anode. Current is transported by these ions as they migrate through the ion exchange membrane towards the cathode. This transport is driven by the potential gradient, and drags with it a shell of solvent. Products from these reactions were analysed by GC-MS and the current supplied was recorded using EG&G Electrochem software. Side reactions causing loss of yield were polymerisation of toluene to tars and splitting of water to oxygen and hydrogen.

The structure of the thesis closely matches with the chronology of the research investigations. First the literature review covers the development of toluene electro-oxidation from the beginning of the century to recent work with mediators and gaseous phase fuel cells. Ion exchange membranes were developed for the chlor alkali industry and water electrolyzers in the late 1950s and early 1960s. The solid polymer electrolyte reactors based on these membranes for electro-organic synthesis are quite recent developments and several early attempts are covered. Most of these concern batch mode synthesis of model reactions, for example the methoxylation of furan. Recent work at the University of Dortmund increased the knowledge of the solid polymer electrolyte reactor although this only concerned the model reaction - the methoxylation of DMF. Many hours electrolysis took place in a continuous operation with recycle. Much effort was concentrated on the performance and pre-treatment of the membranes.

The initial investigations in this research were carried out in two parts. First the kinetics of the toluene oxidation on lead dioxide electrodes was investigated in sulphuric acid using the rotating disk electrode system. Several linear sweep and cyclic voltammograms were performed at different rotation speeds and at different toluene concentrations. Next, batch experiments were conducted to validate work done in the 1920s in nitric acid and acetic acid on platinum electrodes. Experiments were run galvanostatically for up to 10 hours generating products which were analysed using gas chromatography. These experiments were improved upon by eliminating the co-solvent and stirring vigorously with a magnetic stirrer bar in order to disperse the toluene in the aqueous electrolyte. Other supporting electrolytes such as sodium sulphate and sulphuric acid were also tested.

Work in a small glass solid polymer electrolyte reactor was then commenced. Initially cyclic voltammetry was carried out using water as the only source of oxygen. Later other sources such as nitric acid, sulphuric acid and ammonia solution were tested in galvanostatic electrolysis. Several different ion exchange membranes, both cationic and anionic were used. Different anodes were also investigated in the glass solid polymer electrolyte reactor. These included platinum, lead dioxide, nickel foam, nickel mesh and manganese dioxide. A larger, steel, solid polymer electrolyte reactor was then made which offered advantages over the smaller glass one. Steel springs were used to apply pressure to the electrodes forcing them onto the membrane. This ensured a good membrane-electrode contact. Heating chambers allowed electrolysis at higher temperatures. In this reactor other electrode materials were tested. Comparisons between different experiments were made on the basis of current efficiency of benzaldehyde production.

Pre-treatment of the membranes is the subject of Chapter 7. The performance of the solid polymer electrolyte reactor is very much determined by the ion exchange membrane. Pre-treatment of membranes concerns the swelling of the membrane substrate to allow greater solvation of the fixed ions, and an increase in the pore size. Several ion exchange membranes such as Nafion®117, Ionac® MA3470, Neosepta C66, CMB and CMX, and Solvay's CRA, CSP, CDS, ADP and ARA were swollen in several solvents. The solvents chosen were water, sulphuric acid, methanol, toluene and DMF. The effect of temperature was also investigated as was the swelling in more than one solvent. The measured parameters were increase in membrane weight and membrane area. The swollen membranes

were then tested in the large solid polymer electrolyte reactor where the cell potential at constant current was used to compare performance.

Following optimisation of electrode material, membrane type and pre-treatment, electro-oxidation of toluene was carried out in methanol solution. Under investigation in these experiments was the effect of toluene feed concentration, reactor temperature and applied current density on the selectivity and cell voltage. Many reactions were carried out under various conditions with gas and liquid samples being analysed by gas chromatography. The reactor was run continuously, with a recycle stream returning unreacted material back to the anode chamber. Flow rates, temperatures and potentials were recorded every hour for each experiment allowing multiple linear regression analysis of chosen variables. These variables included the electro-osmotic flow, anode overpotential, cell voltage, membrane potential and final product concentrations.

The final piece of work was to develop a computer model of the continuously operated process. Information gained from the experimental work was used in the development of the kinetics and modelling of the membrane potential and electro-osmotic flow. The kinetics are based on Tafel's equation with first order dependency of each reactant. Mass transfer is represented by the mass transfer coefficient and is dependent upon current density. The Runge Kutta method was used to solve the first order partial differential equations. Optimisation of the model was carried out by fitting the results of the model to the 'mean' experimental result data set. This involved adjusting only the rate constants of the desired series and by-product parallel competing reactions. Once a fit of within 1% error was made the simulation was compared with the results of the multiple linear regression analysis.

2. LITERATURE REVIEW

2.1 Introduction

This review covers the literature of direct relevance to electro-organic synthesis in the solid polymer electrolyte reactor. Of particular interest is the development of the reactor for electro-oxidation of toluene. Extensive work was found covering the methoxylation of DMF in the SPE reactor, and the preparation and performance of the ion exchange membrane used in this process. These pieces of work were the most important related references found.

Significant research has been published on SPE electrolysis of several other compounds, both organic and inorganic. These pieces of work investigated different parameters of design and were referred to during the course of the project.

Of paramount importance in the SPE reactor is the conducting polymer electrolyte. Extensive work has been carried out investigating the structure and performance of these membranes, particularly for use in polymer electrolyte membrane (PEM) fuel cells.

The electro-oxidation of toluene has been studied from the beginning of the century to the present day. The initial work concerned the selection of suitable supporting electrolytes, co-solvents and anodes. Later, much research time was spent on the indirect oxidation finding mediators that gave the prime performance required. Some research studied alternative reactors such as the fuel cell for toluene oxidation, while other research looked at different solvents.

2.2 Organic Synthesis Using Solid Polymer Electrolytes

The thesis of Gerl^[1] and his recent paper with Jörissen^[2] formed much of the background work for this project. Their work at the University of Dortmund had been carried out over many years mainly concerning model reactions such as the methoxylation of DMF. Some of the earlier work is reviewed by Simmrock^[3] and co-workers. Their work covered many electro-organic reactions from the oxidation of isopropanol, n-octanol, propargylic alcohol to methoxylation of furan and dimethylformamide. Two different reactors were tested; the 'type 1' cell with attached electrocatalyst layers and the 'type 2' cell with the electrocatalyst

pressed against the membrane in the 'zero gap' configuration. The main area of study reported in this paper^[3] was the methoxylation of furan. This was carried out at current densities of 500A/m^2 with the reactants in an aqueous solvent. The effect of the concentration of water on current efficiencies and cell potential was investigated. Replacing water with sodium sulphate solution was seen to remove the cell potential's dependency on solvent concentration. The transport of species through the ion exchange membrane by electro-osmotic flow was also noted and their relationship to the water content and the methanol concentration were investigated. The diffusion of methanol back across the membrane was also seen to be significant when the concentration gradient increased.

The methoxylation reactions were compared with the oxidation of methanol with water in an identical cell at three different operating temperatures. Formaldehyde and formic acid methyl ester were found to be the major products. Comparing with the furan methoxylation led to the conclusion of a favoured methoxylation reaction rather than the oxidation of methanol, or at least the adsorption of furan onto the platinum catalyst.

Investigations with several other solvents showed that the swelling of the membrane plays an important role in the SPE process. It was thought the dissolution of sulphonic acid groups in the membrane assisted the mobility of the H^+ ions. Furthermore the system as a whole was more likely to be successful for non aromatic rather than aromatic systems. One particular reaction that was highlighted was the methoxylation of DMF. It was this reaction that Gerl^[1] alone and along with Jörissen^[2] investigated further.

Their investigations took place in a continuously operated SPE reactor with an active electrode area of 256cm^2 . Because the conversion per pass was low (10% to 20%) a recycle stream was used to return unreacted electrolyte, methanol and DMF, to the anode chamber. No recycle pump was necessary since electro-osmotic flow provided sufficient driving force. Gerl measured both the potential and current density distribution over the membrane surface. These he found to be even over the height of the membrane and were independent of reactor temperature. From residence time distribution experiments he was also able to propose a mass transfer model of the system that matched well with experimental data. The proposal consisted of:-

- cathode chamber - ideal well mixed region
- membrane - plug flow through pores
- anode chamber divided into three regions of:-

1. lower section - plug flow
2. middle section - mixture of plug and well mixed region
3. upper section - ideal well mixed region

The well mixed regions were due to gas generation. On the cathode side this effect was very large, but only affected the upper regions of the anode chamber due to the packed bed of graphite particles.

A heat transfer model was also proposed by Gerl^[1], and again this fitted well to the experimental data. He found that the heat at the reaction zone, produced by the heat of reaction and electrode overpotentials, was removed by three mechanisms. These were:-

1. conduction through the graphite electrodes and packed bed
2. convection by the electro-osmotic flow
3. evaporation of electrolyte

The evaporation of electrolyte became the most dominant form of heat transfer as the temperature of the cell approached the boiling point of the electrolyte.

2.2.1 Reactions Using Solid Polymer Electrolytes

It was in the late 1970s and early 1980s that synthesis of organics using solid polymer electrolytes began to be investigated. The timing coincided with the development of polymer membranes originally developed for chlor alkali cells and for water electrolyzers. Organic synthesis development was mainly carried out by 4 independent groups. The work of the Dortmund University group was mentioned above. The other groups being Grinberg et al in the Soviet Union, Sarrazin and Tallec in France and Ogumi et al in Japan. This next section covers publications from these three later groups with the addition of work by Chen and Chou^[6]. These papers concern the earliest attempts of electro-organic synthesis using solid polymer electrolytes. Various design permeabilities, reactions, membranes, electrodes and phases were investigated and some of the works are discussed below.

In 1983 Grinberg^[4] published a short abstract regarding his initial investigations into the reduction of several organics at the cathode of an SPE reactor. Table 2-1 summarises the reactions, solvents and cathodes tested. The anodic reaction for all these cases was ionisation of hydrogen in water vapour. The membrane-electrode assembly was made by mixing the catalyst particles with sulphonated perfluorocarbon powder and coating directly onto the cation exchange membrane.

Table 2-1: Summary of Grinberg's SPE Work

Reductant	Solvent	Cathode	Product
CO ₂	water	tin	formic acid
CO ₂	acetonitrile	stainless steel	oxalic acid
acetone	water	lead	isopropanol
acrylonitrile	acetonitrile/water	lead	propionitrile and adiponitrile

Independent research by Sarrazin and Tallec produced 3 papers relating to the use of ion exchange membranes in organic synthesis. Their preliminary note^[5] concerned both oxidation and reduction test reactions. In their second paper on the subject^[6] investigations into methoxylation reactions of 6 separate organics was reported. The methoxylation of furan was considered to be the most successful and this was further developed and reported in their third paper^[7].

All three investigations were carried out in an identically designed reactor. The working compartment consisted of a mesh electrode placed on the surface of an ion exchange membrane. No supporting electrolyte was placed in the working compartment. Aqueous electrolytes were used in the auxiliary compartment where the counter electrode was housed some distance from the membrane.

In the preliminary paper^[5] the reduction of a dibromide organic was carried out using AMV Selemion anion exchange membrane in ethanol and in hexane. The reactions were potentiostatically controlled at 3V in ethanol and 2V in hexane and carried out in a batch operation. The product distribution was monitored as a function of time and as a function of the consumption of electrons. An oxidation reaction was also carried out. This was of hydrazobenzene to azobenzene dissolved in ethanol. For this the chosen membrane was the cationic exchange membrane CMV Selemion. Both these reactions showed the possibility of carrying out electro-organic reactions without supporting electrolyte. The product analysis had shown that these processes were not particularly selective, operated with low current density, although yields were fairly good.

In order to avoid these disadvantages reactions involving solvents were chosen for testing and the results were reported in their second paper^[6]. Six different alkenes were selected for

electro-methoxylation on a platinum mesh:- 1,1-diphenylethylene, trans-stilbene, acenaphthylene, cyclohexene, 2-methyl-3-phenylindenone and furan. The membrane this time was Ionac[®] MC3470. Again the auxiliary compartment was filled with aqueous solution. A constant cell potential of 15V was applied which gave a current density of 120A/m² when only methanol was present. Within a few minutes of adding the alkene (except furan) the current density reached a constant value which depended only the alkene itself. This was thought to be due to increased membrane resistance due to organic permeation, indeed organic product was found in the auxiliary compartment. This prompted the further work on methoxylation of furan to concentrate on membrane selection.

Four cation exchange membranes were tested - Selemion CMV, Ionac[®] MC3470, Nafion[®] 425 and Raipore R-4010. Transport of anionic or cationic species across the membrane was seen again, at different rates for the different membranes. Electro-osmotic flow seemed to be smallest with Ionac and highest for Nafion. A decrease in current density was simultaneously noticed as this transfer happened which was thought to be due to an increase in the membrane resistance caused by organics penetrating the membrane. Chemical yields and current efficiencies reached 83% and 63% respectively for Ionac and the optimum cell potential was situated between 10-15V. Further investigations were made into the energy consumption when using Ionac and graphite anode.

Product analysis showed that, with the exception of furan, the dimethoxylated products were more susceptible to oxidation than the substrate itself. By-products with higher oxidation states were identified and other unidentified by-products such as polymeric methoxylated compounds were felt to be produced. No by-products were observed with furan and the current efficiency for the dimethoxylated product was 75%. The results of this work were compared to traditional electrochemical methods and the conclusion drawn that they were 'not basically different'^[6]. This encouraged further investigation of the methoxylation of furan which was reported in the third paper^[7].

Since the early 1980s Ogumi et al have produced many papers^[8-15] on electro-organic synthesis using the solid polymer electrolyte system. Like Grinberg and Sarrazin and Tallec this work was carried out in batch reactors with, at least, the auxiliary compartment containing aqueous electrolyte. Several different reactions were tested in the SPE reactor with different electrodes, membranes, composite membrane-electrode assemblies, solvents, at potentiostatic as well as galvanostatic operations; these are summarised in Table 2-2:-

Table 2-2: Summary of Ogumi et al.'s Papers on SPE Reactions

Reference	Reactants	Solvents	Electrode	Membrane	Control
[8]	several alkenes	ethanol, hexane	Pt, Au and Pt-Au composites	Nafion [®] 415	current
[9]	acetic acid, monomethyl adipate	none or 0.5M H ₂ SO ₄	single and double Pt composites	Nafion [®] 415	current
[10]	cyclohexanone	aqueous solution of I ₂ or KI	Pt double sided composite	Nafion [®] 415	current
[11]	nitrobenzene	methanol	Pt-Ni and Pt- Cu composites	Nafion [®] 415	current
[12]	geraniol	acetone	Pt-MnO ₂ composite	Nafion [®] 417	potential
[13]	nitrobenzene	methanol, ethanol, 1-propanol, 1-butanol, 1-pentanol, 1-hexanol, 1-heptanol, 1-octanol	Pt-Cu composite	Nafion [®] 415	current
[14]	p-nitrotoluene p-nitrophenol	methanol butanol	Pt-Cu composite	Nafion [®] 415	current
[15]	benzyl alcohol	acetonitrile hexane benzene THF	Pt composite	Nafion [®] 415	current

Many of the conclusions that were drawn from this work were specific to the reaction system under investigation. Some, though, apply to SPE electrolysis in general, and it is these areas that shall be mentioned. Firstly some note should be made of the SPE -Pt composite electrodes and their use in the reactors used by Ogumi et al. All these electrodes were the attached porous electrode layer type with the platinum being deposited onto the Nafion® surface. Frequently other electrocatalysts were deposited on top of the platinum layer. Sometimes both sides of the membrane were coated which allowed both compartments of the reactor to be freed of the need of supporting electrolyte.

Electrolysis was also performed without supporting electrolytes or co-solvents. Many discussions considered the solvent effect in relation to the active ionic clusters in the membrane^[14], active catalyst sites^[11] and the transfer of reactant species to and from these sites^[13]. For the oxidation of benzyl alcohol^[15] the solvents were thought to assist in the stability of the Pt-SPE composite.

There were also several references to transport of different species across the ion exchange membranes. One suggestion was the effect of the back diffusion of hydrogen to the anode. This is normally regarded as having no other effect to play in the reaction scheme, but hydrogen oxidation to protons could occur, reducing the current efficiency.

Two papers by Chen and Chou^[16, 17] compare the performance of metal-SPE composites for the electro-reduction of benzaldehyde. Three different methods were used for the preparation of these composites - diffusion, ion exchange and electroless plating methods. Firstly the Nafion®117 membrane was pre-treated in methanol, hydrogen peroxide, sulphuric acid and water before the depositing took place. Scanning electron micrographs showed that the deposits obtained from the diffusion method were loosely bonded to the membrane. The reactor used by Chen and Chou was different to that used by the 3 previous groups in that it was a continuous process. Again an aqueous electrolyte of 0.25M H₂SO₄ was used in the auxiliary compartment but no co-solvent was used to dilute the benzaldehyde. The three conclusions derived from this work were:-

1. the ion exchange method gave a highly electrochemically active surface area
2. the current efficiency for benzyl alcohol production on SPE electrodes decreased in the order Pt+Pb > Pb > Ni > Cu > Ag+Cu > Ag > Pt
3. the reaction zone is on the inner side of the deposited metal.

2.3 Solid Polymer Electrolyte Membranes

An abundance of scientific papers exists concerning polymer membranes as electrolytes. These stem from the considerable interest in polymer electrolyte fuel cells, water electrolysis, chlor alkali industry and electro-dialysis. These are all aqueous systems rather than organic so much of the data is of limited interest. However, research on the structure of the polymers and their effects on membrane performance is of use in SPE electro-organic synthesis.

Some publications exist which are useful reference books. Scott's handbook^[18] covers properties, structures, uses and data for many membrane types, not only ion exchange membranes. The section on electrodialysis and ion exchange membranes also covers the manufacture processes as well as practical solutions to the measurement of membrane potentials. Yeo and Yeager^[19] review many articles concerning ion exchange membranes and their performance in different aqueous systems. They discuss the development of membranes and the types of applications. The structure of membranes are related to their performance in terms of the ion exchange capacity, clustering, the swelling of membranes due to uptake of water and the state of water within the structure. The transport of different species (ions, water) is also reviewed, and this includes their performance under industrial conditions.

Literature regarding ion exchange membranes as solid polymer electrolytes for electro-organic synthesis is rare. The work at the University of Dortmund has generated the largest number of scientific papers on the subject. A general review of membranes is reported by Jörissen.²⁰ In the first part of this paper he reviews the different reactions, electrodes and membranes tested over a period of time. One of the characteristics of the SPE system which could be advantageous is the electro-osmotic flux. This flux is not available in traditional electrolyzers. This is discussed in detail by Jörissen^[20]. Flux at anion and cation exchange membranes are compared with the conclusion being that anion exchange membranes are more suited to electro-oxidations. This is because the reactants are carried into the reaction zone immediately and the transport of negatively charged reactant ion is enhanced by migration.

Jörissen also reported that all neutral species are unselectively transported. That means that the concentration of species being transferred is identical to that in the reaction zone and at the membrane entrance. However, the overall electro-osmotic flux is highly dependent on the cell electrolyte. As an example Jörissen quotes the electro-osmotic flux of electrolyte as a linear relation from 2 mol/Faraday in pure water to 10 mol/Faraday in pure methanol. More interesting was the discovery that the swelling of the membrane can remarkably influence the electro-osmotic flow.

Swelling of membranes allows the dissociation of the counter ions from the fixed ions. This allows mobility of the ions within larger pores. Because of its high dielectric constant, water is the most suitable solvent and ion exchange membranes are preferably developed for use in this solvent. Jörissen's work on swelling was carried out on Nafion®117. The structure of non-crosslinked polymers was altered as water was absorbed. This phenomena was also repeated in DMF but to a much greater degree. At temperatures ranging from 20°C to 120°C the increase in weight of the membrane was almost exponentially related to temperature. The amount of solvent uptake was also found to be dependent on the fixed ion concentration, measured as the equivalent weight. This work on swelling gave rise to the following conclusions:-

- swelling transforms the membrane to an expanded form
- a membrane swollen in water is too rigid to give satisfactory contact with electrodes
- graphite felt affords a good contact with a swollen membrane
- insufficient contact gives rise to diffusion overpotentials
- swelling led to reduced cell voltages for methanol oxidation, methoxylation of some amides and water electrolysis
- electro-osmotic flux is strongly intensified
- mechanical stability is decreased

These conclusions were also mirrored in the work by Gerl^[1] and Gerl and Jörissen^[2]. The paper concentrates on how the pre-treatment procedure affects the properties of the membrane, and the results of electro-organic synthesis for the model reaction - methoxylation of DMF. An increase in the current efficiency from 65% to 98% was achieved for the chosen reaction, while a fall in the cell potential was noted from 6 to 4V. This was due to the increased membrane electrode contact and the increased swelling producing larger pore size and better ion solvation. The size of the solvation shell was found to be a linear function of the increase in the membrane area during pre-treatment. This

suggested that with no pre-treatment no solvation would occur. Correlating the swelling with the strength of the membrane showed that after an 80% increase in membrane weight the tensile strength had fallen to around 4% of its original raw material value.

During their period of study Gerl and Jörissen^[22] noticed that the equivalent weight of manufactured Nafion®117 membrane had changed. Two distinct equivalent weights could be determined - that in 1993 had a value of 1100g/mole and that in 1994 a value of 1060g/mole. These two types had different characteristics. Comparing also with Nafion®120 (with equivalent weight 120) showed that the higher the equivalent weight the smaller the swelling. Gerl and Jörissen proposed that this was due to structural differences. Lower equivalent weight membranes were thought to have a wider distribution of molecular masses which were more likely to be solvated at lower temperatures. The higher equivalent weight Nafion®117 was thought to have a much narrower distribution so that the solvation rate changed more dramatically above 100°C.

The long-term behaviour of the membrane in the reactor was also investigated. This was done by carrying out the pre-treatment procedure in DMF at 60°C for 2½ days. For a period of 12 hours the solvent temperature was raised to 90°C, after which time the solvent was returned to 60°C. On increasing the temperature the membrane swelled as expected, but on decreasing the temperature the membrane remained in the swollen state even for a period of up to 9 days. The conclusion was drawn that the membrane should be pre-treated at least at the highest temperatures likely to be generated in the reactor. This would prevent swelling in the reactor, potentially causing loss in the membrane - electrode contact.

The solubility of sulphonyl fluoride ion exchange membranes was studied by McCain and Covitch^[23]. Two types of study are reported in their paper. The first concerns swelling of Nafion®117 at ambient temperature, the second concerns the solubility of Nafion®501 and 511 at elevated temperatures. Several organic solvents were used to carry out these studies with correlations being sought linking solubility and swelling with strength of hydrogen bonding, relative volatility and solvent functionality. Although no correlation could be found linking the swelling and the solvent properties the following guidelines were developed:-

- only significant swelling was observed in the solubility parameter range 7.3-9.1Hb
- within this range fluorinated liquids were the most effective swelling agents

- among perhalogenated compounds an increase in relative volatility saw an increase in weight gain
- all amines in the solubility parameter range 7.3-9.1Hb were effective swelling agents
- tertiary nitrogen may play an important role in swelling

A series of organic solvents were then chosen using the above guidelines to completely dissolve the polymer membranes. The dissolution temperature was chosen to be within 10°C of the solvent boiling point. Nine out of the 16 selected solvents completely dissolved the membranes. Of these, Halocarbon Oils (from Halocarbon Products Corporation), barely swelled the polymers at room temperature. Using this solvent the cloud point temperature was correlated with the solids content for both 1100 equivalent weight and 1200 equivalent weight membranes. Rules governing the selection of solvents for complete dissolution were also found:-

1. the solvent must be totally halogenated. The only hydrogens present must be either carboxylic acid or hydroxyl protons
2. another group that are good solvents for dissolution are perfluorotertiary amines
3. the temperature necessary for dissolution is dependent upon the boiling point of the solvent.

Other work concerning solid polymer electrolytes for electro-organic synthesis was reported by Genders, George and Pletcher^[24]. In their work the influence of temperature and current density on the transport of formaldehyde, glycol and water through four different ion exchange membranes was investigated. The process under study was the reduction of formaldehyde to ethylene glycol. Although the system under study was not an SPE reactor the results do impact on membrane performance. For the system at open circuit, the research showed that the flow rate in the reactor has little effect on the transport rate of the organics. The formaldehyde did have a higher flux rate than water or glycol, but this was thought to be due to its higher concentration in the cathode compartment. Also at open circuit an increase in temperature substantially increased the formaldehyde transport rate according to an Arrhenius relationship with an activation energy of 31 kJ/mol.

Increasing the current density from zero to 2000 A/m² gave a decrease in the transport rate of organics and water from the catholyte compartment with cation exchange membranes Nafion[®]324 and RAI 1010. With Tosoh IE-DF34 anion exchange membrane the reverse was true. The magnitude of the water transport was much greater than that of the organics

and was probably due to the low molar concentrations of the organics. The explanation for the increase in rate with anion exchange membranes and decrease with cation exchange membranes was based on the water transport data. The water transports by diffusion due to differences in water activity across the membrane. During electrolysis a bigger effect was the electro-osmotic flow. Using cation exchange membranes the transported ions are protons into the cathode compartment and water transport shows movement in this direction. With anion exchange membranes the formate ions are transported out of the cathode along with a solvation shell of water.

2.3.1 Membranes For Fuel Cells

Ion exchange membranes are used and are being developed for use in solid polymer electrolyte membrane (PEM) fuel cells. The structure of PEM fuel cells is in many ways similar to the SPE reactor - the anode and cathode electrocatalysts can be coated or pressed against the membrane surface, hence, the cell is divided into 2 distinct halves by the membrane-electrode assembly. The transport of species across the membrane is of vital importance. Use of liquid fuel such as in the direct methanol fuel cell brings the two systems closer still. PEM fuel cells are based predominantly on aqueous solutions, and are galvanic, however because of the close relation much of the published work is of interest in both systems.

For an overview of fuel cells the textbook by Blomen and Mugerwa^[25] gives details on much of the historical development and the state of research in 1993. Research publications covering fuel cells are abundant, and here only those related closely with electro-organic synthesis will be discussed. These concern transport across the membranes, potential measurement and modelling.

Seventeen publications regarding transport were reviewed^[26-42]. These should be regarded as only a selection of the total publications on the subject, and as such, give an indication as to the amount and variety of research in this area. All of this work was based in aqueous systems either in pure water^[33,38], methanol/water^[29], acid^[26,28,30-32,35-37] or salt solutions^[27,34,39-41]. The transported species under investigation being sodium^[27], protons^[28,30,35,36], methanol^[29,37], water^[30,34,37,38,40], ions^[28,31,32,39-41], solvent^[31,32] and gases^[26]. Of particular note are the review of transport models in ion exchange membranes by Verbrugge and Pintauro^[29], the work on the temperature effect by Verbrugge et al^[35] and the comparison of

the diffusion and diffusion convection Stefan-Maxwell equations by Schaetzel et al^[42]. As has been discussed previously the transport properties of ion exchange membranes are heavily dependent on their pre-treatment, and although water was one of the solvents used in this project the effect of toluene was such that many of the above papers were only of passing interest. Of more interest were the publications relating to membrane resistance.

Anantaraman and Gardner^[43] performed studies on the effect of humidity on the electrical conduction of Nafion[®]117. In these experiments the membrane was placed in a controlled humidified atmosphere and the water content in the membrane was measured as a function of relative humidity. The membrane impedance was then measured at different relative humidities. The impedance experiments were also carried out with differential relative humidities of air above and below the membrane. The conductivity of the membrane was then calculated from the measured resistances using:-

$$\sigma = \frac{\ln(b/a)}{2\pi \cdot R_T \cdot h} \quad \text{Equation 2-1}$$

where b/a was the ratio of the radii of the probes, R_T is the measured resistance and h is the membrane thickness. Plotting the conductivity against the water content of the membrane showed that increasing the water content increased the conductivity, but it is a non-linear trend. Results from the differential relative humidity experiments showed a conductivity intermediate between the results obtained for two uniform relative humidity experiments.

Büchi and Scherer^[44] carried out measurement of membrane resistance of Nafion[®]117 inside a hydrogen fuel cell. They used a current pulse method of measuring resistance under several conditions of current density, temperature and flow field. They found that the resistance transient was quite large (30s) for a step change in current density from zero to 7770A/m². This corresponded to a change in membrane resistance from 186 mΩcm² to 224mΩcm². The transient was still, however small enough compared with temperature transients to avoid errors due to thermal changes at high current densities. It was found that the membrane resistance increased with increasing current density, except for small irregularities at low current densities. This was thought to be due to changes in water content caused by thermal effects, electro-osmotic flow and production of water at the cathode. Membrane resistance decreased with an increase in temperature. Because the temperature probe was situated at the cell block and not at the membrane surface small thermal effects were used to explain the resistance fluctuations at low current densities. These stemmed from the relative rates of Joule heating and electro-osmotic flows.

2.4 *Electro-Organic Synthesis*

A comprehensive review of all types of electro-organic oxidations was published by Weinberg and Weinberg in 1968^[45]. Nearly 900 papers were reviewed bringing up to date the earlier review by Fichter, also regarding electro-organic synthesis. This review by Fichter was later reprinted in 1970^[46]. Many of the papers regarding oxidation of toluene discussed below came from these works. In 1975 a paper by Fleischmann and Pletcher reviewed the application of electro-organic reactions on an industrial scale. Of particular note was the adiponitrile process, (at that time not commissioned in the UK) and the reduction of phthalic acid. Several other reactions on a smaller scale were mentioned and the development of novel reactors was seen as an area of future work.

2.4.1 Oxidation Of Toluene

The electro-oxidation of toluene can be carried out in two different ways - the direct and indirect methods. These two methods have been developed simultaneously and the review below covers both types. Most interest to this project is the direct method since the reason for the SPE reactor is to eliminate mediators, co-solvents and aqueous electrolytes. The subject of oxidation of toluene and substituted toluenes was reviewed and published by Weinberg and Tilak^[47]. The major issue for the early workers was the location of oxidation. Some reports suggested that oxidation of the aromatic nucleus was the site, but now it is accepted that reaction takes place at the side chain forming a series of compounds in distinct steps - benzyl alcohol, benzaldehyde and benzoic acid. Kinetic studies suggested that the emulsion electrolysis of toluene at lead dioxide electrodes was second order with respect to toluene. The mediated oxidation with Mn^{3+} was reported to be first order with respect to this ion.

The optimal process seemed to be indirect oxidation with either Mn^{3+} or Ce^{4+} on lead dioxide anodes which gave yields of up to 90%. The direct oxidation could only give 20%. Ten years later Wendt et al^[48] compared direct with indirect syntheses for oxidation of toluenes on the basis of selectivity and space time yield. The conclusion being that the choice of method was dependent on the specific toluene. The reduction in selectivity being due to oligomerisation which was found to be suppressed by dilution of the toluenes in inert, polar solvents.

2.4.1.1 Direct Electro-Oxidation of Toluene

Two papers produced by Law and Perkin^[49,50] at the turn of the century were some of the first to examine the direct oxidation of toluene and other similar hydrocarbons. The first paper concerned the oxidation of toluene to benzaldehyde using several co-solvents and electrolytes. A maximum chemical yield of 7-8% benzaldehyde was produced when toluene was electrolysed in acetone and dilute sulphuric acid. Benzyl alcohol was later identified as a second oily product. Without any co-solvent, and using either dilute sulphuric acid or dilute alkali only CO₂ and H₂O were produced. This was carried out with either lead or platinum anodes and as much as 4 kg of toluene! Repeating earlier work by Renard who used ethanol as a co-solvent produced a resinous mass which was thought to be due to the reaction of aldehyde. Electrolysis took place in a divided cell galvanostatically at current density of 120A/m² which gave a cell potential of 3.5-4.5V.

The second paper concentrated on the reactions of ethyl benzene, cumene and cymene in an undivided cell. However, it was reported that when this second cell had been used for toluene oxidation under the same conditions as before then the yield of benzaldehyde had been raised to 18-20%. The absence of any benzoic acid was also confirmed. Law and Perkin also proposed a mechanism for the reaction. This was explained by considering the hydroxyl group as the oxidising agent, first attacking the methyl group to form benzyl alcohol, then again to form benzaldehyde.

The next development in the direct oxidation of toluene was conducted by Mann and Paulson^[51]. An undivided cell was used following Law's reported success, along with platinum anodes. Some confusion had arisen as to the site of oxidation, either the side chain or the aromatic ring. Under the conditions used by Mann the attack took place at the side chain.

Selection of co-solvents was one of the aims of Mann's work. He used sulphuric acid as supporting electrolyte along with several organics which he was able to eliminate quickly. With acetone, large amounts of tar-like products were formed, and difficulties in purifying the benzaldehyde were found. Carbon tetrachloride was tried, but no benzaldehyde could be detected. Ether was the next co-solvent. With this a low yield of 1-2% was found and again large amounts (10g from an original 100g of toluene) of tar-like product. Next, ether was

used as co-solvent along with nitric acid as supporting electrolyte. This reduced the amount of by-product to around 5-8g along with an increase in yield to 6.6%. Tests with nitric acid alone only gave a 1% benzaldehyde yield and a significant proportion (20%) of unconverted toluene. The optimum concentration of nitric acid was chosen to be 20%.

With 20% nitric acid the co-solvents were tested again. Only in the cases with acetic acid was the yield of benzaldehyde above 7%. The optimum combination for the production of benzaldehyde was then determined as:-

- 50ml toluene
- 50ml glacial acetic acid
- 400 - 450ml 20% nitric acid
- 182 - 200A/m² current density
- 4.5 - 4.7V cell voltage

The direct oxidation of toluene and benzene was studied by Clarke, Ehigamusoe and Kuhn^[52]. Kinetic data at 6 different concentrations were published for toluene, along with the variation of current density with concentration. For these studies the anode material was lead dioxide with a sulphuric acid supporting electrolyte. No co-solvent was used. Clarke et al. reported the order of reaction with respect to toluene as approximately 2, although the gradient of the curve was only 1.42. More surprising was their assumption that toluene also underwent the same reaction as benzene i.e. to benzoquinone. The oxidation of toluene in the lower potential region below oxygen evolution was found to be reaction controlled.

Jackson filed a United States Patent in 1982^[53] regarding the electro-organic synthesis of benzyl alcohol, benzaldehyde and benzoic acid (amongst others) from toluene(s). 12 claims were made and these can be separated into 2 distinct types of reactor - the undivided cell and the solid polymer electrolyte reactor. In the undivided cell the claim contains reference to the electrolyte composing of toluene, aqueous solvent and either a tetrafluoroborate salt or a tetraethylammonium salt. The electrodes may be porous. According to the claim, in the reactor divided by an ion selective permionic membrane no solvent or liquid supporting electrolyte is needed, but the toluene should be in contact with the anode and membrane and a reducible source of oxygen should be in contact with the cathode and membrane. The cathode may be graphite. No other claim is made of electrode material, nor is any mention made of applied current or potential.

Examples of experiments carried out to support the claims are made. Non of these use any ion exchange membranes. The 5 examples all used platinum anodes, acetonitrile solvent, tetraethylammonium perchlorate or fluoroborate and cell voltages of 1.7-3.4V. No yields of any of the products were reported, but using IR spectroscopy benzyl alcohol, benzaldehyde and benzoic acid were detected.

Chemisorption of toluene on platinum anodes was reported by Kuliev, Vasil'ev and Bagotskii^[54]. The platinised platinum electrodes were first activated at potentials between 0 and 1.2V. They were then brought to the required initial potential before toluene was added to the 0.5M sulphuric acid. The shift in electrode potential was then measured as a function of time. The lower initial potential of 0.2V corresponded to part coverage of the anode by hydrogen. The potential initially shifts cathodic due to absorption of toluene on the free surface, but quickly recovers as the hydrogen is consumed by interaction with the toluene and reaches a steady value of 0.65V. The highest initial potential of 0.9V corresponded to part coverage by oxygen. No potential shift occurred suggesting that toluene does not interact with absorbed oxygen.

It was also found that the electro-oxidation current of toluene was similar to those of benzene and ethylbenzene under steady state conditions. At constant potential the rate increases with an increase in the bulk concentration giving an order with respect to the aromatic as approximately 0.9. At higher concentrations the current reaches a maximum and then falls. The explanation for this was given by assuming the chemisorbed species are involved in the slow step of the oxidation process.

Two papers report the direct oxidation of toluene using different novel methods. The first, by Mathur, Mukherjee and Zutshi^[55], uses the superoxide anion generated from the reduction of molecular oxygen to oxidise the toluene. This was carried out in an undivided cell using toluene dispersed in acetonitrile and tetramethylammonium bromide. Air was bubbled into the reactor where it was reduced at a mercury pool cathode. The optimum yield of 66.3% benzoic acid was achieved with a current density of 56.7A/m². The cell voltage at this rate was 16-19V.

Otsuka, Ishizuka, Yamanaka and Hatano^[56] used a fuel cell to oxidise toluene in the gas phase to benzaldehyde. Gaseous oxygen and toluene at 373K were fed to the cathode and anode compartments of the fuel cell. Pressures of up to 100kPa were used. A silica wool

disk containing H_3PO_4 acted as an anolyte and separated the two electrodes. The electrocatalyst was mixed with the graphite current collector. Using platinum, ruthenium and nickel the toluene was completely oxidised to carbon dioxide. However, with palladium only benzaldehyde and benzoic acid were produced. Otsuka et al. found that adding chlorides such as HCl , NaCl and MgCl_2 to the anode improved the selectivity of benzaldehyde.

2.4.1.2 Indirect Electro-Oxidation of Toluene

Since indirect routes require more processing it is normally only used when the alternative direct route is unsatisfactory because:-

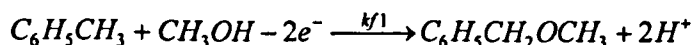
- the rate is low
- there are mass transport problems
- side reactions dominate

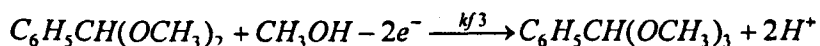
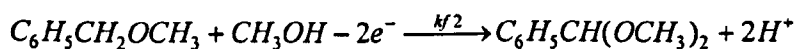
In their review of indirect electro-organic processes Clarke, Kuhn and Okoh^[57] highlighted the oxidation of toluene as one case where all these are true. Fichter^[46] had earlier reviewed work concerning indirect oxidation of toluene with the conclusion that with Mn^{3+} the production of benzaldehyde occurred at high current efficiencies, whereas with Cr^{6+} the major product was benzoic acid.

Several papers report the indirect oxidation of toluenes and substituted toluenes^[58-62]. All used transition metals as the oxidising agent directly, or to generate $\text{OH}\bullet$ radicals as the oxidising agent. In one case toluene was oxidised both by $\text{OH}\bullet$ radicals and transition metal ions in the so called 'paired electro-oxidation'. Selectivities, current efficiencies of generation of ions and yields of products were all high. Commonly used oxidising agents were Ce^{4+} , V^{5+} , V^{4+} , Cu^{2+} , Mn^{3+} , and Co^{3+} .

2.4.1.3 Methoxylation of Toluene

The kinetic study and synthesis of organics from toluenes was studied in detail by Wendt, Bitterlich, Lodowicks and Liu^[63,64]. In their first paper voltammetry was used to investigate the stages of alkoxylation of several toluenes - toluene, p-methoxytoluene and p-chlorotoluene. It was reported that, although the reaction scheme was too simple, the methoxylation took place in 3 distinctive steps:-





The experiments took place at either graphite, glassy carbon or platinum rotating disk electrodes. It was quickly discovered that the half wave potentials at platinum and glassy carbon were much higher than those on graphite so all subsequent experiments were conducted on graphite only. This also suggested that the initial step of the reaction, perhaps the formation of a toluene radical, was heterogeneously catalysed. The electrolyte composed 0.005M methanol in 0.1M NaClO₄. Rotation frequency was in the order of 20Hz and linear sweeps were carried out at 5mV/s.

The voltammetric data showed that toluene was oxidised at intermediate potentials when compared to activated toluenes such as p-methoxytoluene and deactivated toluenes such as p-chlorotoluene. Oxidation of α-methoxytoluene also took place at similar potentials, but α,α-dimethoxytoluene is oxidised at potentials 0.2V higher. This suggested that the intermediate product α-methoxytoluene could not be isolated since it would be immediately oxidised to α,α-dimethoxytoluene.

In contradiction to the proposed 2 electron steps, the number of electrons per toluene molecule was found to be 4.6. It was presumed that this was due to 2 consecutive 2 electron steps to α,α-dimethoxytoluene accompanied by some oligomerisation. Methoxylation of α-methoxytoluene was found to proceed in a 1.2 electron per molecule step.

In Wendt et al's second paper^[64] synthesis of several methoxylated toluenes was carried out. These experiments were performed in a flow through reactor in a closed loop. The anode material was again graphite, and for the methoxylation of toluene the electrolyte contained either 0.1 or 1M methanol, 0.08M NaBF₄ or 0.015M Et₄NBF₄, and sometimes additives such as KF, lutidine, pyridine or sodium methoxylate. These combinations were tested along with three alternative constant current densities - 400, 1200 and 4000A/m². The maximum amounts of α-methoxytoluene and α,α-dimethoxytoluene and the number of electrons consumed per converted molecule of toluene initially and at the time of maximum concentration of α,α-dimethoxytoluene were determined. Higher oxidation states were not identified as α,α,α-trimethoxytoluene but were thought to be oligomers and other non volatile compounds. The highest concentrations of desired products were found when using no additives. These gave maximum concentrations of 10% α-methoxytoluene and 20% α,α-dimethoxytoluene.

The discussion section of this paper^[64] concentrates on the more successful methoxylation reactions with activated toluenes. For toluene the formation of higher oxidation states and oligomers caused much loss of toluene and this occurred at the beginning of the batch process and at the end after all toluene had been consumed. This at least indicated that some higher oxidation states were created from the intermediates. The number of electrons per toluene molecule consumed at the start was always greater than 4. The value of the number of electrons per α -methoxytoluene consumed (with no toluene present) was much less at 2.4. This indicates that much of the toluene was lost through side reactions during the initial step.

2.5 Summary

The review shows that a variety of organic reactions have been attempted in SPE reactor. The majority of these took place in batch reactors with aqueous electrolytes in at least the auxiliary compartment. Reactions with only organic species were model reactions concerning the methoxylation of furan and of DMF. This later reaction is the one that has been studied most extensively in a continuously operated SPE reactor. For this system the current and potential distribution were investigated as were the heat and mass transport.

Several electrode materials have been used in SPE electrolysis normally attached to the membrane surface and based on platinum. Various ion exchange membranes have been used, but the most common one was Nafion[®]117 cation exchange membrane. Very little work has been reported on the properties and performance of membranes in organic species particularly for SPE electrolysis. These works have been limited to Nafion[®]117 for the methoxylation of DMF, the solubility of Nafion[®]117, 501 and 511 in several organic solvents and the transport of water, formaldehyde and glycol across Nafion[®]324, RAI 1010 and Tosoh IE-DF34. Many papers concerning the transport of species across ion exchange membranes used in PEM fuel cells have been published.

Work concerning the direct electro-oxidation of toluene was mainly published in the early part of this century. Use was made of platinum and lead dioxide electrodes in sulphuric and nitric acids. Maximum yields of 19% benzaldehyde were reported for electrolysis with acetic acid as co-solvent. Kinetic studies of toluene electro-oxidation at lead dioxide rotating disk electrodes were reported. The order of reaction was 2 and in the lower

potential region the reaction was kinetically controlled. Two more novel methods of direct oxidation were reported concerning the generation of the superoxide anion and the gas phase oxidation in a fuel cell.

Methoxylation of toluene was shown to give α -methoxytoluene and α,α -dimethoxytoluene in two stages. This was carried out in a solution of methanol and aqueous electrolytes, but gave low yields and higher oxidation products.

3. EXPERIMENTAL

This chapter describes the apparatus and the general procedures used for carrying out the experimental section of the project. The development of the reactor system such as piping arrangements is discussed in more detail in the relevant chapters as is specific work associated with minor testing. This chapter also gives information on the chemicals used, their purity and the risks associated with using them. Instruments used for the analysis of known and identification of unknown compounds, and the programs used are also listed.

3.1 Apparatus

The following paragraphs describe in detail the apparatus used throughout the project. This includes final designs of reactors, the power supplies, electrodes, apparatus for pre-treatment of ion exchange membranes, pumps and flowmeters.

3.1.1 Reactors

3.1.1.1 Undivided Cell

The reactor used for experiments conducted on the rotating disk electrode apparatus was a simple glass undivided cell with 2 compartments. The anode chamber had a volume of 300ml and contained 4 connections. One of these was the smaller cathode chamber of 40ml volume. The other 3 connections were for filling/emptying, sampling and potential measurement via a luggin probe.

3.1.1.2 H - Cell

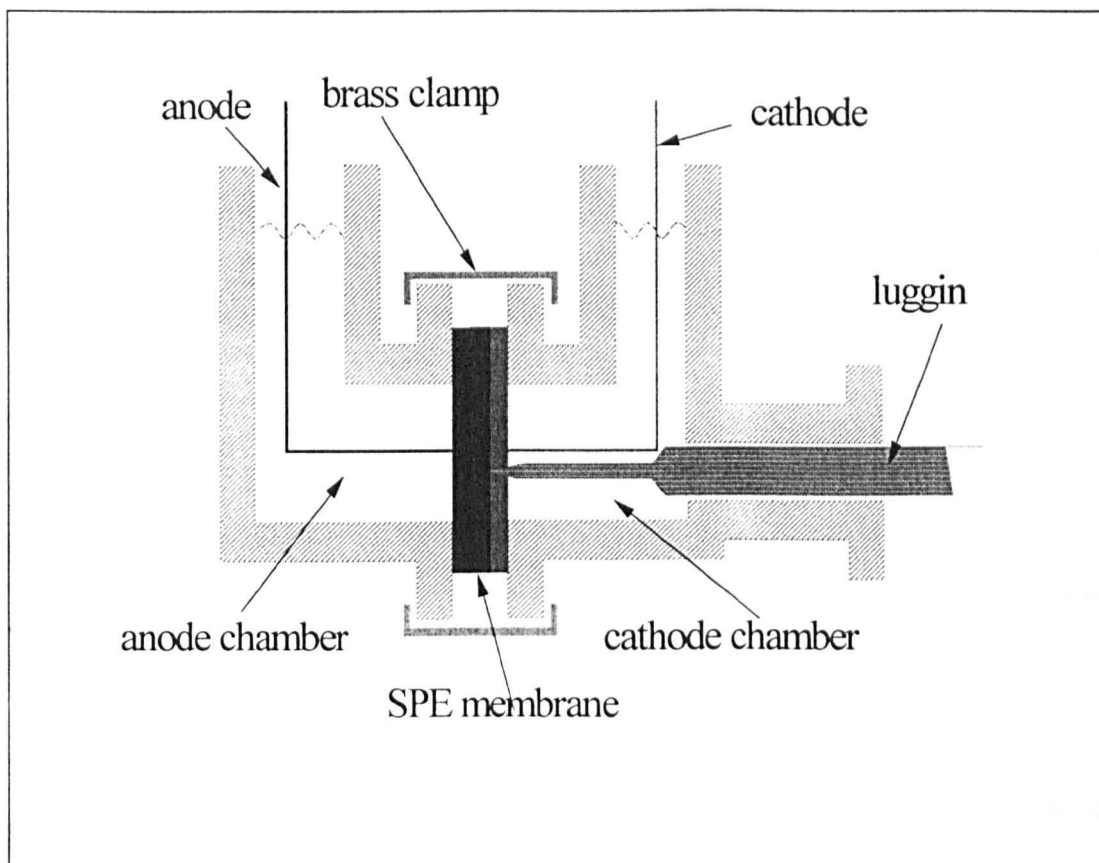
A simple H-cell was used for emulsion electrolysis. The 60cm³ anode chamber was separated from the 30cm³ cathode chamber by a glass frit. Mixing was by magnetic stirrer.

3.1.1.3 Glass SPE reactor

The glass SPE reactor (see Figure 3-1) consisted of two glass flanged chambers of 40cm³ which were clamped together, sandwiching anode, membrane and cathode. The flange was kept small to ensure that a good electrode/membrane contact was made; the area in contact

with the electrolyte being 5cm². A glass luggin was placed through the cathode and pressed against the membrane. Saturated KCl gel filled the probe and in this way the anode-membrane potential could be recorded. Teflon seals were used to prevent leakage from the membrane, electrode and flange joints. The brass clamps were held tight with nuts and bolts. The glass flange being protected with silicon rubber gaskets.

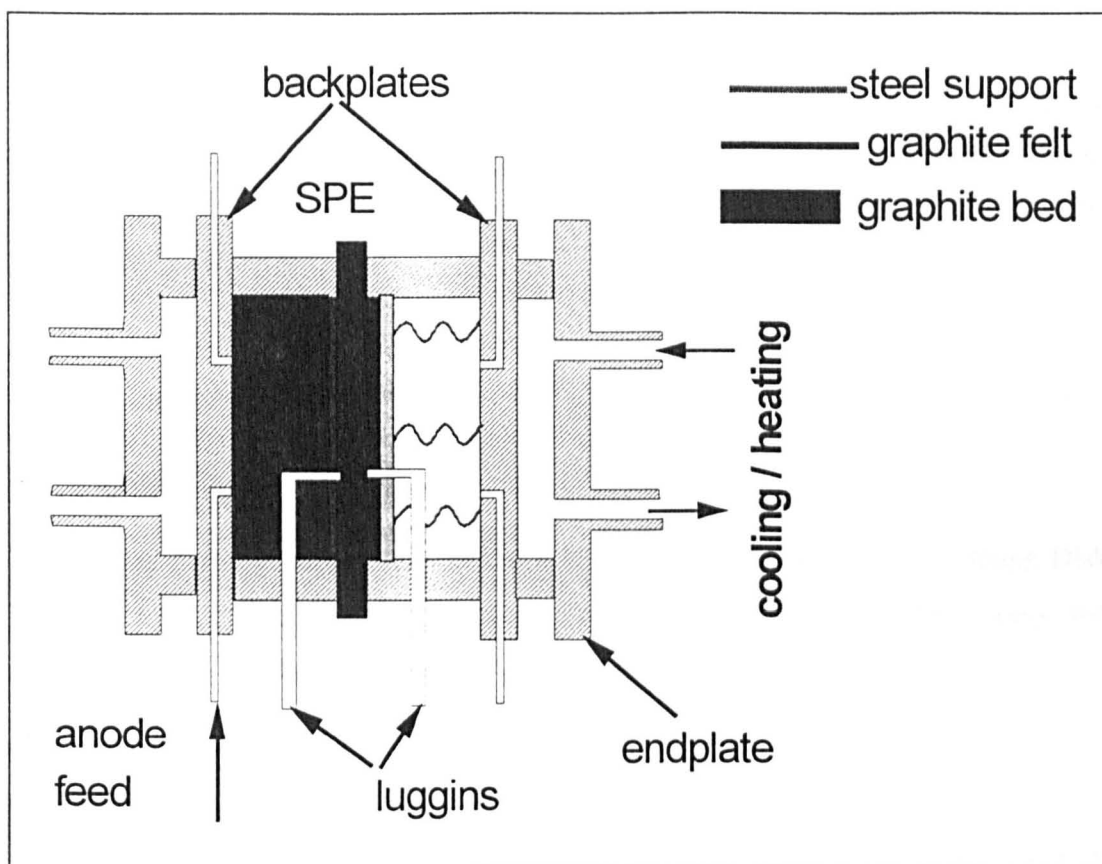
Figure 3-1: The Glass SPE Reactor



3.1.1.4 Steel SPE Reactor

The steel SPE cell also consisted of 2 chambers (see Figure 3-2) clamped together around the anode, membrane and cathode. A 1cm deep packed bed of graphite particles of irregular size (approximately 2mm diameter) filled the anode chamber. The 7cm x 3cm x 5mm graphite felt anode was placed on top of this, followed by the SPE membrane which was sized at 9cm x 5cm. A 2mm deep graphite felt cathode, also 7cm x 3cm rested on the opposite side. Pressure was applied to the cathode by sprung stainless steel mesh current contactors in order to maintain an even contact on the membrane. 3mm diameter stainless steel probes on either side of the membrane allowed the anode potential to be measured. Heating or cooling was through the outer chambers which were 1cm deep.

Figure 3-2: The Steel SPE Reactor



3.1.2 Power Supply

The electrical supply to the experiments was controlled in one of 2 ways. The majority of experiments needed less than 10V cell potential and current less than 1A. Hence, use was made of a personal computer controlled potentiostat. For power requirements greater than these a stabilised DC power supply was sufficient.

3.1.2.1 Potentiostat/Galvanostat

An EG&G Princeton Applied Research Potentiostat/Galvanostat Model 273 was used throughout the experimental process when the power requirement was sufficient. It was always controlled by a personal computer using the EG&G Echem Software Model 270/250 Research Electrochemistry Software. This allows several types of experiment to be performed. The ones used throughout this project were cyclic voltammetry (cv), linear sweep voltammetry (lsv), controlled potential coulometry (cpc) and chronopotentiometry (ce).

3.1.2.2 DC Supply

For experiments requiring greater power than that provided by the Model 273, a DC supply was used. This was a Farnell LS60-5 Autoranging Power Supply with a 60 Watt power limit. No provision was made for measurement of electrode potentials so this had to be carried out separately, see Chapter 8.

3.1.3 Electrodes

3.1.3.1 Rotating Disk Electrode

The rotating disk electrode (rde) was the H.B.Thompson and Associates' Rotating Disk Electrode System. The EG&G potentiostat was used to control the power supply and rotation speed was controlled manually within the range of 0-5400rpm.

3.1.3.2 Reference Electrode

The reference electrodes used were standard saturated calomel electrodes (SCE), and all values of electrode potentials quoted are with respect to the SCE unless otherwise stated. The particular type used in this project was Russel's PHM-105-010Y, CRL.

3.1.3.3 Anode and Cathode Material

A range of electrode materials were tested throughout the duration of the project and are listed in Table 3-1, page 35. The final selection was Sigratherm GFA5 or GFA10 soft graphite felt supplied by SGL Carbon Group. These were 5mm or 10mm in thickness respectively and allowed a much greater surface contact with the solid polymer electrolyte than was achieved with any metallic mesh. Several metals were tested, usually as a mesh but some as foam, sheet or deposited chemically and electrochemically.

3.1.4 Pumps and Flowmeters

Several pumps were considered for use in the flow system, but since the electro-osmotic flow controls the maximum rate only low flow rate pumps were suitable. Initially a March-May TE-3P-MD centrifugal pump with a magnetically driven PVDF impeller was used but even with a bypass the flow rate was difficult to control. The ideal pump was a Watson-

Marlow 101-U Peristaltic pump. This was able to deliver the low flow rate required (~20ml/hour). The flow rate was controlled via the pump mounted flow counter and this was calibrated by collecting a known volume over a measured time. Several solutions were used to do this and the results are shown in Figure 3-3.

Figure 3-3: Pump Calibration Curve

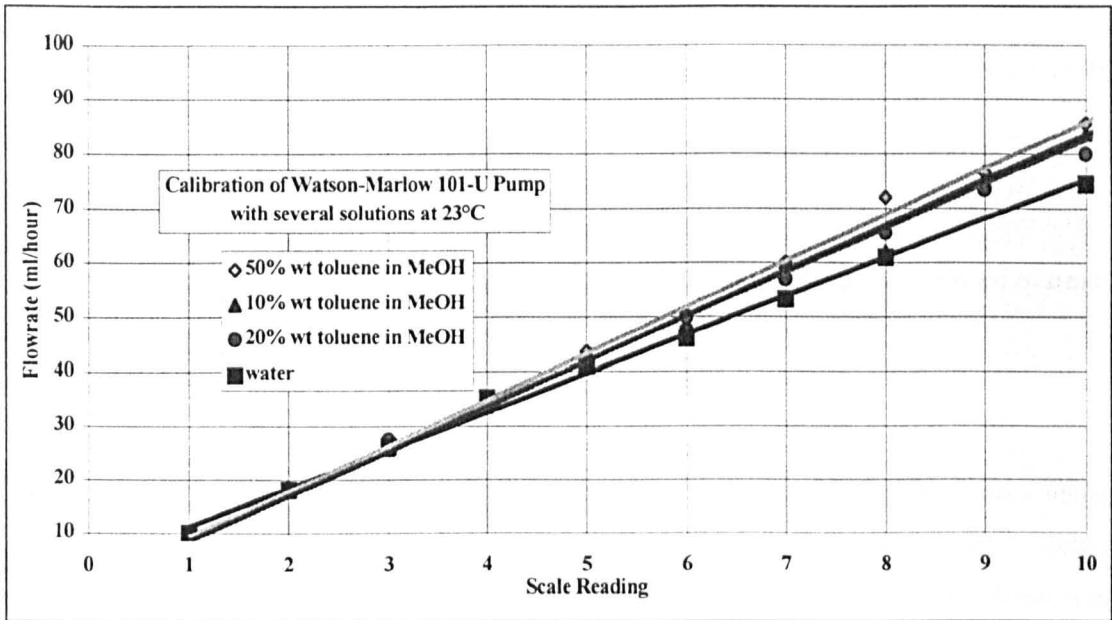
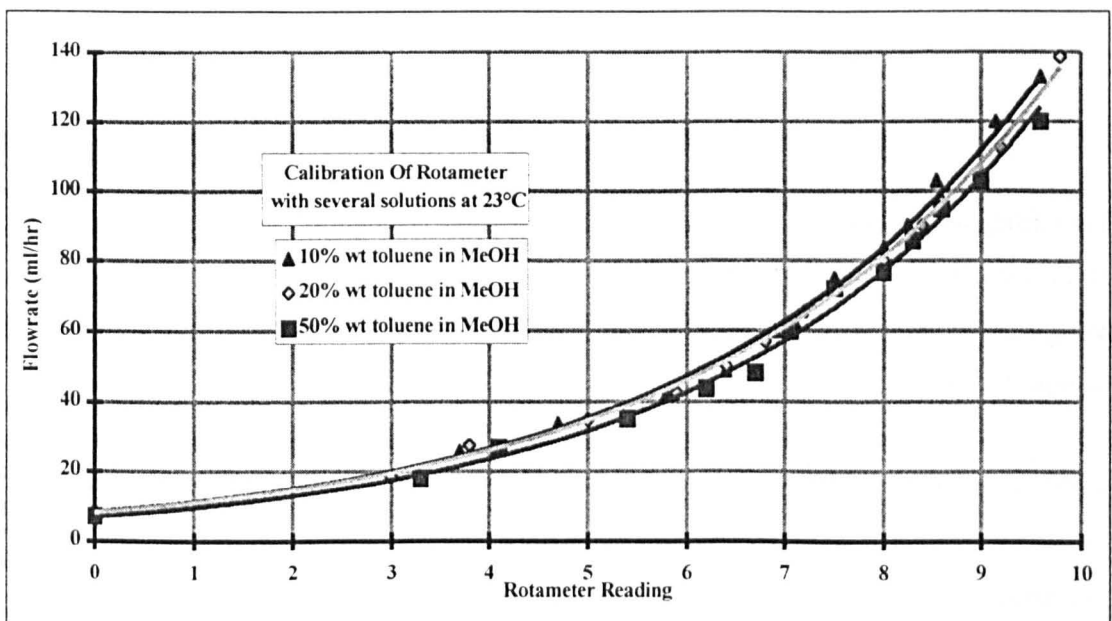


Figure 3-4: Calibration of Rotameter



The rotameter used to measure recycle flow rate was a Fischer Porter Flowrator. The tube number was FP 1/16-10-G-5/81 and a silicon float was used. This was calibrated with

several solutions of toluene in methanol, see Figure 3-4, showing that it was suitable for a range of flows from 8-130 ml/hour.

3.1.5 Experimental Procedures

3.1.5.1 *Pretreatment of Ion Exchange Membranes*

The swelling procedure adopted for pre-treatment of the ion exchange membranes was as follows:-

1. cut dry membranes to the desired size
2. weigh and measure dimensions
3. place membrane in swelling solvent at the correct temperature for desired period of time
4. remove membrane from solvent with forceps
5. remove surface liquid by drying between paper towels
6. reweigh and remeasure

The solvents were heated to the desired temperature in a beaker covered with parafilm using a magnetic stirrer-hotplate. The temperature was monitored manually using a thermometer. For more accurate control, for example during a non boiling pre-treatment, the solvent was heated using a water bath with automatic temperature control. Membranes subsequently used in electrolysis were placed directly in the appropriate reactor or stored in Millipore water.

3.1.5.2 *Electrolysis Experiments*

The procedure adopted during electrolysis experiments was basically the same regardless of power supply, or whether the operation was galvanostatic, potentiostatic or potential scan. If an SPE reactor was to be used the first task was to pretreat the membrane using the procedure described in Section 3.1.5.1. The steps in the experimental procedure followed were:-

1. Installation of the SPE - for SPE reactors the first task was to install the pre-treated ion exchange membrane. For the glass reactor the membrane was first sandwiched between the mesh electrodes before a Teflon seal was placed on either side. This membrane-electrode assembly was then fixed into the reactor and held tight by brass clamps fixed against the glass flange. Silicon rubber seals protected the flange from the brass clamp. For the steel SPE reactor the assembly was more complicated. The steel reactor was made up of several plates which were mounted on tie bolts. Installation of the SPE was

part of the reactor assembly procedure. Each plate in turn was mounted on the tie bolts starting with the anode endplate followed by the anode heating chamber, anode backplate, anode chamber, consisting of a packed bed of graphite particles and the graphite felt anode, and then the SPE. Separating each section was PTFE tape acting as sealant. The anode chamber, membrane and cathode chamber were sealed with 1mm thick Teflon gaskets. After the SPE and gasket came the graphite felt cathode and sprung steel support surrounded by the cathode chamber. Placing the cathode chamber backplate on the tie bolts compressed the membrane-electrode assembly. This was followed by the cathode heating chamber and finally the cathode endplate. This whole assembly from anode endplate to cathode endplate was held together by tightening the nuts on the tie bolts.

2. Filling the reactor - for the H-cell, rde, glass SPE reactor and batch experiments in the steel SPE reactor, filling was carried out manually to the required level. For continuous flow experiments in the steel SPE reactor filling was carried out by pumping electrolyte from the feed tank first to the catholyte chamber, allowing it to overflow to the anode chamber via the recycle loop. The feed line was then re-routed to the anode chamber ready for start up.
3. Connection of power supply - for H-cell and glass SPE reactors the connection to the supply was simply by crocodile clip direct to the electrodes. For occasions when the EG&G power supply was used without a reference electrode this lead was connected to the cathode so that the measured potential was the cell potential. For the rde experiments the cathode and reference electrodes were also connected directly. The anode (rotating) connection was through the Thompson rotating disk electrode. The connections to the steel SPE reactor were to the backplates. If used the reference electrode was connected to the luggin probe, otherwise it was connected to the cathode backplate.
4. Temperature control - the majority of experiments were carried out at room temperature. For experiments in the glass SPE reactor at more elevated temperatures the whole reactor assembly was immersed in a water bath at the desired temperature. The steel SPE reactor was heated through conduction of heat across the backplates. The heating chambers were filled with continuously recirculating hot water from a water bath with a thermostat. The reactor temperature was measured in the cathode chamber with a thermocouple. Time to reach steady state was in the order of 30 minutes for an operating temperature of 50°C.
5. Experiment control - parameters relating to the potential or current supply were controlled at the DC supply or via the M270 Echem software. These parameters included

scan rate, initial potential, final potential, current and time. Electrolyte feed was controlled at the pump manually. Reactor temperature was controlled through the water bath providing heat to the heating chambers.

6. Measurements - the EG&G software recorded all potential and current data. With the DC supply recording was done manually as was the recording of all other experimental data e.g. feed temperature, product temperature, recycle rate, membrane potential, gas volumes and temperatures. Samples were periodically taken from both anode and cathode chambers as well as the feed tank and final product. Gas product samples were also collected when experiments were conducted in the steel SPE reactor.

3.2 Chemicals

3.2.1 Purity And Supplier

Table 3-1, page 35 lists the names of chemical suppliers along with the concentrations used for the project.

3.2.2 Ion Exchange Membranes

Ten different ion exchange membranes were used during the project. Those tested were a variety of cation and anion exchange membranes, free and supported, fluorocarbon and hydrocarbon types. Table 3-3, page 36 gives details of membranes used and some of their properties.

3.2.3 Control of Substances Hazardous to Health (COSHH) Assessments

The following Risk Phrases were applied to all experiments, meaning that all had to be carried out in either a fume cupboard or some other evacuated container. Local Exhaust Ventilation was also required for the pump/feed vessel in case of major spillage.

R11:highly flammable

R21:harmful in contact with skin

R23:toxic by inhalation

R25:toxic if swallowed

R36:irritating to the eyes

R61: may cause harm to unborn child

3.3 Product Analysis

Products, by-products and reactants were analysed using several methods as described below.

3.3.1 Gas Chromatography

This was the method of analysis used most frequently in the project. The particular model used was a Perkin Elmer Autosystem oven with model 1020 integrator software. An Alltech Econo-Cap capillary column was used throughout. This was an SE-30 column of 15m length, internal diameter of 0.54mm and a film thickness of 1.2 μ m. Flame ionisation was used to detect reactants methanol and toluene, as well as products methoxytoluene, dimethoxytoluene, benzyl alcohol, benzaldehyde and benzoic acid. The program was a direct temperature rise from 50°C to 110°C over 4 minutes i.e. a ramp rate of 15°C/min. The carrier gas was nitrogen at 8psi at a flow rate of 1.3ml/min. Calibration was by external standard. In order to analyse for both reactants and products an attenuation change from 64 to 8 was made after 0.91 minutes.

3.3.2 Mass Spectrometry

Identification of unknown products took place on a Hewlett Packard GC-MS model VGTrio-1 in the Department of Environmental Medicine at the University of Newcastle upon Tyne.

3.3.3 Gas Analysis

Analysis of gases collected from the flow cell were analysed for hydrogen, oxygen, carbon monoxide and carbon dioxide using a Shimadzu GC-8A gas chromatograph. Two packed columns were installed in this machine. The first being a molecular sieve of mesh size 40-60; the second is packed with Chromosorb 101 of 80-100 mesh. Both columns were 2m long stainless steel tubes with an internal diameter of 3mm. The chromatograph was run isothermally at 40°C with helium as the carrier gas at 100kPa (30ml/min) in column 1 and at 85kPa (35ml/min) in column 2.

A Shimadzu C-R6A Chromatopac integrator was used to calculate gas composition. Adjustment of the values obtained was carried out to compensate for oxygen from the

atmosphere. This was done on the basis of the nitrogen content, since no nitrogen containing species were present in the reaction mix.

Table 3-1: List of Electrode Suppliers

Material	Form	Supplier
CoMn_2O_x	mesh 50	University of Dörtmund
copper	mesh 50	W. Pattersons
graphite felt	5-10mm felt	SGL Carbon
lead	wire	Aldrich
MnO_2	mesh 50	University of Dörtmund
nickel	mesh 26	Philip Cornes
nickel	foam	Electrosynthesis Co.
palladium	mesh 26	electrochemical deposition
PbO_2	coating on SPE or rde	chemical or electrodeposition
platinum	mesh 50	Aldrich
stainless steel	mesh 45	W. Pattersons

Table 3-2: List of Chemical Suppliers

Name	Purity	Supplier
α,α -dimethoxytoluene	99%	Sigma-Aldrich Chemical Co.
α -methoxytoluene	99%	Fischer Scientific UK
ammonium hydroxide	30% NH_3 in water, 99%	Sigma-Aldrich Chemical Co.
benzaldehyde	99+%	Sigma-Aldrich Chemical Co.
benzoic acid	99.5%	Sigma-Aldrich Chemical Co.
benzyl alcohol	99+%	Sigma-Aldrich Chemical Co.
dimethylformamide	99.9+%	Sigma-Aldrich Chemical Co.
methanol	99.9+%	Sigma-Aldrich Chemical Co.
nitric acid	63%	Fisher Scientific UK
potassium chloride	99+%	Sigma-Aldrich Chemical Co.
sulphuric acid	98%	Fisons Scientific Equipment
toluene	99.5%	Sigma-Aldrich Chemical Co.
Millipore water	resistivity>10M Ω cm	Millipore Milli U10

Table 3-3: Summary of Ion Exchange Membranes

Type	Manufacturer	Name	Structure	IEC* (Meq/g)	Backing
cationic	Du Pont	Nafion® 117	perfluorinated sulphonic acid	0.9	-
	Tokuyama Soda	Neosepta C66-10F	strongly acidic, Na ⁺ form	1.7-2.2	poly-vinyl- chloride
		Neosepta CMX-5B	strongly acidic, Na ⁺ form	1.5-1.8	poly-vinyl- chloride
		Neosepta CMB			polyethylene
	Solvay	CRA	sulphonic acid fluorinated film	1.4-2.2	-
		CSP	sulphonic acid fluorinated film	2.6-3.1	-
		CDS	sulphonic acid fluorinated film	1.7-2.2	-
	Solvay	ARA	vinyl pyridine fluorinated film	0.9-1.3	-
		ADP		0.8-1.2	-
anionic	Ionac	MA3475		1.4	Tergal

* ion exchange capacity

4. ROTATING DISK ELECTRODE

4.1 Introduction

The initial investigations for the oxidation of toluene took place on the rotating disk electrode (rde) in order to identify a number of kinetic parameters. It was hoped that this would go some way towards understanding the reaction mechanisms. This was followed by some electrolysis in various electrolytes in order to generate products in sufficient quantity to analyse in the gas chromatograph.

The undivided cell described in Chapter 3 was used as the flask for these experiments. A lead dioxide film was obtained on the rotating disk electrode (using the method of Clarke et al^[52]) by oxidising a lead anode at 2V vs SCE for 30 minutes followed by 30 minutes at 2.5V vs SCE. The rde had an outside diameter of 1.3cm and an active electrode area of 0.283cm². This ensured no further change in current at constant potential over the range of study. The counter electrode was a 4cm² lead sheet. Base electrolyte was 1M H₂SO₄ prepared from 98% H₂SO₄ and Millipore water. Sufficient volume of electrolyte ensured the active area was at least 3cm below the liquid surface. Rotation speeds ranged from 100rpm to 800rpm ensuring the flow regime was well within the laminar region, and that the critical flow rate was not exceeded. Concentrations of toluene in base electrolyte ranged from 0 to 9.39mol/m³, the approximate saturation concentration of toluene in 1M H₂SO₄. Linear sweep voltammetry scans were carried out over the range of 1.4 to 1.8V vs SCE at scan rates of 1mV/s. The resulting current densities were low enough to ensure that toluene concentrations remained within 95% of the initial concentration.

4.2 Linear Sweep Voltammetry

First, a series of scans were made only on the base electrolyte at rotation speeds of 10.5, 20.9, 41.8 and 83.8rad/s. The results of these scans show very little effect of rotation speed on current density, see Figure 4-1. Next, a series of experiments were made in which toluene mixed with sulphuric acid was used as the electrolyte. These experiments used the same rotating disk electrode system and followed the same electrode preparation as described by Clarke et al^[52]. These experiments can be divided into two. The first concerned the effect of toluene concentration and so several different amounts of toluene were

dispersed in the sulphuric acid giving a range of concentrations from 0.6 to 9.39 mol/m³. These experiments took place with an electrode rotation speed of 10.4 rad/s. The second involved only the 9.39 mol/m³ concentration of toluene, but rotation speeds from 10.5 to 84 rad/s.

Figure 4-1: Background Scans

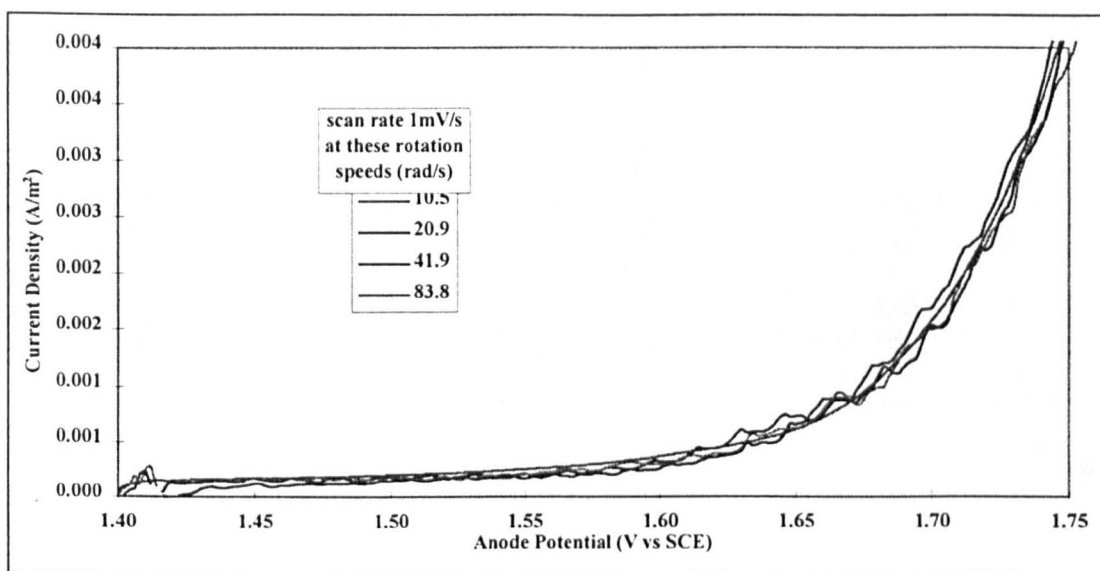
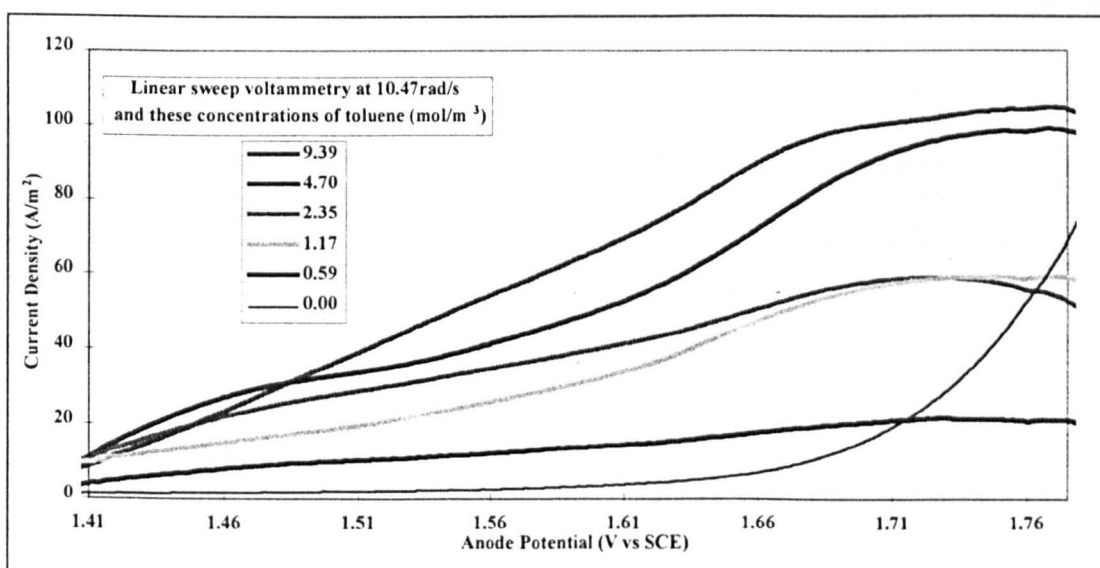


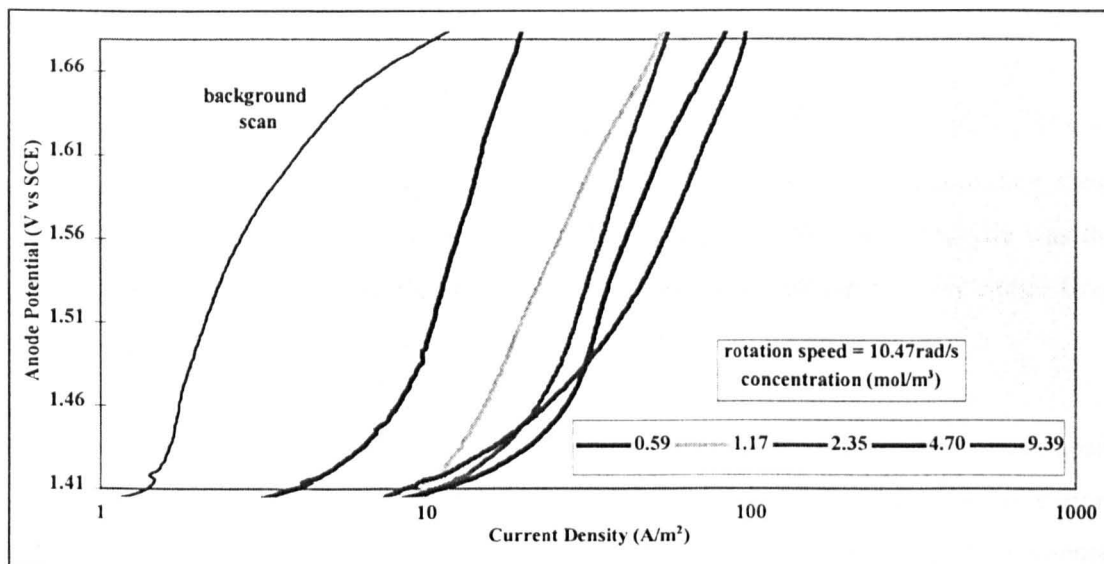
Figure 4-2: Linear Sweep Voltammogram For Toluene in Sulphuric Acid



The results are shown in Figure 4-2, Figure 4-3 and Figure 4-4. In Figure 4-2 the axes are plotted normally, whereas in the other two figures they are plotted in the Tafel representation i.e. $\log\{\text{current density}\}$ versus potential. Figure 4-2 shows that toluene affects the scan, and that its effect is increased with increasing concentration. At higher

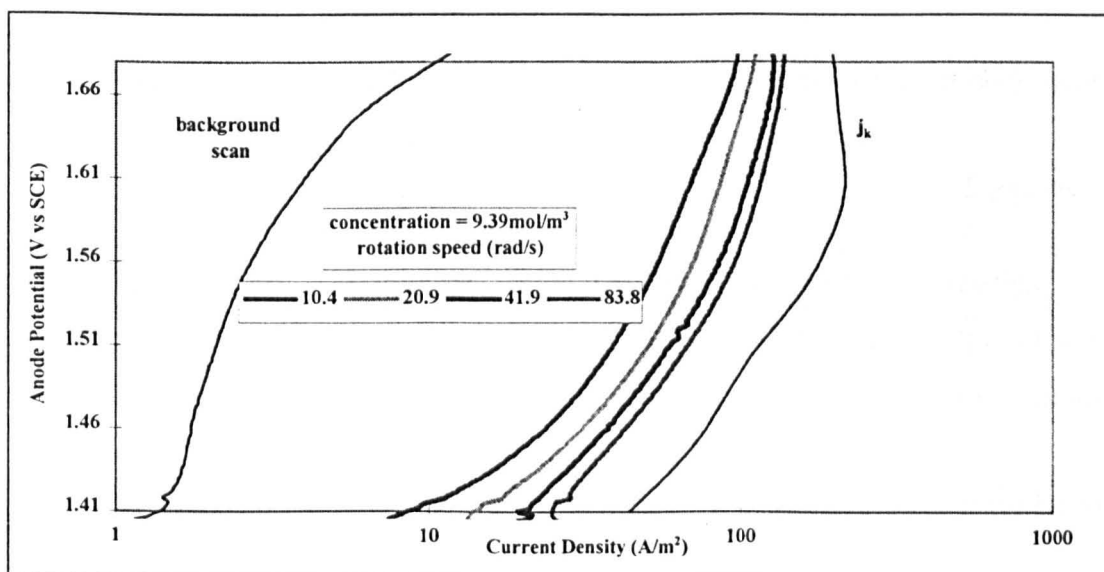
anode potentials, from 1.7 to 1.77V vs SCE a limiting current is noticed. After these potentials gas evolution becomes dominant, shown by a rise in the scan with no toluene (the background scan), and the current density noticed with toluene falls.

Figure 4-3: Linear Sweep Voltamogram With Various Concentrations



Similar results are noticed with the experiments at fixed concentration and various rotation speeds. As the speed increases the size of the response increases although the size of the current density increase produced on changing the rotation speed is not as large as the change seen with a change in concentration.

Figure 4-4: Linear Sweep Voltamogram At Various Rotation Speeds



Data from Figure 4-2 and Figure 4-2 have been fitted to the Tafel equation to obtain exchange current densities and transfer coefficients. Rearranging the well known Tafel equation

$$j = j_o \cdot \exp[-\beta \cdot n \cdot f \cdot \eta] \quad \text{Equation 4-1}$$

to

$$\eta = \frac{1}{\beta \cdot n \cdot f} \ln[j_o] - \frac{1}{\beta \cdot n \cdot f} \ln[j] \quad \text{Equation 4-2}$$

and fitting this to the linear portion of the scans, in the potential range greater than 1.51V vs SCE, gives the transfer coefficient in the range of 0.023 to 0.034. In calculating these constants the value of n was chosen as 4 using the assumption that benzaldehyde was the product of oxidation. The corresponding values of exchange current density range from 6.15×10^{-3} to $1.51 \times 10^{-1} \text{ A/m}^2$.

These values show a wide variation which would normally indicate a different mechanism for the reactions under differing concentrations. However, in this case the variation is more likely to indicate that the oxidation of toluene is not a model system. Large experimental errors are also likely to be introduced because of the low concentrations of toluene being used close to its solubility limit in water. Fitting Tafel slopes to 'straight curves' from experimental data also introduces subjective decisions. Despite the inaccuracies in this experimental method the values of Tafel constants are in the same order of magnitude as Clarke's results, see section 4.6.

4.3 Mass Transfer Limiting Current Density

For an irreversible reaction such as the oxidation of toluene the mass transfer limiting current density j_d can be written as:-

$$j_d = \frac{n \cdot F \cdot C_b \cdot D}{\delta} = n \cdot F \cdot k_L C_b \quad \text{Equation 4-3}$$

where δ is the diffusion layer thickness. Under laminar flow conditions δ is given by:-

$$\delta = 1.61 D^{1/2} \nu^{1/2} \omega^{-1/2} \quad \text{Equation 4-4}$$

Combining Equation 4-3 and Equation 4-4 gives the mass transfer limiting current density in terms of the speed of rotation:-

$$j_d = 0.62 n F D^{1/2} \nu^{-1/2} \omega^{1/2} C_b \quad \text{Equation 4-5}$$

or more simply

$$j_d = B\omega^{1/2}C_b$$

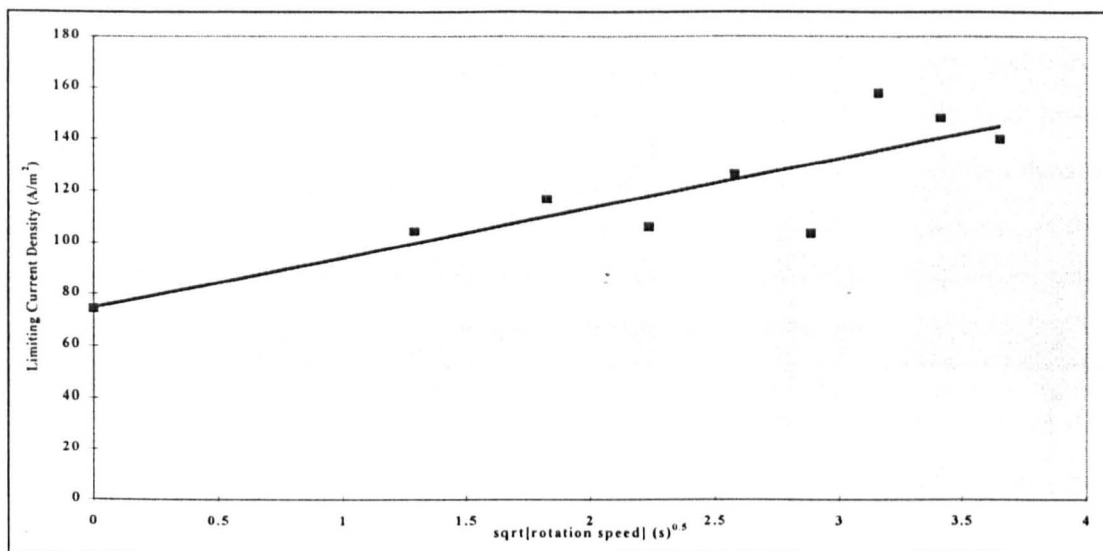
Equation 4-6

where

$$B = 0.62n.F.D^{2/3}\nu^{-1/6}$$

Equation 4-7

Figure 4-5: Limiting Current Density



Hence, the mass transfer limiting current density can be plotted against the rotation speed to give a straight line through the origin. The gradient gives the diffusion coefficient if all other variables are known. This plot is shown in

Figure 4-5 and shows a straight line passing through the ordinate at a large positive value. This indicates the reaction exhibits mixed control over the regions chosen so no further data can be extracted from this Figure. However, the diffusion coefficient can be calculated using the mixed control Levich equation, see Section 4.4.

4.4 Diffusion Coefficient

The value of the diffusion coefficient can be found by separating the kinetic and mass transfer current densities. The overall current density j is made up of the kinetic current density j_k and the mass transfer limiting current density j_d according to the mixed control Levich Equation:-

$$\frac{1}{j} = \frac{1}{j_k} + \frac{1}{j_d}$$

Equation 4-8

j_d is defined by Equation 4-5 and for a first order irreversible reaction j_k can be defined as:-

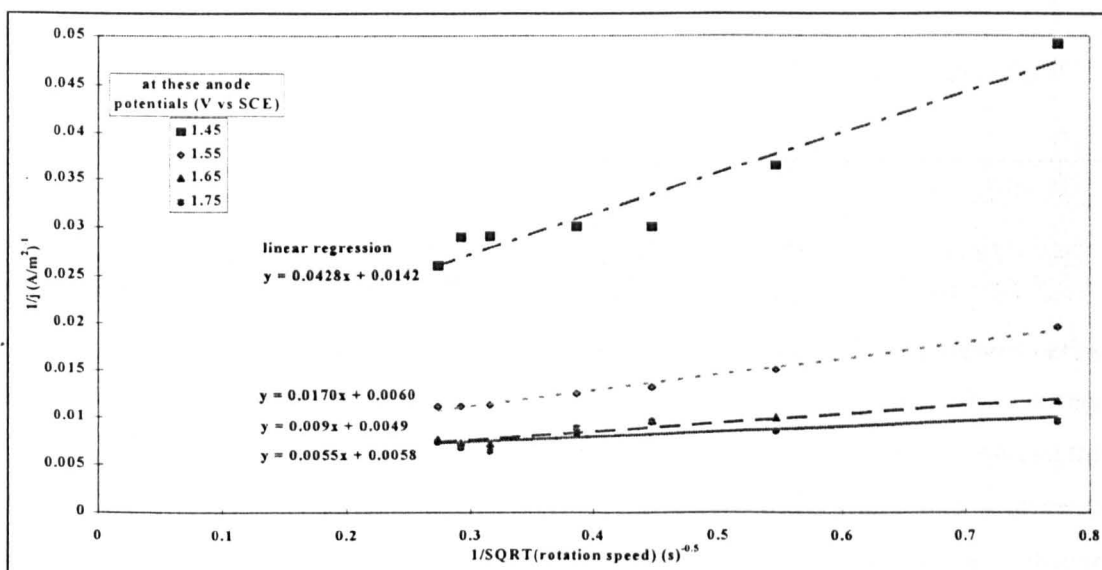
$$j_k = n.F.k_f.C_s$$

Equation 4-9

So by plotting $1/j$ against $1/\omega^{1/2}$ the diffusion coefficient can be found from the gradient, and the intercept should give j_k . This is shown in Figure 4-6.

The diffusion coefficients calculated from this figure range from 1.1×10^{-9} m/s for 1.45V to 23×10^{-9} m/s for 1.75V. The corresponding values of j_k are 70.4 and 172 A/m^2 , respectively. These values of j_k can be plotted against the anode potential to form a polarisation curve and compared with experiment. This is shown in Figure 4-4, page 38. The polarisation curve resembles closely the shape of the experimental data although it is shifted to lower potentials as expected. The transfer coefficient for it is 0.054 and exchange current density $3.1 \times 10^{-8} \text{ A/m}^2$.

Figure 4-6: Determination Of Diffusion Coefficient



4.5 Order Of Reaction And Rate Constant

The order of reaction and rate constant can also be calculated from data obtained using the rde. To carry this out the mass transfer limiting current density is required at several potentials. Due to the mixed control nature of this reaction the simpler change in concentration effect was used to determine the order. This is shown in Figure 4-7 and the order was determined directly from the gradient as 0.57 .

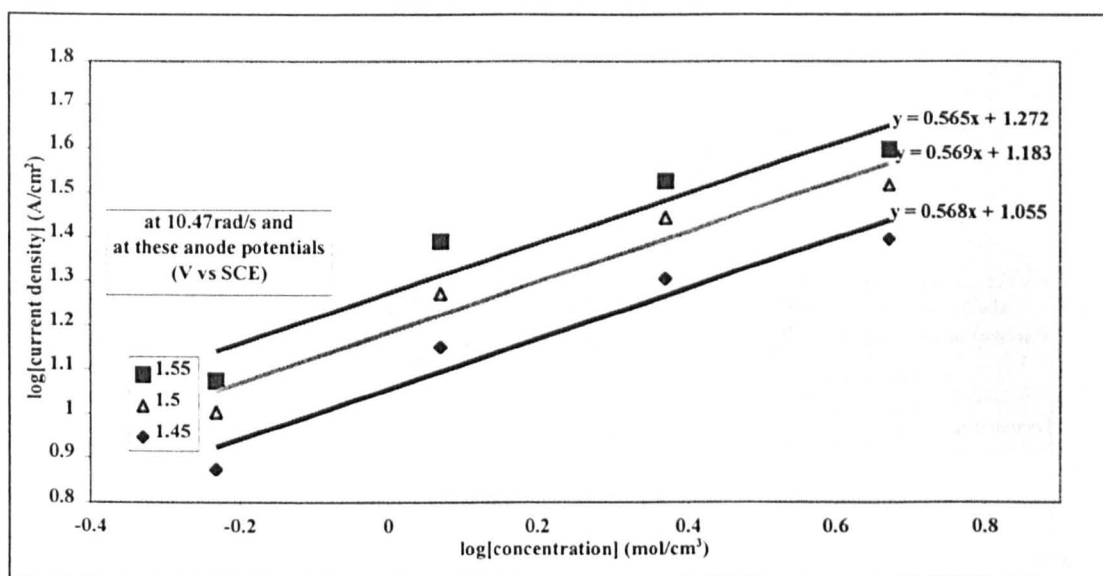
Values of the rate constant k_f can also be calculated from the intercept of Figure 4-7. This can be derived from Equation 4-10:-

$$\log[j] = p \cdot \log[C_b] + \log[n \cdot F \cdot k_f]$$

Equation 4-10

Again this is strictly only applicable in the absence of mass transfer. Values calculated ranged from 2.9×10^{-5} to $4.9 \times 10^{-5} \text{ mol}^{-0.5} \text{ m}^{-0.5} \text{ s}^{-1}$.

Figure 4-7: Effect Of Concentration



4.6 Comparison With The Literature

The work carried out by Clarke et al^[52] is compared with this work in the two figures below and the results are summarised in Table 4-1. In Figure 4-8 polarisation curves show a very similar pattern with transfer coefficients from Clarke^[52] ranging from 0.033 to 0.046 and the exchange current density ranging from 1.2×10^{-5} to $1.43 \times 10^{-4} \text{ A/m}^2$. These values compare well with the results reported for this project, but again the variation indicates a large degree of experimental error.

Figure 4-9 compares the results of the concentration dependency. For data recorded at similar electrode potentials Clarke's experiments^[52] gave an order of reaction more than twice that calculated for these experiments, 1.39 compared with 0.57. The only major difference in experimental technique was Clarke's larger electrode (outer diameter 2.4cm, active area 1 cm^2). The discrepancy in order is thought to be due to the miscibility of toluene in sulphuric acid. The results from this work fit well to a linear regression, but the first two points at both potentials can be seen to give a larger gradient than the linear regression chosen. This would give a closer order of reaction to Clarke's results^[52]. However, in this project higher current densities were achieved with concentrations much lower than was used by Clarke et al^[52]. Clarke's data^[52] give a linear fit with less deviation and this may be

due to higher rotation speeds improving mixing, or due to higher temperatures. Unfortunately the rotation speed, temperature and scan rate for Clarke's experiments^[52] were not reported.

Figure 4-8: Tafel Comparison

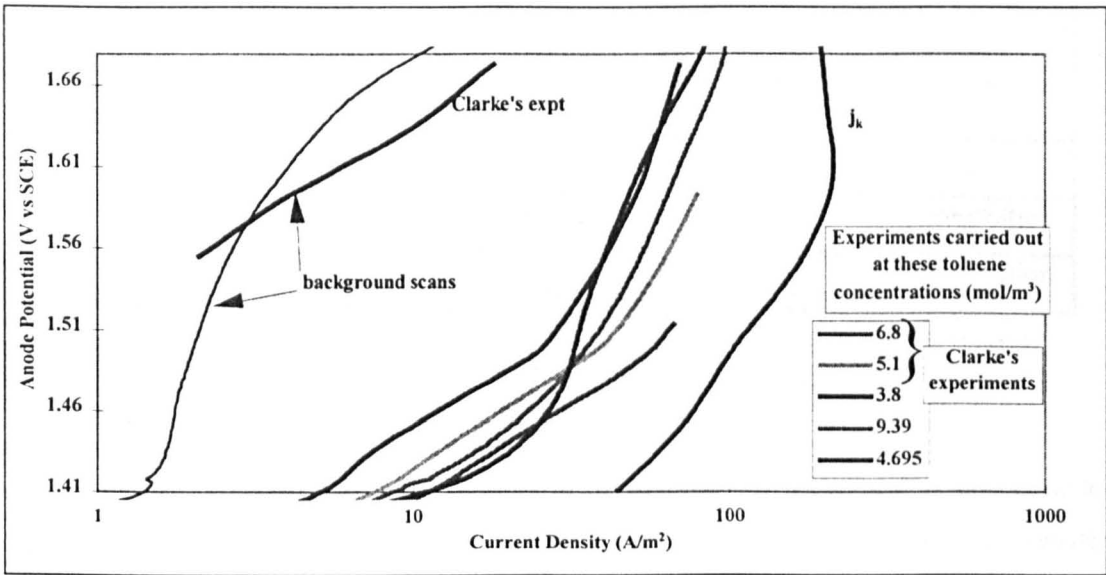


Figure 4-9: Concentration Dependence Comparison

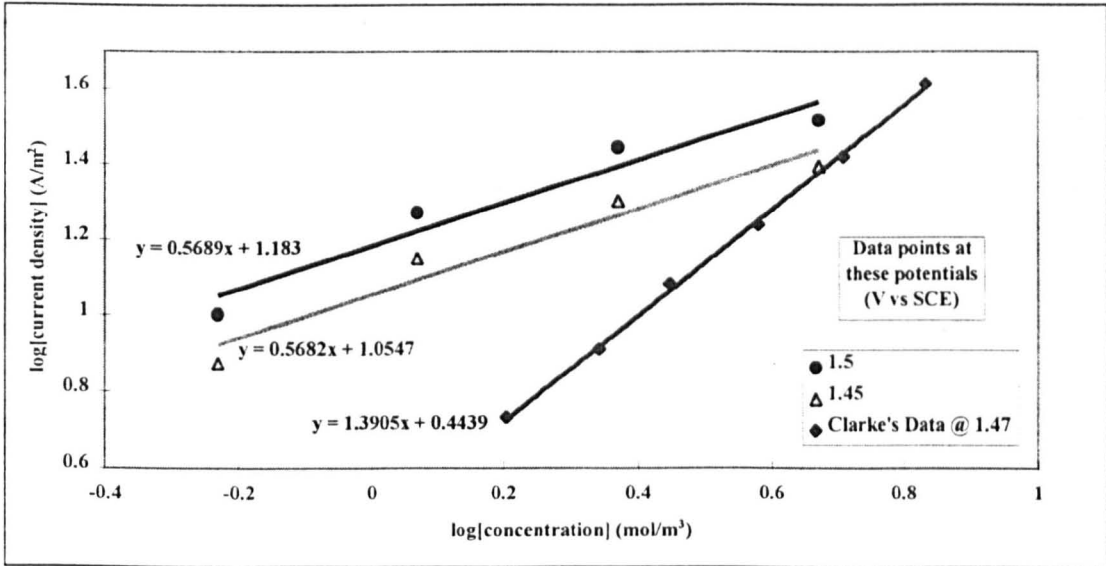


Table 4-1: Summary of Data from Kinetic Investigations

Property	This Project		Clarke's Experiments ^[52]	Method
	maximum	minimum		
β	0.034	0.023	0.033-0.046	Tafel plot
	0.054	0.054		j_k
j_o (A/m ²)	1.51×10^{-1}	6.15×10^{-3}	$0.12-1.43 \times 10^{-4}$	Tafel plot
	3.1×10^{-8}	3.1×10^{-8}		j_k
D (m ² /s)	4.2×10^{-9}	1.1×10^{-9}		1/j
p	0.569	0.565	1.39	concentration
k_f (mol ^{-0.5} m ^{-0.5} s ⁻¹)	4.9×10^{-5}	2.9×10^{-5}	9.3×10^{-3}	concentration

4.7 Conclusions

These results show that oxidation of toluene in aqueous sulphuric acid is not a model system. However it may be said that the system exhibits mixed kinetic and mass transfer control. The range of potential in which kinetics limit the rate is small and this is due to the low miscibility of toluene in aqueous solvents. Normally the addition of co-solvent increases the solubility and is the usual method for solving these problems. These are discussed in Chapter 5: Emulsion Electrolysis.

5. EMULSION ELECTROLYSIS

5.1 Introduction

This Chapter reports on the experiments carried out in order to determine some optimum conditions for the oxidation of toluene. The basis of the experiments were Mann's experiments^[51] carried out in the early 1920s. In his experiments a platinum anode was used to oxidise toluene in a solution of base electrolyte and co-solvent. The base electrolytes used were 1M H₂SO₄ or 4M HNO₃. Various co-solvents were tested and Mann's conclusions^[51] were that a mixture of nitric acid and acetic acid were the best combinations. Under these conditions a maximum conversion of toluene to benzaldehyde of 19.5% at 180A/m² was obtained. Here, the early experiments were validated using modern laboratory equipment. Platinum anodes were used throughout, and the effect of co-solvent and base electrolyte were quantified by considering the extent to which toluene was converted.

5.2 With Acetic Acid

In the following experiments the H-Cell was used as the reactor; the main differences between this and Mann's reactor^[51] were a glass frit to separate the two compartments, the size (90cm³ compared to 2 litres), and the use of mesh rather than sheet platinum. The reactor was divided to lower the chances of oxidation products being reduced to toluene at the cathode. Without this the current efficiency would be underestimated

The platinum mesh had an open surface area of 4cm², compared with Mann's electrodes which had an area of 68cm²; and was cleaned in concentrated nitric acid followed by washing in Millipore water. The counter electrode was of graphite. Experiments were performed galvanostatically at the values quoted in Table 5-1. Figure 5-1 and Figure 5-2 show the concentration and current efficiency profiles of benzaldehyde for the first three galvanostatic experiments over a 5-6 hour period. The first of these, EXP365, was carried out with glacial acetic acid as a co-solvent.

Figure 5-1: Concentration Profile of Benzaldehyde for Conditions Given In Table 5-1

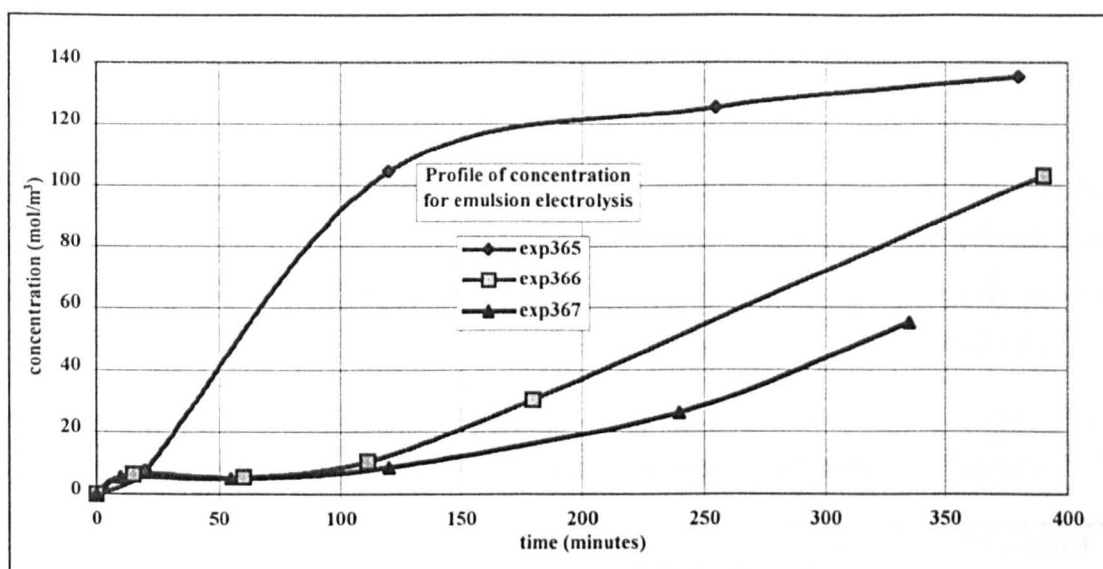
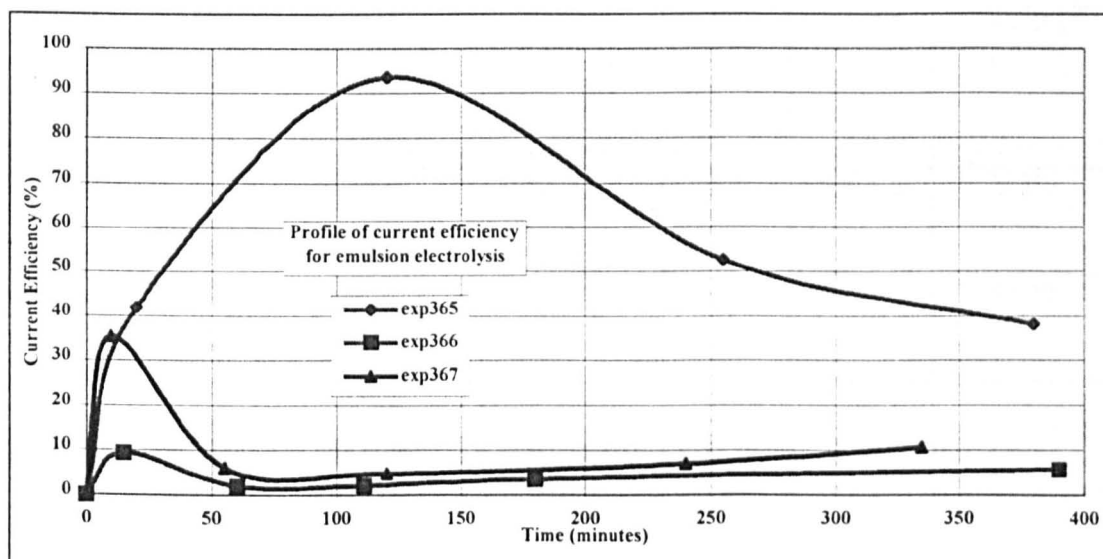


Figure 5-2: Current Efficiency Profile for Conditions Given In Table 5-1



The initial experiment used the same ratio of reactants as Mann's^[51] most successful experiments (as shown in Table 5-1), but the current density was increased by a factor of 4. The final current efficiency, with respect to benzaldehyde production, of this experiment was twice that reported by Mann, probably due to the separator preventing reduction of product back to toluene. As can be seen in Figure 5-1 the current efficiency goes through a maximum of 93.4% and then falls which may be due to the conversion of toluene reducing the amount available for further reaction. Gas evolution was noticed throughout all the experiments and was assumed to be the major reason for loss of current efficiency.

Using the diffusion coefficient calculated in Chapter 4 the mass transfer limiting current density was calculated using the correlation of Mizushima et al^[75] for forced convection in agitated vessels. These were at least twenty times greater than the applied current density for this experiment. This only applied initially since as the reaction progressed the concentration of toluene fell, so the mass transfer limiting current density also fell. The applied current density would only become mass transfer limiting after 380 minutes if the toluene concentration reached 4% of its initial concentration and this would only occur if, overall, the number of electrons per converted toluene molecule (n) was less than 1.58.

Table 5-1: Emulsion Electrolysis Summary on Platinum

Experiment Reference Number	Electrolyte Composition	Catholyte	Current Density (A/m^2)	Cell Potential (V)	Maximum Current Efficiency
EXP365	5ml toluene 40ml 4M HNO ₃ 5ml acetic acid	4M HNO ₃	750	5.1-7.2	93.4%
EXP366	10ml toluene 40ml 4M HNO ₃	4M HNO ₃	750	5.6-5.2	9.3%
EXP367	10ml toluene 40ml 4M HNO ₃	4M HNO ₃	250	3.6-3.8	35.4%
EXP368	10ml toluene 40ml 4M HNO ₃	4M HNO ₃	50	2.9	-
EXP369	10ml toluene 40ml 1M Na ₂ SO ₄	1M Na ₂ SO ₄	375	8.8	-
EXP370	10ml toluene 40ml 2M Na ₂ SO ₄	2M Na ₂ SO ₄	375	9.2-7.9	-
EXP371	10ml toluene 40ml 1M H ₂ SO ₄	1M H ₂ SO ₄	750	4.2	-

The most evident side reaction causing loss of efficiency was hydrogen and oxygen evolution from the water present in the base electrolyte. Other side reactions were possible such as reaction of benzyl alcohol with acetic acid, reaction with nitric acid and oligomerisation of toluene. Figure 5-3 shows a typical chromatogram for the emulsion electrolyses, and as can be seen more than one oxidation product was isolated. The

unknown product was never identified even using GC-MS although benzoic acid, benzyl benzoate, benzyl acetate, *p*-nitrotoluene and *o*-nitrotoluene were eliminated.

5.3 The Effect of Acetic Acid Co-Solvent

The next step was to remove the co-solvent. One reason for having the co-solvent was to increase the solubility of toluene in base electrolyte, but in an SPE reactor co-solvents (and electrolytes) are unnecessary. Removing co-solvent created a 2-phase system. In order to disperse toluene in the base electrolyte vigorous stirring was employed using a magnetic stirrer. Some success was noted in the following experiment labelled EXP366. The same conditions applied as before with the exception of co-solvent. A much reduced current efficiency was noted, but some oxidation product was formed. Again using the correlation of Mizushima^[75] and the diffusion coefficients from Chapter 4, the mass transfer limiting current density was predicted at a least 47 times greater than the applied current density for the initial concentration of toluene. Mass transfer limiting current density would not be reached unless the overall electron stoichiometry was as low as 0.77 according to these predicted mass transfer coefficients. Another significant observation was the fall in formation of unknown by-product, with respect to benzaldehyde formation.

Comparing these last two experiments, (EXP365 and EXP366), shows the effect of acetic acid. Increasing the solubility allowed the toluene to diffuse evenly throughout the supporting electrolyte and in so doing gaining access to the anode where the reaction took place. Removing the co-solvent caused the aqueous electrolyte and toluene to separate. Therefore, the toluene concentration in the aqueous phase was significantly reduced. The effect of this is shown in the lower concentration of oxidation product and the much reduced current efficiency.

Mann^[51] had used a current density of 180-200A/m² so the next step was to attempt electrolysis at, or near, this rate. At 250A/m² the final current efficiency increased to 10.6% with respect to benzaldehyde, although the amount of benzaldehyde was much reduced, but the ratio of the unknown by-product to benzaldehyde fell again, as can be seen from Table 5-2.

In experiment EXP368 the current density was reduced further, (see Table 5-1) to 50A/m², to see if the trend continued. No products or by-products were detected from this

experiment. The final 3 experiments were designed to test the effect of base electrolyte. Mann^[51] had carried out some experiments on sulphuric acid and concluded that it was not a suitable electrolyte as too much condensation product was formed. In experiment EXP371 no oxidation nor by-product was formed. In a neutral sodium sulphate electrolyte the results were just as disappointing with no products or by-products detected.

Figure 5-3: Emulsion Chromatogram

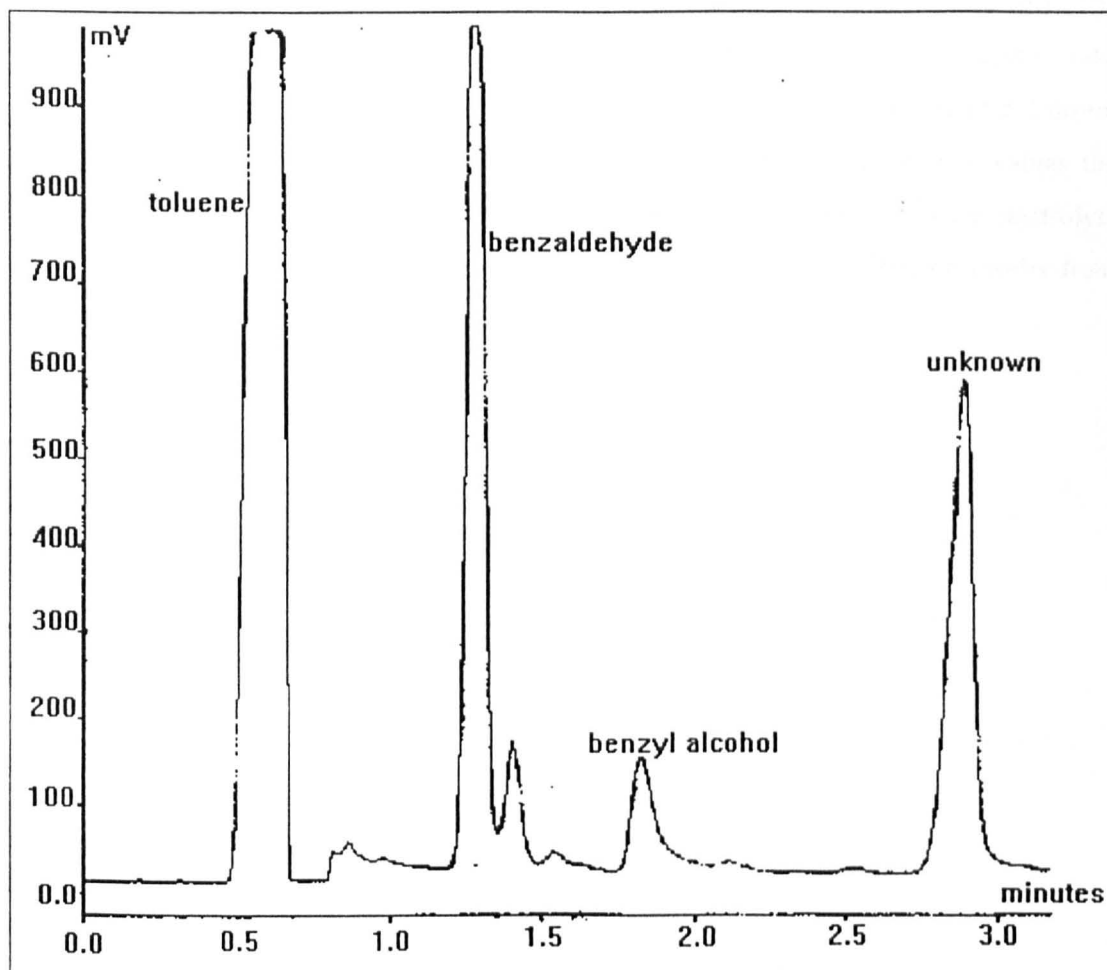


Table 5-2: By-product Ratio

Experiment Reference Number	Reaction Time (Minutes)	Benzaldehyde Peak Area	By-product Peak Area	Ratio Of Areas
EXP365	380	88.52×10^6	148×10^6	0.60
EXP366	390	419×10^6	33.6×10^6	1.25
EXP367	335	25.2×10^6	9.66×10^6	2.61

5.4 Summary

These experiments supported the findings of Mann^[51], and moved the project a step closer to oxidising toluene directly in an SPE reactor. The product of oxidation was found to be benzaldehyde and this was thought to be formed via the intermediate benzyl alcohol. No oxidation of benzaldehyde to benzoic acid was evident. It was proved that toluene could be oxidised directly without co-solvent, but that without one the current efficiency was much reduced and this was thought to be simply due to the lowering of the reactant solubility. The major side reactions were gas evolution and some unidentified low volatile compounds. Formation of these unidentified compounds was reduced after removing acetic acid. Current density was also shown to have an effect on current efficiency since at low values the desired oxidation of toluene and formation of by-product was limited. The base electrolyte was also thought to take part in the reaction since nitric acid gave differing results from sulphuric acid and sodium sulphate.

6. BATCH ELECTROLYSIS

6.1 Introduction

At this stage in the project some kinetic data had been collected regarding the oxidation of toluene on lead dioxide, and oxidation products had been formed from electrolysis in a divided reactor on platinum. The next stage was to see if an SPE reactor could be used to oxidise toluene without any co-solvent or base electrolyte. This was a step-by-step process evaluating kinetic data, membranes, electrodes and the two SPE reactors in turn. The first series of experiments took place in the glass SPE reactor.

An advantage of using solid polymer electrolytes is that liquid phase electrolytes and co-solvents need not be used. The ion exchange membranes used as solid polymer electrolytes function by allowing the transport of ions and a shell of solvent molecules. The major driving force for this transport is migration due to the high potential gradient caused by the close proximity of the two electrodes. Ion exchange membranes are either cation or anion selective (bipolar membranes are also commercially available). Membranes are not 100% selective so anions are also transported in cation exchange membranes. The property of selective transport is used in SPE electrolysis to enhance the particular reaction under study.

The mechanism of the toluene oxidation process is not known, but it is possible to consider several alternative initiation steps. For example the reaction may start by the formation of a toluene cation:-



or perhaps the first step involves hydroxide ions:-

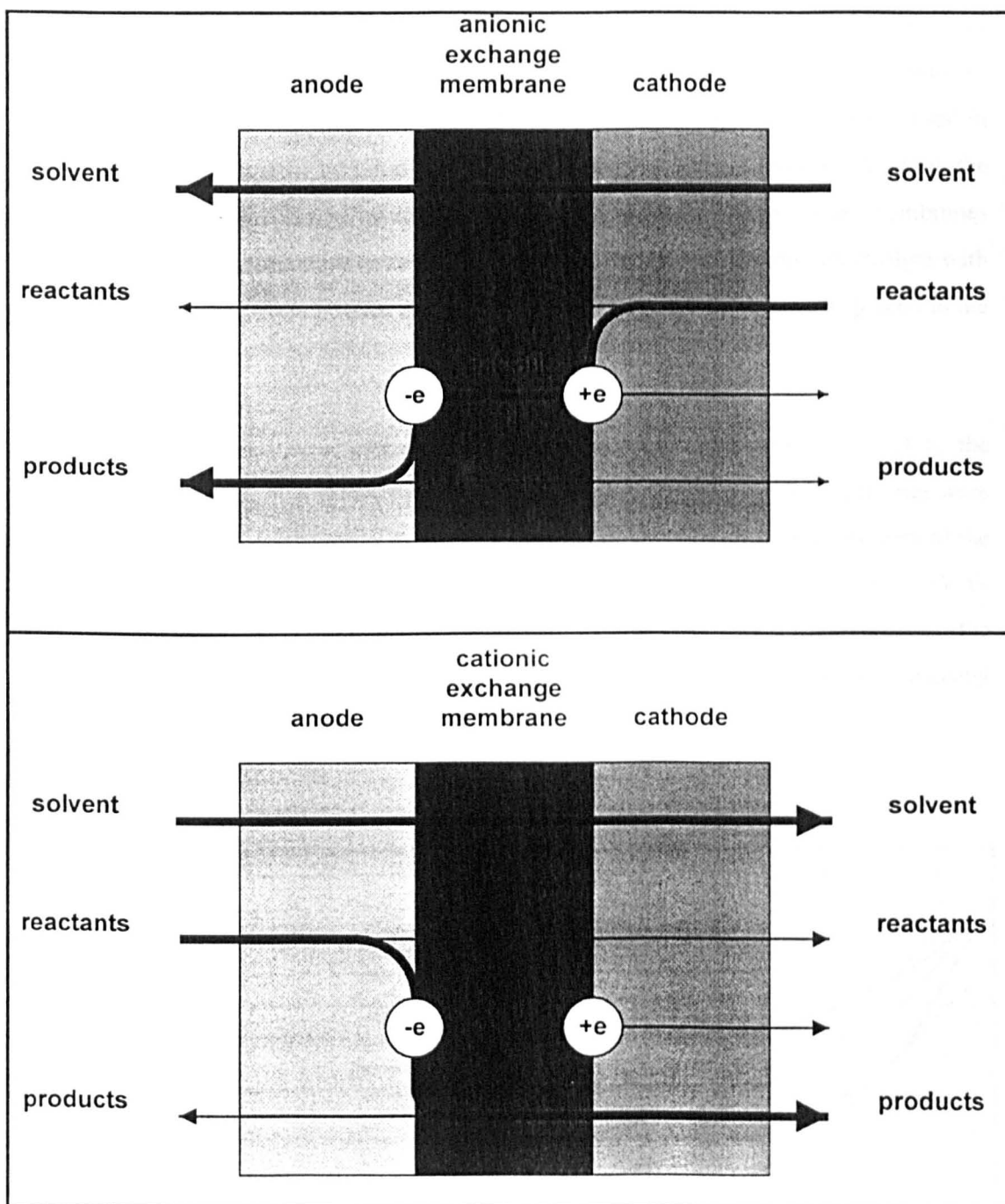


For mechanisms involving transport of hydroxide ions an anion exchange membrane would be used. For mechanisms involving transport of species such as a toluene cations or protons a cation exchange membrane would be selected. In the work reported here both types of membrane were tested in the hope that this would lead to greater understanding of the mechanism through enhancement of the transport of the reactive species.

In the following experiments only toluene was placed in the anode chamber. The cathode compartment was filled with water or other aqueous solvents. In Figure 6-1 the transport of

species when anion and cation exchange membranes are used is shown. For toluene oxidation anion exchange membrane would be used to aid the transport of hydroxide generated at the cathode from the reduction of water. Transport of anions such as nitrate from nitric acid would also be aided. Cation exchange membranes would help the transport of protons or toluene cations.

Figure 6-1: Schematics Of Transport In SPE Reactors



6.2 Glass SPE Reactor

6.2.1 Cyclic Voltammetry

Cyclic voltammetry was first to be carried out in an SPE reactor. The aim was to gain an insight into the mechanism of the reactions when toluene was oxidised in this environment. This time a platinum mesh anode was used, the counter electrode being a stainless steel mesh. Electrodes were cleaned in concentrated nitric acid, then washed in water prior to use. The active anode area was 5cm^2 . The Nafion[®] 117 cation exchange membranes used in these tests were pre-treated by simply soaking in boiling water for 30 minutes to allow the fixed ions in the membrane to be solvated. Because conducting ion exchange membranes and the zero-gap configuration were being used there was no need to mix electrolyte with toluene. Pure toluene could be used as the anolyte; the aqueous electrolyte was placed in the catholyte chamber.

First background scans were carried out and these are shown in Figure 6-2. Only the forward and reverse scan is shown for 100mV/s for clarity. The scans at the other rates were similar. These cyclic voltamograms were performed with water in both compartments of the reactor. Scan rates of 200, 100, 50 and 25mV/s were used to scan between 1 and 2.5V vs SCE. As expected the current density increased as the scan rate increased since the thickness of the diffusion layer is smaller at higher scan rates. This is due to the increasing non-steady state at higher scan rates.

Figure 6-2: Cyclic Voltamograms of the Water-Water System

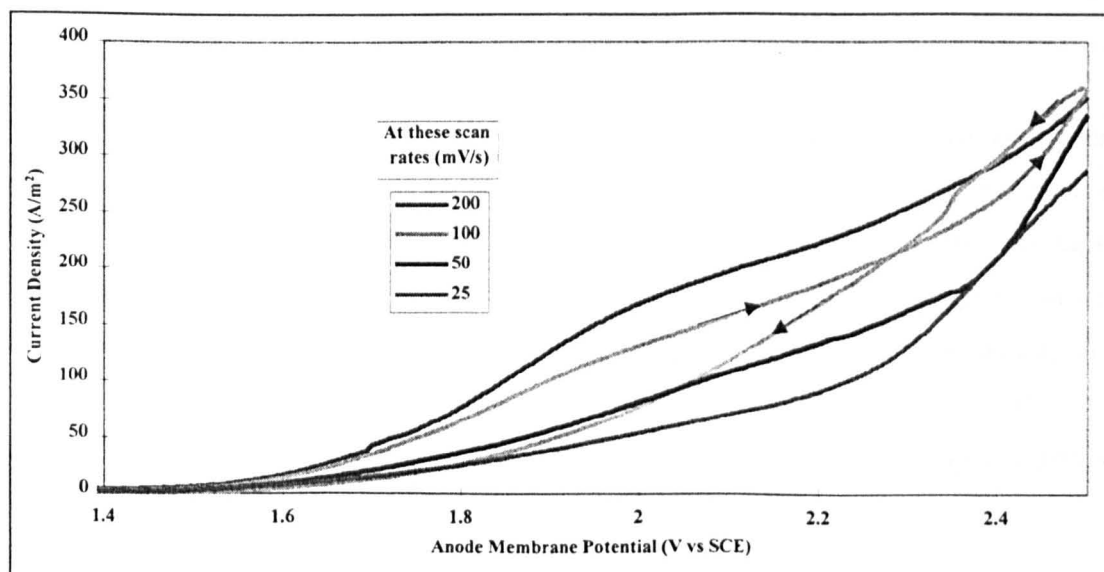


Figure 6-3: Cyclic Voltamograms of the Toluene-Water System

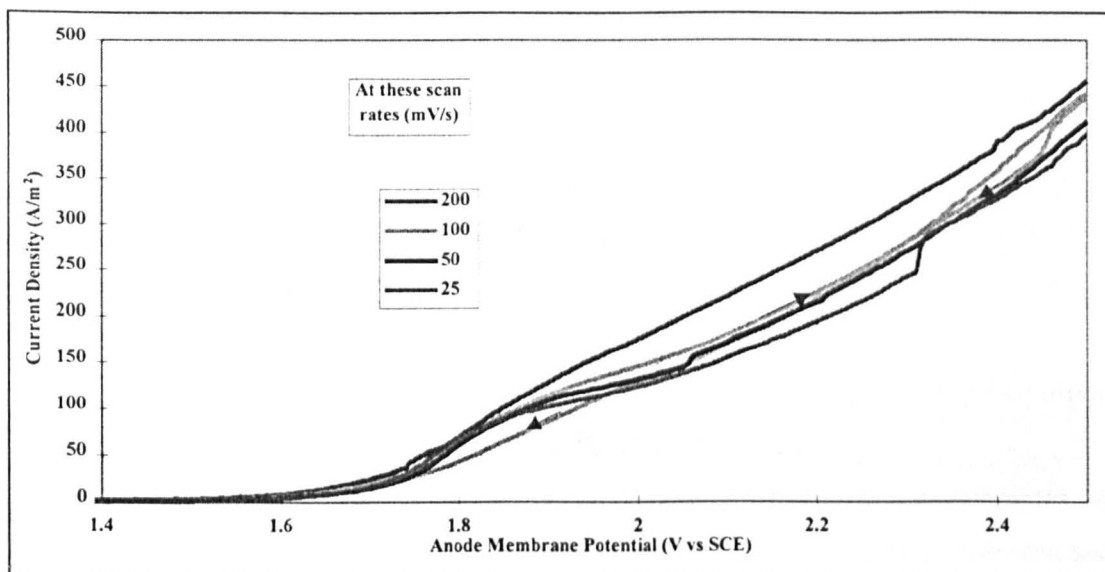
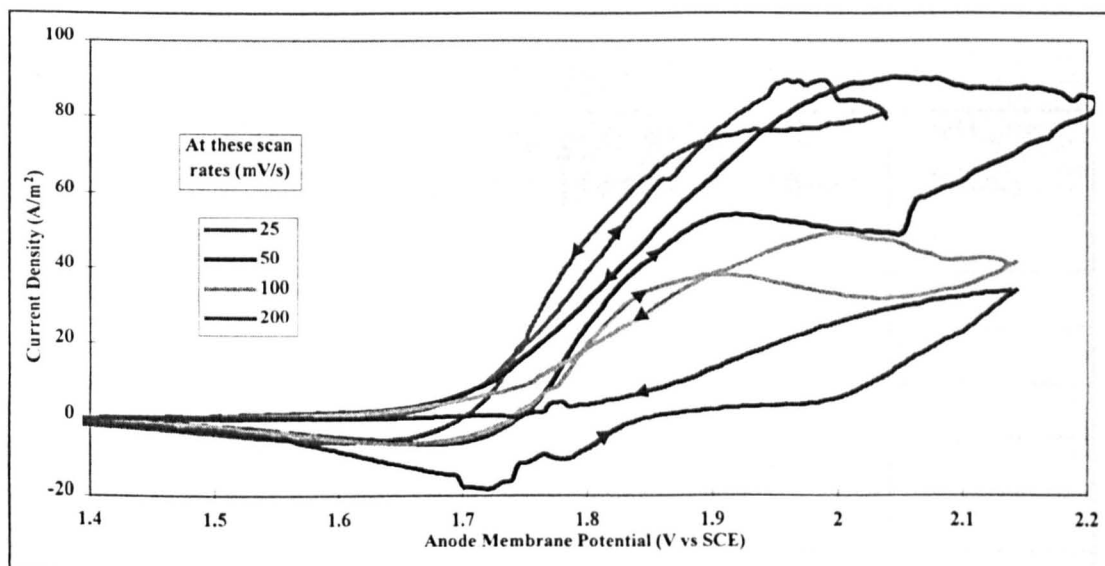


Figure 6-4: Cyclic Voltamograms Of Toluene Oxidation



These scans were repeated for experiments where pure toluene was the anolyte and water the catholyte. These are shown in Figure 6-3, and again the forward and reverse scans are only shown for 100mV/s for clarity. The results in Figure 6-2 and Figure 6-3 are very similar, with the toluene-water system producing a wave at 1.85V and slightly higher current density. This shows that toluene affected the system in some way although at this stage in the investigation no oxidation products had been identified. Theoretically, subtracting the scan of the water-water system from the toluene-water scan should give a current-potential relationship for toluene oxidation. This is shown in

Figure 6-4. Due to the similarities of the two scans to produce this figure the errors become large and dominate the result. Hence, no further data or information about the system can be extracted using this technique

6.2.2 Membrane Tests

The aim of these experiments was to:-

1. perform oxidation electrolysis in an SPE system, and
2. to gain an understanding of the mechanism of toluene oxidation by observing the current efficiencies for different combinations of membrane and catholyte

Particular attention was paid to the effect of different membranes and catholytes. A selection of ion exchange membranes were used - both anionic and cationic, reinforced and self supporting. These were pre-treated by soaking in boiling catholyte for 30 minutes, then washing in Millipore water.

Table 6-1: Membrane/ Electrolyte Test Summary on Platinum

Catholyte	Membrane	Current Density (A/m ²)	Average Cell Potential (V)	Time (hours)	Final Current Efficiency (%)
4M HNO ₃	Nafion [®] 117	380	2.5	20	0.8
	Nafion [®] 117	320	2.5	20	4.2
1M HNO ₃	ADP	360	4.0	10	1.8
	Nafion [®] 117	100	2.5	10	
0.1M HNO ₃	Nafion [®] 117	100	2.6	10	
1M H ₂ SO ₄	Nafion [®] 117	360	2.5	20	
	ARA	260	9.0	10	
	ADP	360	3.4	10	
water	Nafion [®] 117	360	3.5	10	
	ADP	360	8.4	10	
1M NH _{3(aq)}	Nafion [®] 117	360	4.5	10	
	Ionac [®] 3475	360		10	
	ADP	360	4.8	10	

The catholytes used were based on the emulsion work. Initially 4M HNO₃ was used, but successive experiments used a lower concentration. Sulphuric acid was again tested even though previous work by Mann^[51] and in here in Chapter 5 had shown this was not suitable. Neutral (water) and basic (ammonia solution) catholytes were also assessed in order that a full range of pH was tested. Again the anolyte was pure toluene. All these experiments ran for at least 10 hours galvanostatically at, normally, 360A/m². Cell potentials were found to be between 2.5V and 9.0V. Very little oxidation product was made; but as with the emulsion electrolysis the greatest amount was formed with nitric acid catholytes. The by-product isolated with the emulsion test was not evident with the SPE reactor.

Table 6-1 summarises the membrane tests. The current efficiency was based on benzaldehyde production which was much lower than in the emulsion tests. This information points to gas evolution being the major reaction and not the oxidation of toluene. This is most likely to be due to the construction of the SPE reactor preventing good contact between electrodes and membrane, or to the performance of the membranes altering the quantity and type of species being available at the anode.

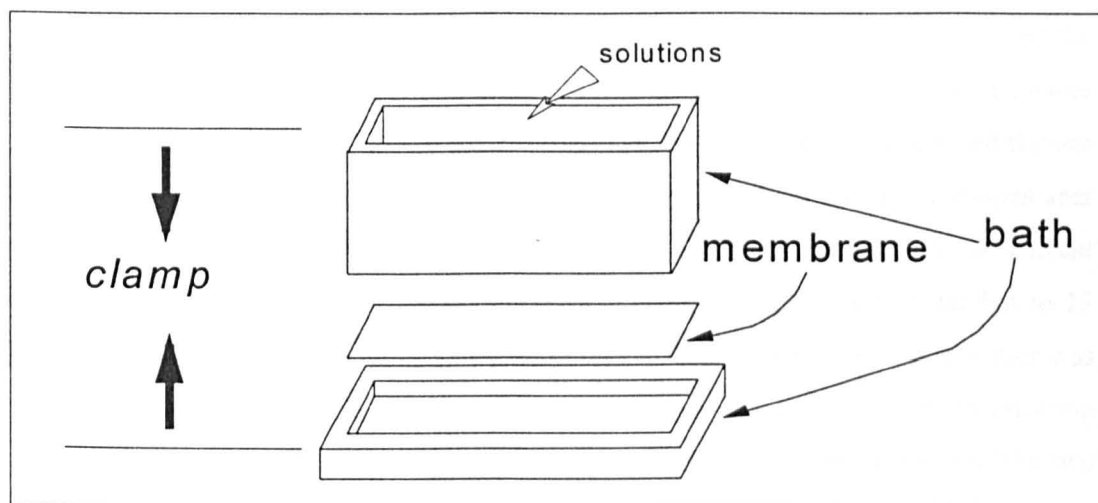
6.2.3 Electrode Tests

In the SPE system the role of the electrode material is not only to act as a current collector. The electrodes provide active sites where reactant and/or intermediate species can be converted. Different materials and identical compounds in different states contain sites of different characteristics. These characteristics determine the suitability of the material for the relevant reaction. A simple method of selecting one anode material from another is to carry out galvanostatic experiments and quantify the conversion of reactant to desired product. In this section the results of testing four alternative anodes are reported. They are lead dioxide, nickel foam, nickel mesh and MnO₂.

It is important that electrodes used in SPE reactors are porous. This allows transport of reactants and products to and from the reaction zones. One way of producing a porous electrode is to deposit a thin layer of substance on the ion exchange membrane. This is termed an Attached Porous Electrode. In this way an anode of lead dioxide was produced for use in the SPE reactor. The method used was the ion exchange method of Chen and Chou^[16]. The Nafion®117 cation exchange membrane was first soaked in boiling Millipore water for 1 hour. A rectangular bath, 7cm x 3cm, made from perspex was used to secure the

membrane during the ion exchange process, see Figure 6-5. The membrane was left to soak in 0.1M $\text{Pb}(\text{NO}_3)_2$ for 2 hours at 60°C. After this it was washed in Millipore water before 5ml of reducing agent (0.4wt% NaBH_4) was added. A layer of metal ions were deposited on the surface of the membrane which were subsequently oxidised to lead dioxide with NaOCl .

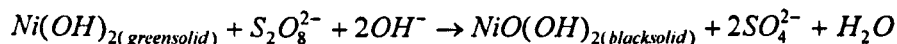
Figure 6-5: Deposition Bath



Two stainless steel mesh electrodes were placed, one on either side of the membrane-electrode assembly to act as current collectors. This sandwich was clamped in place in the glass SPE reactor. Toluene was again the anolyte and Millipore water the catholyte. In this way electrolysis took place for 6 hours at 1800A/m^2 , the anode potential being steady at 0.4V vs SCE. Analysis of samples taken from the anode chamber during the period of galvanostatic operation showed no oxidation products. Hence, it is thought that oxygen evolution was the main reaction taking place.

Several successful investigations of direct electro-oxidation of alcohols, and in particular benzyl alcohol electro-oxidation, have taken place on nickel based anodes (Do & Chou^[65], Cognet et al^[66], Hwang et al^[67]). It was because of this that nickel foam and nickel mesh were used as anodes in the SPE reactor. In order to reduce the expected deterioration of the anodes due to low pH at the electrode-membrane interface an anionic exchange membrane was used. It was hoped that this would increase the selective transfer of hydroxide (generated at the cathode) through the membrane. The first to be tested was nickel foam. Electrolysis took place at 100A/m^2 for 10 hours. At the end of this time gc analysis showed that a significant proportion of toluene had been oxidised to benzaldehyde. The final current efficiency for this experiment was 52.4%. Also evident were insoluble pale green particles

located on the nickel foam. Following chemical analysis with alkaline sodium persulphate these were identified as nickel hydroxide.



The main problem associated with the nickel foam was its brittle nature. To ensure good contact between anode and membrane a large force was necessary. This force caused the foam to crumble. This, together with the chemical deterioration made foam an unsuitable anode material. As a substitute nickel mesh was tested. This was much stronger and thinner so was much less likely to break under compression. The mesh used had a larger open area than that of the foam and of the platinum mesh used earlier. Because of this the current density was reduced to 40A/m², but the duration of the experiments were extended to 15 hours. Even so no oxidation product was formed, but the same type of insoluble matter was found on the mesh surface. Poor anode-membrane contact and the possibility of differing oxidation states were thought to be the reason for the difference in performance of the two types of nickel.

A low current efficiency was also recorded with an MnO₂ coated titanium dioxide electrode. This time the current density was 50A/m², and the temperature of operation was also increased to 75°C. Benzaldehyde was the only detected product, produced at a final current efficiency of 3%.

6.2.4 Oxidation Of Benzyl Alcohol

Before work proceeded on the steel SPE reactor some investigation was undertaken regarding other oxidations. The work of Do & Chou^[65], Cognet et al^[66] and Hwang et al^[67] had instigated the investigation of nickel. This work was extended to cover the oxidation of benzyl alcohol. Three different anodes were tested - nickel foam, nickel mesh and platinum mesh. A current density of 10A/m² was used and oxidation lasted at least 2 hours. With nickel foam oxidation was extended to 10 hours. Membranes used were pre-treated in boiling water. With nickel foam Ionac[®]MA3475 anion exchange membrane was used; the other experiments took place with Nafion[®]117 cation exchange membrane. No products or by-products were detected with platinum or nickel mesh. However, with nickel foam the highest conversion of reactant took place. A final current efficiency of 85.4% was recorded for benzaldehyde production, thought to take place according to Equation 6-3. Some toluene

was also produced which was thought to be due to disproportionation of benzyl alcohol according to Equation 6-4:-



Oxidation of the anode was also evident; again this was confirmed as $Ni(OH)_2$. These results indicated that nickel foam was a good electro-catalyst for the oxidation of both toluene and benzyl alcohol. Unfortunately its deterioration made it unsuitable for use in the SPE reactor. Another important find was that the oxidation of benzyl alcohol took place with higher current efficiency suggesting that the step from toluene to benzyl alcohol was the more difficult one.

6.3 Steel SPE Reactor

The steel SPE reactor was commissioned because it offered advantages over the glass SPE reactor. These advantages related to the sealing of the membrane-electrode assembly and the membrane electrode contact. Because a steel frame was used higher pressure could be applied to the gaskets thus reducing the potential for leaks. A steel mesh with a sprung backing was used as a current collector on both sides of the membrane which increased the pressure applied to the electrodes. It was hoped this would increase the area of the electrodes in contact with the membrane. The steel SPE reactor also had the advantage of using a range of operating temperatures. Until now all experiments, (except those with MnO_2), had been carried out at ambient conditions. The temperatures used in the following batch experiments in the steel SPE reactor were conducted at 70°C in the hope that this would improve the kinetics of the oxidation process. Also the experience of Gerl^[1] had shown that higher temperatures reduced cell voltages

6.3.1 Electrode Tests

The steel reactor allowed a larger electrode to be used. The size used in these experiments was 7cm x 3cm, compared with the circular electrodes of 5cm² used in the glass reactor. Pure toluene was again used as the anolyte and Millipore water as the catholyte. Table 6-2 summarises the experiments carried out with a range of anodes.

Several values in Table 6-2 are worth noting. Nickel mesh gave a similar performance as in the glass SPE reactor. It was felt that foam would be too brittle for the higher compression

in the steel SPE reactor so was not used. The graphite felt gave the highest conversion of all the SPE experiments so far, except nickel foam. This was probably due to its compressible nature allowing a much greater and more even contact area between anode and membrane. Being felt it was also less likely to cause puncturing of the membranes which often occurred with the metallic electrodes. Some success was noted with platinum mesh although this was still well below that achieved in the emulsion experiments.

Table 6-2: Steel SPE Electrode Test Summary

Experiment Number	Anode Material	Membrane Type	Current Density (A/m ²)	E _{AM} (V vs SCE)	Duration (mins)	Final Current Efficiency (%)
EXP412	Ni mesh	Ionac® 3475	23.8	2.3	300	-
EXP427	graphite felt	Nafion® 117	11	1.6	180	20.3
EXP429	Pt mesh	Nafion® 117	450	4.4	120	4.3
EXP441	Pd mesh	Nafion® 117	100	0.18	180	10.7

The palladium anode was manufactured by electrodeposition on nickel mesh according to Cleghorn and Pletcher's^[68,69] method. The nickel mesh was a 26 wires per inch standard and was prepared by degreasing in dichloromethane then etching in 1M HNO₃. This assisted in the adhesion of the deposit. Plating took place at 10A/m² in a 1M HCl bath containing 5g/l palladium (II) chloride. At 100A/m² the deposit was very powdery, but at the reduced current density it was more satisfactory. The resulting experiment showed a reasonably higher conversion to benzaldehyde at a current efficiency of 10.7%.

6.4 Summary

Batch experiments in the SPE reactor produced vital information on the reaction and the system. It had been shown that electro-oxidation of toluene was possible without supporting electrolytes or co-solvents and, in general, the current efficiency was low. The majority of this work had been carried out with water, as a source of oxygen, and toluene. Because these are immiscible they were placed on opposite sides of the membrane. Future work was

aimed at alternative sources of oxygen that could be mixed with toluene with the most obvious being methanol.

The importance of a good contact between electrodes and membranes was highlighted. The compressibility and texture of graphite felt made it the obvious choice for longer term experiments. Applying pressure to the membrane electrode assembly had also assisted in making the good contact.

Oxidation with nickel foam had been successful in terms of production of desired product with high current efficiencies. Deterioration of the anode was the major disadvantage. However, this reaction had suggested that the initial oxidation of toluene to benzyl alcohol may be the most difficult step.

7. MEMBRANE PRE-TREATMENT

7.1 Introduction

Pre-treatment of ion exchange membranes is important for a variety of reasons. These reasons all relate to the structure of the fixed and counter ions within the polymer network. Swelling in solvents alters the performance of ion exchange membranes when used as SPEs. The performance relates to the ability of the ion exchange membrane to conduct ions. For this to be carried out with low resistance the fixed and counter ions must be dissociated and this is done by solvation. Mobility of the counter ions within the pores of the membrane also affects the performance of the ion exchange membrane and this is also increased by greater solvation. Ion exchange membranes were developed for use in aqueous systems such as water electrolysis and fuel cells and, hence, most literature relates to the swelling and performance in aqueous systems. Gerl and Jörissen^[2], and Jörissen^[20], have carried out extensive work on the pre-treatment of ion exchange membranes for use as SPEs for the methoxylation of DMF. Their system was completely organic so DMF was used as the sole swelling medium with interesting results particularly regarding the high level of osmotic flow. This chapter of the thesis records the attempts to evaluate the physical, chemical and electrochemical stability of several ion exchange membranes for use in the SPE system for oxidation of toluene in methanol. This process was carried out in two parts - the first involved pretreating membranes under various conditions, the second concerned testing the pre-treated membranes in the steel SPE reactor to assess such characteristics as cell potential and physical strength.

Transport across membranes can be caused by several driving forces such as pressure, concentration and electrical potential. These give rise to viscous flow, diffusion and migration respectively. Electro-osmotic flow is the movement of species driven by electrical potential. In the SPE reactor this takes place across the ion exchange membrane. Any ionic species, for example OH^- or H^+ , will be readily transported by the high potential gradient, which in this project was in the order of 5000V/m. These ions are likely to be surrounded by molecules of solvents which are then transported along with the ions. Movement of the ions and solvent shells will drag with them bulk solution. Together, these ions and solvents make up the electro-osmotic flow.

The size of the electro-osmotic flow in the SPE reactor is determined by several parameters. These consist of the potential gradient and hence current density, the ions produced, the solvents' affinity for the ions, the size of the solvent shell and the characteristics of the membrane. In the work reported below the characteristics of the membrane were altered by soaking them in solvents under different conditions. The membranes used consisted of a network of polymeric substrate linked to ionic groups. The ionic groups are positioned in clusters and when placed in solvents these clusters of ions dissociate. It is this dissociation of co and counter ions that enables the membranes to conduct electrical charge. During swelling, especially at high temperatures, some of the polymeric substrate may dissolve which may lead to physical deterioration.

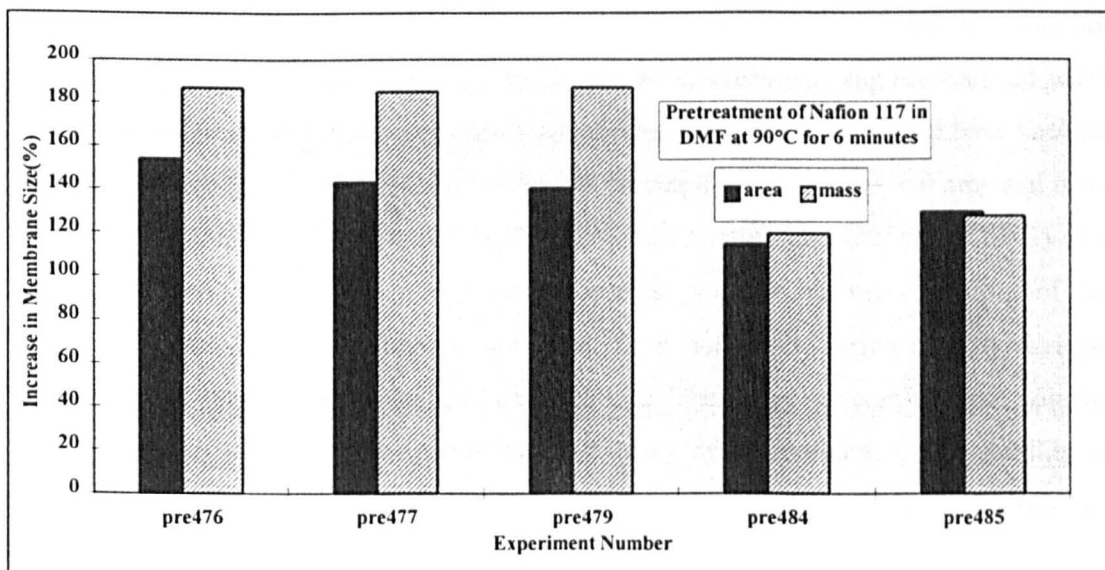
7.2 Swelling Tests

Swelling tests were carried out using the apparatus described in Chapter 3 which also describes the ion exchange membranes. The increase in size was calculated for membrane area and mass using Equation 7-1 and Equation 7-2 respectively.

$$\text{increase} = \frac{(\text{final area} - \text{initial area})}{\text{initial area}} \times 100 \quad \text{Equation 7-1}$$

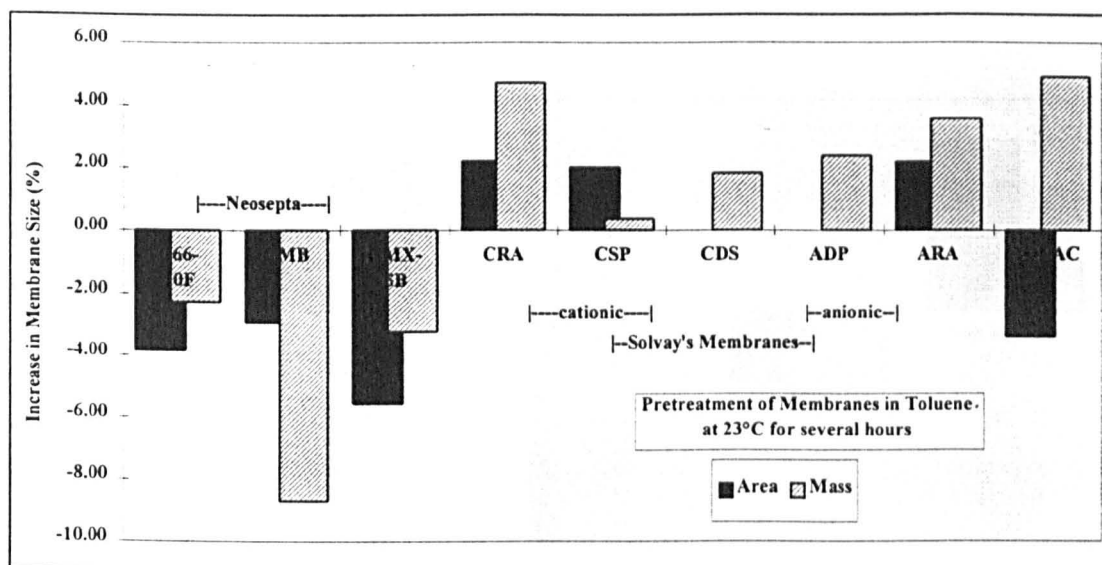
$$\text{increase} = \frac{(\text{final mass} - \text{initial mass})}{\text{initial mass}} \times 100 \quad \text{Equation 7-2}$$

Figure 7-1: Swelling in DMF



Several solvents were used to pretreat the membranes, some in combinations with others, at different temperatures and for various durations. The initial investigations involved swelling Nafion[®]117 in DMF to compare with the results obtained by Gerl and Jörissen^[2]. These were carried out in DMF at 90°C for 6 minutes and the increase in area and mass was comparable with those of Gerl^[2] (shown in Figure 7-1). These results were compared to swelling tests which took place in pure toluene at 23°C (Figure 7-2) and again at 100°C (Figure 7-3)

Figure 7-2: Swelling in Toluene at 23°C

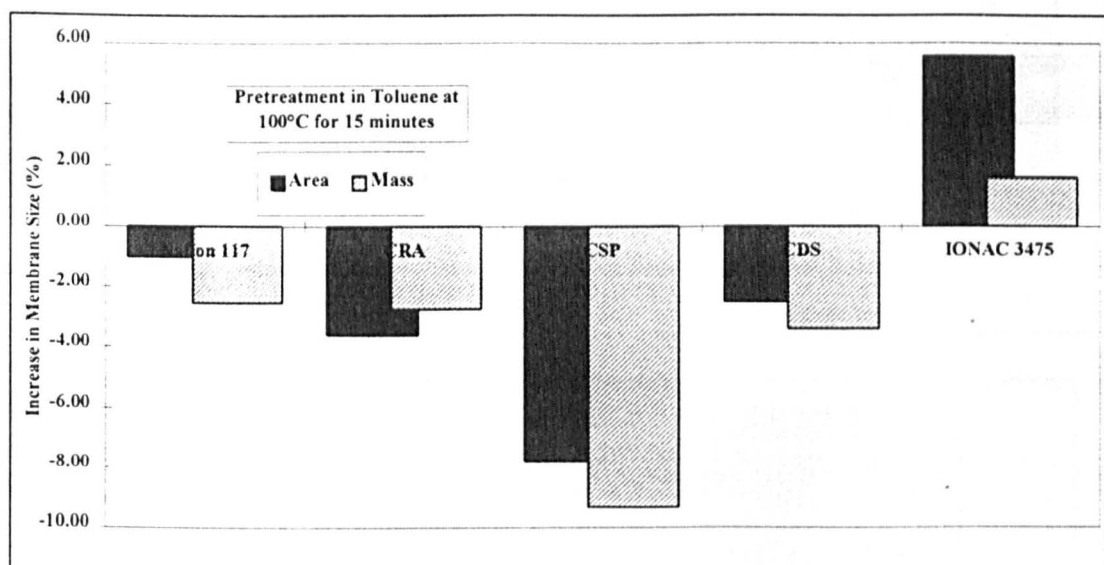


The tests in pure toluene showed a remarkable difference to those in DMF. It was obvious from these two experiments that swelling of the membranes by pure toluene was not possible, in fact the area and mass of many of the membranes was slightly reduced when compared to their normal form. Neosepta's membranes and Ionac[®] 3475 both have backing supports which may have affected the results. All Neosepta's membranes lost area and mass during the pre-treatment, and Ionac[®] 3475 showed the strange phenomena (at 23°C) of a smaller area but greater mass. Of particular interest was the chemical stability of the Neosepta membranes as the supports are made from polyvinylchloride or polyethylene, substances not recommended for use with toluene. These results confirm that toluene dissolves part of the polymer substrate, or the backing of the membrane. The stability of membranes used in the SPE reactor with toluene was therefore likely to be reduced somewhat.

In the next investigation the increase in membrane size was calculated as a function of toluene in methanol composition. This was carried out at 45°C, a temperature thought to be close to the subsequent operating temperature of the reactor. The membranes were soaked in the relevant solvent for 15 minutes before weighing took place. Several membranes were tested, with the highest amount of swelling again being with Nafion®117. This took place in a concentration of approximately 0.04 moles of toluene to 1 mole of methanol, see

Figure 7-4. The swelling was still much less than had been achieved in DMF, but was greater than that achieved in pure toluene alone

Figure 7-3: Swelling in Toluene at 100°C



In general, membranes other than Nafion®117 did not swell significantly. Of those membranes, Solvay's CRA exhibited the greatest increase in area (only 20%) although this increase in area was much less than with Nafion®117 (52%). This maximum increase occurred at a mole ratio of 0.1:1 which was also the same ratio as the maximum increase in the Solvay's CSP membrane.

Pre-treatment of Nafion®117 in methanol alone was investigated at the normal boiling point. As expected an increase in temperature increased the swelling. These experiments were carried out for a much longer period of time to enable solvation to reach equilibrium. Of course at higher temperatures and for prolonged periods a significant amount of substrate dissolution may have occurred although this was never investigated.

Figure 7-5 shows the results which approached some of those achieved following pre-treatment in DMF (Figure 7-1).

Figure 7-4: Pre-treatment in Methanol/Toluene

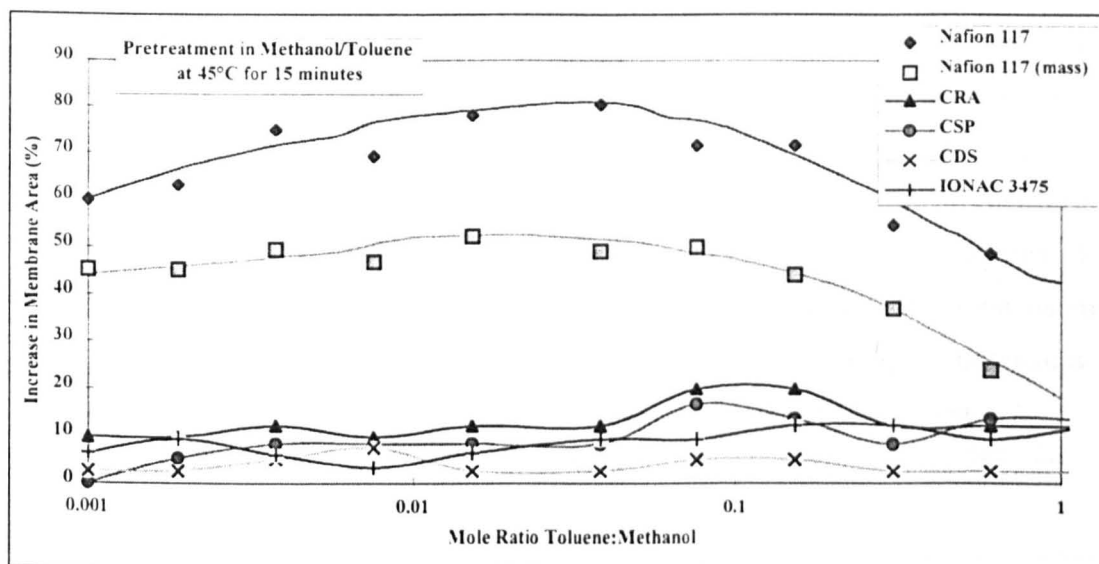
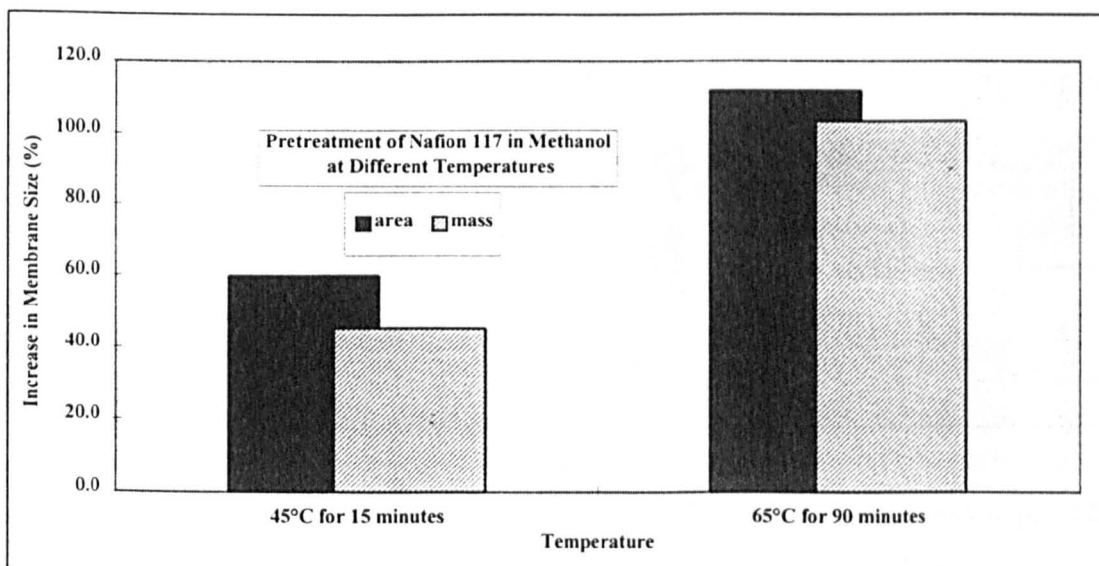


Figure 7-5: Pre-treatment in Methanol

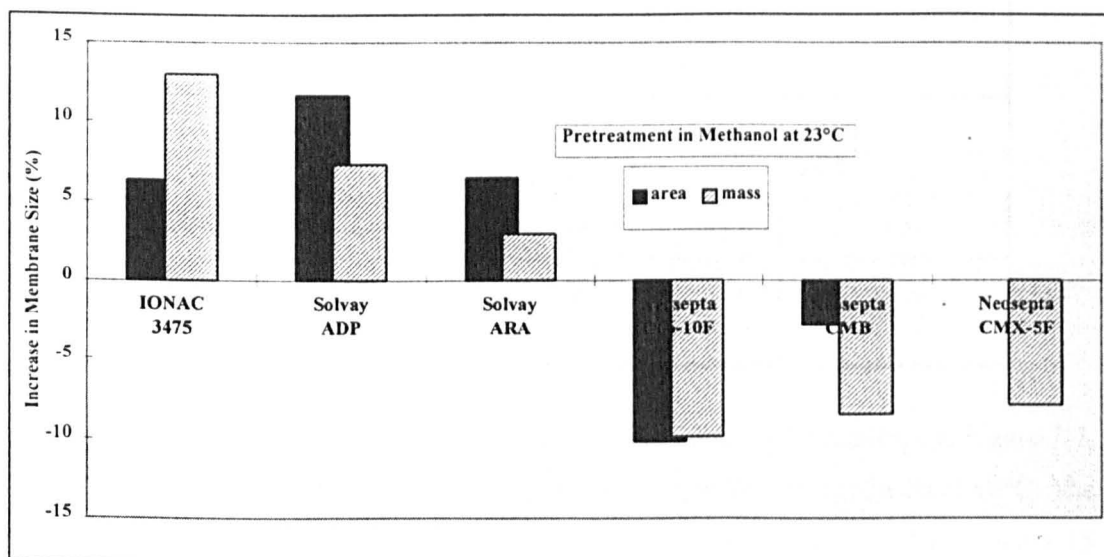


Several other membranes were also pre-treated in methanol but only at 23°C. These were anion exchange membranes - Ionac®MA3475, Solvay's ADP and ARA and Neosepta cation exchange membranes - C66-10F, CMB, CMX-5B. They were placed in the solution for either 18 hours (cation exchange membranes) or 50 hours (anion exchange membranes). After this time they were reweighed and measured. Figure 7-6 shows that in comparison to

Nafion[®]117 only modest swelling occurred, and in the case of Neosepta, as with swelling in toluene, the membranes lost mass and area.

According to the investigations by Gerl^[1,21] regarding the pre-treatment temperature, the membrane should be pre-treated at least at the highest temperature used in the electrolysis process. This conclusion was made following pre-treatment of Nafion[®]117 in DMF first at 60 °C for 3 days, then a short term (12 hours) temperature rise to 90°C followed by a 10 day period again at 60°C. Even after 10 days the membranes still retained their swollen size to within 95%. The next series of experiments were based upon this knowledge. The investigations concerned the selection of the swelling medium and the subsequent stability during electrolysis. This work was prompted primarily by the swelling characteristics in pure toluene and in pure methanol which were shown to be completely different.

Figure 7-6: Pre-treatment in Methanol at 23°C



In the first examination, Nafion[®]117 was soaked in methanol at its normal boiling point for a period of 90 minutes. It was then weighed and measured before being returned to methanol at room temperature (23°C) for 4 days. It was then transferred into toluene also at 23°C and left for 2 days. After this period of time the membrane was reweighed and measured. The results in Table 7-1 show a remarkable difference in swelling. The membrane nearly doubled in area and mass when placed in methanol and then returned to its near normal state when soaked in toluene. This evidence suggested that pretreating in methanol at 65°C was not sufficient to permanently alter the membrane structure in a

similar way that it was in DMF^[1]. Toluene seemed not to be able to swell Nafion®117 on its own even following pre-treatment in methanol.

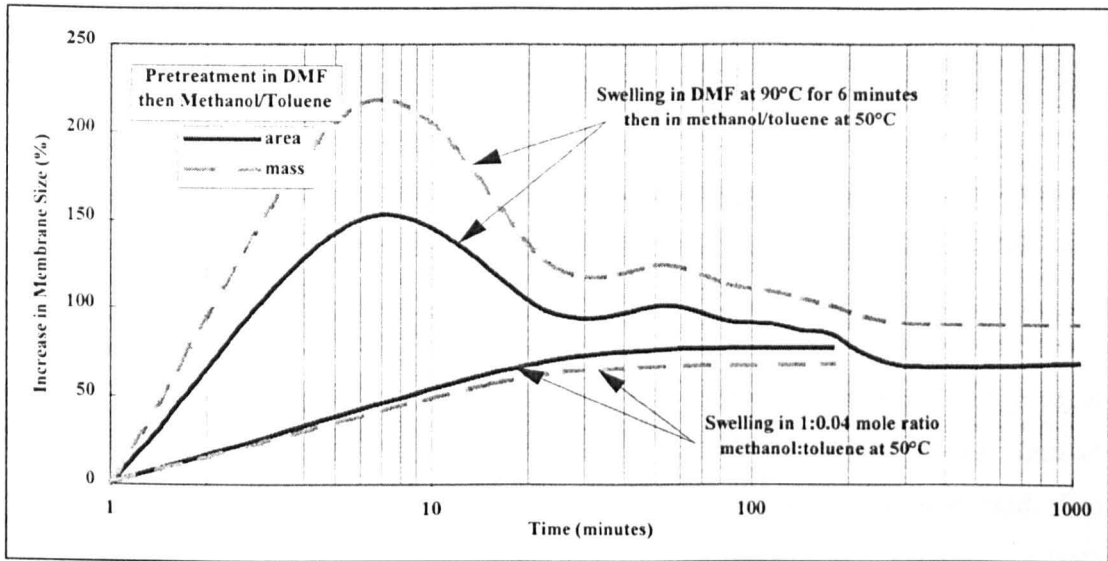
If swelling in DMF at 90°C does dissolve some of the membrane substrate and allow relaxation of the crosslinking as Gerl^[1] suggests then pretreating in DMF followed by soaking in other solvents should improve the swelling of the membrane and, hence, its performance in the reactor. This was investigated in the next series of experiments where Nafion®117 was soaked first in DMF then in a combination of methanol and toluene. The particular concentration of toluene chosen was that giving the greatest swelling, which according to Figure 7-4 was a mole ratio of 1:0.04 (methanol:toluene).

Table 7-1: Pre-treatment in Methanol then Toluene

Time Of Measurements	Area (cm ²)	Mass (g)	Increase In Size Relative To Initial	
			Area (%)	Mass (%)
Initially	32.0	1.12	-	-
After Soaking In Methanol	63.2	2.20	97.5	96.4
After Soaking In Toluene	33.8	1.18	5.6	5.4

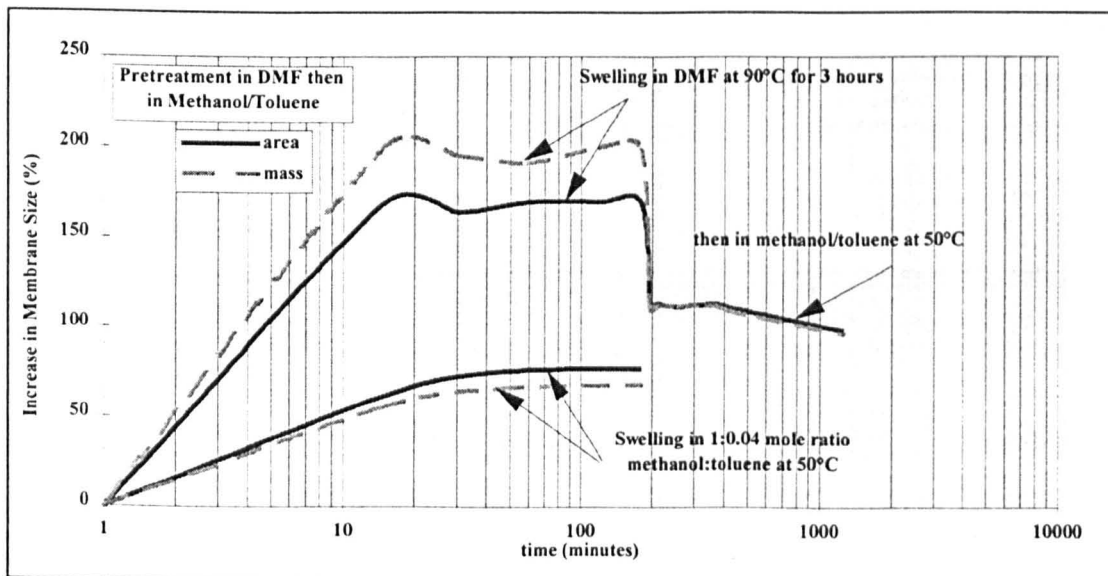
First a sample of Nafion®117 was pre-treated in DMF at 90°C for 6 minutes, see Figure 7-7. This was then weighed, measured and placed in the methanol/toluene solution at 50°C. The membrane behaved as expected in the DMF where it increased in area by 151%. After 15 minutes in the methanol/toluene solution it had already reduced in area to 97%. For the next 5 hours the membrane continued to shrink to a final state of 67%. A direct comparison of pretreating in methanol/toluene of the same composition and temperature showed that after 3 hours the membrane had returned to the area that would be expected from pretreating solely in methanol/toluene. This meant that only 3 hours of increased performance i.e. possible greater electro-osmotic flow, would be gained by using this pre-treatment procedure.

Figure 7-7: Pre-treatment in DMF for 6 Minutes then in Methanol/Toluene



A repeat was made of the pre-treatment in DMF followed by soaking in methanol/toluene, (Figure 7-8). This time the Nafion[®]117 was left in DMF for 3 hours to see if the swelling could be extended, hence, increasing the advantages for a greater length of time. At the end of 3 hours in DMF the area increase was 169%, but after only 15 minutes in methanol/toluene it had reduced to 113%. Over the next 18 hours some of this swelling was lost and a final area of 98% was achieved. Again comparing with the results achieved with only methanol/toluene showed a significant period of time at an increased area. If the reduction in area continued at the same rate then the advantage would be prolonged for a total of 40 hours.

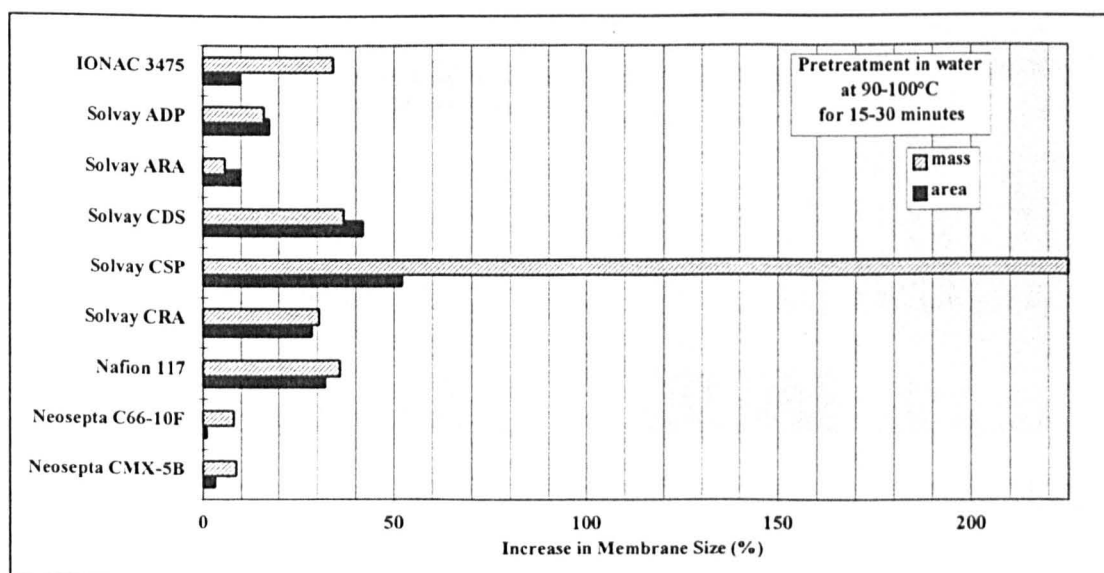
Figure 7-8: Pre-treatment in DMF for 3 hours then in Methanol/Toluene



The period of swelling in DMF was not itself without concern. It was noticed that after 1 hour the membrane contained distinct areas of enlargement of approximately 1mm diameter. These were evenly distributed across the whole of the membrane and existed throughout the experiment even during the period of soaking in methanol/toluene. This was thought to be due to solvent clusters in the membrane causing dissolution of substrate, and therefore loss of physical stability.

The concern regarding the loss in physical stability, and the consideration of product contamination meant that DMF no longer featured as a potential swelling solvent. Instead investigations moved towards aqueous solvents such as water or sulphuric acid. The previous electrolysis experiments with water and toluene showed that water was a poor reagent and that any contamination during electrolysis would result in loss of current efficiency by gas evolution. Several membranes were pre-treated in Millipore water at 90-100°C for 15-30 minutes and the results are shown in Figure 7-9. What was immediately obvious was that Solvay's CSP membrane absorbed a vast amount of water compared to its initial mass. Its area increase was not so great although it was the greatest by some 9% over Solvay's CDS. Nafion®117 again performed reasonably well, increasing its area by 32%, closely followed by Solvay's CRA at 29%. Solvay's anion exchange membranes did not swell as well as their cationic cousins, but Ionac®MA3475 absorbed enough water to increase its mass by 33%. This was thought to be due to absorption by its backing support rather than the membrane itself. Neosepta's membranes again remained largely unchanged.

Figure 7-9: Pre-treatment in Water



The Nafion[®]117 used was the H⁺ type and so to ensure that all available cationic sites were full of H⁺ ions it was pre-treated in boiling H₂SO₄ for 15 minutes, and also 30 minutes. Due to the remarkable swelling performance of Solvay's CSP this pre-treatment was also carried out on this membrane. Figure 7-10 shows the result after 15 minutes; after 30 minutes the swelling was within $\pm 2\%$ of this. Solvay's CSP again showed a remarkable increase in mass of 135% but it's area increased by only 22%, similar to the swelling achieved by Nafion[®]117. These were all less than that achieved in water.

A final experiment was carried out to complete these swelling tests. Many pre-treatment procedures are more complicated than simple swelling in one solvent. The method used for Nafion[®]117 prior to use in direct methanol fuel cells is a series of treatments and was carried out to compare with the simple tests carried out above:-

1. cut membrane
2. boil in Millipore water for 30 minutes
3. soak in 5% H₂O₂ at 80°C for 1 hour to destroy residual organic impurities
4. wash thoroughly with water to remove traces of hydrogen peroxide
5. boil in 1M H₂SO₄ for 2 hours
6. wash again in Millipore water followed by boiling in Millipore water for 2 hours
7. storage should be in plastic containers to avoid contamination with leached Na⁺ and membranes should be boiled in Millipore water again before use.

Figure 7-10: Pre-treatment in Sulphuric Acid

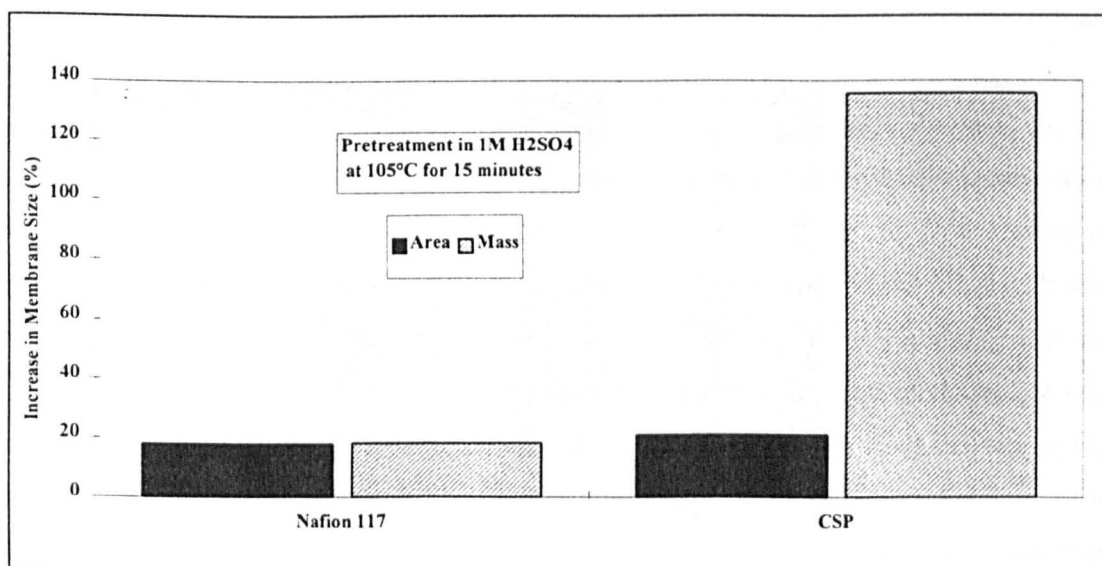
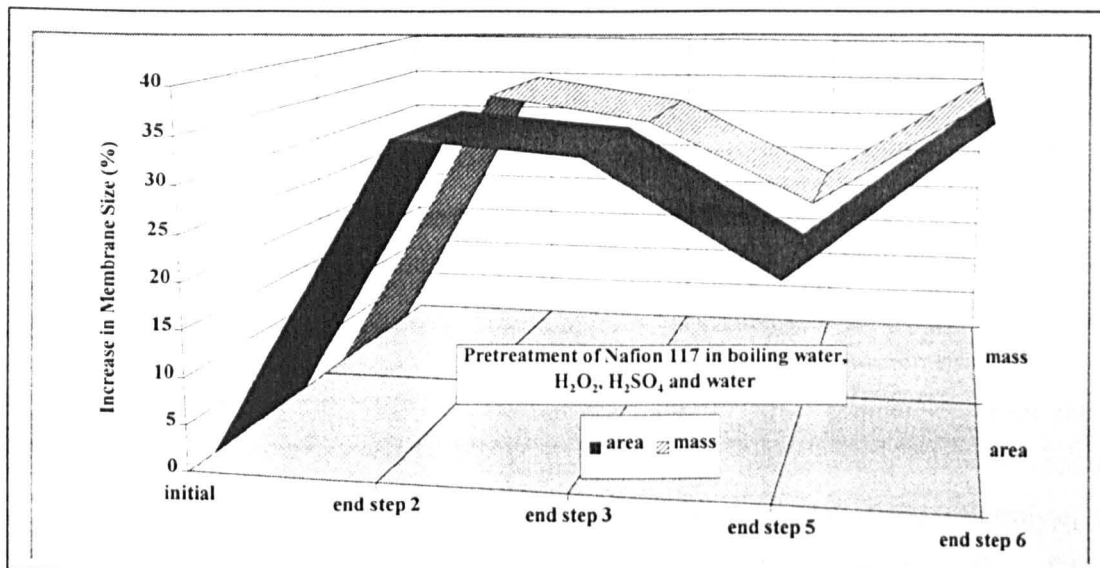


Figure 7-11: Pre-treatment in Various Aqueous Solutions



It was interesting to note the swelling characteristics during this procedure and these are shown in Figure 7-11. A large amount of swelling occurred in water followed by peroxide. The membrane returned to a smaller area during the period of boiling in the acid, (to within 1% of the area in acid alone) and then back to its maximum area again in water.

7.3 In-Situ Testing Of Pre-treated Membranes

Following the swelling of membranes executed above several electrolysis experiments were undertaken. These experiments not only completed the examination of the membranes but formed part of the development and commissioning of the reactor system. Not all membranes were tested, and not all solvents were tested - a process that would take excessive time. Instead effort was concentrated on the cation exchange membranes; all solvents except toluene were used, (but not for all membranes).

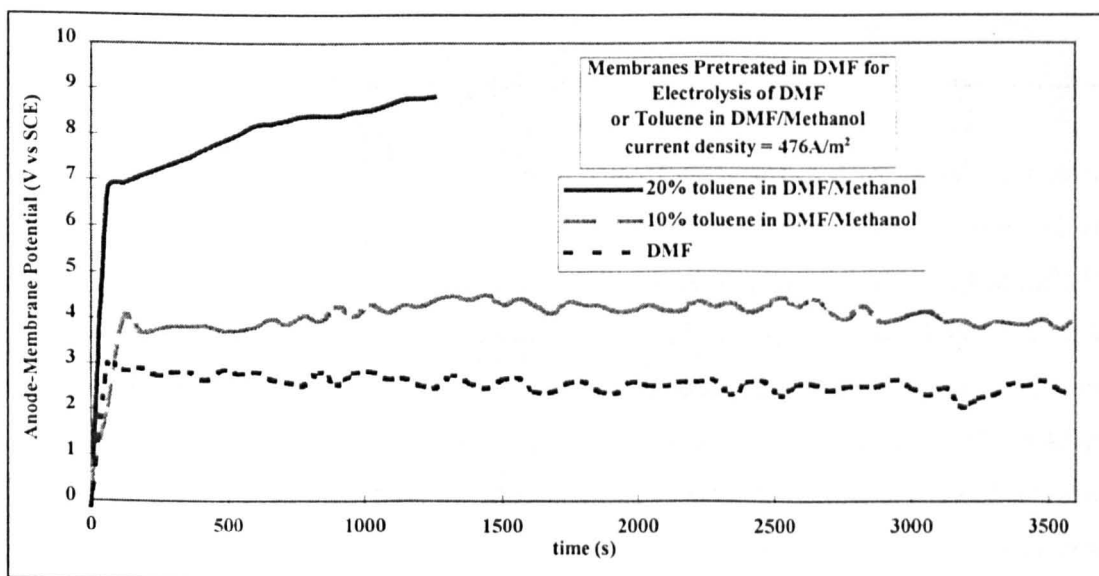
Testing of the membranes involved electrolysis of 10% weight toluene in methanol (the concentration of toluene giving the greatest swelling of Nafion®117) or 10% toluene in methanol:DMF in a ratio of 1:2. Both anode and cathode chambers were filled with this electrolyte. Both electrodes were graphite felt and a range of current densities, subject to the potentiostat limit of $476A/m^2$, were applied for a period of 1 hour. Feed of electrolyte was to the anode chamber by peristaltic pump; the product being taken from the top of the cathode chamber and part recycled to the feed point. This meant that electro-osmotic flow would take reactant through the membrane so the feed rate had to be controlled in order to prevent flooding. The anode-membrane potential was measured as the potential difference

across both anode and cation exchange membrane using a Luggin capillary connected to a standard calomel electrode. The membrane performance was assessed by:-

1. the size of the anode-membrane potential
2. the amount of current flowing subject to an anode-membrane potential maximum of 10V,
3. any physical deterioration observed during electrolysis or afterwards by visual inspection.

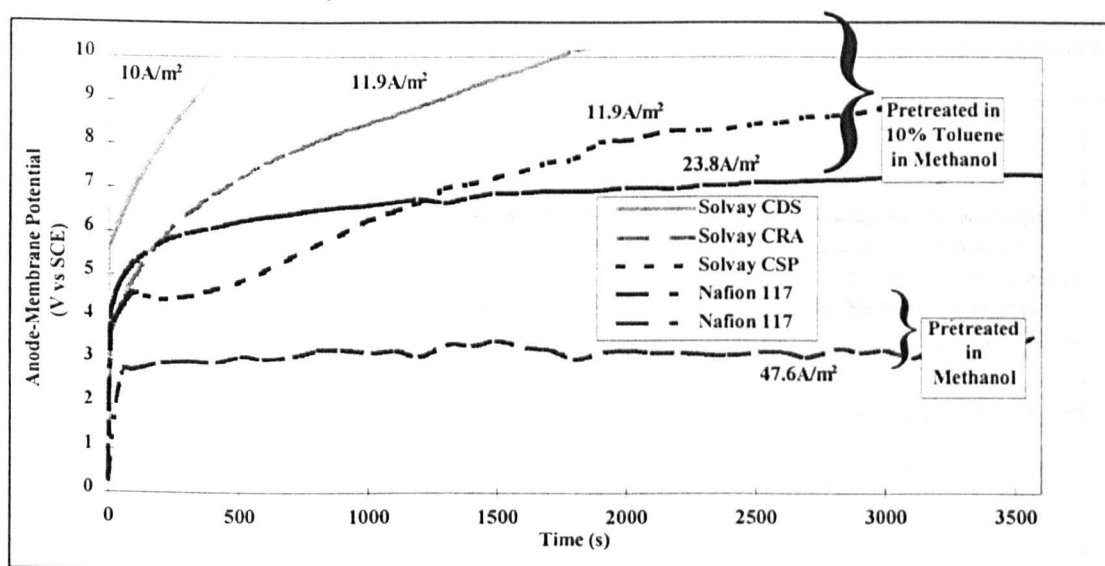
The starting point was with DMF pre-treated Nafion[®]117. Direct comparisons were then made with the results of Gerl^[1,21] and these provided a base line to which following results were assessed. These experiments, therefore, used DMF as part of the electrolyte, a substance that was feared could cause a loss in current efficiency by formation of by-products. In DMF alone the anode-membrane potential was very similar to that achieved by Gerl^[1,21] ranging between 2-3V vs SCE. This was a good indication that the reactor system was working at the expected rate. Replacing the electrolyte solution with 10% toluene in DMF/methanol caused a rise of 1-2V vs SCE in the anode-membrane potential. On increasing the toluene concentration further to 20% the anode-membrane potential significantly shifted by 4-6V to 7-8.6V vs SCE. These results, shown in Figure 7-12, confirm those of the swelling tests where toluene caused a loss in the swelling of pre-treated membranes. No deterioration in the membranes was noticed by visual inspection, but as expected methoxylated products of DMF were found in the product stream.

Figure 7-12: Electrolysis Tests with DMF Pre-treated Membranes



Four types of cation exchange membranes pre-treated in methanol solution were tested in the steel SPE reactor and the results are shown in Figure 7-13. These were Solvay's membranes and Nafion®117. These were pre-treated in 10% toluene in methanol for the electrolysis of the same solution. Much lower current densities were applied compared with those pre-treated in DMF and higher potentials were recorded. Solvay's membranes, in general, operated at higher potentials than Nafion®117 although for 20 minutes Solvay's CSP membrane was some 1.5V lower than Nafion®117. Solvay's CRA and CDS membranes reached 10V vs SCE after 30 and 8 minutes respectively. An additional test was conducted with Nafion®117 pre-treated in pure methanol. At 47.6A/m² this membrane gave a much better result in terms of anode-membrane potential. For 1 hour the potential remained around 2.8-3.1V vs SCE, approximately 3-4V less than the next best (with Nafion®117 at 23.8A/m²).

Figure 7-13: Electrolysis Tests with Membranes Pre-treated in Methanol/Toluene



Water pre-treated Neosepta membranes were tested and compared to water pre-treated Nafion®117 membranes, see Figure 7-14. These tests were carried out at 100A/m² (2-10 times greater than in methanol) again for the oxidation of toluene in methanol. Nafion®117 gave an anode-membrane potential of between 4.3 - 5.1V vs SCE compared with 8.5-9.5V vs SCE for Neosepta CMX-5B. Neosepta C66-10F gave an equally high anode-membrane potential but for only 2 minutes and at a much reduced current density of 9.5A/m². Comparing these results with those of Nafion®117 pre-treated in methanol showed a higher anode-membrane potential (4.7V compared with 2.95V vs SCE) but at a higher current density (100A/m² compared with 47.6A/m²).

Figure 7-14: Electrolysis Tests with Membranes Pre-treated in Water

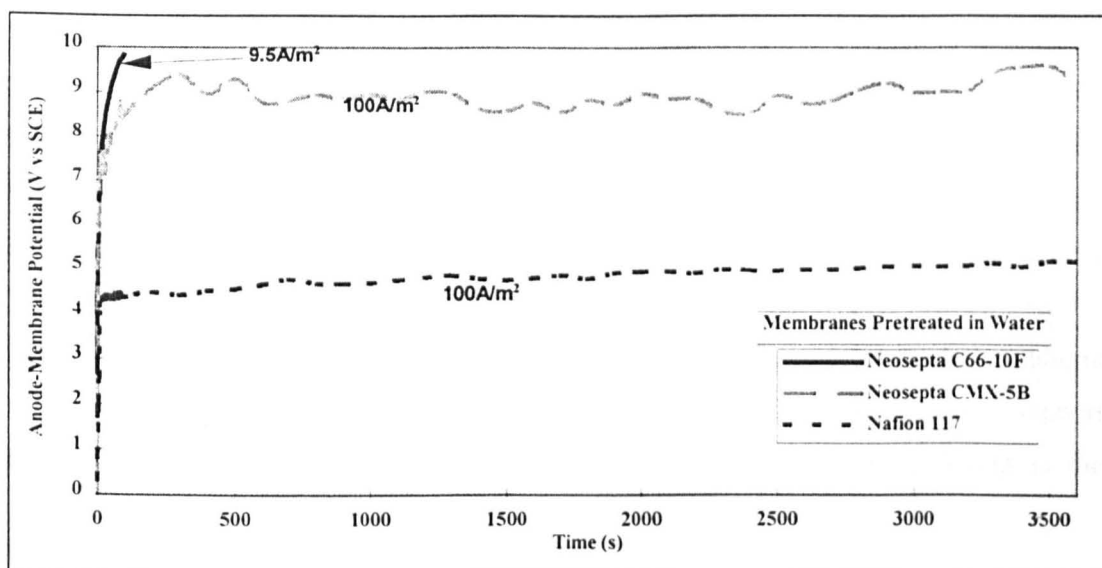


Figure 7-15: Electrolysis Tests with Membranes Pre-treated in Various Aqueous Solvents

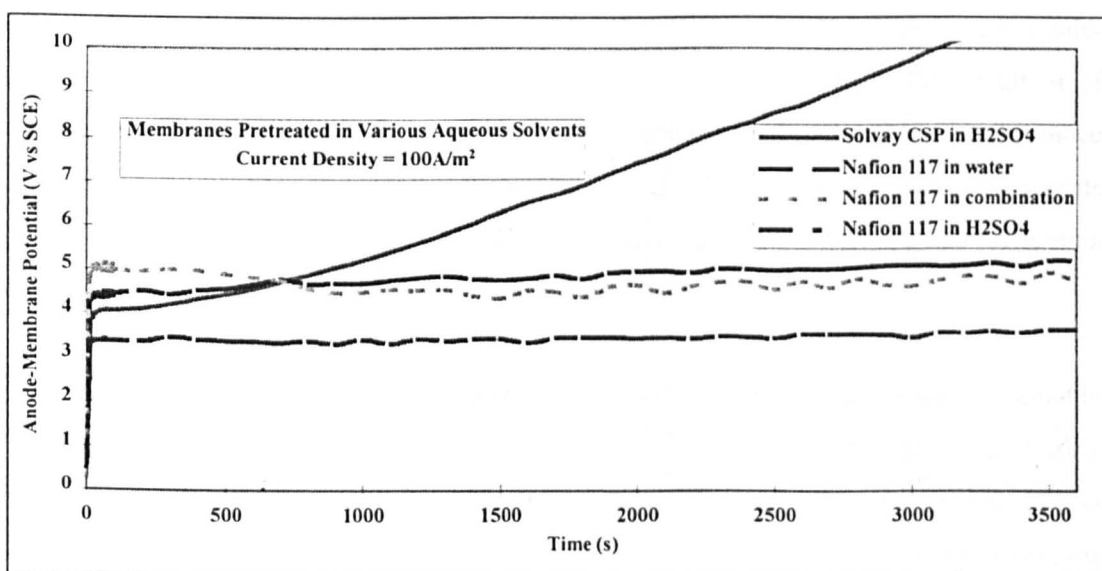


Figure 7-15 shows further tests of membranes pre-treated in aqueous solvents. Following the remarkable swelling of Solvay's CSP membrane in H₂SO₄ it was tested in the SPE reactor, again for the oxidation of toluene in methanol. During this experiment the anode-membrane potential rose steadily from 4 to 10V vs SCE over 50 minutes. In comparison with this was the performance of a similarly pre-treated Nafion[®]117 membrane which gave an anode-membrane potential constant over 1 hour at 3.3V vs SCE. This was also much better, by 1-1.5V, than the water pre-treated Nafion[®]117 membrane. The Nafion[®]117

membrane pre-treated in a series of aqueous solvents (including water, hydrogen peroxide and sulphuric acid) gave a similar result as that with a water only pre-treated Nafion[®]117 membrane, i.e. some 0.5V vs SCE lower.

7.4 Final Membrane and Pre-treatment Selection

The final selection of membrane was one of the simplest tasks undertaken in this project. Of the 10 ion exchange membranes tested the performance of Nafion[®]117 was consistently better. Solvay's CSP did show remarkable swelling characteristics in water and sulphuric acid, but the others were largely unaffected. This may be due to the backing support hindering absorption of solvents or to a much greater amount of cross linking in the polymer substrate.

A much more difficult task was the selection of a membrane pre-treatment process. The first solvent to be ruled out was toluene which had not swollen any membrane alone and had reduced swelling obtained in other solvents. Overall DMF had given the lowest anode-membrane potential although it was only tested for the electrolysis of DMF itself or of toluene in DMF/methanol. Increasing the toluene content had reduced its performance considerably but the main reason for dismissing it as the sole pre-treatment solvent was its contribution to by-product formation. Health risks associated with DMF use also favoured a different solvent.

A better option seemed to lie with methanol since swelling performance was reasonably high. Also a relatively low anode-membrane potential was seen during electrolysis testing but at much reduced current densities. The main concern for pre-treatment in methanol was the action of toluene. During swelling tests it had been shown that the area of the membrane eventually returned to that obtained in the final solvent. One option was to pretreat in methanol/toluene but the anode-membrane potential associated with this was quite high at 6.5-7V vs SCE at low (23.8A/m^2) current densities. A second option was to first pretreat in DMF then in methanol/toluene. A 6 minute pre-treatment in DMF had increased the area of the membrane for only 3 hours over that obtained in methanol/toluene alone. A 3 hour pre-treatment had increased this time potentially to 18 hours, but with membrane deterioration. The optimum seemed to lie in pretreating for a period (between 6 minutes and 3 hours) in DMF. As discussed above this was rejected for reasons of contamination, health and deterioration.

The final selection was pre-treatment in the series of aqueous solvents. Although this didn't give the largest swelling, nor the lowest anode-membrane potential it was a simple operation that gave reasonable performance at a medium current density and is well established in polymer electrolyte fuel cells where several days of operation have been recorded.

8. FLOW REACTOR

8.1 Introduction

This chapter describes in detail the development of the steel SPE reactor for the electrolysis of methanol and toluene. Important details such as selection of membrane and its pre-treatment were discussed in the previous chapters. Other considerations are discussed below such as flow regime, temperature effects, membrane support, gaseous product collection, potential measurement and practical problems such as gasket material.

Experiments carried out in the flowcell include potentiodynamic scans for determination of modelling parameters as well as long duration (10hours) electrolyses. Analysis of samples and of experimental data gathered during electrolysis are discussed followed by their implications for the development of a computer simulation. The data gathered during these experiments is given in Appendix 2.

8.2 Flow Set-up

A characteristic of using the SPE system compared to traditional electrochemical reactors (other than the ability to carry out electrolysis with non conducting species) is that reactants are transported through the reaction zone by electro-osmotic flow. The feed to the reactor must be selected carefully to capitalise on this characteristic. For electrolysis with an anion exchange membrane the transport of reactants is from the cathode to anode. For cation exchange membrane the transport is in the reverse direction.

Selection of the membrane type depends upon the reaction mechanism. For the oxidation of toluene in methanol the reaction is thought to proceed with the removal of H^+ ions from methanol. These H^+ ions are then solvated with methanol and toluene and are transported across the membrane by the potential driving force. This electro-osmotic flow from anode to cathode is enhanced by the use of a cation exchange membrane such as Nafion[®]117.

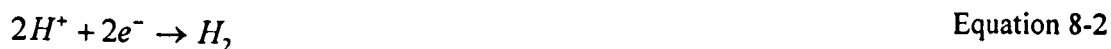
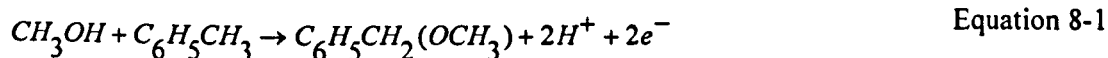
To take advantage of the electro-osmotic flow, feed of electrolyte must be to the anode chamber. Gerl^[1,21] recorded electro-osmotic flow of 60ml/hr for a membrane area of $\sim 20\text{cm}^2$ and with a current density of 100A/m^2 for the methoxylation of DMF. Feed rates up to this

value meant that all electrolyte passed through the membrane to the cathode chamber i.e. the reactor was of the plug flow type. Unreacted electrolyte was then recycled to the anode. This was also the configuration adopted for the oxidation of toluene in methanol. The feed rate was controlled via the pump mounted control panel. The recycle flow rate was measured with a Fischer-Porter rotameter and the product stream was calculated as the mass rate. External liquid lines were made from 1mm internal diameter PTFE tubing, Omnifit connectors and valves. A flowsheet of the reactor system is given in Appendix 4 showing the reactor configuration.

8.2.1 Gas Collection

From the work by Gerl^[1,21] it was known that much hydrogen generation could be expected from the reaction. Gaseous by-products from the oxidation of methanol, carbon dioxide and carbon monoxide, were also expected. Gas outlet lines were designed for the purpose of separating liquid and gaseous phases, one for each half of the reactor. The gaseous phases would then be collected and analysed separately. The system was modelled on that used by Gerl^[1,21] where the gas phase was collected by displacement of a weak salt solution. Water cooled condensers were included to enable the separation of volatile materials such as methanol and methyl ester. These items are also shown on the flowsheet in Appendix 4.

The rate of hydrogen generation is directly related to the current density. Loss of current efficiency may have meant a reduction in hydrogen evolution, but if the reduction was due to methanol decomposition, for example, this may have been compensated for by an increase in the rate of carbon dioxide formation. Assuming 100% current efficiency and the reaction schemes:-



enabled the amount of hydrogen evolved to be calculated from:-

$$\dot{M}_{\text{H}_2} = \frac{j \cdot A}{n \cdot F} \quad \text{Equation 8-3}$$

where A is the area of electrode in contact with the membrane.

8.3 Flowcell Development

The design of the reactor was based on that developed at the University of Dortmund for the methoxylation of DMF^[1]. The reactor used in this project was different in size and shape.

The active electrode area was rectangular with dimensions 7cm x 3cm. Other parts such as the PTFE tubing were also of different size. Much time was spent commissioning the original reactor design before a final design was reached. This involved carrying out experiments galvanostatically and potentiostatically in order to assess the performance of the system, as a whole and as individual parts. Items such as sizing of gas outlet piping, cathode type, reactor packing and sealants are discussed below. Much of this work concerned the amount and type of data to be collected in order to assess the reactor. Chemical analysis on the gas chromatograph had already been programmed from earlier work. Temperatures, pressures and flows in different parts of the system were measured at regular intervals to confirm changes with time. The applied current and cell potential were easily recorded from the power supply, but other potentials needed special probes. These are also discussed below.

These initial experiments were also aimed at selecting the range of best conditions under which the reactor should be tested in detail. This involved running several experiments at different temperatures and at different current densities. Membrane swelling was thought to depend strongly upon feed concentration so this was based on the results of the membrane pre-treatment as discussed in Chapter 7. The membrane gave highest swelling in a 10%wt toluene in methanol solution and so this was adopted as the standard concentration. Other concentrations close to this value were also tested.

8.3.1 Gas Outlet

The outlet lines from the reactor carried two-phases and so they were sized to allow for the large flow of gas in order to prevent entrainment of liquid. Sizing of these lines was closely related to the electrolyte feed rate, the electro-osmotic flow and the current, which were all dependent upon the membrane performance, hence, the importance of the pre-treatment procedure.

The current density range used in the experiments was from 190-952A/m². Higher rates of 1900A/m² were tried for short periods and this led to liquid entrainment in the outlet lines causing complete emptying of the chambers. Much gas evolution was noticed on both sides of the reactor, as had been noted by Gerl^[1]. He found that this was mainly hydrogen, and that the hydrogen found on the anode side was due to back diffusion across the membrane. The problem of liquid entrainment was reduced by enlarging the diameter of the lines from

3mm to 5mm internal diameter. Using Equation 8-3 the velocity of hydrogen evolution was reduced from 0.0356m/s to 0.0128m/s at the highest rate of 952A/m².

A consequence of a large amount of hydrogen evolution was blocking of reaction sites at the cathode surface. A platinum mesh cathode was tested to see if the releasing of hydrogen bubbles would be aided by a less tortuous construction than graphite felt. Unfortunately, this caused another problem to develop. Due to the pressure applied by the steel springs the mesh cathode punctured the Nafion[®]117 in several places. A compromise was reached by using a thinner layer of graphite felt on the cathode side. Instead of 5mm thickness the felt was reduced to 2mm.

8.3.2 Packed Bed

On the anode side of the membrane Gerl^[1] had used a packed bed of graphite particles. This eventually became the chosen set-up for this project. For several experiments steel springs were used on both sides of the membrane. This caused practical problems when assembling the reactor and also stretching of the membrane as the reactor was compressed. The graphite packed bed was a solid platform on which the anode and membrane could rest. Pressure could then be applied from the cathode side without causing deformation of the membrane.

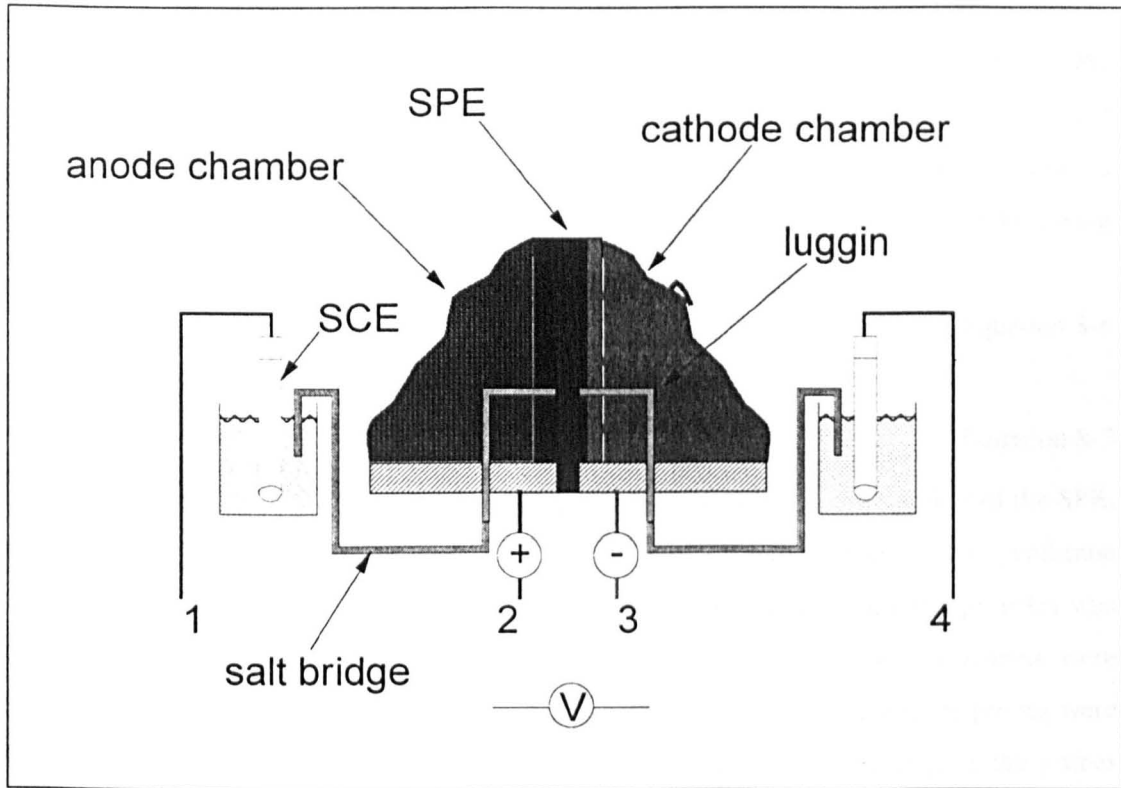
It was found that 1mm thick Teflon gaskets were suitable sealants around the membrane and reactor body. These were chemically resistant, didn't deform under pressure and so could be reused.

8.3.3 Potential Measurement

In the earlier experiments in the glass SPE reactor, see Chapter 6, only one reference electrode had been used. The flowcell was improved by including two reference electrodes which meant that the membrane potential could also be measured. Figure 8-1 shows the scheme for the measurement of membrane and other potentials. The Luggin probes were made from 1mm internal diameter brass tubing and were fixed into the chamber frames with steel locking nuts. Holes were cut in the graphite felt electrodes to allow the probes to rest on the surface of the membrane. This allowed liquid electrolyte to fill the probes. When the electrolyte was seen to flow out of the reactor through the probes they were connected to the salt bridges. These were made from 1mm internal diameter PTFE tubing filled with

saturated KCl gel. Connection to the standard calomel electrodes was via two baths of saturated KCl gel.

Figure 8-1: Schematic Of Potential Measurement Apparatus



To measure potentials a voltmeter was connected between two of the four connections labelled in Figure 8-1. It was found that simultaneous recording of potentials, for example with 4 voltmeters, was not possible even with high impedance voltmeters. Each reading had to be made separately to avoid current leakage. Table 8-1 summarises the measured potentials.

Table 8-1: Potential Measurements

Connections	Name	Symbol
2-3	Cell Potential	E_{cell}
2-4	Anode-Membrane Potential	E_{ACM}
1-3	Cathode-Membrane Potential	E_{CAM}
1-4	Membrane Potential	E_{M}

From these readings the anode potential (E_A) and the cathode potential (E_C) could be calculated from:-

$$E_A = E_{ACM} - E_M \quad \text{Equation 8-4}$$

$$E_C = E_{CAM} - E_M \quad \text{Equation 8-5}$$

Theoretically the anode and cathode potentials could be measured using the system shown in

Figure 8-1 by connecting the voltmeter across 1-2 and 3-4 respectively. Unfortunately the Luggin probes were not in the 'current path' for these measurements and so incorrect readings were obtained. The above equations were used instead. As a means of checking the system's order the cell potential was also calculated from three readings using the following equations:-

$$E_{CELL} = E_A + E_M + E_C \quad \text{Equation 8-6}$$

hence,

$$E_{CELL} = E_{ACM} + E_{CAM} - 2.E_M \quad \text{Equation 8-7}$$

One practical problem associated with the Luggin probes concerned the stability of the SPE. Positioning the probes too close to the membrane caused hot spots to form on the membrane which led to early failure. Many experimental runs were performed until this problem was solved. Positioning the probes too far from the membrane and the measurements were affected by gas evolution at the electrode surface. Gas bubbles penetrating the probes were easily noticed from wildly fluctuating voltmeter readings. Periodic purging of the probes kept the system working well.

8.3.4 Temperature Range

The electrolysis experiments were tested across a range of easily achievable operating temperatures. The lower limit was restricted by the temperature of cooling water (19-23°C), the upper by the boiling point of the methanol/toluene mix. Although the boiling point of the mix was never determined the normal boiling point of methanol is 64.6°C. Temperatures of 66°C were achieved but only resulted in vast amounts of gas evolution, presumably from methanol vaporisation. A simultaneous rise in cell potential was also noticed.

The reactor temperature was controlled by recirculating the heating/cooling water around both heating chambers. The heating/cooling water was heated in a 1 litre beaker on a hot plate. This was pumped around the system by a small centrifugal pump. A thermostat mounted on the hot plate was used to control the bulk water temperature.

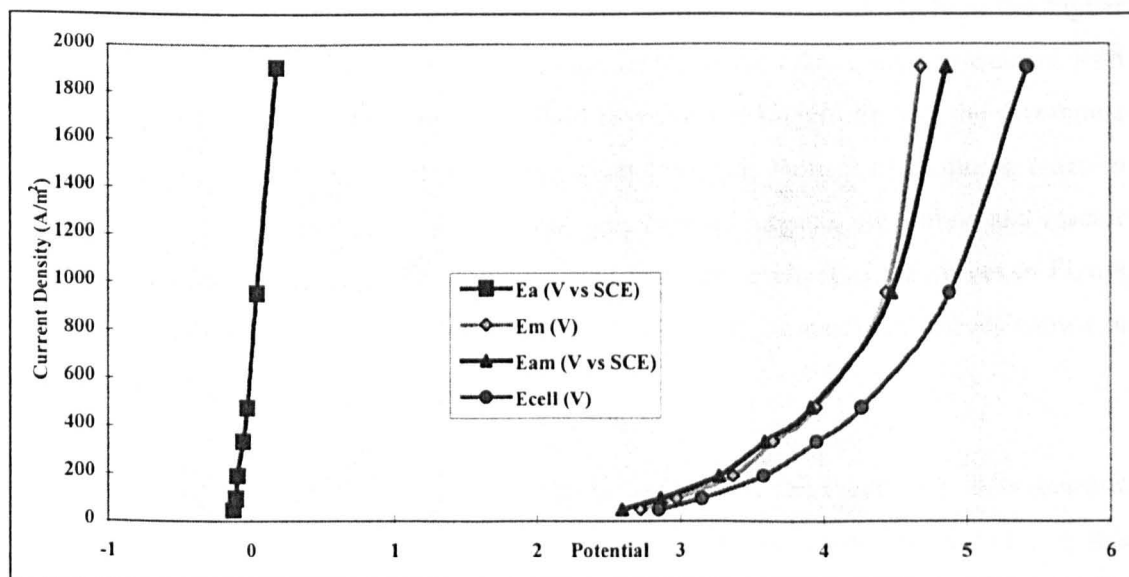
8.3.5 Current Range

The current was limited by the rate of gas generation as discussed in Section 8.3.1. Above 1000A/m^2 the amount of gas being generated caused a large rise in cell potential such that the power supply reached its upper limit. The minimum current chosen was 200A/m^2 . The cell potential was also found to be affected by the feed concentration of toluene. At the higher feed concentration of 30%wt toluene the power limit of the DC supply was reached at 500A/m^2 .

8.4 Calculation of Transfer Coefficient

The transfer coefficient for the oxidation of toluene in the SPE reactor using methanol was calculated by first carrying out some potentiodynamic scans. The applied current density was held constant for 2 minutes at each chosen value ranging between 0 and 2000A/m^2 . At the end of this period the cell, membrane, anode-membrane and cathode membrane potentials were taken. Using Equation 8-4 the anode potential was calculated by subtracting the membrane potential from the anode-membrane potential. An example of the readings is shown in Figure 8-2 and the subsequent anode potentials are shown in Figure 8-3.

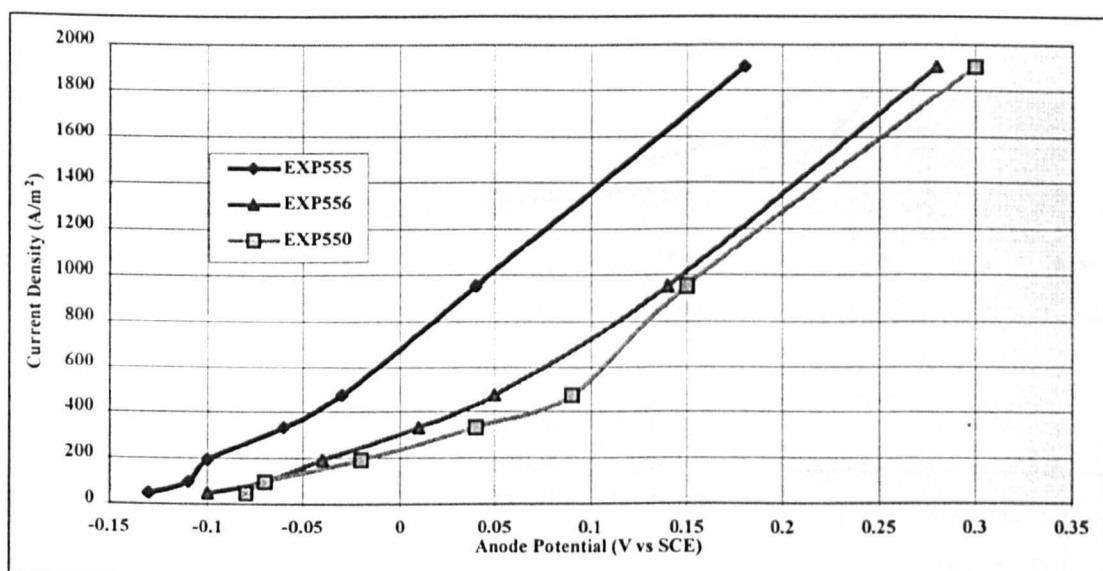
Figure 8-2: Potentiostatic Scan for EXP555



All experiments showed that the membrane potential was very similar to the cell potential and so when subtracting these two similar values the anode potentials were very small and

approximately zero. Due to the large errors incurred in this process the anode potentials were not thought to accurately reflect the true potentials for the oxidation of toluene in methanol. This can be seen when compared with Wendt's work ^[63] where the half wave potential on graphite anodes was given as 1.77 V vs NHE. However, the conditions in the SPE reactor were different from those in Wendt's flowcell, and so the data generated in this project was used for the purposes of modelling.

Figure 8-3: Potentiostatic Scans Of Toluene in Methanol



The anode potentials, in Figure 8-3, show linear characteristics particularly at the higher current densities. Since the membrane potential included the Ohmic drop associated with the electrolyte resistance in the potential field between the Luggin tip and the membrane surface, and had already been removed, this linear form was thought to be due to junction potentials between graphite felt, graphite bed, gas bubbles, organic electrolyte and reactor support. The resistance, 0.0667Ω , was calculated from the gradient of the curves in Figure 8-3 using Ohm's Law and was removed to produce the iR compensated curves shown in Figure 8-4.

The compensated curves were then plotted in the Tafel form, see Figure 8-5. Galvanostatic experiments took place in the current range from 100 to 1000A/m^2 and correlating this range for the scans gave the equations shown in Figure 8-5. This gave transfer coefficients of 0.31, 0.34 and 0.77 for EXP550, EXP555 and EXP556 respectively. The average of these

values, 0.47, was used in the reactor model for each of the electrochemical reactions i.e. the methoxylation, dimethoxylation and oligomerisation reactions.

Figure 8-4: iR Compensated Potentiostatic Scans

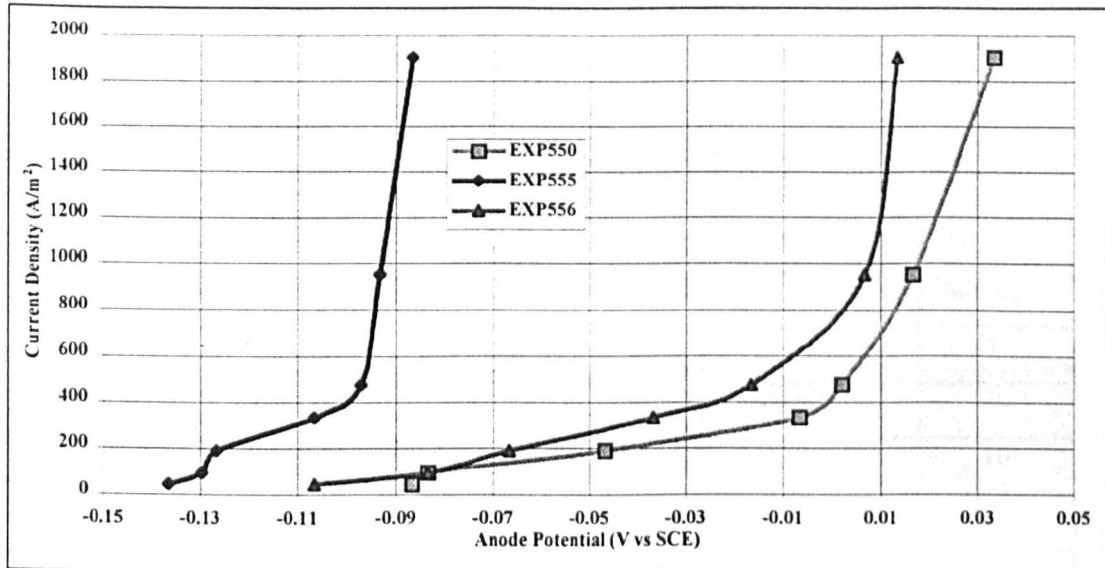
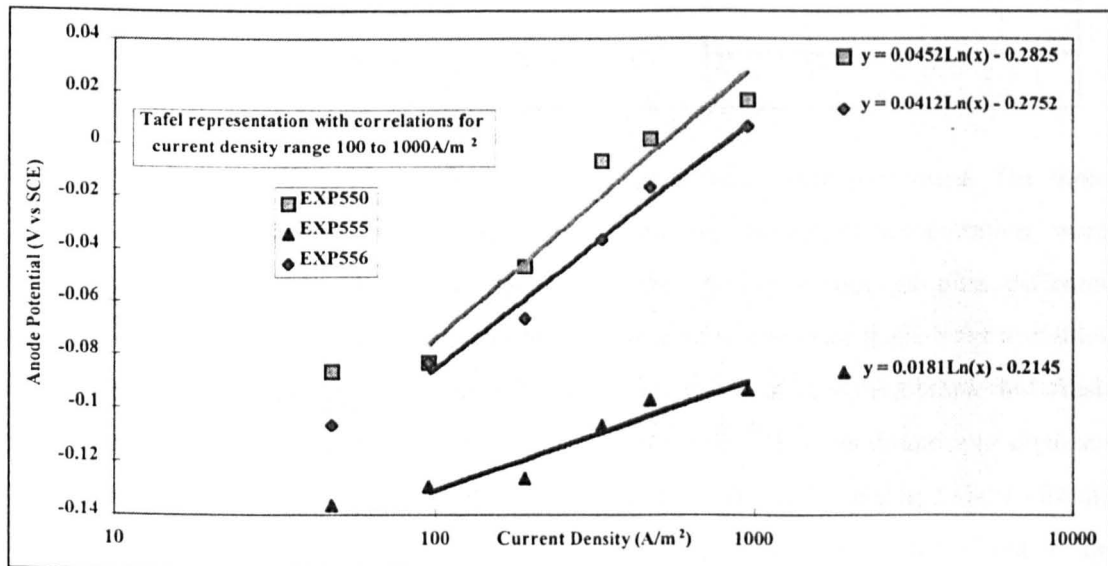


Figure 8-5: Tafel Plot



8.5 Electrolysis

Several different experiments were undertaken for the oxidation of toluene in methanol in the steel SPE reactor under galvanostatic conditions. All experiments utilised a Nafion®117 membrane pre-treated in a series of aqueous solvents, as discussed in Chapter 7. The reactor configuration included graphite felt electrodes, a graphite bed packed anode chamber, and a

stainless steel sprung cathode current collector. The electrolyte feed was controlled to ensure it matched the electro-osmotic flow. Data readings were taken every hour. These included all potential measurements, feed, anode chamber, cathode chamber, anode gas and cathode gas temperatures as well as gas volumes. Electrolyte samples were taken from the cathode chamber outlet every hour for analysis. Gas samples were taken at the end of the experiments.

Table 8-2: Summary of Electrolysis Conditions

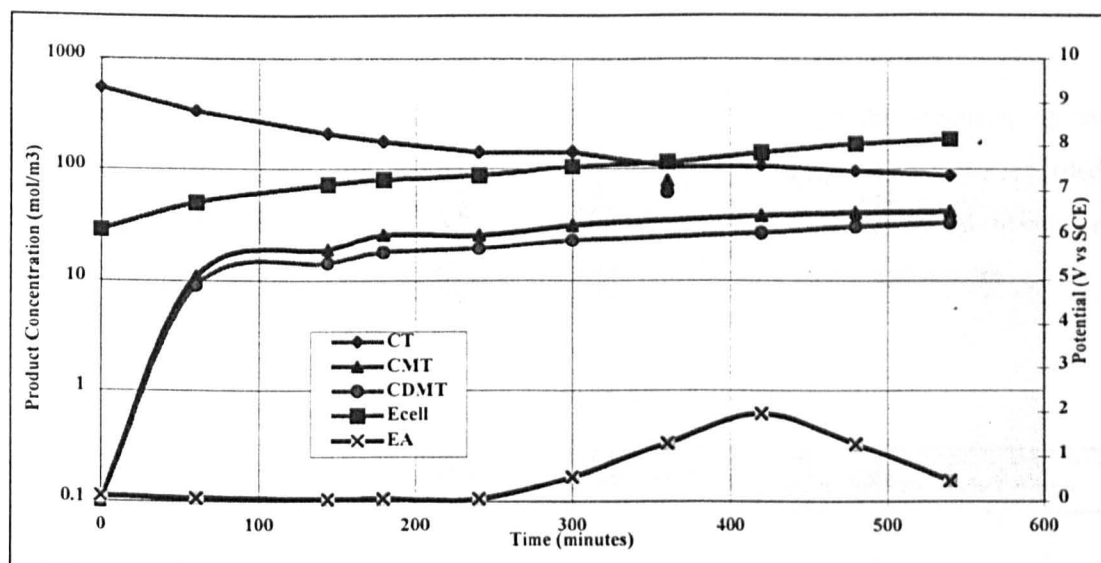
Experiment Number	Current Density (A/m ²)	Toluene Feed Concentration (%)	Temperature (°C)	Duration (hours)
EXP547	476	10	40	9
EXP548	952		50	7
EXP549	190		30	10
EXP552	190	30	50	9
EXP553	476		30	9
EXP554	333		40	4
EXP557	190	20	40	9
EXP558	476		50	9
EXP559	952		30	5.5

Table 8-2 shows the conditions under which the experiments were performed. The three main controlling parameters, i.e. current, temperature and electrolyte concentration, were tested at low, medium and high values three times giving a total of nine different combinations. Multiple linear regression (MLR) was used to correlate these input variables to several output parameters. The original plan was to use a new membrane and fresh electrolyte for each reaction. This was not always the case. The membrane was changed either after it had reached its useful life (after it had burnt through causing a short circuit) and always after a change in feed concentration. The experiments were carried out in the order of increasing current density as it was expected that the product distribution would rapidly reach a new steady state, certainly before the end of the 10 hours. The reactor system was completely refilled with fresh electrolyte only after the end of each set of 3 experiments. This allowed a steady state to be reached much quicker than if fresh electrolyte had been introduced each time the current density or temperature was changed.

8.6 Results And Data Analysis

The raw data from the galvanostatic experiments and chemical analysis are tabulated in Appendix 2. An example of the results are shown graphically in Figure 8-6 for experiment number EXP547 and a summary of the data is also given in Table 8-7. The results are discussed below with attention being paid to the amount and types of products produced by the reactions. The effect of the three applied parameters, current density, feed concentration and temperature, are aided by MLR analysis. A direct comparison between experimental data and the data produced by the MLR equations is shown in Appendix 6. A detailed discussion of the MLR equations is made in section 8.7.1, and the effect of the three main parameters on reactor performance is discussed in Chapter 9.

Figure 8-6: Example Result, EXP547



8.6.1 General Comments

Before the analysis of the data some general comments should be made which apply to all the experiments conducted in this set. The electro-osmotic flow was not as high as expected, in fact it was difficult to obtain an accurate reading from the rotameter because

1. the recycle flow rate was near the lower limit of the rotameter,
2. the recycle flow rate was not steady, and
3. the electrolyte sample size and frequency of sampling were large compared with the flow rate.

The electro-osmotic flow rate data in Appendix 2 are instantaneous readings. The average readings may be completely different as they take into account the mass balance, i.e. the electro-osmotic flow must be equal to the sum of the product rate and recycle flow rate.

Each electrolyte sample was analysed on the Perkin Elmer gc. This was calibrated for both reactants and two products, α -methoxytoluene and α,α -dimethoxytoluene. Four peaks were identified on the chromatograms relating to the two reactants and two products. The raw data (Appendix 2) also gives the results from the chromatograph and it can be seen that the methanol reactant concentration, in many cases, rises during the period of electrolysis. This obviously infringes the mass balance and is thought to be as a result of:-

- a change in density of the electrolyte due to production of species of greater density and/or
- the accuracy of the gc at its range limit.

8.6.2 Hydrogen Generation

Gaseous products generated in the reactor were collected over the duration of the experiment. The volume collected along with its temperature and pressure were recorded. When the volumeters were full, samples were taken which were analysed using gas chromatography. Table 8-3 shows the data collected and the chromatograph results.

Table 8-3: Summary Of Gas Analysis

Experiment Number	Chamber	Chromatograph Results (%)				Corrected Values (%)			Actual Rate (ml/hr)	Theoretical Rate (ml/hr)	Difference (%)
		H ₂	O ₂	N ₂	CH ₄	H ₂	O ₂	CH ₄			
EXP547	Anode	55.0	23.0	21.0	0.0	75.9	24.1	0.0	59.3	417.9	2.5
	Cathode	86.5	10.0	3.5	0.0	90.5	9.5	0.0	348.0		
EXP548	Anode	59.0	13.0	26.0	2.0	87.9	9.1	3.0	127.5	835.8	18.9
	Cathode	89.0	8.0	3.0	0.0	92.5	7.5	0.0	550.0		
EXP549	Anode	75.5	11.0	13.5	0.0	91.1	8.9	0.0	23.2	167.2	4.8
	Cathode	89.5	2.0	8.5	0.0	100.3	-0.3	0.0	136.0		
EXP552	Anode	78.0	4.5	17.5	0.0	100.2	-0.2	0.0	26.3	167.2	-13.4
	Cathode	64.0	17.0	19.0	0.0	84.3	15.7	0.0	163.3		
EXP553	Anode	88.0	7.5	4.5	0.0	93.3	6.7	0.0	58.0	417.9	0.0
	Cathode	90.0	2.0	8.0	0.0	100.1	-0.1	0.0	360.0		
EXP554	Anode	79.0	11.0	10.0	0.0	90.4	9.6	0.0	38.0	292.5	-0.5
	Cathode	77.0	11.0	12.0	0.0	90.8	9.2	0.0	256.0		
EXP557	Anode	49.0	20.0	31.0	0.0	80.6	19.4	0.0	21.8	167.2	-5.4
	Cathode	91.0	8.0	1.0	0.0	92.2	7.8	0.0	154.4		
EXP558	Anode	60.0	21.0	19.0	0.0	79.0	21.0	0.0	61.7	417.9	-4.0
	Cathode	92.5	6.5	1.0	0.0	93.7	6.3	0.0	372.9		
EXP559	Anode	87.0	3.0	10.0	0.0	99.6	0.4	0.0	98.2	835.8	-0.1
	Cathode								738.2		

The compositions have been corrected for the quantity of air based upon the nitrogen content. This was due to air trapped within the system at start-up. According to the chromatograph results the vast majority of gaseous product was hydrogen, the rest being made up of oxygen. One experiment detected a very small (3%) amount of methane although this was not detected in any of the other experiments. The production of oxygen was thought to be highly unlikely from methanol and toluene. A more likely source was the oxidation of water remaining in the pre-treated membrane. The theoretical amount generated is shown in Table 8-4. The value calculated is in the range 4.4 to 21.8% of the theoretical rate of hydrogen generation and this matches closely with the corrected values in Table 8-3.

Also noticeable is the amount of hydrogen collected at the anode side. Any hydrogen formed was expected to be by reduction of hydrogen ions at the cathode. Observation of hydrogen at the anode suggests that hydrogen is diffusing back through the membrane to the anode chamber as observed by Gerl^[1,21].

Table 8-4: Theoretical Oxygen Generation

Water Absorbed (g)	0.586
Moles of O ₂	0.0163
Volume at 22°C, 1 atm (ml)	364.6
Flow rate over 10 hours (ml/hr)	36.5

A comparison between the actual and theoretical quantity of producable hydrogen was made. This was based on 1 mole of hydrogen ions produced per mole of electrons. In the calculation all gas was regarded as hydrogen since the volume collected was the volume displaced by gas evolution and not necessarily the gas evolved itself. The comparisons show that 7 out of 9 of the experiments were within 5.4% of the theoretical value, and overall the difference was averaged to just 2.8% suggesting that the assumption was reasonably accurate.

8.6.3 Toluene Mass Balance

After 10 hours of electrolysis at new current densities and temperatures the electrolysis experiments were assumed to be at steady state. This allowed the performance of the reactor to be assessed. The first assessment involved the calculation of the current efficiency of the

system to produce the desired products, α -methoxytoluene and α,α -dimethoxytoluene. This was calculated on the basis of a 2 electron reaction for α -methoxytoluene and a 4 electron reaction for α,α -dimethoxytoluene. The concentration of products at steady state were taken as the final outlet concentrations and are shown in Table 8-7, on page 94. The product stream flow rate was assumed to be the same as the feed rate. Using these values the current efficiency for product formation lies between 1.39 and 8.96% indicating the formation of by-product(s) being the dominant reaction. These results are shown in Table 8-5.

On close inspection the amount of toluene contained in the products and in the unreacted toluene do not match the amount entering the reactor system. A mass balance on the toluene compounds revealed that a large proportion of toluene was unaccounted for. The results are shown in Table 8-5. These very low efficiencies suggest the major reaction was the formation of a by-product and this is discussed in Section 8.6.3.1. A mass balance on methanol was not possible due to the chemical analysis showing a greater concentration of unreacted methanol than in the feed stream alone (see Appendix 2).

Table 8-5: Current Efficiency for the SPE Reactor

Experiment Number	Applied Current (A)	Current Efficiency (%)	Toluene Flow (mol/s)			
			Reactor Feed	in Products	Unreacted	Unaccounted
EXP547	1.0	5.72	2.41E-06	2.06E-07	4.69E-07	1.73E-06
EXP548	2.0	8.15	2.41E-06	4.83E-07	2.14E-07	1.71E-06
EXP549	0.4	1.39	2.41E-07	1.93E-08	4.89E-08	1.73E-07
EXP552	0.4	5.53	3.18E-06	1.04E-07	5.24E-07	2.55E-06
EXP553	1.0	4.42	4.83E-06	1.99E-07	8.58E-07	3.77E-06
EXP554	0.7	8.96	5.84E-06	2.78E-07	1.02E-06	4.53E-06
EXP557	0.4	3.05	2.20E-06	5.69E-08	3.61E-07	1.78E-06
EXP558	1.0	3.59	4.14E-06	1.62E-07	6.75E-07	3.30E-06
EXP559	2.0	3.85	4.86E-06	3.25E-07	6.78E-07	3.86E-06

8.6.3.1 By-product Identification

A change in colour of the electrolyte during all experiments was evidence of some formation of a by-product. Both reactants are colourless as are the two identified products. The identification of the by-product of electrolysis was investigated first by chromatography using the existing temperature program extended to 30 minutes. No additional peak was detected. GC-MS identified several peaks with mass numbers 329, 461,

973, 1124, 1247 and 1484 but no compound from the database matched with the chromatogram sufficiently, nor was thought possible from the two reactants.

Separation of the product was also attempted using a silica packed capillary column. The column was first washed through with petroleum ether and 21 samples were collected. This left a brown phase on the silica thought to be the by-product. This was then washed off successfully with acetone and ten samples were collected numbered 101-110. The first samples (1-21) contained some methanol, toluene, α -methoxytoluene and α,α -dimethoxytoluene, but the last ten (101-110) gave no peaks on the SE-30 GC column.

Distillation of the final product managed to separate methanol, toluene, α -methoxytoluene and α,α -dimethoxytoluene from the unknown by-product which was tar like: viscous and nearly black. This was left in a fume cupboard for several days allowing the solvents to evaporate. Elemental analysis was then carried out to assess carbon, hydrogen and nitrogen content. The first analysis only detected ~65% of the mass. The remaining 35% was thought to be due either to oxygen from the by-product (the only other element in the reactant mixture) or from solvent that had not evaporated. If this was methanol then the carbon and hydrogen would have been included in the analysis. Ignoring this undetected amount gave a compound with a carbon to hydrogen molar ratio of 1:1.2. These results are shown under the experiment number EXP559 in Table 8-6.

Table 8-6: Elemental Analysis

Experiment Number	Mass Concentrations (%)			Molar Ratios			
	C	H	N	C	H	O*	N
EXP559	59.44	6.10	0.00	4.95	6.10	2.15	0.00
	59.44	6.10	0.00	4.95	5.88	2.17	0.00
EXP516	61.29	5.21	0.27	5.11	5.21	2.08	0.02
	61.12	5.07	0.11	5.09	5.07	2.11	0.01

* assuming unknown amount is oxygen

Another sample was prepared, labelled EXP516, this time by storing in an oven at 100°C for 1 month. This allowed 26% of its mass to be lost through solvent evaporation. The by-product solidified during this time. Elemental analysis again showed an undetected amount this time 34%. The carbon to hydrogen ratio of 1:1 was again similar. These results point to a by-product mainly based upon toluene which has a carbon to hydrogen ratio of 1:1.14.

8.7 Multiple Linear Regression (MLR)

Statistical analysis was carried out on data from the galvanostatic experiments to generate empirical relations governing some process variables. This was done for two reasons:-

1. for further use in modelling of the system , or
2. to compare the generated model over a range of conditions.

Since only a small number of experiments were carried out on the system statistical analysis enabled trends to be calculated to fill in gaps where only more experiments was the alternative.. Using a small data set meant that the fit of the generated empirical equations was not always as high as desired. The value of ρ , the correlation coefficient between the real and empirical values, ranged from 0.69 to 0.94. The error ranged from 0.25 to 0.84.

Electro-osmotic flow is known to be dependent only upon the applied current density and so this was used as a basis for the particular MLR equation. The anode potential is related to the current density and temperature via the Tafel equation. It's relationship with reactant concentration is found by considering a simple rate equation. Hence, this MLR equation also has some theoretical justification. A similar relationship is also used for the two product concentrations.

The data used in the MLR analysis is shown in Table 8-7 and the resulting equations are tabulated in Table 8-8. A direct comparison between the experimental data and the MLR results is shown in Appendix 6. Table 8-9 shows equations used to asses the fit of the MLR equations to experimental data.

Table 8-7: Data Used in MLR

Experiment Number	Duration (hr)	Average Values			Steady State Values							
		Current Density (mA/cm ²)	T _A (°C)	C _{Tr} (%)	SPE Age (hr)	E _{CELL} (V)	E _M (V)	E _A (V vs SCE)	F _{OS} (ml/hr)	C _{MT} (mol/m ³)	C _{DMT} (mol/m ³)	C _T (mol/m ³)
EXP547	9.0	47.6	37.6	10	9.0	8.4	7.00	0.65	10.5	41.5	32.6	169
EXP548	7.0	95.2	51.3	10	16.0	14.3	12.97	0.20	49.0	44.0	130.0	77
EXP549	10.0	19.0	32.2	10	26.0	11.9	11.09	0.30	1.0	35.6	34.0	176
EXP552	9.0	19.0	49.2	30	9.0	8.1	7.29	0.39	4.3	77.0	9.1	436
EXP553	9.0	47.6	28.7	30	18.0	14.2	10.75	2.05	6.6	92.4	16.5	470
EXP554	4.0	33.3	38.3	30	22.0	11.5	8.65	2.07	7.9	104.6	21.4	464
EXP557	9.0	19.0	37.7	20	9.0	4.6	3.70	0.14	4.5	40.1	5.1	287
EXP558	9.0	47.6	49.0	20	18.0	5.2	4.08	0.77	8.5	58.4	10.1	285
EXP559	5.5	95.2	34.8	20	23.5	15.0	10.53	2.12	33.4	90.5	26.5	244

Some variables used were the steady state variables i.e. at the end of the experiment. With the exception of membrane age these variables were the response variables. The independent variables used in the MLR were average values, with the exception of membrane age, which was defined as the age of the membrane at the start of the experiment.

The MLR was carried out using MATLAB software and the Multi-Dat toolbox. Correlations generated were based upon functions of the 5 independent variables: current density(j), anode temperature(T_A), toluene concentration(C_{Tf}), membrane age (A_M) and duration(t). The most significant variable for all dependent variables, except unreacted toluene, was the current density. Toluene feed concentration was also highly significant for the product concentrations, and most significant for unreacted toluene concentration

Table 8-8: Empirical Equations from Multiple Linear Regression

Equation	Error	ρ^2
$F_{OS} (ml / hr) = 1.7 \times 10^8 j - 3.2 \times 10^{10}$	0.33	-
$E_A (V \text{ vs } SCE) = 2.0 \log_{10} j - 0.062 T_A - 2.9 \log_{10} \left[\frac{1}{C_{Tf}} \right] + 9.5$	0.40	0.86
$E_M (V) = 4.7 \times 10^{-3} j - 0.058 T_A - 2.6 \times 10^{-4} C_{Tf} + 5.1 \times 10^{-5} A_M + 22$	0.84	0.48
$E_{CELL} (V) = 9 \times 10^{-3} j - 0.20 T_A + 9.2 \times 10^{-4} C_{Tf} + 4.9 \times 10^{-5} A_M + 63$	0.62	0.71
$C_T (mol / m^3) = -0.081 j - 1.9 T_A + 0.17 C_{Tf} + 640$	0.13	0.99
$C_{MT} (mol / m^3) = 0.075 j + 1.7 \times 10^{16} \exp \left[\frac{-F}{R T_A} \right] + 6.8 \times 10^{-3} C_{Tf} + 2.0 \times 10^{-3} t - 44$	0.26	0.95
$C_{DMT} (mol / m^3) = 0.072 j + 6.2 \times 10^{16} \exp \left[\frac{-F}{R T_A} \right] - 0.017 C_{Tf} - 4.1 \times 10^{-4} t + 29$	0.72	0.60

Independent variables are in SI units

Table 8-9: Assessment Equations

Correlation Coefficient	$\rho = \frac{\text{cov}\{y_{real}, y_{model}\}}{s_{real}, s_{model}}$
Covariance	$\text{cov} = \frac{\sum (y_{real} - \bar{y}_{real})(y_{model} - \bar{y}_{model})}{n}$
Standard Deviation	$s_{real} = \sqrt{\frac{\sum (y_{real} - \bar{y}_{real})^2}{n}}$
Standard Error	$error = \frac{\sum (y_{real} - y_{model})^2}{n_s - (n_v + 1)}$

8.7.1 Analysis of MLR

Although detailed examination of the effect of the applied parameters is carried out in Chapter 9, some analysis is made here comparing the MLR equations with the experimental data. The current density and feed concentration had greatest influence on the reactor performance. Temperature was thought to have little effect at the ranges considered when compared with the other two variables.

Increasing the current density increased the yield of both products, but not at the same rate. The yield of α,α -dimethoxytoluene increased at a faster rate causing a shift in selectivity away from α -methoxytoluene. This is seen most easily for the experiments at 20% toluene feed concentration where the ratio of final product concentrations fell from 7.9 to 3.4 on increasing the current density from 190 to 952A/m². However, according to the MLR equations the concentration of α -methoxytoluene should increase at a slightly higher rate compared to α,α -dimethoxytoluene. This small error is due to the very small number of data points used in the MLR analysis.

The effect of the feed concentration of toluene was much easier to detect. For 10% the α -methoxytoluene concentrations were approximately 40mol/m³, for 20% they were 60mol/m³ and 30% they were 90mol/m³. For α,α -dimethoxytoluene the situation was not quite so clear, with most values below 35mol/m³ and smaller with higher feed concentrations. This gave three discrete bands, one for each feed concentration. The product ratios, in order of increasing feed concentration, were 1.2, 5.7 and 6.3. This showed that the toluene feed

concentration not only increased the α -methoxytoluene concentration, but reduced the α,α -dimethoxytoluene concentration. This situation was also reflected in the MLR equations.

The effect of reactant feed may be explained by considering the availability of the two reactants. With a very high concentration of methanol, α,α -dimethoxytoluene would be expected to feature strongly as this is formed from two rather than one methanol molecule. With a high concentration of toluene the opposite situation would be expected.

According to the MLR equations an increase in temperature increases the yield of both products. This was difficult to determine from the data alone as the effect was much smaller than the effect of feed concentration or current density. Using the range of conditions used in the experiments the strength of the parameters were assessed by substituting into the MLR equation for α -methoxytoluene concentration. The result showed that current density had the highest effect, and temperature the lowest.

The amount of unreacted toluene also showed the same features as the products. These are reflected in the MLR generated equation. This showed that on increasing the current density and temperature the amount of unreacted toluene would fall. Increasing the feed concentration of toluene increased the amount of unreacted toluene.

8.8 Summary

The flowcell reactor was used successfully for the oxidation of toluene in methanol. No solvents or liquid phase electrolytes were used. Performance of the reactor was assessed over a range of temperatures, current densities and feed concentrations. Chemical analysis showed that no oxidation of methanol to carbon dioxide took place. The main gaseous product was hydrogen and this reaction took place with an electron stoichiometry of 2. Liquid products were formed at low current efficiencies, with the main reaction consuming large quantities of toluene.

Multiple linear regression was used to assist in the analysis of the reactor. This showed that increasing the current density increased the selectivity of α,α -dimethoxytoluene. The feed concentration also played a large part in selectivity. Increasing the toluene feed concentration favoured the production of α -methoxytoluene. The effect of reactor

temperature was much smaller than the current density or feed concentration effect, but an increase in temperature was shown to increase the yield of both products.

9. MODELLING

9.1 Introduction

A model of the SPE oxidation of toluene in methanol was developed in order to simulate the experimental results discussed in Chapter 8. The effect of changing forcing variables (current density, temperature and feed concentrations) was seen on the output from the simulation (cell potential, anode overpotential, and product distribution). A further use of the simulation was to predict performance of scaled-up reactors. To this end changing dimensions of the notional reactor design was sufficient.

For the model the SPE reactor was divided into a series of blocks. The model connected mass balances over each block to build an overall mass balance of the process. Initially feed conditions, reactor dimensions and electrochemical constants were input. From this the flows through the reactor were calculated. The model assumes the SPE reactor to be a plug flow reactor with recycle. The flow through the reactor being determined by the electro-osmotic flow. The feed rate to the reactor is limited by the size of the electro-osmotic flow so that the anode chamber cannot be overfilled.

The reaction model was based on that developed by Haines^[70]. Two reaction schemes were considered and developed and the final selection of a parallel competing reaction was included in the reactor model. Use was made of the empirical equations derived from the flow reactor for data not available and the model was compared with the data generated from experimental runs.

9.2 Reaction Schemes

The first task in developing the model was to decide on the reaction scheme. Two such schemes were developed, and one was chosen for inclusion in the model. The first to be considered (Scheme 1) was a two electron step process involving both reactants. The second proposal (Scheme 2) involved generation of a methoxy radical as the initial step in the reaction. Scheme 1 was chosen for the model because it was based on work published by Wendt et al^[63,64]. The following Sections describe the two schemes.

9.2.1 Scheme 1

This reaction scheme involved only electrochemical and mass transfer reactions and the proposed routes are shown in Table 9-1. Because the reactants were in high concentration (in effect they were solvents as well as reactant species) and the conversion over a small time step was small then the concentration gradient was zero. This meant that mass transfer of reactants was also zero since bulk and surface concentrations for reactant were equal.

Table 9-1: Reaction Scheme 1 - e-e Mechanism

Number	Reaction	Type
r_1	$M_{surface} + T_{surface} \xrightarrow{k_{f1}} MT_{surface} + 2H^+ + 2e^-$	e
r_2	$M_{surface} + MT_{surface} \xrightarrow{k_{f2}} DMT_{surface} + 2H^+ + 2e^-$	e
r_3	$M_{surface} + H_2O_{surface} \xrightarrow{k_{f3}} CO_2 + 6H^+ + 6e^-$	e
r_4	$2T_{surface} \xrightarrow{k_{f4}} P_{surface} + 2H^+ + 2e^-$	e
r_5	$H_2O_{bulk} \xrightarrow{k_{tH}} H_2O_{surface}$	mt
r_6	$MT_{surface} \xrightarrow{k_{tMT}} MT_{bulk}$	mt

Mass transfer was only considered for transport of intermediate α -methoxytoluene to the surface and also that of water. Water was included as it was known to take part in the oxidation of methanol to carbon dioxide. Although the methanol was 99.9 % pure, some moisture was expected. Absorbed water remaining in the membrane from the pre-treatment process was also expected to take part in some oxidation.

The oxidation of methanol was considered to be one of two reactions resulting in the loss of current efficiency. The other was the dimerisation of toluene. From the work of Wendt,^[63,64] and the evidence of the elemental analysis, toluene polymerisation was thought to be the major competing reaction.

The electrochemical reactions were assumed to be irreversible first order reactions in each component and described by Tafel type equations. Diffusional mass transfer of water and α -methoxytoluene were explained by Fick's First Law. The six rates were expressed by the following equations:-

$$r_1 = k_{f1} \cdot C_M \cdot C_T \quad \text{Equation 9-1}$$

$$r_2 = k_{f2} \cdot C_M \cdot C_{MT_{surface}} \quad \text{Equation 9-2}$$

$$r_3 = k_{f3} \cdot C_M \cdot C_{W_{surface}} \quad \text{Equation 9-3}$$

$$r_4 = k_{f4} \cdot C_T^2 \quad \text{Equation 9-4}$$

$$r_5 = N_W = -D_W \frac{\partial C_W}{\partial z} = k_{LW} (C_{W_{bulk}} - C_{W_{surface}}) \quad \text{Equation 9-5}$$

$$r_6 = N_{MT} = -D_{MT} \frac{\partial C_{MT}}{\partial z} = k_{LMT} (C_{MT_{surface}} - C_{MT_{bulk}}) \quad \text{Equation 9-6}$$

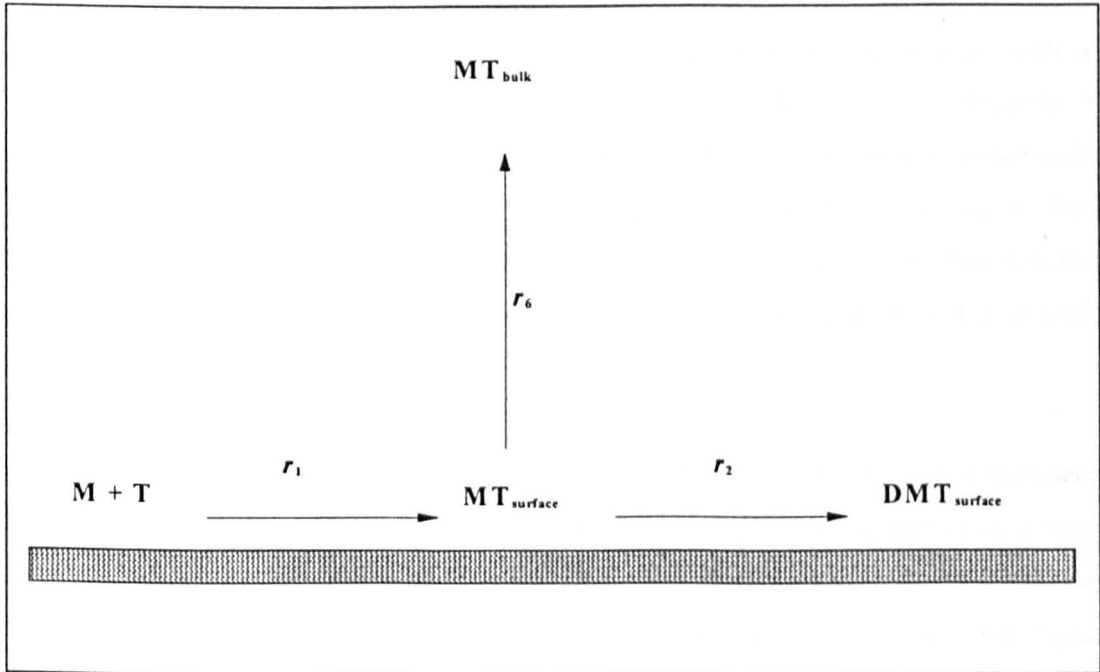
In order to eliminate the surface concentration of water, Equation 9-3 and Equation 9-5 were combined giving:-

$$\frac{r_3}{k_{f3} \cdot C_M} = C_{W_{bulk}} - \frac{r_4}{k_{LW}} \quad \text{Equation 9-7}$$

At steady state the diffusion of water to the electrode surface equals the rate of reaction of water at the surface. This means that at steady state $r_3=r_4$. Rearranging Equation 9-7 gives the rate in terms of the bulk concentrations only:-

$$r_3 = r_4 = \frac{k_{LW} \cdot k_{f3} \cdot C_M \cdot C_{W_{bulk}}}{(k_{LW} + k_{f3} \cdot C_M)} \quad \text{Equation 9-8}$$

Figure 9-1: Electrode Surface At Steady State



To eliminate the surface concentration of methoxytoluene from Equation 9-2 and Equation 9-6 a steady state mass balance at the surface was also made. Figure 9-1 shows

diagrammatically the three rates considered. At steady state the rate of formation of methoxytoluene equals the rate of disappearance. This disappearance can arise in either of two ways. The first is the reaction of α -methoxytoluene with methanol to produce α,α -dimethoxytoluene; the second is diffusion from the surface to the bulk.

At steady state $r_1 = r_2 + r_6$, or

$$k_{f1} \cdot C_M \cdot C_T = k_{f2} \cdot C_M \cdot C_{MT_{surface}} + k_{LMT} \cdot (C_{MT_{surface}} - C_{MT_{bulk}}) \quad \text{Equation 9-9}$$

rearranging in terms of the surface concentration gives:-

$$C_{MT_{surface}} = \left[\frac{k_{f1} \cdot C_M \cdot C_T + k_{LMT} \cdot C_{MT_{bulk}}}{(k_{f2} \cdot C_M + k_{LMT})} \right] \quad \text{Equation 9-10}$$

Substituting this into the rate equations gives the rate of formation in terms of the bulk concentrations:-

$$r_2 = k_{f2} \cdot C_M \left[\frac{k_{f1} \cdot C_M \cdot C_T + k_{LMT} \cdot C_{MT_{bulk}}}{k_{f2} \cdot C_M + k_{LMT}} \right] \quad \text{Equation 9-11}$$

The equations used in the model were Equation 9-1, Equation 9-4, Equation 9-8 and Equation 9-11.

9.2.2 Scheme 2

An alternative reaction scheme was also derived that involved chemical as well as electrochemical reactions. The first step involved the electrochemical generation of methoxy radicals. These were then free to take part in homogeneous reactions either at the surface or in the diffusion layer, (the concentration of radicals in the bulk being zero). These subsequent reactions could involve many other species forming a variety of products that are typical of free radical reactions. The ones considered for this model are listed in Table 9-2.

The reactions again were assumed to be irreversible and first order in each component. Reactions such as the oxidation of methanol with water, and the dimerisation of toluene were also included. The electrochemical reactions were developed as in the first scheme; the homogeneous chemical reactions were more complicated due to the non linear concentration gradient in the diffusion layer caused by significant rates of reactions taking place in this layer. The reactions considered for the second scheme were:-

$$r_{11} = k_{f11} \cdot C_{M_{surface}} = k_{f11} \cdot C_{M_{bulk}}$$

$$r_{12} = k_{12} \int_0^{\delta} C_{MR_z} \cdot C_{T_z} \cdot dz = k_{12} \cdot C_{T_{bulk}} \int_0^{\delta} C_{MR_z} \cdot dz$$

$$r_{13} = k_{13} \int_0^{\delta} C_{MT_z} \cdot C_{MR_z} \cdot dz$$

$$r_{14} = N_{MR} = -D_{MR} \frac{\partial C_{MR}}{\partial z}$$

$$r_{15} = N_{MT} = -D_{MT} \frac{\partial C_{MT}}{\partial z}$$

as well as r_3 , r_4 and r_5 from Scheme 1.

Table 9-2: Reaction Scheme 2: Free Radical Mechanism

Number	Reaction	Type
r_{11}	$M \xrightarrow{k_{f11}} MR \bullet + H^+ + e^-$	e
r_{12}	$MR \bullet + T \xrightarrow{k_{12}} MT + \frac{1}{2} H_2$	c
r_{13}	$MR \bullet + MT \xrightarrow{k_{13}} DMT + \frac{1}{2} H_2$	c
r_3	$M_{surface} + H_2O_{surface} \xrightarrow{k_{f3}} CO_2 + 6H^+ + 6e^-$	e
r_4	$2T_{surface} \xrightarrow{k_{f4}} P_{surface} + 2H^+ + 2e^-$	e
r_5	$H_2O_{bulk} \xrightarrow{k_{1W}} H_2O_{surface}$	mt
r_{14}	$MR_{surface} \xrightarrow{k_{LMR}} MR_{bulk}$	mt
r_6	$MT_{surface} \xrightarrow{k_{LMT}} MT_{bulk}$	mt

To derive an expression for the concentrations of α -methoxytoluene and methoxy radical in the diffusion layer an instantaneous molar balance was carried out over a thickness Δz .

$$0 = in - out + produced - reacted$$

$$0 = (N_{MR_z} - N_{MR_{z+\Delta z}}) + 0 - \Delta z (k_{12} \cdot C_{MR_z} \cdot C_T + k_{13} \cdot C_{MT_z} \cdot C_{MR_z})$$

$$0 = -\frac{(N_{MR_{z+\Delta z}} - N_{MR_z})}{\Delta z} - (k_{12} \cdot C_{MR_z} \cdot C_T + k_{13} \cdot C_{MT_z} \cdot C_{MR_z})$$

In the limit as $\Delta z \rightarrow 0$,

$$0 = \frac{\partial N_{MR_z}}{\partial z} + k_{12} \cdot C_{MR_z} \cdot C_T + k_{13} \cdot C_{MT_z} \cdot C_{MR_z}$$

$$\text{but } N_{MR_z} = -D_{MR} \frac{\partial C_{MR_z}}{\partial z}$$

therefore

$$\frac{\partial^2 C_{MR_z}}{\partial z^2} - \left(\frac{k_{12} \cdot C_T + k_{13} \cdot C_{MT_z}}{D_{MR}} \right) C_{MR} = 0$$

A similar process for α -methoxytoluene gave:-

$$\frac{\partial^2 C_{MT_z}}{\partial z^2} - \frac{k_{13} \cdot C_{MR_z} \cdot C_{MT_z}}{D_{MT}} = \frac{-k_{12} \cdot C_{MR_z} \cdot C_T}{D_{MT}}$$

Solving these two equations would give the concentrations of methoxy radical and methoxytoluene as a function of position in the diffusion layer. This would allow r_{12} and r_{13} to be solved analytically.

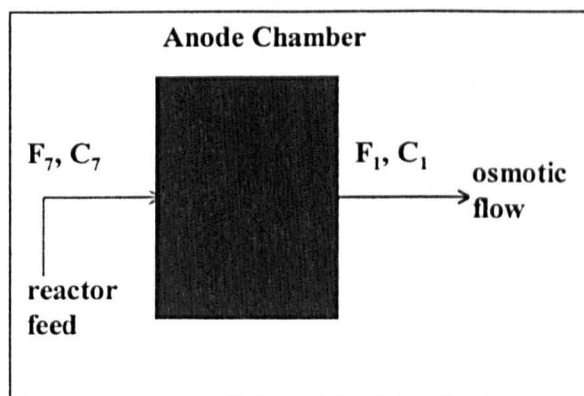
9.3 Mass Balances

The material balances which form the basis of the reactor model are developed here using Scheme 1, Table 9-1, as the model reaction mechanism.

9.3.1 Anode Mass Balances

Appendix 5 shows the reactor block diagram used to develop the mass balances. The most complicated mass balances were carried out over the anode where the electrochemical reactions took place and Figure 9-2 shows the schematic of the anode block.

Figure 9-2: Anode Mass Balance



Applying the mass balance to each component in the anode gave the differential change in concentration. This is demonstrated using methanol:-

Reacted + In - Out = Accumulation

$$r_M \cdot A_a + F_7 \cdot C_{M7} - F_1 \cdot C_{M1} = \frac{d}{dt}(V_A \cdot C_{M1})$$

but since

$$r_M = -r_1 - r_2 - r_3$$

$$\left[k_{f1} \cdot C_{M1} \cdot C_{T1} + k_{f2} \cdot C_{M1} \left(\frac{k_{f1} \cdot C_{M1} \cdot C_{T1} + k_{LAW} \cdot C_{M1} \cdot C_{W_{\infty}}}{k_{f2} \cdot C_{M1} + k_{LAW}} \right) + \frac{k_{LW} \cdot k_{f3} \cdot C_{M1} \cdot C_{W_{\infty}}}{(k_{LW} + k_{f3} \cdot C_{M1})} \right] \frac{A_a}{V_A} + \frac{F_7 \cdot C_{M7}}{V_A} - \frac{F_1 \cdot C_{M1}}{V_A} = \frac{d}{dt}(C_{M1})$$

Similar equations were developed for the other components in the system. These were then solved separately using a fourth order Runge Kutta method. This was possible by using a small time step and assuming that other components were constant over this time step. For example, when differentiating the above equation for methanol the concentrations of water, α -methoxytoluene and toluene were assumed steady. When the respective toluene equation was differentiated the methanol and α -methoxytoluene concentrations were assumed constant. According to Runge Kutta:-

$$C_{M1}(t+1) = C_{M1}(t) + \frac{h}{6} \{g_1 + 2g_2 + 2g_3 + g_4\}$$

where g_1 , g_2 , g_3 and g_4 are the differentials evaluated with $C_{M1}(t)$ equal to $C_{M1}(t)$,

$$C_{M1}(t) + \frac{h}{2} \cdot g_1, C_{M1}(t) + \frac{h}{2} \cdot g_2 \text{ and } C_{M1}(t) + h \cdot g_3 \text{ respectively.}$$

9.3.2 Other Mass Balances

Mass balances over the other blocks were less complex. This was due to the reaction term disappearing. Runge Kutta was again used to solve the differential equations. In the cathode chamber mass balance the formation of hydrogen was based, not upon the amount of H^+ ions generated at the anode, but on 100% current efficiency. The result of these other mass balances was either a new block concentration, for example in the cathode chamber, or a new stream concentration, for example with the recycle separator. Figure 9-3 shows the schematic for the recycle loop. The time lag due to the length of the recycle line was calculated by compensation for the volumetric recycle flow rate. The lagtime was calculated from:-

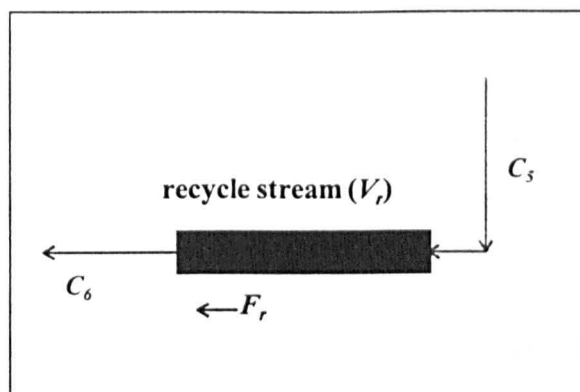
$$\text{lagtime} = t - \tau_r = t - \frac{V_r}{F_r}$$

where V_r = recycle line volume, and F_r = recycle flow rate. This allowed the exit of the recycle stream to be calculated knowing the inlet history from:-

$$C_6(t) = C_5(t - \tau_r)$$

For those occasions where τ_r was greater than t then the lagtime was set to zero.

Figure 9-3: Time-Lag in the Recycle Line



9.4 Galvanostatic Operation

The experimental runs were all controlled galvanostatically. In order to ensure constant current operation in the model the following procedure was adopted. First the four rate constants were calculated using a guessed anode overpotential and a Tafel type function. From this the four rates and, hence, the current density were calculated. A comparison between this calculated current density and the applied current density was made. If the error was less than 0.5% the guessed overpotential was accepted, otherwise a new guess was made. This process was repeated for each time through the loop. As the reactions progressed concentrations changed which altered the rates of reaction. Changing the anode overpotential ensured the overall rate was set at the limit defined by the applied current density.

New guesses of overpotential were made by incrementing previous values. For errors greater than $\pm 2\%$ the change was $\pm 0.001\text{V}$; errors between 2 and 0.5% were incremented by 0.00001V . This method gave a sufficiently rapid convergence to a reasonably accurate level without resorting to more complex techniques such as Newton-Raphson approximation. The convergence was measured by counting the number of times around the increment loop. For a number greater than 5000 the program stopped.

9.5 Mass Transfer Coefficient

Diffusion of water and α -methoxytoluene from the bulk electrolyte to the reaction surface was assumed to take place according to Fick's Law. A linear concentration profile in the diffusion layer was also assumed. No concentration gradient was necessary for the bulk electrolyte due to large concentrations at the surface.

Calculation of mass transfer coefficients were based upon the work by Carta et al^[71]. They correlated the Reynolds and Sherwood Numbers for Sigri's carbon felt using the equation:-

$$Sh = 3.19 Re^{0.69} \quad \text{Equation 9-12}$$

This equation was developed for hydraulic Re values between 1 and 10 for the reduction of ferricyanide and cupric ions. The empirical equation was compared to the results of other workers who examined several types of porous electrodes including different carbon felts. . The constant term contains the often used Schmidt term to the power 1/3 and was calculated as 602 for this system Equation 9-12 was used in the model using the physical properties of the felt supplied in the paper^[71] and by expanding the dimensionless groups.

$$k_L = 3.19 \times \left(\frac{D}{d_{fh}} \right) \left(\frac{\rho \cdot u \cdot d_{fh}}{\mu} \right)^{0.69}$$

In this expression d_{fh} is the hydraulic felt diameter and is calculated from the porosity of the felt by:-

$$d_{fh} = 4\epsilon / S_B$$

The specific electrode area S_B is also calculated from the porosity:-

$$S_B = \frac{4}{d_f} \cdot (1 - \epsilon)$$

d_f is the diameter of the felt fibres and for the carbon felt used by Carta^[71] was measured as $(11.0 \pm 0.5) \times 10^{-6}$ m. The Reynolds number for the experimental results was 3.78×10^{-4} using an electro-osmotic flow of 10 ml/hr indicating laminar type flow. This gave a mass transfer coefficient of 8.07×10^{-8} m/s. However, the mass transfer correlation of Carta^[71] exhibits a dependence on the Reynolds number which is more representative of turbulent flow, although reduced dependency on the Reynolds number is indicated at low values. Insufficient data in this region does not permit adequate correlation, thus, predicted mass transfer coefficients are likely to be underestimated using this correlation. Despite this limitation Carta's correlation was adopted since it was the closest set of data available in the literature and was initially adequate for the purposes of the model.

9.6 Transfer Coefficient

The value of the transfer coefficient used in the model was derived from the potentiostatic scans of the flowcell experiments, see Section 4 in Chapter 8. These gave values of the transfer coefficient as 0.472.

9.7 Electro-Osmotic Flow

The ionic species generated during electrolysis were H^+ ions. Methanol, toluene, α -methoxytoluene, α,α -methoxytoluene and by-products were dragged across the membrane by movement of the protons from the anode to the cathode driven by the potential gradient. This transport was detected by analysing the catholyte. The electro-osmotic flow, which was defined in Chapter 7 was, for the purposes of modelling, assumed to equally apply to all the species present in the anode chamber. Hence, the concentration of species flowing through the membrane was assumed to be the same concentration as that present in the anode chamber. In reality this assumption may not be true due to the differing abilities of the species to solvate protons.

Pressure driven viscous flow was not thought to be a major mode of transport in the SPE reactor since even at maximum swelling the pore size was small (the feed rate of electrolyte only reached a maximum of 10 ml/hr). The concentration driving force was also thought relatively small compared to the potential driving force. Only in the diffusion layer was a concentration driving force expected to be significant since the conversion was small and reactant concentration high.

The empirical equation generated by multiple linear regression of the experimental data was used in the model. Dependence only on current density gave a good fit over the data and a low error value. For the model the empirical equation was altered to allow performance testing to be simulated with other membrane areas A_a .

$$F_{os} = \frac{(0.479j - 8.888)}{0.021} \times A_a$$

9.8 Potentials

The anode overpotential was calculated as described above in Section 9.4 in order to control the simulation galvanostatically. The cell potential was made up of this overpotential plus the membrane and cathode potentials. The membrane potential was calculated from the empirical equation generated from multiple linear regression which was based upon current density, temperature, electrolyte composition and age of the membrane:-

$$E_M = 0.047j - 0.058T_A - 0.023C_{Tf} + 0.182A_M + 5.938$$

The cathode potential was calculated using Tafel data for hydrogen evolution on graphite cathodes. Pickett^[72] lists Tafel data for several electrodes at 20°C. The one for graphite is:-

$$\eta_c = -0.39 - 0.21 \log j$$

where the overpotential is in Volts and the current density in A/m².

9.9 Side Reaction

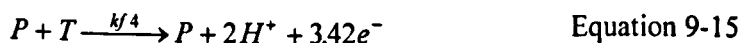
Before the model could be optimised the side reaction scheme had to be resolved. It was decided that this must be an electrochemical step, since such a large proportion of current was lost in the experimental runs. Also it couldn't involve methanol since the final concentration of this reactant was high. Literature^[63,64] and experimental evidence had pointed towards some polymer-like compound being formed. This could be modelled in several ways. The first to be tried involved the formation of a toluene dimer according to :-



Using this model caused a rapid loss of toluene due to the reaction consuming one mole of toluene per mole of electrons. For a fixed rate of reaction (fixed rate constant and potential) a smaller consumption of reactant takes place when the electron stoichiometry is high. A more realistic model was based on the addition of a toluene molecule onto an existing polymer chain. In this case only half a mole of toluene is consumed per mole of electrons:-



Even with this model there were some instances where the toluene concentration in the reaction zone became negative. Again this was due to the low ratio of electrons to toluene. The final model chosen, Equation 9-15, was based upon a mass balance carried out on the data generated purely from the multiple linear regression. This gave an electron to toluene ratio in the polymerisation reaction of 3.42, see the final column in Table 9-4.



9.10 Optimisation

Optimisation of the model involved selection of parameters that had not already been fixed. These were the electrochemical rate constants k_{f1} , k_{f2} , k_{f3} and k_{f4} . To do this, data was first generated for several combinations of applied variables by utilising the MLR equations. Next, values of the rate constants in the model were changed until the model gave results matching those predicted by MLR experiment H3. The model was then run using the same combination of applied variables so that comparisons could be made with experimental data and MLR generated data

9.10.1 MLR Experiments

These experiments were created for two reasons. The first was to enable the rate constants to be determined. For this the three main independent variables, current density, feed concentration and anode temperature, were fixed at their mean values for the SPE experiments. Those were 500A/m², 20% toluene and 40°C. The empirical equations generated from the MLR were then used to calculate the resulting product stream concentrations, anode overpotential and cell potential. The electro-osmotic flow was also calculated. The rate constants in the model could then be adjusted to give matching dependent variables.

The alternative would have been to optimise the model with an SPE experiment. Unfortunately no one experiment had the mean values for all independent variables and comparing directly with one experiment, as opposed to the MLR generated expressions, was thought to be more susceptible to experimental errors.

The second reason for the MLR experiments was to compare the model to the experimental results over a range of operating conditions. Several such experiments were created using thirteen combinations of current density, temperature and feed concentration. These are shown in Table 9-3, along with the results; the highlighted experiment H3 being the one chosen for model optimisation.

The dependent variables in Table 9-3 were the results that were compared with the model results once the rate constants had been optimised. For experiment H1 the predicted osmotic flow and α,α -dimethoxytoluene concentration were negative. For the α,α -dimethoxytoluene concentration this was not such a problem and was assumed to mean

'approximately zero'. The osmotic flow was a bigger problem. This was because the electro-osmotic flows in the simulation program were also based on the same empirical equation.

Table 9-3: MLR Data Set

experiment number	Independent Variables				Dependent Variables						
	Duration (hr)	j (A/m ²)	T _A (°C)	C _{Tf} (%)	E _{CELL} (V)	E _M (V)	E _A (V vs SCE)	F _{OS} (ml/hr)	C _{MTS} (mol/m ³)	C _{DMTS} (mol/m ³)	C _{TS} (mol/m ³)
H1	10	100	40	20	5.87	5.47	-0.12	-4.10	47.22	-2.49	319.53
H2	10	250	40	20	7.22	6.18	0.70	3.08	58.40	8.28	307.37
H3	10	500	40	20	9.47	7.36	1.32	15.05	77.05	26.23	287.10
H4	10	750	40	20	11.72	8.54	1.69	27.02	95.70	44.18	266.83
H5	10	1000	40	20	13.97	9.72	1.94	38.99	114.34	62.13	246.57
H6	10	500	30	20	11.43	7.93	1.94	15.05	76.11	22.74	306.47
H7	10	500	35	20	10.43	7.65	1.63	15.05	76.44	24.00	296.79
H8	10	500	45	20	8.50	7.07	1.01	15.05	78.11	30.14	277.42
H9	10	500	50	20	7.52	6.78	0.71	15.05	79.93	36.86	267.73
H10	10	500	40	10	8.67	7.59	0.46	15.05	71.12	40.76	139.04
H11	10	500	40	15	9.07	7.47	0.96	15.05	74.08	33.49	213.07
H12	10	500	40	25	9.88	7.24	1.60	15.05	80.02	18.97	361.13
H13	10	500	40	30	10.28	7.13	1.83	15.05	82.98	11.71	435.16

The program code included two corrections and a warning if the osmotic flow was lower than 0.5ml/hr, or if the feed rate was higher than the osmotic flow. The first correction increased low osmotic flows to a set value of 1ml/hr. The second corrected the feed rate to the same rate as the osmotic flow.

Since the MLR data were statistically related to the experimental data set they gave similar current efficiencies and mass balances. Table 9-4 shows the results of these calculations. H1 was calculated for a positive osmotic flow so that future model results could be directly compared. The others gave current efficiencies in the expected range of 2.37-7.84%. The toluene mass balance was also very similar to experimental results with unreacted toluene in the order of 10⁻⁷mol/s. This left an unaccounted amount of toluene also in the expected range of 10⁻⁶mol/s. This was thought to be the toluene which made the polymer by-product. The penultimate column shows the amount of toluene that would have been consumed by the 2 electron polymerisation model proposed by Equation 9-14. For experiments H2 to H12 the amount of unaccounted toluene was between 34% and 94% of this proposal. For experiment H13 the unaccounted amount was greater than the proposal by 14%. The final column shows the value of the ratio of electrons to toluene in the polymerisation reaction so that the unaccounted amount of toluene and the remaining current matched. Again excluding experiment H1, the average of the electron:toluene ratio was 3.42. This then was the basis for the modification of Equation 9-14.

Table 9-4: Mass Balance and Current Efficiency of the MLR Data

experiment number	applied current (A)	Feed rate (ml/hr)	current efficiency (%)	toluene flows (mol/s)					value of e to match unaccounted
				reactor feed	in products	unreacted	unaccounted	consumed with e=2	
H1	0.21	1.0	1.08	4.9E-07	1.2E-08	8.9E-08	3.8E-07	1.1E-06	5.60
H2	0.53	3.1	2.37	1.5E-06	5.7E-08	2.6E-07	1.2E-06	2.7E-06	4.49
H3	1.05	10.0	6.61	4.9E-06	2.9E-07	8.0E-07	3.8E-06	5.1E-06	2.69
H4	1.58	10.0	6.26	4.9E-06	3.9E-07	7.4E-07	3.7E-06	7.7E-06	4.10
H5	2.10	10.0	6.09	4.9E-06	4.9E-07	6.8E-07	3.7E-06	1.0E-05	5.55
H6	1.05	10.0	6.21	4.9E-06	2.7E-07	8.5E-07	3.7E-06	5.1E-06	2.73
H7	1.05	10.0	6.35	4.9E-06	2.8E-07	8.2E-07	3.8E-06	5.1E-06	2.71
H8	1.05	10.0	7.06	4.9E-06	3.0E-07	7.7E-07	3.8E-06	5.1E-06	2.67
H9	1.05	10.0	7.84	4.9E-06	3.2E-07	7.4E-07	3.8E-06	5.0E-06	2.65
H10	1.05	10.0	7.79	2.4E-06	3.1E-07	3.9E-07	1.7E-06	5.0E-06	5.87
H11	1.05	10.0	7.20	3.6E-06	3.0E-07	5.9E-07	2.8E-06	5.0E-06	3.67
H12	1.05	10.0	6.02	6.1E-06	2.7E-07	1.0E-06	4.8E-06	5.1E-06	2.13
H13	1.05	10.0	5.43	7.4E-06	2.6E-07	1.2E-06	5.9E-06	5.1E-06	1.75

9.10.2 Rate Constants

These are related to the anode overpotential using a Tafel type equation in the form:-

$$k_{f1} = k_{f10} \exp\{-\beta n f \eta\}$$

To optimise the model to fit experiment H3 the values of the constants k_{f10} , k_{f20} , k_{f30} and k_{f40} were calculated. The model was run until steady state was reached (2000 minutes) and the results compared with experiment H3. Of particular interest were E_A , C_{MT} , and C_{DMT} and, hence, these were the values optimised at 1.079V vs SCE, 77mol/m³ and 26mol/m³ respectively. The values of E_{CELL} and C_T were not optimised; the cell potential was calculated as the sum of the membrane, anode and cathode potentials, whilst the concentration of toluene was determined by the mass balance. The value of k_{f30} was set to zero since no carbon dioxide nor any other oxidation product of methanol had been detected. E_A was controlled by adjusting k_{f40} - the by-product rate constant; C_{MT} by adjusting k_{f10} - the methoxylation rate constant and C_{DMT} by adjusting k_{f20} - the dimethoxylation rate constant. The rate constants giving the best fit (to within $\pm 1\%$) of those results in experiment H3 are shown in Table 9-5.

Table 9-5: Rate Constants At 1.079V Anode Potential

k_{j10}	$4.858 \times 10^{-28} \text{mol}^{-1} \text{m}^4 \text{s}^{-1}$	k_{j1}	$3.692 \times 10^{-12} \text{mol}^{-1} \text{m}^4 \text{s}^{-1}$
k_{j20}	$7.665 \times 10^{-28} \text{mol}^{-1} \text{m}^4 \text{s}^{-1}$	k_{j2}	$5.825 \times 10^{-12} \text{mol}^{-1} \text{m}^4 \text{s}^{-1}$
k_{j30}	0	k_{j3}	0
k_{j40}	$3.960 \times 10^{-37} \text{mol}^{-1} \text{m}^4 \text{s}^{-1}$	k_{j4}	$3.009 \times 10^{-21} \text{mol}^{-1} \text{m}^4 \text{s}^{-1}$

9.11 Comparisons

9.11.1 Comparison With MLR Generated Data

The data generated by the model are shown in Table 9-6 and Table 9-7. For model experiments M1, M5 and M10 the duration was shorter than expected. This was due to the concentration of toluene in the anode chamber falling below zero. Three factors account for this:-

- the osmotic flow was very low (M1). Osmotic flow was proportional to current density and according to the multiple linear regression equation ($F_{os}=0.479j-8.888$) was slightly negative for 100A/m^2 . This value was corrected to 1ml/hr , but this was too small for the rate of depletion of toluene.
- the current density was too high (M5). The high rate of reaction used up all the available toluene.
- the original amount of toluene in the anode chamber was too small (M10). Although the rate was slower the concentration reached zero because insufficient toluene was available.

These three experiments highlight the importance of electro-osmotic flow.

The current efficiencies predicted by the model ranged from 0% to 18.02% with the modal value at 6.61%. These values compared well with the experimental and MLR results. The current efficiencies of experiments M2, M4, M10 and M11 were approximately 2-3 times greater. What was also noticeable was that these four experiments all had a much lower concentration of toluene in the product stream than the others. This was because these experiments caused the toluene concentration in the anode compartment to approach zero by one of the three conditions described above. This had the effect of shifting the reaction away from the polymerisation towards methoxylation or dimethoxylation, hence, increasing the efficiency.

Table 9-6: Modelling Results

experiment number	Independent Variables				Dependent Variables					
	Duration (hr)	j (A/m ²)	T _A (°C)	C _{Tf} (%)	E _{CELL} (V)	E _A (V)	F _{OS} (ml/hr)	C _{MTS} (mol/m ³)	C _{DMTS} (mol/m ³)	C _{TS} (mol/m ³)
M1	19	10	40	20	10	1	1	1	1	1737
M2	33	25	40	20	13	1	3	20	275	74
M3	33	50	40	20	14	1	15	78	26	582
M4	33	75	40	20	16	1	27	27	159	56
M5	8	100	40	20	12	1	39	20	142	18
M6	33	50	30	20	15	1	15	78	26	582
M7	33	50	35	20	15	1	15	78	26	582
M8	33	50	45	20	14	1	15	78	26	582
M9	33	50	50	20	14	1	15	78	26	582
M10	7	50	40	10	10	1	15	14	120	44
M11	33	50	40	15	15	1	15	51	81	159
M12	33	50	40	25	14	1	15	77	13	1027
M13	33	50	40	30	14	1	15	72	7	1478

Table 9-7: Mass Balance and Current Efficiency for the Model

experiment number	applied current (A)	Feed rate (ml/hr)	current efficiency (%)	toluene flows (mol/s)			
				reactor feed	in products	unreacted	in byproduct
M1	0.21	1.0	0.07	4.9E-07	5.1E-10	4.8E-07	2.9E-09
M2	0.53	3.1	18.02	1.5E-06	2.5E-07	6.4E-08	1.2E-06
M3	1.05	10.0	6.65	4.9E-06	2.9E-07	1.6E-06	3.0E-06
M4	1.58	10.0	11.72	4.9E-06	5.2E-07	1.6E-07	4.2E-06
M5	2.10	10.0	7.74	4.9E-06	4.5E-07	5.1E-08	4.4E-06
M6	1.05	10.0	6.65	4.9E-06	2.9E-07	1.6E-06	3.0E-06
M7	1.05	10.0	6.65	4.9E-06	2.9E-07	1.6E-06	3.0E-06
M8	1.05	10.0	6.65	4.9E-06	2.9E-07	1.6E-06	3.0E-06
M9	1.05	10.0	6.65	4.9E-06	2.9E-07	1.6E-06	3.0E-06
M10	1.05	10.0	12.99	2.4E-06	3.7E-07	1.2E-07	1.9E-06
M11	1.05	10.0	10.93	3.6E-06	3.7E-07	4.4E-07	2.8E-06
M12	1.05	10.0	5.24	6.1E-06	2.5E-07	2.9E-06	3.0E-06
M13	1.05	10.0	4.44	7.4E-06	2.2E-07	4.1E-06	3.0E-06

9.11.2 Comparison With Experimental Data

The model was compared directly with every experiment and these are shown graphically in Appendix 7. For four out of nine experiments the model terminated before the steady state condition was reached and so no comparisons could be made for these cases. The reasons for the termination of the model are the same as described above in Section 9.11.1, i.e. the concentration of toluene fell to zero at the anode surface. Three of the terminations,

EXP549, EXP552 and EXP557 were caused by low electro-osmotic flow as a result of low applied current density. The other, EXP548 was caused by high current density depleting the toluene through reaction. In EXP547 and EXP559 the toluene concentration in the anode compartment almost reached zero, at which stage the dimethoxylation reaction became very dominant resulting in very high concentrations of α,α -dimethoxytoluene.

The best fits occurred with those experiments having higher toluene feed concentrations and intermediate current densities. EXP553 and EXP554 both had 30% toluene feed concentrations and current densities of 476 and 333 A/m² respectively. This resulted in final product concentrations that were lower than experimental values, although the reactant concentration was over estimated. The cell potentials predicted by the model for these two experiments showed good agreement with experimental values although the anode potential was lower than expected.

The best fit of all occurred with EXP558. This was expected since the applied current density and feed concentration were very similar to the conditions used to optimise the model. All concentrations were higher than experimental values, as was the cell potential, but were in the same order of magnitude. The anode potential showed a reasonable fit to experimental data.

9.12 Effect of Independent Variables

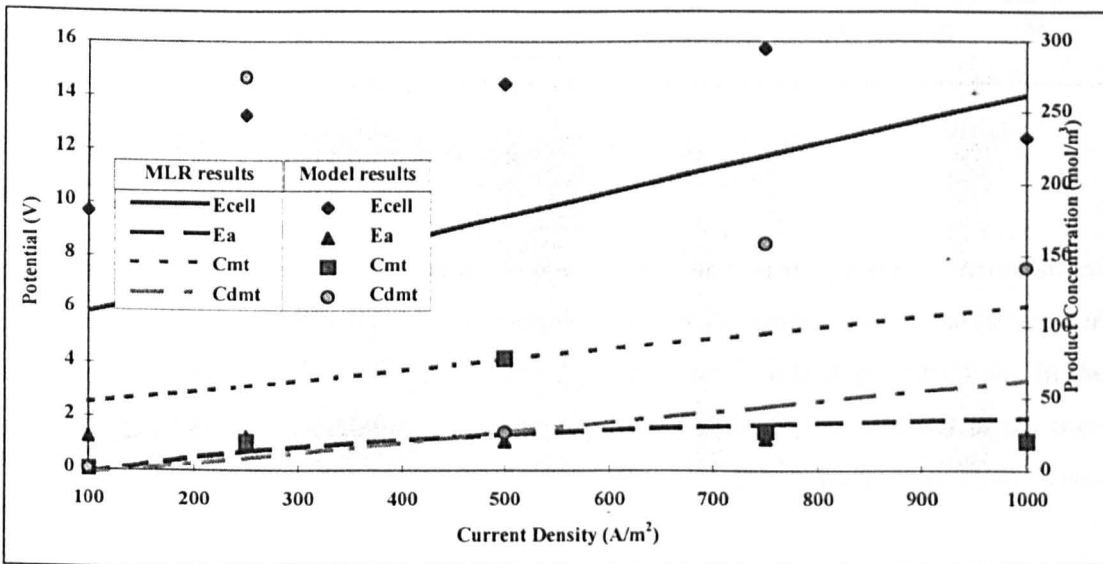
By plotting the results of the model experiments (Table 9-6) against those predicted by MLR equations (see Table 9-3) the effect of the independent terms was seen. Product concentrations and the anode overpotential had been optimised by setting the rate constants so that the output fitted MLR experiment H3 within 1%. Deviations from this fit occurred as the applied variables were adjusted to higher and lower values. These effects are discussed below. In general the following statements can be made:-

- cell potential - the model gave much higher values due to the time dependence term.
- anode overpotential - this fit was good over the whole range.
- product distribution - the fit was good except for the effect of current density and at low toluene concentrations.

9.12.1 Current Density

Figure 9-4 shows the effect of current density on the cell and anode potentials as well as the product concentrations. According to the MLR equations increasing the current density increased all these dependent variables. In the model the current density had the effect of reducing the toluene concentration in the anode compartment to, or near to, zero at both low and high values due to either low electro-osmotic flow or rapid reaction of toluene respectively. When the toluene concentration reached zero the model terminated so no comparison could be made. When the concentration became close to zero the model predicted high concentrations of product as the desired reactions became more dominant than the oligomerisation. In these cases too, no comparison could be made. Because of these extremes no effect of current density on the potentials can be made using the results from the model.

Figure 9-4: Effect of Current Density on Product Distribution and Potentials

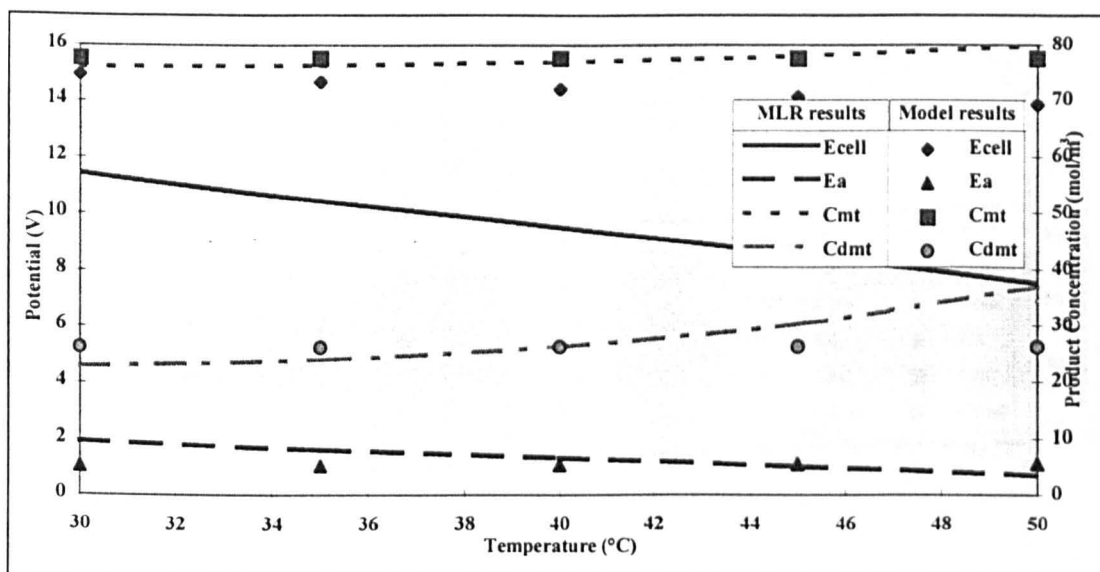


9.12.2 Temperature

Figure 9-5 shows the effect of reactor temperature on the product distribution and the anode and cell potential. According to the experimental results (generated by MLR) an increase in temperature caused a decrease in both potentials and a rise in the concentration of both products. The increase in concentration occurred with increasing rate at higher temperatures.

According to the model results little change occurred in anode potential and only a small decrease in cell potential was noticed as the temperature was increased. Both products were formed in the same concentrations at all temperatures in the range.

Figure 9-5: Effect of Temperature on Product Distribution and Potentials



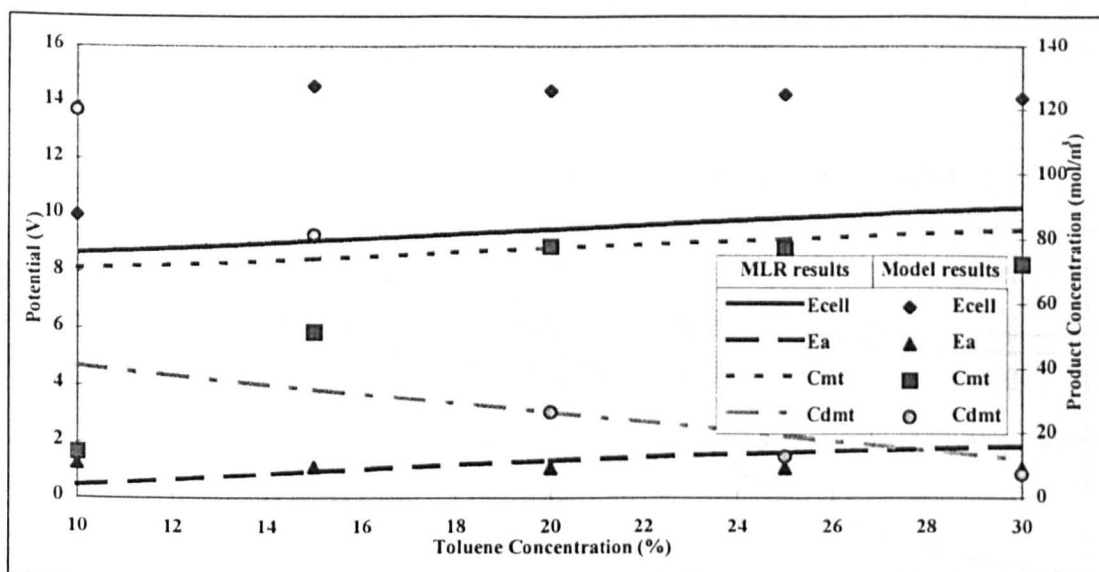
9.12.3 Feed Concentration

Figure 9-6 shows the effect that the feed concentration had on the product concentrations and on the anode and cell potentials. According to the MLR generated results an increase in the toluene concentration in the feed caused a slight increase in both potentials and in the concentration of α -methoxytoluene. A more significant change was observed in the α,α -dimethoxytoluene concentration. This was seen to decrease as the toluene concentration was increased.

The effect of feed concentration according to the model was complicated by the results at 10% and 15% toluene feed concentrations. In these cases the toluene concentration in the anode compartment became close to zero and the dimethoxylation reaction became dominant. This causes the effect of feed concentration to be intensified at low concentrations, whereas at higher feed concentrations the fall in α,α -dimethoxytoluene concentration is less rapid. At low feed concentrations the α -methoxytoluene concentration rises quickly, but as the feed concentration increases from 20% to 30% a decrease is seen.

According to the model results the anode potential falls as the toluene feed concentration increases. This is also similar for the cell potential except for the range 10 to 15% where the cell potential rises.

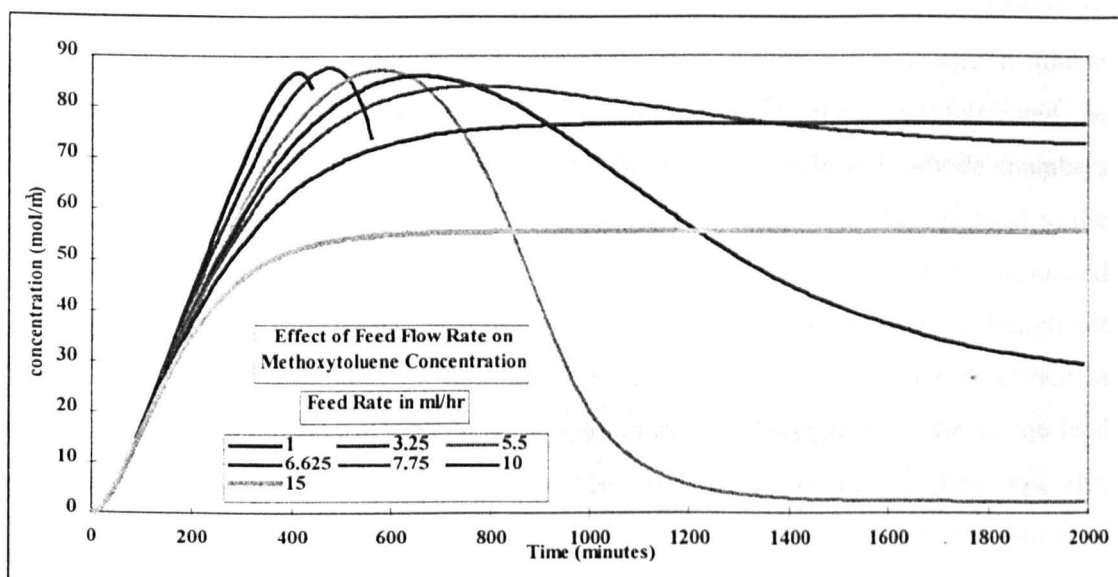
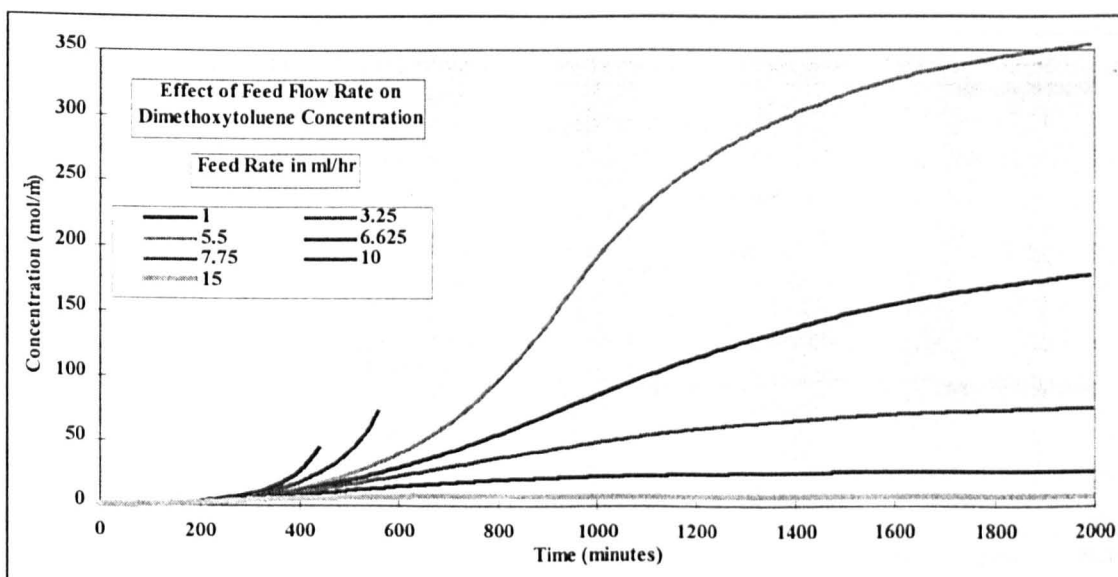
Figure 9-6: Effect of Feed Concentration on Product Distribution and Potentials



9.12.4 Effect Of Feed Rate

It can now be seen that for a given current density, temperature and feed concentration the flows through the system had a great effect on the performance. This is demonstrated below by considering the mean independent variable set. The model was run with various feed rates between 1ml/hr and 15ml/hr. The limit of 15ml/hr was set because of the electro-osmotic flow. Figure 9-7 and Figure 9-8 show the effect on the steady state product concentrations. At 1ml/hr and 3.25ml/hr feed rates the simulation terminated early because the toluene concentration in the anode chamber reached zero. This condition was reached earlier for the lowest rate, as expected. Increasing the feed rate to 5.5ml/hr showed that the α -methoxytoluene reached a maximum product concentration of 87mol/m^3 after 600 minutes and then fell to reach a steady state value of less than 5mol/m^3 . The α,α -dimethoxytoluene concentration shows a typical s-shaped curve as it approaches a steady state condition of 360mol/m^3 after 2000 minutes. As the feed rate increased the final α -methoxytoluene concentration was reached much earlier and at a value closer to the maximum achieved. At 15ml/hr the steady state concentration fell again. For α,α -dimethoxytoluene the final steady state condition fell as the feed rate was increased.

These observations are all explained by considering the mass balance over the anode chamber. The rate of depletion of toluene due to reaction remained the same for all experiments; the changes in feed rate only altered the rate at which fresh toluene was supplied. At high feed rates the dominant reaction was the oligomerisation of toluene. At low feed rates the desired reactions became more dominant. At low rates the α,α -dimethoxylation became very dominant, and at very low rates the toluene concentration reached zero.

Figure 9-7: Feed Flow Effect On α -Methoxytoluene ConcentrationFigure 9-8: Feed Flow Effect On α,α -Dimethoxytoluene

9.13 Scale-Up

The modelling program was written so that the scale-up of the reactor could be predicted. This involved the consideration of the effect of the electrode (or membrane) area upon every variable. Since electrochemical reaction rates are proportional to the electrode area a simple scale-up factor could be used:-

$$\text{Scale - Up Factor} = \frac{\text{Area 2}}{\text{Area 1}}$$

Thus simulations were carried out with scale-up factors of 10, 100 and 476 as examples. Although theoretically no limit exists, in practice the size of commercially available membranes would limit the active area per cell. Increasing the area directly affected the electro-osmotic flow and the applied current. The depth of the anode and cathode chambers was kept at 1cm so that the scale-up factor of the reactor volume was also identical to the area scale-up factor. The velocity of electrolyte through the graphite electrodes remained the same so the mass transfer coefficients remained unaffected. The feed rate, although not directly affected by scale-up needed to be changed to avoid the conditions described in Section 9.12.4 i.e. depletion of toluene concentration to zero. To compare scale-up the feed rate was also increased by the same factor. The volume of the recycle line was also increased by the same factor to take into account the extra length of pipework required to connect the chambers together.

Figure 9-9: Scale-up Of The SPE Reactor

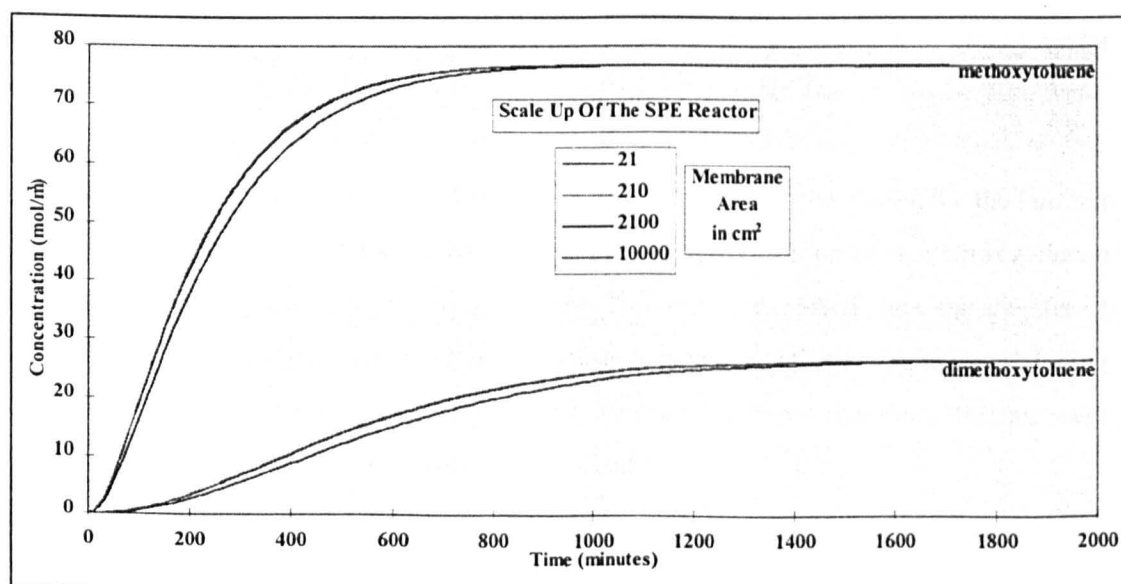


Figure 9-9 shows the scale-up results for the situation described above. It shows that the same steady state conditions exist for this reactor up to a membrane/electrode area of 1 m^2 (the maximum scale-up used). The shape of the membrane in the scale-up remained the same. No account was taken of the increased volume of gas that would be produced by the increased applied current. As already discussed in Chapter 8 large gas evolution caused entrainment of electrolyte into the gas stream. The shape and volume of the chambers and the size of the gas manifolds would have to be sized to prevent this occurring, although this has not been taken into account in the model. An advantage of the large production of gas is the increase in mass transfer coefficients caused by the mixing effect of the bubbles. The model assumed that a high concentration of reactant would be permanently available, but this work has shown that in many cases the concentration approaches zero. This may cause some mass transfer limit to be imposed.

9.14 Dependence on Mass Transfer Coefficient

In Section 9.5, page 108, the selection of mass transfer coefficient-Reynolds Number correlation was discussed. The reactor model used in all the work discussed so far was based on the high Reynolds Number dependence region. In this section the model results are compared for an experiment using both low and high Reynolds Number correlations. In the low dependence region the mass transfer coefficient may be nearly constant particularly at flow rates of 10^{-6} m/s as in the SPE reactor under investigation. According to Carta⁽⁷¹⁾ this mass transfer coefficient may be as high as $4.6 \times 10^{-6}\text{ m/s}$, compared with a value of $8.1 \times 10^{-8}\text{ m/s}$ using the high Reynolds Number dependency correlation. The model was run for the data of EXP558 (the experiment giving the best fit to the model) using both mass transfer coefficients.

In Figure 9-10 the effect on product distribution can be seen. The correlation for the laminar region (larger mass transfer coefficient) gave a greater concentration of α -methoxytoluene and a reduced amount of α,α -dimethoxytoluene. This was as expected since the transfer of α -methoxytoluene away from the electrode surface was enhanced and in doing so reducing the amount converted to α,α -dimethoxytoluene. Figure 9-11 shows that the potentials were unaffected by the change in mass transfer coefficient.

Figure 9-10: Effect of Mass Transfer Coefficient on Product Distribution

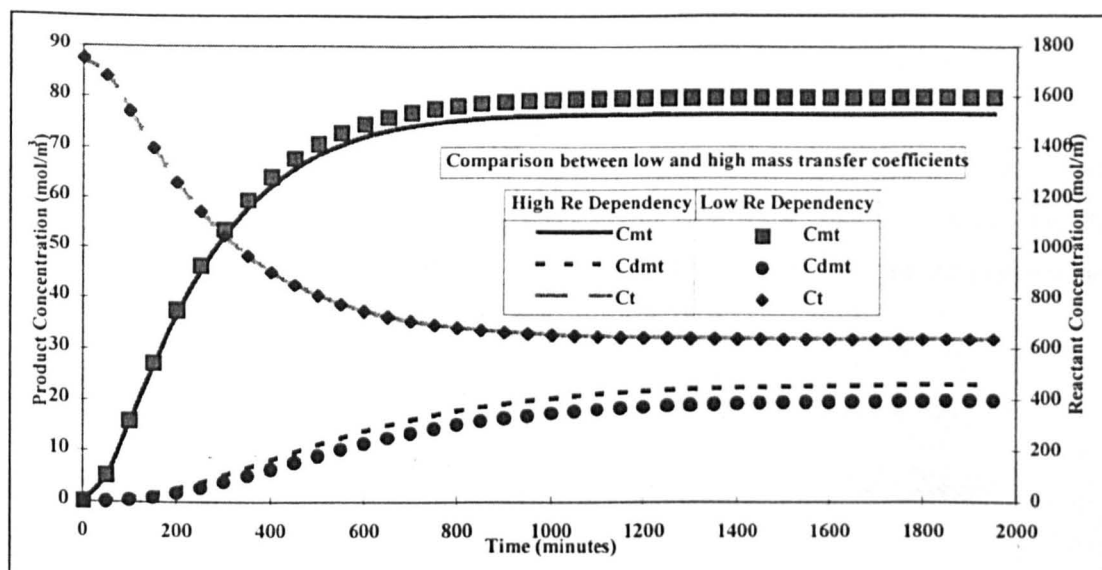
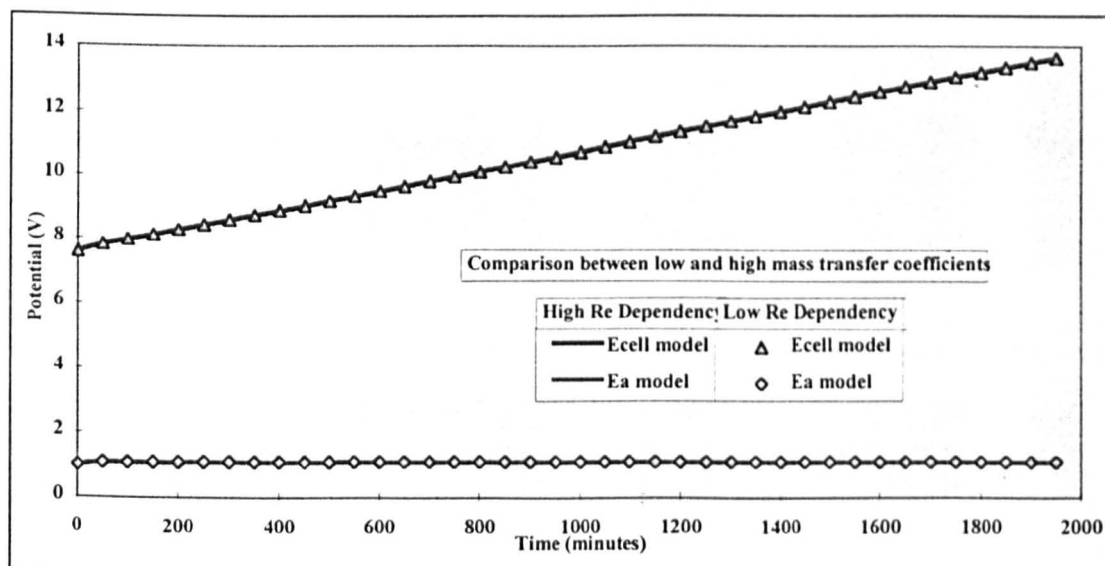


Figure 9-11: Effect of Mass Transfer Coefficient on Potentials



9.15 Summary

A computer simulation was carried out of the oxidation of toluene in methanol in the steel SPE reactor. The reaction scheme was based on proposals available in the literature, Tafel type kinetics and first order reaction dependency.

The decision to use Reaction Scheme 1, based on a series of two electrochemical reactions as described by Wendt^[63,64] was felt adequate for the purposes of the simulation. Preliminary

examination of Reaction Scheme 2 did not indicate that an improved reactor model could be realised due to the dominance of the toluene oligomerisation.

Optimisation of the rate constants was carried out to fit the model results to MLR data generated from experiments. The model was then used to predict the effect of current density, temperature, toluene feed concentration, feed flow rate and mass transfer coefficient on the reactor performance. The major factor affecting the reactor performance was found to be the rate of oligomerisation of toluene.

IMAGING SERVICES NORTH

Boston Spa, Wetherby
West Yorkshire, LS23 7BQ
www.bl.uk

**PAGE NUMBERING AS
ORIGINAL**

10. CONCLUSIONS

The main objective of this project was to develop a solid polymer electrolyte reactor for the oxidation of toluene. This has been completed successfully by first investigating the kinetics, looking at the background research into electro-oxidation of toluenes, studying the pre-treatment of several ion exchange membranes before the reactor was used and modelled.

The initial investigations carried out on a lead dioxide rotating disk electrode system gave information on the kinetic behaviour of toluene oxidation. The concentration dependency was calculated giving an order of reaction with respect to toluene as 0.5 a rate constant in the order of $10^{-5} \text{mol}^{0.5} \text{m}^{-0.5} \text{s}^{-1}$. The transfer coefficient and exchange current density were calculated from the Tafel equation as 0.028 and 10^{-3} to 10^{-1}A/m^2 . The diffusion coefficient was in the order of $2 \times 10^{-9} \text{m/s}$.

The direct oxidation of toluene was tested on platinum electrodes with, and without, acetic acid co-solvent. Removing the acetic acid decreased the maximum current efficiency for benzaldehyde from 94% to 10%. This was thought to be due to the reduced toluene solubility. The other products were benzyl alcohol and unknown low volatile compounds. Reducing the current density, without co-solvent, caused the current efficiency to go through a maximum of 10% at 250A/m^2 . This also corresponded to a decrease in the formation of the unknown by-products. Performance with nitric acid electrolyte was much better than with sulphuric acid or sodium sulphate where the current efficiency was 0-0.5%.

Experiments conducted in a glass batch reactor with membrane area of 5cm^2 showed the need for good reactor design. Of great importance was the electrode-membrane contact. A poor contact gave high cell potentials and low current efficiencies. Gas evolution was thought to be the competing reaction. Electrodes giving best performance were graphite felt, nickel foam and palladium coated mesh. At the end of the experiments these gave current efficiencies for benzaldehyde of 20.3%, 52.4% and 10.7% respectively. Nickel foam was thought to be unsuitable because of its rapid deterioration caused by low pH levels at the electrode-membrane interface. Oxidation of benzyl alcohol was successfully accomplished on nickel foam with a current efficiency for benzaldehyde of 85.4% after 10 hours. This

showed that the difficult step in the oxidation of toluene was the first reaction to benzyl alcohol.

Investigations regarding the swelling of ion exchange membranes for use in the solid polymer electrolyte synthesis reactor identified Nafion®117 as the most suitable of the tested membranes. Of the other membranes only Solvay's CSP showed a significant uptake of water. Membranes with backing support such as Ionac®MA3475 were thought unsuitable for organic synthesis because the support restricted swelling.

The solvents used for swelling were shown to have different characteristics. In general, and in particular for Nafion®117, the increase in swelling was in the order

DMF > methanol > methanol/toluene > water > sulphuric acid > toluene.

For Nafion®117 swelling in DMF increased the membrane area up to 165%, although this soon returned to the 76% value when subsequently placed in methanol/toluene solution. In methanol alone the membrane area increased by 112%, but the effect of toluene was to adversely reduce the uptake of solvent. In toluene alone the membrane area decreased relative to the 'as received' condition. In water and 1M sulphuric acid the swelling was similar. Area increases of 34% and 19% respectively were achieved.

Comparisons of the performance of different membranes swollen in different solvents was made during electrolysis in the steel SPE reactor. This testing involved galvanostatic operation for 10 hours for the oxidation of toluene in methanol, sometimes in DMF. The anode-membrane potential was measured as a function of time and current density. These values were lowest for Nafion®117 in DMF even at current densities of 476A/m². Next was Nafion®117 in aqueous solvents at 100A/m², followed by Nafion®117 in methanol at 47.6A/m². The best of the other membranes were Neosepta® CMX-5B and Solvay® CSP in water at 100A/m². The final selection of a pre-treatment procedure was based on a series of aqueous solvents. Although this did not give the greatest uptake of solvent, nor the lowest anode-membrane potential, it was a simple and safe procedure that gave reasonable performance at medium current densities.

Oxidation of toluene in methanol was carried out in a continuous SPE process. The effect of current density, temperature, toluene feed concentration and mass transfer coefficient on the selectivity, current efficiency and potentials were investigated. The products of this reaction were found to be α-methoxytoluene, α,α-dimethoxytoluene and higher oxidation states

based upon oligomerisation of toluene. This appeared as tar-like low volatile matter. Current efficiencies for toluene products were low, between 1.4% and 9% at steady state. These results were recorded at temperatures of 30°C to 50°C using current densities ranging from 200A/m² to 1000A/m². Feed concentrations of toluene were between 10% and 30% toluene in methanol.

Gases produced in the reactor were collected and analysed. These were identified as nearly pure hydrogen. No carbon dioxide was detected and only small amounts of oxygen were found (8-9%). The volume of gas collected gave good agreement (within 2.8%) to the theoretical amount based upon 2 electrons per hydrogen molecule. In the liquid phase no formic acid nor methyl esters were detected.

Measurement of the membrane potential took place with 2 Luggin probes. This allowed the anode overpotential to be calculated. This parameter along with cell potential, electro-osmotic flow and product distribution were analysed using multiple linear regression. This showed how these parameters were affected by the three applied variables. Of particular interest was the electro-osmotic flow which was found to be highly dependent on current density.

The results of the multiple linear regression were used in the building of a computer model of the SPE reactor for toluene oxidation. Tafel type kinetics were based on a transfer coefficient of 0.472 calculated from the experimental results. The reactions were based on a series of 2 electron steps for the oxidation of toluene to α -methoxytoluene then α - α -dimethoxytoluene. A competitive parallel electrochemical reaction based on the oligomerisation of toluene was used to model the loss of current efficiency. Rate constants of these three electrochemical steps were optimised to fit the mean data set from the experiments. They were based on a Tafel type equation which allowed the model to simulate galvanostatic operation by adjusting the anode overpotential.

Computer simulations showed that oligomerisation was the most dominant reaction, making the SPE reactor unsuitable for the oxidation of toluene. For this system the effect of the applied variables was investigated. Increasing current density was shown to increase the product concentration of both desired products. Increasing the reactor temperature increased the concentration of both products, but more so for α - α -dimethoxytoluene. An increase in

toluene concentration in the feed slightly increased the concentration of α -methoxytoluene and decreased the concentration of α - α -dimethoxytoluene.

The electro-osmotic flow was also shown to have a large influence on product distribution for this system. Since a large proportion of toluene was consumed by the oligomerisation its concentration in the anode compartment depended strongly on the rate of flow through the reactor. This was limited by the electro-osmotic flow.

A slight increase in selectivity of α -methoxytoluene was noticed by using a low Reynolds Number dependency correlation when compared to the high dependency correlation proposed by Carta^[71]. The simulation also showed that this type of reactor can, in principle, be easily scaled up by a simple increase in active membrane-electrode area.

The following conclusions can be drawn regarding the overall project:-

- It is possible to develop the solid polymer electrolyte reactor, but only for selected electro-organic reactions.
- The oxidation of toluene is not a suitable reaction as it proceeds slowly with low selectivity. Oligomerisation of toluene was the main reaction.
- The performance of the membrane is critical to the efficiency of the reactor as a whole. Toluene adversely affects the swelling of ion exchange membranes so its concentration must be kept low.
- Graphite felts give excellent electrode membrane contact and, hence, are a good choice for electrode material. They also offer the possibility of coating with catalyst and/or Nafion[®] solution.
- Increasing the electro-osmotic flow would enhance the reactor performance by increasing the contact of reactants and electrode surface. Using 'flow-by' configuration is not thought to be a suitable option as the membrane-electrode interface is bypassed.
- Increasing the toluene feed concentration increases the selectivity of α -methoxytoluene.
- A simple area scale-up factor can be used to predict performance of larger SPE reactors.



IMAGING SERVICES NORTH

Boston Spa, Wetherby

West Yorkshire, LS23 7BQ

www.bl.uk

PAGE NUMBERING AS ORIGINAL

REFERENCES

- 1 Gerl, R., 'Scale Up Einer SPE Elektrolysezelle Fur Die Elektro-Organische Synthese Am Beispiel Der Methoxylierung Von N,N-Dimethylformamid', PhD Thesis, University Of Dortmund, Germany, 1996.
- 2 Gerl R. And Jörissen, J., 'Scale Up Of A Solid Polymer Electrolyte (SPE) Cell For Electro-Organic Synthesis', In Preparation, Pp1-12, 1997.
- 3 Simmrock, K.H., Gregel, R., Fabiunke, R., Jörissen, J., And Kohler, M., 'Electro-Organic Synthesis In Solid Polymer Electrolyte Cells', Proceedings Of The Symposium On Electrochemical Engineering In The Chlor-Alkali And Chlorate Industries', The Electrochemical Society, V88-2, Pp383, 1988.
- 4 Grinberg, V.A., Zhuravleva, V.N., Vasil'ev, Y.B., And Kazarinov, V.E., 'Electrosynthesis Of Organic Compounds Using A Solid Polymeric Electrolyte', Soviet Electrochemistry, V19, Pp1299, 1983.
- 5 Sarrazin, J., And Tallec, A., 'Use Of Ion Exchange Membranes In Preparative Organic Electrochemistry: New Processes For Electrolysis', Journal Of Electroanalytical Chemistry, V137, Pp183-188, 1982.
- 6 Raoult, E., Sarrazin, J., And Tallec, A., 'Use Of Ion Exchange Membranes In Preparative Organic Electrochemistry. I. Anodic Methoxylation Of Some Olefins', Journal Of Applied Electrochemistry, V14, Pp639-643, 1984.
- 7 Raoult, E., Sarrazin, J., And Tallec, A., 'Use Of Ion Exchange In Preparative Electrochemistry II. Anodic Dimethoxylation Of Furan', Journal Of Applied Electrochemistry, V15, Pp85-91, 1985.
- 8 Ogumi, Z., Nishio, K., And Yoshizawa, S., 'Application Of The SPE Method To Organic Electrochemistry - II. Electrochemical Hydrogenation Of Olefinic Double Bonds', Electrochimica Acta, V26, N12, Pp1779-1782, 1981.
- 9 Ogumi, Z., Yamashita, H., Nishio, K., Takehara, Z-I., And Yoshizawa, S., 'Application Of The SPE Method To Organic Electrochemistry - III. Kolbe Type Reactions On Pt-SPE', Electrochimica Acta, V28, N11, Pp1687-1693, 1983.
- 10 Ogumi, Z., Ohashi, S., And Takehara, Z-I., 'Application Of The SPE Method To Organic Electrochemistry - VI. Oxidation Of Cyclohexanol To Cyclohexanone On Pt-SPE In The Presence Of Iodine And Iodide', Electrochimica Acta, V30, N1, Pp121-124, 1985.

-
- 11 Ogumi, Z., Inaba, M., Ohashi, S., Uchida, M., And Takehara, Z-I., 'Application Of The SPE Method To Organic Electrochemistry - VII. The Reduction Of Nitrobenzene On A Modified Pt-Nafion', *Electrochimica Acta*, V33, N3, Pp365-369, 1988.
 - 12 Ogumi, Z., Inatomi, K., Hinatsu, J.T., And Takehara, Z-I., 'Application Of The SPE Method To Organic Electrochemistry - XIII. Oxidation Of Geraniol On Mn, Pt-Nafion', *Electrochimica Acta*, V37, N7, Pp1295-1299, 1992.
 - 13 Inaba, M., Ogumi, Z., And Takehara, Z., 'Application Of The Solid Polymer Electrolyte Method To Organic Electrochemistry XIV. Effects Of Solvents On The Electro-reduction Of Nitrobenzene On Cu, Pt-Nafion', *Journal Of The Electrochemical Society*, V140, N1, Pp19-22, 1993.
 - 14 Inaba, M., Hinatsu, J.T., Ogumi, Z., And Takehara, Z., 'Application Of The Solid Polymer Electrolyte Method To Organic Electrochemistry XV. Influence Of The Multiphase Structure Of Nafion On Electro-reduction Of Substituted Aromatic Nitro Compounds On Cu, Pt-Nafion', *Journal Of The Electrochemical Society*, V140, N3, Pp706-711, 1993.
 - 15 Yasuzawa, M., Kan, K., Ogumi, Z., And Takehara, Z., 'Electro-Oxidation Of Benzyl Alcohol On Pt-Nafion Composite Electrode', *Electrochimica Acta*, V40, N11, Pp1785-1787, 1995.
 - 16 Chen, Y.-L., And Chou, T.-C., 'Electrochemical Reduction Of Benzaldehyde Using Pt-Pb/Nafion As Electrode', *Journal Of Applied Electrochemistry*, V24, Pp434-438, 1994.
 - 17 Chen, Y.-L., And Chou, T.-C., 'Metals And Alloys Bonded On Solid Polymer Electrolyte For Electrochemical Reduction Of Pure Benzaldehyde Without Liquid Supporting Electrolyte' *Journal Of Electroanalytical Chemistry*, V360, Pp247-259, 1993.
 - 18 Scott, K., 'Handbook of Industrial Membranes', 1st Edition, Elsevier Science Publishers, Oxford, 1995.
 - 19 Yeo, R.S., And Yeager, H.L., 'Structural And Transport Properties Of Perfluorinated Ion Exchange Membranes', *Modern Aspects of Electrochemistry*, V16, Pp437-505, 1985.
 - 20 Jörissen, J., 'Ion Exchange Membranes As Solid Polymer Electrolytes (SPE) In Electro-Organic Syntheses Without Supporting Electrolytes', *Electrochimica Acta*, V41, N4, Pp553-562, 1996.
 - 21 Gerl, R., And Jörissen, J., 'Pre-treatment Of Ion Exchange Membranes For Use As A Solid Polymer Electrolyte (SPE) In Electro-Organic Synthesis Without Supporting Electrolyte', In Preparation, 1997
-

- 22 Gerl, R., And Jörissen, J., 'Pre-treatment Of Ion Exchange Membranes For Use As A Solid Polymer Electrolyte (SPE) In Electro-Organic Synthesis Without Supporting Electrolyte', In Preparation, 1997
- 23 McCain, G.H., And Covitch, M.J., 'Solubility Characteristics Of Perfluorinated Polymers With Sulfonyl Fluoride Functionality', Journal Of The Electrochemical Society, V131, Pp1350-1352, 1984.
- 24 Genders, D.J., George, E.L., And Pletcher, D., 'A Study Of The Transport Of Formaldehyde And Ethylene Glycol Through Ion Permeable Membranes In Electrolysis', Journal Of The Electrochemical Society, V143, N1, Pp175-178, 1996.
- 25 Blomen, L.J.M.J., and Mugerwa, M.N., 'Fuel Cell Systems', Plenum Press, New York and London, 1993.
- 26 Yeo, R.S., And McBreen, J., 'Transport Properties Of Nafion Membranes In Electrochemically Regenerative Hydrogen/Halogen Cells', Journal Of The Electrochemical Society, V126, N10, Pp1682-1687, 1979.
- 27 Yeager, H.L., Kipling, B, And Dotson, R.L., 'Sodium Ion Diffusion In Nafion® Ion Exchange Membranes', Journal Of The Electrochemical Society, V127, Pp303-307, 1980.
- 28 Yeo, R.S., 'Ion Clustering And Proton Transport In Nafion Membranes And Its Applications As Solid Polymer Electrolyte', Journal Of The Electrochemical Society, V130, N3, Pp533-538, 1983.
- 29 Verbrugge, M.W And Pintauro, P.N., in ., 'Modern Aspects Of Electrochemistry', V19, Bockris, J.O'M., Conway, B.E., And White, R.E., Editors, Plenum Press, New York, Pp1-66, 1987.
- 30 Verbrugge, M.W., 'Methanol Diffusion In Perfluorinated Ion Exchange Membranes', Journal Of The Electrochemical Society, V136, N2, Pp417-423, 1989.
- 31 Verbrugge, M.W., And Hill, R.F., 'Transport Phenomena in Perfluorosulfonic Acid Membranes During The Passage Of Current', Journal Of The Electrochemical Society, V137, N4, Pp1131-1138, 1990.
- 32 Verbrugge, M.W., And Hill, R.F., 'Ion And Solvent Transport In Ion Exchange Membranes, I. A Macrohomogeneous Mathematical Model', Journal Of The Electrochemical Society, V137, N3, Pp886-892, 1990.
- 33 Verbrugge, M.W., And Hill, R.F., 'Ion And Solvent Transport In Ion Exchange Membranes, II. A Radiometer Study Of The Sulfuric Acid, Nafion-117 System', Journal Of The Electrochemical Society, V137, N3, Pp893-898, 1990.

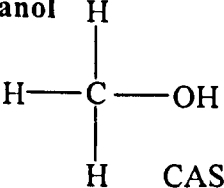
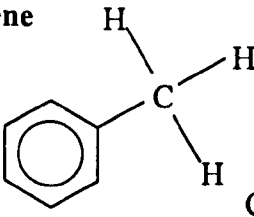
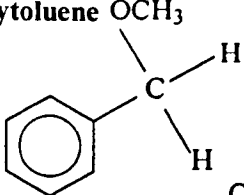
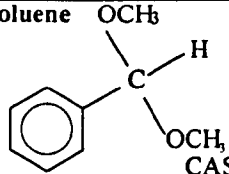
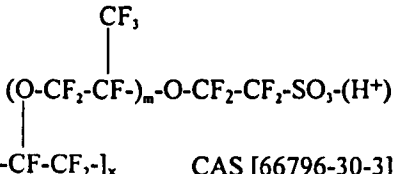
-
- 34 Zawodzinski, T.A., Springer, T.E., Davey, J., Valerio, J., And Gottesfeld, S., 'Water Transport Properties Of Fuel Cell Ionomers', Modelling Of Batteries And Fuel Cells, Electrochemical Society Meeting, 1991.
- 35 Verbrugge, M.W., Schneider, E.W., Conell, R.S., And Hill, R.F., 'The Effect Of Temperature On The Equilibrium And Transport Properties Of Saturated Poly(Perfluorosulfonic Acid) Membranes', Journal Of The Electrochemical Society, V139, N12, Pp3421-3428, 1992.
- 36 Cahan, B.D., And Wainright, J.S., 'AC Impedance Investigations Of Proton Conduction In Nafion®', Journal Of The Electrochemical Society, V140, N12,, L185-186, 1993.
- 37 Weng, D., Wainright, J.S., Landau, U., And Savinell, R.F., 'Electro-Osmotic Drag Coefficient Of Water And Methanol In Polymer Electrolytes At Elevated Temperatures', Journal Of The Electrochemical Society, V143, N4, Pp1260-1263, 1996.
- 38 Nguyen Q.T., Favre, E., Ping, Z.H., And Néel, J., 'Clustering Of Solvents In Membranes And Its Influence On Membrane Transport Properties', Journal Of Membrane Science, V113, Pp137-150, 1996.
- 39 Zhao, H., Price, W.E., Too, C.O., Wallace, G.G., And Zhou, D., 'Parameters Influencing Transport Across Conducting Electroactive Polymer Membranes', Journal Of Membrane Science, V119, Pp199-212, 1996.
- 40 Okada, K., Kjelstrup-Ratkje, S., Møller-Holst, S., Jerdal, L.O., Friestad, K., Xie, G, And Finally Holmen, R., 'Water And Ion Transport In The Cation Exchange Systems NaCl-SrCl₂ And KCl-SrCl₂', Journal Of Membrane Science, V111, Pp159-167, 1996.
- 41 Lehmani, A., Turq, P., Périé, M., Périé, J., And Simonin, J-P., 'Ion Transport In Nafion® 117 Membrane', Journal Of Electroanalytical Chemistry, V428, Pp81-89, 1997.
- 42 Schaetzel, P., Favre, E., Auclair, B., And Nguyen, Q.T., 'Mass Transfer Through Ion Exchange Membranes: Comparison Between The Diffusion And The Diffusion Convection Stefan Maxwell Equations', Electrochimica Acta, V42, N16, Pp2475-2483, 1997.
- 43 Anantaraman, A.V., And Gardner, C.L., 'Studies On Ion Exchange Membranes. Part 1. Effect Of Humidity On The Conductivity Of Nafion®', Journal Of Electroanalytical Chemistry, V414, Pp115-120, 1996.
- 44 Büchi, F.N., And Scherer, G.G., 'In-Situ Resistance Measurements Of Nafion® 117 Membranes In Polymer Electrolyte Fuel Cells', Journal Of Electroanalytical Chemistry, V404, Pp37-43, 1996.
- 45 Weinberg, N.L., And Weinberg, H.R., Electrochemical Oxidation Of Organic Compounds, Chem. Rev., v68, Pp449-522, 1968.
-

-
- 46 Fichter, F., 'Organische Electrochemie', Leipzig, Steinkopf, Reissued By Salford University Bookshop, Pp35-39, 60-65, 75-77, 83, 103-118, 124, 1970.
- 47 Weinberg, N.L., And Tilak, B.V., 'Techniques Of Chemistry, Volume 5, Part III, Technique Of Electro-Organic Synthesis', J.Wiley, New York, Pp126-141, 1982.
- 48 Wendt, H., And Bitterlich, S., 'Anodic Synthesis Of Benzaldehydes - I Voltammetry Of The Anodic Oxidation Of Toluenes In Non-Aqueous Solutions', *Electrochimica Acta*, V37, N11, Pp1951-1958, 1992.
- 49 Law, H.D., And Perkin, M., 'Electrolytic Oxidation Of Hydrocarbons Of The Benzene Series. Part I., Hydrocarbons Containing The Methyl Group', *Transactions Of The Faraday Society*, V1, Pp31-41, 1905.
- 50 Law, H.D., And Perkin, M., 'Electrolytic Oxidation Of Hydrocarbons Of The Benzene Series. Part II, Ethyl Benzene, Cumene And Cymene', *Transactions Of The Faraday Society*, V1, Pp251-261, 1905.
- 51 Mann, C.A., And Paulson, P.M., 'The Electrochemical Oxidation Of Toluene To Benzaldehyde', *Transactions Of The Electrochemical Society*, V47, Pp101-115, 1925.
- 52 Clarke, J.S., Ehigamusoe, R.E., And Kuhn, A.T., 'The Anodic Oxidation Of Benzene, Toluene And Anisole', *Journal Of Electroanalytical Chemistry*, V70, Pp333-347, 1976.
- 53 Jackson, P.J., 'Electrolytic Synthesis Of Aryl Alcohols, Aryl Aldehydes, And Aryl Acids', United States Patent, US 4,402,804, Pp7, 6-Sept-1983.
- 54 Kuliev, S.A., Vasilev, Y.B., And Bagotskii, V.S., 'Effect Of Substituents On Electro-oxidation Of Aromatic Compounds And On Their Interaction With The Platinum Electrode Surface', *Soviet Electrochemistry*, V22, N6, Pp706-709, 1986.
- 55 Mathur, R.S., Mukherjee, S.K., And Zutshi, K., 'Electrosynthesis Of Benzoic Acids Via Superoxide Anion', *Journal Of The Electrochemical Society Of India*, V38, N3, Pp210-212, 1989.
- 56 Otsuka, K., Ishizuka, K., Yamanaka, I And Hatano, M., 'The Selective Oxidation Of Toluene To Benzaldehyde Applying A Fuel Cell System In The Gas Phase', *Journal Of The Electrochemical Society*, V138, N11, Pp3176-3182, 1991.
- 57 Clarke, R., Kuhn, A., And Okoh, E., 'Indirect Electrochemical Processes', *Chemistry In Britain*, V11(2), Pp59-64, 1975.
- 58 Kramer, K., Robertson, P. M., And Ibl, N., 'Indirect Electrolytic Oxidation Of Some Aromatic Derivatives', *Journal Of Applied Electrochemistry*, V10, Pp19-36, 1980.
- 59 Tomat, R., And Rigo, A., 'Electrochemical Oxidation Of Toluene Promoted By OH Radicals', *Journal Of Applied Electrochemistry*, V14, Pp1-8, 1984.
-

-
- 60 Wendt, H., And Schneider, H., 'Reaction Kinetics And Reaction Techniques For Mediated Oxidation Of Methylarenes To Aromatic Ketones', *Journal Of Applied Electrochemistry*, V16, Pp134-146, 1986.
- 61 Kreysa, G., And Medin, H., 'Indirect Electrosynthesis Of p-Methoxy Benzaldehyde', *Journal Of Applied Electrochemistry*, V16, Pp757-767, 1986.
- 62 Jow, J-J., Lee, A-C., And Chou, T-C., 'Paired Electro-Oxidation. I. Production Of Benzaldehyde', *Journal Of Applied Electrochemistry*, V17, Pp753-759, 1987.
- 63 Wendt, H., And Bitterlich, S., 'Anodic Synthesis Of Benzaldehydes - I Voltammetry Of The Anodic Oxidation Of Toluenes In Non-Aqueous Solutions', *Electrochimica Acta*, V37, N11, Pp1951-1958, 1992.
- 64 Wendt, H., Bitterlich, S., Lodowicks, E., And Liu, Z., 'Anodic Synthesis Of Benzaldehydes - II. Optimisation Of The Direct Anodic Oxidation Of Toluenes In Methanol And Ethanol', *Electrochimica Acta*, V37, N11, Pp1959-1969, 1992.
- 65 Do, J.-S., And Chou, T.-C., 'Anodic Oxidation Of Benzyl Alcohol To Benzaldehyde In The Presence Of Both Redox Mediator And Polymer-Supported Phase-Transfer Catalyst', *Journal Of Applied Electrochemistry*, V22, Pp966-972, 1992.
- 66 Cognet, P., Berlan, J., And Lacoste, G., 'Application Of Metallic Foams In An Electrochemical Pulsed Flow Reactor. Part III: Oxidation Of Benzyl Alcohol', *Journal Of Applied Electrochemistry*, V26, Pp631-637, 1996.
- 67 Hwang, B.J., Yu, B.Y., And Lo, Y.L., 'Kinetics Of Benzyl Alcohol Oxidation On A Pure Nickel Electrode In KOH Solution', 187th Meeting Of The Electrochemical Society, Reno Nevada, Paper 602, 1995.
- 68 Cleghorn, S.J.C., And Pletcher, D., 'Investigations Of The Electrocatalytic Hydrogenation Of Organic Molecules At Palladium On Nickel Cathodes', *Electrochimica Acta*, V38, N18, Pp2683-2689, 1993.
- 69 Cleghorn, S.J.C., And Pletcher, D., 'The Mechanism Of Electrocatalytic Hydrogenation Of Organic Molecules At Palladium Black Cathodes', *Electrochimica Acta*, V38, N2/3, Pp425-430, 1993.
- 70 Haines, A.N., 'Mathematical Modelling Of Industrial Electrolytic Reactions' PhD Thesis, Teesside Polytechnic, 1988.
- 71 Carta, R., Palmas, S., Polcaro, A.M., And Tola, G., 'Behaviour Of A Carbon Felt Flow By Electrodes. Part 1. Mass Transfer Characteristics', *Journal Of Applied Electrochemistry*, V21, Pp793-798, 1991.
-

- 72 Electrochemical Reactor Design, David J. Pickett, Elsevier Scientific Publishing Company, Amsterdam, Oxford, New York, 1997.
- 73 Perry, R.H., and Green, D.W., 'Perry's Chemical Engineers' Handbook', 6th Edition, McGraw-Hill, New York, Pp.-258, 1984.
- 74 Van Der Weilen, L.A.M., Zomerdijk, M., Houwers, J., And Luyben, K.C.A.M., 'Diffusivities Of Organic Electrolytes In Water', Chemical Engineering Journal, V66, Pp111-121, 1997.
- 75 Mizushina, T., 'The Electrochemical Method In Transport Phenomena', Pp87-161, 1970.

APPENDIX 1: PROPERTIES

Structure	Properties (25°C, 1 atm)	
Methanol  CAS [67-56-1]	M_r density viscosity dielectric constant	32 781 kg/m ³ 4.7x10 ⁻⁴ Ns/m ² 32.63
Toluene  CAS [108-88-3]	M_r density viscosity dielectric constant	92 864 kg/m ³ 5x10 ⁻⁴ Ns/m ² 2.38
α-methoxytoluene  CAS [538-86-3]	M_r density	122 963 kg/m ³
α,α-dimethoxytoluene  CAS [538-86-3]	M_r density	152 1014 kg/m ³
Nafion[®] 117  CAS [66796-30-3]	IEC [*] thickness resistance	0.9 Meq/g 2mm 1.5 Ω cm ²
	fibre diameter porosity bulk density true density	11x10 ⁻⁶ m 0.94 122 kg/m ³ 2100 kg/m ³

*ion exchange capacity

Appendix 2: Flowcell Results

Batch Number	547
Date	09/5/97
j (mA/cm ²)	47.6
C _{T0}	867mol/m ³ 10%

APPENDIX 2

Reaction time (hr)		0	1	2.7	3	4	5	6	7	8	9	10	Average	Steady State
F	ml/hr	0	10	10	10	10	10	10	10	10	10		10	10
P	g/hr	0	10	10	10	10	10	10	10	10	10		10	10
R	ml/hr	0											0	0
E _{cell}	V	6.4	7.0	7.4	7.5	7.6	7.8	7.9	8.1	8.3	8.4		7.8	8.4
E _{ACM}	V vs SCE	5.69	6.59	6.97	7.01	6.91	7.12	7.30	7.47	7.71	7.45			
E _{CAM}	V vs SCE	5.70	6.90	7.35	7.38	7.51	7.10	6.45	5.87	7.00	7.96			
E _A	V vs SCE	0.13	0.08	0.05	0.06	0.06	0.56	1.32	1.97	1.30	0.47		0.65	
E _C	V vs SCE	0.31	0.39	0.43	0.43	0.66	0.54	0.47	0.37	0.59	0.98		0.54	0.98
Em	V	5.56	6.51	6.92	6.95	6.85	6.56	5.98	5.50	6.41	6.98		6.51	7.00
Tw	°C	34.0	37.0	38.0	38.5	39.0	38.5	38.5	38.5	38.0	39.5			
Tp	°C			29.3	25.1	27.0	29.1	28.6	29.9	28.9	32.1			
Tf	°C													
Tr	°C													
T _A	°C	31.2	35.8	37.3	38.0	37.8	38.1	37.9	38.0	37.2	38.3		37.6	38.0
T _C	°C	30.9	35.8	37.1	38.0	37.6	37.9	37.7	37.7	37.2	38.3			
Tag	°C		19.5	20.0	20.0	20.0	20.0	20.0						
Tcg	°C		19.5	20.0										
Vag	ml		50	80	22	68	66	70					59.3	
Vcg	ml		170(.5hr)	178(.5hr)									348	
C _M	mol/m ³	22311	22339		22511	21963	22817	21436	22635	22756	22837			22837
C _T	mol/m ³	219	206		188	182	182	164	174	171	169			169
C _{MT}	mol/m ³	0.0	10.7	18.5	25.9	26.1	31.5	78.4	37.7	40.0	41.4			41.4
C _{DMT}	mol/m ³	0.0	8.5	13.5	17.8	19.5	23.0	61.9	26.7	30.4	32.5			32.5
C _{CO} ²	%				0									0
C _H ² anode	%				75.9									75.9
C _H ² cathode	%							90.5						90.5

Appendix 2: Flowcell Results

Batch Number	548
Date	12/5/97
j (mA/cm ²)	95.2
C _{T0}	867mol/m ³ 10%

Reaction time (hr)		0	1	2	3	4	5	6	7	8	9	10	Average	Steady State
F	ml/hr	10	10	10		10	10	10	10				10	
P	g/hr	10	10	10		10	10	10	10				10	11
R	ml/hr		8	8		8	10	34	38				16	38
E _{cell}	V	9.5	8.7	9.4		11.1	12.1	13.0	14.3				11.4	14.3
E _{ACM}	V vs SCE	8.88	8.15	8.88		10.50	11.47	12.34	13.56					
E _{CAM}	V vs SCE	8.80	8.51	9.23		10.90	11.90	12.77	13.62					
E _A	V vs SCE	0.40	0.07	0.11		0.17	0.11	0.14	0.59				0.20	
E _C	V vs SCE	0.32	0.43	0.46		0.57	0.54	0.57	0.65				0.54	
E _m	V	8.48	8.08	8.77		10.33	11.36	12.20	12.97				10.62	12.97
T _w	°C	50.0	52.5	50.5		49.5	52.5	52.0	49.0					
T _p	°C		45.1			43.1	45.1	44.6	45.2					
T _f	°C													
T _r	°C													
T _A	°C	48.7	51.9	49.9		50.1	53.0	52.5	50.1				51.3	50.1
T _C	°C	49.2	51.6	50.1		50.1	52.7	51.9	50.1					
T _{ag}	°C		20.0	20.0	20.0									
T _{cg}	°C				20.0									
V _{ag}	ml		115	124	186 in 80 minutes								128	
V _{cg}	ml				550 in 60 minutes								550	
C _M	mol/m ³		22402	22875		22793	11360	22435	22187					
C _T	mol/m ³		157.0	140.0		112.0	63.0	87.9	77.0					77.0
C _{MT}	mol/m ³		36.3	41.1		42.9	166.0	44.7	36.8					44.0
C _{DMT}	mol/m ³		50.2	72.3		106.3	356.0	136.7	130.9					130.0
C _{CO} ²	%				0.0									
C _H ² anode	%				87.9									
C _H ² cathode	%				92.5									

Appendix 2: Flowcell Results

Batch Number	549
Date	13/5/97
j (mA/cm ²)	19.04
C _{T0}	867 mol/m ³ 10%

Reaction time (hr)		0	1	2	3	4	5.25	6	7	8	9	10	Average	Steady State
F	ml/hr				10		0				10	10	3	
P	g/hr						10						10	
R	ml/hr												0	
E _{cell}	V	16.0	11.8		11.6		11.1	11.1	11.2		11.6	11.9	11.5	11.9
E _{ACM}	V vs SCE	15.00	10.72		10.99		10.45	10.47	10.44		10.71	11.10		
E _{CAM}	V vs SCE	14.92	11.39		10.89		10.48	10.96	11.19		11.51	11.86		
E _A	V vs SCE	0.62	0.51		0.70		0.56	0.31	-0.02		0.03	0.01	0.30	
E _C	V vs SCE	0.54	0.18		0.60		0.59	0.80	0.73		0.83	0.77	0.64	
Em	V	14.38	10.21		10.29		9.89	10.16	10.46		10.68	11.09	10.40	11.09
Tw	°C	26.0	32.0		33.0		34.0	34.0	34.0		34.0	33.0		
Tp	°C		25.2		27.6		27.6	28.4			34.6			
Tf	°C													
Tr	°C													
T _A	°C	24.4	30.8		31.6		33.0	33.1	33.1		32.4	31.6	32.2	31.0
T _C	°C	24.5	30.9		31.7		33.1	33.2	33.0		32.4	31.8		
T _{ag}	°C	20.0	20.0		20.0		21.0	22.0	22.0					
T _{cg}	°C	20.0	20.0		20.0									
V _{ag}	ml		3		42		72	20	26				23	
V _{cg}	ml		146		262								136	
C _M			24239		22787		22770	22709	22735		22779	22777		111
C _T	mol/m ³		217.0		199.0		189.0	186.0	183.6		178.6	176.0		176.0
C _{MT}	mol/m ³		16.1		18.5		26.0	28.9	29.6		34.2	35.6		35.6
C _{DMT}	mol/m ³		18.8		21.2		29.8	32.0	31.0		34.0	34.0		34.0
C _{CO} ²	%				0									
C _H ² anode	%								91.1					
C _H ² cathode	%				100									

Appendix 2: Flowcell Results

Batch Number	552
Date	20/5/97
j (mA/cm ²)	19.04
C_{T0}	2646 mol/m ³ 30%

Reaction time (hr)		0	1	2	3	4	5	6	7	8	9	10	Average	Steady State
F	ml/hr	10.00	10.00		0.00	0.00	0.00	0.00	10.00	0.00	0.00		3.33	3.33
P	g/hr												8.00	4.33
R	ml/hr												0.00	
E _{cell}	V	6.30	8.04		8.12	8.30	8.22	8.10	8.12	8.24	8.14		8.16	8.24
E _{ACM}	V vs SCE	6.16	7.64		7.54	7.84	7.75	7.65	7.68	7.65	7.68			
E _{CAM}	V vs SCE	5.98	7.62		7.83	7.95	7.79	7.69	7.58	7.75	7.64			
E _A	V vs SCE	0.49	0.38		0.24	0.32	0.38	0.37	0.52	0.43	0.45		0.39	
E _C	V vs SCE	0.31	0.36		0.53	0.43	0.42	0.41	0.42	0.53	0.41		0.44	
E _m	V	5.67	7.26		7.30	7.52	7.37	7.28	7.16	7.22	7.23		7.29	7.29
T _w	°C	49.0	51.0		52.0	50.0	50.0	50.5	50.0	50.0	50.5			
T _p	°C													
T _f	°C		20.0		20.0									
T _r	°C													
T _A	°C	44.7	48.9		50.4	49.0	49.1	48.9	49.1	49.0	49.0		49.2	49.0
T _C	°C	43.9	49.4		50.2	49.2	49.3	49.4	49.2	49.3				
T _{ag}	°C	20.0	20.0		20.0	20.0	20.0	20.0	20.0	20.0				
T _{cg}	°C	20.0	20.0		20.0									
V _{ag}	ml	0	20		48	18	24	23	23	28			26	
V _{cg}	ml	0	170		320								163	
C _M	mol/m ³		18077		17400	17677	18001	18648	18225	18242	18131			
C _T	mol/m ³		408.0		403.0	424.0	441.0	469.0	441.0	438.0	436.0			436.0
C _{MT}	mol/m ³		56.7		62.7	65.3	67.0	73.1	68.6	76.2	77.1			77.0
C _{DMT}	mol/m ³		11.2		8.7	8.5	8.2	8.8	9.2	9.2	9.1			9.1
C _{CO} ²	%				0									
C _H ² anode	%				84.3									
C _H ² cathode	%										100			

Appendix 2: Flowcell Results

Batch Number	553
Date	21/5/97
j (mA/cm ²)	47.6
C _{T0}	2646 mol/m ³ 30%

Reaction time (hr)		0	1.5	2	3	4	5	6	7	8	9	10	Average	Steady State
F	ml/hr	10	10	10	10	10	10		10		10		10	10
P	g/hr			0.00	5.00	6.27	5.46		12.21		12.63		4.62	6.57
R	ml/hr			0.00									0.00	
E _{cell}	V	13.31	11.72	11.77	11.91	12.08	12.47		13.51		14.24		12.50	14.24
E _{ACM}	V vs SCE	12.26	10.79	10.87	10.99	11.17	11.66		12.45		13.29			
E _{CAM}	V vs SCE	11.06	9.72	9.69	9.68	9.81	10.14		10.87		11.41			
E _A	V vs SCE	1.91	1.74	1.82	1.96	2.00	2.09		2.22		2.54		2.05	
E _C	V vs SCE	0.71	0.67	0.64	0.65	0.64	0.57		0.64		0.66		0.64	
E _m	V	10.35	9.05	9.05	9.03	9.17	9.57		10.23		10.75		9.55	10.75
T _w	°C	21.5	27.0	28.0	28.5	29.0	29.5		29.5		29.5			
T _p	°C			27.0	27.0	28.2	29.0		29.1		29.0			
T _f	°C	20.0	20.0	20.0	20.0	20.0	20.0		21.0		21.0			
T _r	°C													
T _A	°C	20.6	26.8	27.6	28.3	29.3	29.2		29.5		29.9		28.7	30.0
T _C	°C	20.4	26.9	27.6	28.4	29.0	29.3		29.7		30.1			
T _{ag}	°C			20.0	20.0	20.0	20.0		21.0					
T _{cg}	°C			20.0	20.0									
V _{ag}	ml				58	52	56		124				58	
V _{cg}	ml				360									
C _M	mol/m ³		18161	18505	18319	17943	17919		17852		17068			
C _T	mol/m ³		415.0	427.0	419.0	415.0	430.0		465.0		470.0			470.0
C _{MT}	mol/m ³		81.9	86.0	89.8	91.0	91.9		94.8		92.4			94.0
C _{DMT}	mol/m ³		12.9	13.6	14.8	16.8	16.9		17.1		16.5			17.0
C _{CO} ²	%				0				0					
C _{II} ² anode	%				90.8									
C _{II} ² cathode	%								90.4					

Appendix 2: Flowcell Results

Batch Number	554
Date	22/5/97
j (mA/cm ²)	33.3
C _{T0}	2646 mol/m ³ 30

Reaction time (hr)		0	1	2	3	4	5	6	7	8	9	10	Average	Steady State
F	ml/hr	0	0	10	10	10							7.5	10
P	g/hr			2.45	7.73	5.63							3.34	7.9
R	ml/hr													
E _{cell}	V	9.45	11.41	11.51	11.37	11.49							11.45	11.49
E _{ACM}	V vs SCE	8.87	10.6	10.71	10.61	10.73								
E _{CAM}	V vs SCE	6.82	9.17	9.16	9.04	9.16								
E _A	V vs SCE	2.4	2	2.11	2.1	2.08							2.07	
E _C	V vs SCE	0.35	0.57	0.56	0.63	0.51							0.57	
E _m	V	6.47	8.6	8.6	8.51	8.65							8.59	8.65
T _w	°C	41	33	37	38.5	39.5								
T _p	°C			31.1	4									
T _f	°C			21	21	21								
T _r	°C													
T _A	°C	40.9	31.9	36.2	44	38.5							38.3	38.3
T _C	°C	40.8	31.9	36.1	37.7	38.5								
T _{ag}	°C	20	20	20	21	21								
T _{cg}	°C	20	20	20	21	21								
V _{ag}	ml	0	34	38	42	38							38	
V _{cg}	ml	0	250	252	280	242							256	
C _M	mol/m ³		17352	17484	18501	17606								
C _T	mol/m ³		480.0	468.0	500.0	464.0								464.0
C _{MT}	mol/m ³		105.9	105.0	104.7	104.6								104.6
C _{DMT}	mol/m ³		23.1	22.3	22.5	21.4								21.4
C _{CO} ²	%					0								
C _H ² anode	%					90.4								
C _H ² cathode	%					90.8								

Appendix 2: Flowcell Results

Batch Number	557
Date	28/5/97
j (mA/cm ²)	19.04
C _{T0}	1749 mol/m ³ 20%

Reaction time (hr)		0	1	2	3	4	5	6	7	8	9	10	Average	Steady State
F	ml/hr	10	10	0	10	10	0	10	0	10	10		6.67	10
P	g/hr		0.57	3.1	3.16	5.83	3.72	1.53	3.25	2.95	3.44		3.06	4.53
R	ml/hr													
E _{cell}	V	4.39	4.53	4.5	4.42	4.38	4.51	4.58	4.5	4.6	4.57		4.51	
E _{ACM}	V vs SCE	3.86	4	3.96	3.84	3.8	3.88	3.93	3.79	3.85	3.81			
E _{CAM}	V vs SCE	4.11	4.41	4.39	4.23	4.22	4.41	4.3	4.23	4.35	4.26			
E _A	V vs SCE	0.07	0.09	0.07	0.14	0.11	0.14	0.18	0.19	0.16	0.21		0.14	
E _C	V vs SCE	0.32	0.5	0.5	0.53	0.53	0.67	0.55	0.63	0.66	0.66		0.58	
E _m	V	3.79	3.91	3.89	3.7	3.69	3.74	3.75	3.6	3.69	3.6		3.73	3.7
T _w	°C	42	35	37	40	41	40	40	40	40	40			
T _p	°C		26.9		27		32		27.6		29.8			
T _f	°C	20	20	21	21	21	22	22	23		22			
T _r	°C													
T _A	°C	39.9	33.6	35.5	38.2	39.6	39	38.7	38.7	38.4	38.2		37.7	38.2
T _C	°C	39.9	33.6	35.5	38.2	39.6	38.9	38.8	38.6	38.4	38.2			
T _{ag}	°C	20	20	21	21	22	22	23	24	24				
T _{cg}	°C	20	20	21	21	22	22	23	24	24				
V _{ag}	ml		10	18	21.5	24	28	24	27	22			21.81	
V _{cg}	ml		186	154	164	146	152	150	138	145			154.38	
C _M	mol/m ³		19859		20661		20096		21382		19769			
C _T	mol/m ³		312.0		304.0		292.0		295.0		287.0			287.0
C _{MT}	mol/m ³		29.7		34.8		38.1		40.1		38.6			40.1
C _{DMT}	mol/m ³		4.6		4.9		5.1		5.0		4.8			5.1
C _{CO} ²	%										0			
C _H ² anode	%										80.6			
C _H ² cathode	%										92.2			

Appendix 2: Flowcell Results

Batch Number	558
Date	29/5/97
j (mA/cm ²)	47.6
C _{T0}	1749 mol/m ³ 20%

Reaction time (hr)		0	1	2	3	4	5	6	7	8	9	10	Average	Steady State
F	ml/hr	10	10	10	10	10	10	10	10	10	10		10	10
P	g/hr		4.68	8.38	5.62	6.35	6.42	18.84	4.39	7.81	6.65		7.68	8.52
R	ml/hr													
E _{cell}	V	4.89	4.51	4.56	4.63	4.7	4.82	4.86	4.96	5.05	5.19		4.81	
E _{ACM}	V vs SCE	3.92	3.92	4.01	4.09	4.16	4.21	4.27	4.3	4.37	4.54			
E _{CAM}	V vs SCE	4.54	4.18	3.81	3.47	3.46	2.39	4.21	4.35	4.42	4.63			
E _A	V vs SCE	0.1	0.26	0.62	1.02	1.06	2.06	0.49	0.5	0.5	0.42		0.77	
E _C	V vs SCE	0.72	0.52	0.52	0.4	0.36	0.24	0.43	0.55	0.5	0.55		0.46	
Em	V	3.82	3.66	3.39	3.07	3.1	2.15	3.78	3.8	3.87	4.08		3.43	4.08
Tw	°C	46	52	52	51.5	51.5	50.5	51	50.5	50.5	50.5			
Tp	°C		32.2		34.2		35.4		35.9		38.8			
Tf	°C	20	22	23	22	22	22	22	22	22	22			
Tr	°C													
T _A	°C	42.6	49.9	50.5	50	50.4	49.4	49.6	49.3	49.4	49.3		49.04	49.3
T _C	°C	42.5	49.9	50.6	50	50.4	49.3	49.6	49.3	49.3	49.3			
Tag	°C	22	22	22	22	22	22	22						
Tcg	°C	22	22	22	22	22	22	22	22		22			
Vag	ml		36	68	66	66	68	66					61.67	
Vcg	ml		380	340	380	380	400	400	330				372.8	
C _M	mol/m ³		20742		22644				21142		20978			
C _T	mol/m ³		274.0		307.0				280.0		285.0			285.0
C _{MT}	mol/m ³		41.0		52.2				55.3		57.7			58.4
C _{DMT}	mol/m ³		5.3		7.8				8.6		9.6			10.1
C _{CO} ²	%							0						
C _H ² anode	%							79						
C _H ² cathode	%								93.7					

Appendix 2: Flowcell Results

Batch Number	559
Date	29/5/97
j (mA/cm ²)	95.2
C _{T0}	1749 mol/m ³ 20%

Reaction time (hr)		0	1	2	3	4	5	5.5	7	8	9	10	Average	Steady State
F	ml/hr	10	10	10	10	10	10	10					10	10
P	g/hr		3.45	5.5	6.2	5.7	5.68	32.11					5.35	7.44
R	ml/hr		10	10	10	10	26	26					15.33	26
E _{cell}	V	8.26	7.2	8.96	9.96	11.6	14.95	20					12.12	
E _{ACM}	V vs SCE	7.07	6.21	6.3	8.4	9.83	13.6							
E _{CAM}	V vs SCE	7	6.16	6.96	7.14	7.2	10.97							
E _A	V vs SCE	0.71	0.84	1.08	2.17	3.42	3.07						2.12	
E _C	V vs SCE	0.64	0.79	1.74	0.91	0.79	0.44						0.93	
E _m	V	6.36	5.37	5.22	6.23	6.41	10.53						6.75	10.53
T _w	°C	35	31.5	31.5	33	34	36	36						
T _p	°C		28.8		31.7	34.1	38.3	38						
T _f	°C	20	21	22	22	23	23	23						
T _r	°C		21	22	22	23	23	23						
T _A	°C	34.5	31.5	32.3	33.8	35.5	37.8	38						38
T _C	°C	34.5	31.6	32.3	33.8	35.5	37.8	38					34.77	
T _{ag}	°C	22	22	22	23	23	23							
T _{cg}	°C	22	22	22		23	23							
V _{ag}	ml		44	90	94	96	167						98.2	
V _{cg}	ml		340(.5hr)	790		510(45 min)	390(.5hr)						738.2	
C _M	mol/m ³		21080		20852	23995	20260	20282						
C _T	mol/m ³		268.0		252.0	269.0	245.0	244.0						244.0
C _{MT}	mol/m ³		61.3		75.3	91.6	89.8	90.2						90.5
C _{DMT}	mol/m ³		12.1		18.2	23.0	25.6	26.1						26.5
C _{CO} ²	%						0							
C _H ² anode	%						99.6							
C _H ² cathode	%													

APPENDIX 3: PROGRAM CODE

```
REM
REM          SPEmodel.bas
REM          written by R.S.Girt
REM          as part of PhD Thesis
REM  "Scale Up Of Solid Polymer Electrolyte for Electro-Organic Synthesis"
REM          Department of Chemical and Process Engineering
REM          University of Newcastle Upon Tyne
REM
REM
*****
*
REM-----
REM          declaration of subroutines
DECLARE SUB properties ()
DECLARE SUB reynolds ()
DECLARE SUB pcmassbalance ()
DECLARE SUB pgmassbalance ()
DECLARE SUB pamassbalance ()
DECLARE SUB update ()
DECLARE SUB mtgmassbalance ()
DECLARE SUB dmtgmassbalance ()
DECLARE SUB wgmassbalance ()
DECLARE SUB mgmassbalance ()
DECLARE SUB tgmassbalance ()
DECLARE SUB wcmassbalance ()
DECLARE SUB mtcmassbalance ()
DECLARE SUB dmtcmassbalance ()
DECLARE SUB tcmassbalance ()
DECLARE SUB mcmassbalance ()
DECLARE SUB initial ()
DECLARE SUB anodemassbalance ()
DECLARE SUB anodepotential ()
```

```

DECLARE SUB anodecurrentbalance ()
DECLARE SUB cathodechambermb ()
DECLARE SUB cathodemassb ()
DECLARE SUB dimensions ()
DECLARE SUB dmtamassbalance ()
DECLARE SUB feedconditions ()
DECLARE SUB feedmassb ()
DECLARE SUB flowsandvolumes ()
DECLARE SUB graphitebedmassbalance ()
DECLARE SUB initialcalculations ()
DECLARE SUB initialconditions ()
DECLARE SUB initparameters ()
DECLARE SUB loopmassb ()
DECLARE SUB mamassbalance ()
DECLARE SUB membranemassb ()
DECLARE SUB mtamassbalance ()
DECLARE SUB potentials ()
DECLARE SUB separatormassb ()
DECLARE SUB tamassbalance ()
DECLARE SUB wamassbalance ()
DECLARE SUB dataoutput ()
REM-----
REM
REM-----
REM
REM      declaration of all variables shared by subroutines
REM
REM
REM      E - potentials (V)
REM      C - concentrations (mol/m3)
REM      m - methanol
REM      t - toluene
REM      mt - methoxytoluene
REM      dmt - dimethoxytoluene
REM      p - polymer

```

```

REM      w - water
REM      f,1,2,4,5,6,7,r - feed, block numbers, recycle
REM      ini, fin - initial and final conditions
REM      kf - rate constants for electrochemical reactions (m4/mol.s)
REM      beta - transfer coefficients
REM      n - electron stoichiometry
REM      Far, f, R, temp - Faraday constant (C/mol), F/R.temp (per V), gas constant
(J/mol.K), temperature (K)
REM      A, d - area (m2) and diameter (m)
REM      kL - mass transfer coefficients (m/s)
REM      j - calculated current density (A/m2)
REM      currenterror - difference between applied and calculated current densities
REM      r - rates (mol/m2.s)
REM      F - flows (m3/s)
REM      V - volumes (m3)
REM      A, C - anode and cathode
REM      t, runtime, h - time (minutes), maximum time, step time
REM      a, g - Runge Kutta constants
COMMON SHARED ETAa(), ETAc(), Ea, Ecell(), EM
COMMON SHARED cmf, cm1ini, cm1fin, cm2, cm4ini, cm4fin, cm5(), cm6, cm7
COMMON SHARED ctf, ct1ini, ct1fin, ct2, ct4ini, ct4fin, ct5(), ct6, ct7
COMMON SHARED cmtf, cmt1ini, cmt1fin, cmt2, cmt4ini, cmt4fin, cmt5(), cmt6, cmt7
COMMON SHARED cdmtf, cdmt1ini, cdmt1fin, cdmt2, cdmt4ini, cdmt4fin, cdmt5(),
cdmt6, cdmt7
COMMON SHARED cwf, cw1ini, cw1fin, cw2, cw4ini, cw4fin, cw5(), cw6, cw7
COMMON SHARED cpf, cp1ini, cp1fin, cp2, cp4ini, cp4fin, cp5(), cp6, cp7
COMMON SHARED kf1, kf10, kf2, kf20, kf3, kf30, kf4, kf40
COMMON SHARED beta1, beta2, beta3, beta4
COMMON SHARED n1, n2, n3, n4
COMMON SHARED Far, f, R, temp
COMMON SHARED Aa, dmean, dhydraulicfibre, viscosity, density, diffusivity, porosity
COMMON SHARED kLMT, kLW, electrodeheight, electrodewidth
COMMON SHARED jt, currentdensity, currenterror
COMMON SHARED r1, r2, r3, r4
COMMON SHARED F1, F2, F4, F6, F7, Ff, Fp, Fr

```

```

COMMON SHARED Va, Vg, Vc, Vr, Vh(), Vht()
COMMON SHARED t, runtime, counter
COMMON SHARED a(), g(), h
CLS
REM-----
REM
REM
REM-----
REM      sets initial conditions in the reactor - feed, current, dimensions
REM      temperatures, osmotic flow, times, mass transfer coefficients
CALL initial
REM
REM-----
REM-----
REM      THE PROGRAM
REM
FOR t = 1 TO runtime
    REM
    CALL anodepotential
    CALL anodemassbalance
    CALL membranemassb
    CALL cathodemassb
    CALL cathodechambermb
    CALL separatormassb
    CALL loopmassb
    CALL feedmassb
    CALL potentials
    CALL update
    IF ct1ini < 0 THEN GOTO 4
    REM      terminates for negative toluene concentration
NEXT t
REM
REM
REM-----
REM-----

```

```

REM
4 CALL dataoutput
REM
BEEP
END
REM
REM-----
REM      Data statements
REM      This data is in A/m2, K, m3/s, and mol/m3
REM
REM
REM
DATA 500, 313, 2.777777e-9, 20114, 1749.1, 0, 0, 0, 0
REM DATA 500, 308, 2.777777e-9, 20114, 1749.1, 0, 0, 0, 0
REM DATA 476, 310.6, 2.777e-9, 22436, 867.11, 0, 0, 0, 0
REM DATA 952, 324.2, 2.77e-9, 22436, 867.11, 0, 0, 0, 0
REM DATA 190.4, 305.2, 8.33e-8, 22436, 867.11, 0, 0, 0, 0
REM DATA 190.4, 322.2, 9.25e-10, 17753, 2646.4, 0, 0, 0, 0
REM DATA 476, 301.6, 2.777e-9, 17753, 2646.4, 0, 0, 0, 0
REM DATA 333.3, 311.3, 2.083e-9, 17753, 2646.4, 0, 0, 0, 0
REM DATA 190.4, 310.7, 1.85e-9, 20114, 1749.1, 0, 0, 0, 0
REM DATA 476, 322.0, 2.777e-9, 20114, 1749.1, 0, 0, 0, 0
REM DATA 952, 307.7, 2.77e-9, 20114, 1749.1, 0, 0, 0, 0
REM-----
*****
*
SUB anodecurrentbalance
REM
REM  calculates current density for the guessed anode overpotential
REM
REM-----
REM
REM  calculates rate constants at the guessed overpotential
REM
LET kfl = kf10 * EXP(-1 * (beta1) * n1 * f * Ea)

```

```

LET kf2 = kf20 * EXP(-1 * (beta2) * n2 * f * Ea)
LET kf3 = kf30 * EXP(-1 * (beta3) * n3 * f * Ea)
LET kf4 = kf40 * EXP(-1 * (beta4) * n4 * f * Ea)
REM
REM-----
REM
REM  calculates rates of each reaction
REM
LET r1 = kf1 * cmlini * ctlini
LET r2 = kf2 * cmlini * (kf1 * cmlini * ctlini + kLMT * cmtlini) / (kf2 * cmlini +
kLMT)
LET r3 = kLW * kf3 * cmlini * cwlini / (kLW + kf3 * cmlini)
LET r4 = kf4 * ctlini * ctlini
REM
REM-----
REM
REM  current density is the sum of the individual rates
REM
LET jt = (r1 * n1 + r2 * n2 + r3 * n3 + r4 * n4) * Far
REM
REM
END SUB
*****
*

SUB anodemassbalance
REM
REM  carries out a mass balance over the anode chamber
REM  for all the components
REM
REM
CALL mamassbalance
CALL tamassbalance
CALL mtamassbalance
CALL dmtamassbalance

```

CALL wamassbalance

CALL pamassbalance

REM

REM

REM

REM

END SUB

*

SUB anodepotential

REM calculates the anode overpotential for the given current

REM-----

REM

LET Ea = ETAa(t) 'sets the variable at the guessed overpotential

LET counter = 0 'sets the loop counter to zero

REM

REM-----

REM

10 CALL anodecurrentbalance 'goes to calculate the current density at the

REM guessed overpotential

REM

REM-----

REM

REM calculates the error and if less than 0.5% jumps to

REM the main program

REM

LET currenterror = 100 * (jt - (currentdensity)) / (currentdensity)

IF ABS(currenterror) < .5 THEN GOTO 40

REM

REM-----

REM

LET counter = counter + 1 'checks to see if the loop is converging

IF counter > 5000 THEN GOTO 50

REM

```

REM-----
REM
IF currenterror < 0 GOTO 20      'sends the program to the respective
IF currenterror > 0 GOTO 30      'iteration section
REM
REM-----
REM
20 IF currenterror < -2 THEN      'increments the overpotential
LET Ea = Ea + .001
ELSE LET Ea = Ea + .00001
END IF
GOTO 10
REM
REM-----
REM
30 IF currenterror > 2 THEN      'increments the overpotential
LET Ea = Ea - .001
ELSE LET Ea = Ea - .00001
END IF
GOTO 10
REM
REM-----
REM
40 LET ETAa(t + 1) = Ea          'sets the overpotential at the
REM                               'correct value
REM
REM
50 END SUB

*****
*

SUB cathodechambermb
REM
REM  carries out a mass balance over the cathode chamber
REM  for all the components

```

```

REM
REM
CALL mcmassbalance
CALL tcmassbalance
CALL mtcmassbalance
CALL dmtcmassbalance
CALL wcmassbalance
CALL pcmassbalance
REM
REM
REM
END SUB

*****
*

SUB cathodemassb
REM
REM calculates the cathode overpotential and the amount of hydrogen evolved
REM
LET ETAc(t) = .39 + .21 * LOG(currentdensity)
LET Vh(t) = currentdensity * Aa * 22400 / (2 * Far) * 60
LET Vht(t) = Vht(t - 1) + Vh(t)
REM
REM
REM
END SUB

*****
*

SUB dataoutput
REM
REM writes the results to the file modata.xls
REM
OPEN "c:\steve\speproje\modellin\modata.xls" FOR OUTPUT AS #1
FOR cell = 1 TO runtime STEP 10

```

WRITE #1, cell, Ecell(cell), ETAa(cell), ct5(cell), cmt5(cell), cdmt5(cell)

NEXT cell

CLOSE

REM

REM

REM

END SUB

*

SUB dimensions

REM

REM defines the size of all arrays

REM

REM-----

REM

DIM cm5(runtime + 1)

DIM ct5(runtime + 1)

DIM cmt5(runtime + 1)

DIM cdmt5(runtime + 1)

DIM cw5(runtime + 1)

DIM cp5(runtime + 1)

DIM ETAa(runtime + 1)

DIM ETAc(runtime + 1)

DIM Ecell(runtime + 1)

DIM Vh(runtime + 1)

DIM Vht(runtime + 1)

DIM g(4)

DIM a(4)

REM

REM-----

REM

LET a(1) = 2

LET a(2) = 4 'sets the Runge Kutta constants

LET a(3) = 3

LET a(4) = 1

REM

REM

REM

END SUB

*

SUB dmtamassbalance

REM

REM mass balance on dimethoxytoluene in anode using Runge Kutta

REM

REM

LET conc = cdmt1ini

FOR n = 1 TO 4

LET b2 = kf2 * cm1ini * (kf1 * cm1ini * ct1ini + kLMT * cmt1ini) / (kf2 * cm1ini + kLMT)

LET b5 = F7 * cdmt7

LET b6 = F1 * conc

LET g(n) = (b2 * 60 * Aa + b5 - b6) / Va

LET conc = cdmt1ini + n * h * g(n) / a(n)

NEXT n

LET cdmt1fin = cdmt1ini + h * (g(1) + 2 * g(2) + 2 * g(3) + g(4)) / 6

END SUB

*

SUB dmtcmassbalance

REM

REM mass balance on dimethoxytoluene in the cathode chamber

REM

LET conc = cdmt4ini

FOR n = 1 TO 4

LET b5 = F2 * cdmt2 / Vc

```

    LET b6 = F4 * conc / Vc
    LET g(n) = b5 - b6
    LET conc = cdmt4ini + n * h * g(n) / a(n)
NEXT n
LET cdmt4fin = cdmt4ini + h * (g(1) + 2 * g(2) + 2 * g(3) + g(4)) / 6
REM
REM
REM
END SUB

*****
*

SUB feedconditions
REM
REM      sets all block concentrations to the feed conditions
REM
LET cm1ini = cmf
LET cm1fin = cmf
LET cm2 = cmf
LET cm4ini = cmf
LET cm4fin = cmf
LET cm5(0) = 0
LET cm6 = cmf
LET cm7 = cmf
LET ct1ini = ctf
LET ct1fin = ctf
LET ct2 = ctf
LET ct4ini = ctf
LET ct4fin = ctf
LET ct5(0) = 0
LET ct6 = ctf
LET ct7 = ctf
LET cmt1ini = cmtf
LET cmt1fin = cmtf
LET cmt2 = cmtf

```

```

LET cmt4ini = cmtf
LET cmt4fin = cmtf
LET cmt5(0) = 0
LET cmt6 = cmtf
LET cmt7 = cmtf
LET cdmt1ini = cdmtf
LET cdmt1fin = cdmtf
LET cdmt2 = cdmtf
LET cdmt4ini = cdmtf
LET cdmt4fin = cdmtf
LET cdmt5(0) = 0
LET cdmt6 = cdmtf
LET cdmt7 = cdmtf
LET cw1ini = cwf
LET cw1fin = cwf
LET cw2 = cwf
LET cw4ini = cwf
LET cw4fin = cwf
LET cw5(0) = 0
LET cw6 = cwf
LET cw7 = cwf
LET cp1ini = cpf
LET cp1fin = cpf
LET cp2 = cpf
LET cp4ini = cpf
LET cp4fin = cpf
LET cp6 = cpf
LET cp7 = cpf
END SUB

*****
*

SUB feedmassb
REM
REM   mass balance on the feed and recycle streams

```

```

REM
LET cm7 = (Ff * 60 * cmf + Fr * cm6) / F7
LET ct7 = (Ff * 60 * ctf + Fr * ct6) / F7
LET cmt7 = (Ff * 60 * cmtf + Fr * cmt6) / F7
LET cdmt7 = (Ff * 60 * cdmtf + Fr * cdmt6) / F7
LET cw7 = (Ff * 60 * cwf + Fr * cw6) / F7
LET cp7 = (Ff * 60 * cpf + Fr * cp6) / F7
REM
REM
REM
END SUB
*****
*

SUB flowsandvolumes
REM      defines reactor dimensions then
REM      calculates flows around the system
REM
REM-----
REM
LET electrodeheight = .07      'reactor dimensions
LET electrodewidth = .03
LET Aa = electrodeheight * electrodewidth
LET Vr = 1.28E-06 / .0021 * Aa
LET Vht = 0
LET Vc = electrodeheight * electrodewidth * .01 + 1.96E-06
LET Va = electrodeheight * electrodewidth * .01 + 3.338E-06
REM
REM-----
REM
LET F1 = (currentdensity / 10 * .478767 - 8.88764) / (.0021 * 1000000 * 60) * Aa
IF F1 < (Ff * 60) THEN PRINT "WARNING - Feed Too HIGH"
IF F1 < 1.38888E-10 THEN LET F1 = 2.777777E-10
IF F1 < (Ff * 60) THEN LET Ff = F1 / 60
LET F2 = F1      'calculates flows through the system

```

```

LET F4 = F1                'based on the electro-osmotic flow
LET Fp = (Ff * 60)         'Increases the feed rate if it is negative
LET Fr = F1 - (Ff * 60)    'and decreases it if it is bigger than Fos
IF Fr < 0 THEN LET Fr = 0
LET F7 = (Ff * 60) + Fr
REM
REM-----
REM
PRINT Ff * 60, F1, F2, F4, Fp, Fr, F7    'prints the flows as a check
REM
REM
REM
END SUB

*****
*

SUB initial
REM
REM      sets all variables and arrays used in the main program
REM
CALL initialconditions
CALL dimensions
CALL feedconditions
CALL flowsandvolumes
CALL properties
CALL reynolds
CALL initparameters
REM
REM
REM
END SUB

*****
*

SUB initialconditions

```

```

REM
REM      reads the independent variables
REM
READ currentdensity, temp, Ff, cmf, ctf, cmtf, cdmf, cwf, cpf
LET h = 1
LET runtime = 2000
REM
REM
REM
END SUB
*****
*

SUB initparameters
REM
REM      sets the constants
REM
REM-----
REM
LET R = 8.314      'universal constants
LET Far = 96485
LET f = Far / (R * temp)
REM
REM-----
REM
REM
REM
LET kf10 = 4.858732E-28
LET kf20 = 7.665269E-28  'rate constants
LET kf30 = 0
LET kf40 = 3.96E-37
REM
REM
REM-----
REM

```

```

REM
LET kLW = kLMT      'sets all mass transfer coefficients equal
REM
REM
REM-----
REM
REM
LET beta1 = -.472
LET beta2 = -.472   'transfer coefficients
LET beta3 = -.472
LET beta4 = -.472
REM
REM
REM-----
REM
REM
LET n1 = 2
LET n2 = 2          'electron stoichiometry
LET n3 = 6
LET n4 = 3.42
REM
REM
REM-----
REM
REM
LET ETAa(1) = 0      'overpotentials
LET ETAc(1) = 0
REM
REM
REM
END SUB
*****
*

SUB loopmassb

```

```

REM
REM    mass balance on the recycle stream
REM-----
REM
REM
IF Fr = 0 THEN
LET tau6 = 1E+10    'calculates the residence time in the stream
ELSE
LET tau6 = Vr / Fr
END IF
REM
REM
REM-----
REM
REM
LET lagtime = INT(t - tau6)    'calculates the lagtime
IF lagtime < .5 THEN LET lagtime = 1
REM
REM
REM-----
REM
REM
LET cm6 = cm5(lagtime)
LET ct6 = ct5(lagtime)    'calculates the concentrations exiting
LET cmt6 = cmt5(lagtime)    'from the recycle stream
LET cdmt6 = cdmt5(lagtime)
LET cw6 = cw5(lagtime)
LET cp6 = cp5(lagtime)
REM
REM
REM-----
REM
REM
END SUB

```

*

SUB mamassbalance

REM

REM mass balance on methanol in anode

REM-----

REM

REM

LET conc = cm1ini

FOR n = 1 TO 4

LET b1 = kf1 * conc * ct1ini

LET b2 = kf2 * conc * (kf1 * conc * ct1ini + kLMT * cmt1ini) / (kf2 * conc + kLMT)

LET b3 = kW * kf3 * conc * cw1ini / (kW + kf3 * conc)

LET b5 = F7 * cm7

LET b6 = F1 * conc

LET g(n) = (b5 - (b1 + b2 + b3) * 60 * Aa - b6) / Va

LET conc = cm1ini + n * h * g(n) / a(n)

NEXT n

LET cm1fin = cm1ini + h * (g(1) + 2 * g(2) + 2 * g(3) + g(4)) / 6

REM

REM

REM-----

REM

REM

END SUB

*

SUB mcmassbalance

REM

REM

REM mass balance on methanol in cathode

REM-----

REM

```

LET conc = cm4ini
FOR n = 1 TO 4
LET b5 = F2 * cm2 / Vc
LET b6 = F4 * conc / Vc
LET g(n) = b5 - b6
LET conc = cm4ini + n * h * g(n) / a(n)
NEXT n
LET cm4fin = cm4ini + h * (g(1) + 2 * g(2) + 2 * g(3) + g(4)) / 6
REM
REM
REM
END SUB
*****
*

SUB membranemassb
REM
REM    mass balance over the membrane
REM-----
REM
REM
LET cm2 = F1 * cm1ini / F2
LET ct2 = F1 * ct1ini / F2
LET cmt2 = F1 * cmt1ini / F2
LET cdmt2 = F1 * cdmt1ini / F2
LET cw2 = F1 * cw1ini / F2
LET cp2 = F1 * cp1ini / F2
REM
REM
REM-----
REM
REM
END SUB
*****
*

```

SUB mtamassbalance

REM

REM mass balance on methoxytoluene in anode

REM-----

REM

REM

LET conc = cmt1ini

FOR n = 1 TO 4

LET b1 = kf1 * cm1ini * ct1ini

LET b2 = kf2 * cm1ini * (kf1 * cm1ini * ct1ini + kLMT * conc) / (kf2 * cm1ini + kLMT)

LET b5 = F7 * cmt7

LET b6 = F1 * conc

LET g(n) = ((b1 - b2) * 60 * Aa + b5 - b6) / Va

LET conc = cmt1ini + n * h * g(n) / a(n)

NEXT n

LET cmt1fin = cmt1ini + h * (g(1) + 2 * g(2) + 2 * g(3) + g(4)) / 6

REM

REM

REM-----

REM

REM

END SUB

*

SUB mtcmassbalance

REM

REM mass balance on methoxytoluene in cathode

REM-----

REM

REM

LET conc = cmt4ini

FOR n = 1 TO 4

LET b5 = F2 * cmt2 / Vc

```

LET b6 = F4 * conc / Vc
LET g(n) = b5 - b6
LET conc = cmt4ini + n * h * g(n) / a(n)
NEXT n
LET cmt4fin = cmt4ini + h * (g(1) + 2 * g(2) + 2 * g(3) + g(4)) / 6
REM
REM
REM-----
REM
REM
END SUB

*****
*

SUB pamassbalance
REM
REM    mass balance on polymer in anode
REM-----
REM
REM
LET conc = cplini
FOR n = 1 TO 4
LET b4 = kf4 * ctlini * ctlini
LET b5 = F7 * cp7
LET b6 = F1 * conc
LET g(n) = (b4 * 60 * Aa + b5 - b6) / Va
LET conc = cplini + n * h * g(n) / a(n)
NEXT n
LET cplfin = cplini + h * (g(1) + 2 * g(2) + 2 * g(3) + g(4)) / 6
REM
REM
REM-----
REM
REM
END SUB

```

*

SUB pcmassbalance

REM

REM mass balance on polymer in cathode

REM-----

REM

REM

LET conc = cp4ini

FOR n = 1 TO 4

LET b5 = F2 * cp2 / Vc

LET b6 = F4 * conc / Vc

LET g(n) = b5 - b6

LET conc = cp4ini + n * h * g(n) / a(n)

NEXT n

LET cp4fin = cp4ini + h * (g(1) + 2 * g(2) + 2 * g(3) + g(4)) / 6

REM

REM

REM-----

REM

REM

END SUB

*

SUB potentials

REM

REM calculates cell and membrane potentials

REM-----

REM

REM

LET em1 = currentdensity * .1 * .047231

LET em2 = (temp - 273) * .05769

LET em3 = .02281 * ctf / 87.46 'membrane potential based on MLR

```

LET em4 = .182139 * t / 60
LET EM = 5.937778 + (em1) - (em2) - (em3) + (em4)
LET Ecell(t) = ETAa(t) + ETAc(t) + EM
REM
REM
REM-----
REM
REM
END SUB

*****
*

SUB properties
REM
REM    graphite felt and electrolyte properties
REM-----
REM
REM
LET dmean = 4 * Aa / (2 * (electrodewidth + electrodeheight))
LET porosity = .94
LET fibrediameter = .000011
LET Sb = (4 / fibrediameter) * (1 - porosity)
LET dhydraulicfibre = 4 * porosity / Sb
REM
REM
REM-----
REM
REM
LET density = 786.7
LET viscosity = .0004724
LET diffusivity = 1E-09
REM
REM
REM-----
REM

```

```

REM
END SUB
*****
*

SUB reynolds
REM
REM    calculates mass transfer coefficients from reynolds number
REM-----
REM
REM
LET uosmotic = F1 / Aa / 60
LET re = density * uosmotic * dhydraulicfibre / viscosity
LET kLMT = (3.19 * (diffusivity / dhydraulicfibre) * re ^ .69) * 60
REM
REM
REM-----
REM
REM
END SUB
*****
*

SUB separatormassb
REM
REM    calculates product stream concentration
REM-----
REM
REM
LET cm5(t) = cm4ini
LET ct5(t) = ct4ini
LET cmt5(t) = cmt4ini
LET cdmt5(t) = cdmt4ini
LET cw5(t) = cw4ini
LET cp5(t) = cp4ini

```

```

REM
REM
REM-----
REM
REM
END SUB
*****
*

SUB tamassbalance
REM
REM    mass balance on toluene in anode
REM-----
REM
REM
LET conc = ct1ini
FOR n = 1 TO 4
LET b1 = kf1 * cm1ini * conc
LET b4 = kf4 * conc * conc
LET b5 = F7 * ct7
LET b6 = F1 * conc
LET g(n) = (b5 - b6 - (b1 + b4) * 60 * Aa) / Va
LET conc = ct1ini + n * h * g(n) / a(n)
NEXT n
LET ct1fin = ct1ini + h * (g(1) + 2 * g(2) + 2 * g(3) + g(4)) / 6
REM
REM
REM-----
REM
REM
END SUB
*****
*

SUB tcmassbalance

```

```

REM
REM   mass balance on toluene in cathode chamber
REM-----
REM
REM
LET conc = ct4ini
FOR n = 1 TO 4
LET b5 = F2 * ct2 / Vc
LET b6 = F4 * conc / Vc
LET g(n) = b5 - b6
LET conc = ct4ini + n * h * g(n) / a(n)
NEXT n
LET ct4fin = ct4ini + h * (g(1) + 2 * g(2) + 2 * g(3) + g(4)) / 6
REM
REM
REM-----
REM
REM
END SUB
*****
*

SUB update
REM
REM   resets initial values for next increment
REM   and prints current product status
REM-----
REM
REM
LET cm1ini = cm1fin
LET ct1ini = ct1fin
LET cmt1ini = cmt1fin
LET cdmt1ini = cdmt1fin
LET cw1ini = cw1fin
LET cplini = cplfin

```

```

LET cm4ini = cm4fin
LET ct4ini = ct4fin
LET cmt4ini = cmt4fin
LET cdmt4ini = cdmt4fin
LET cw4ini = cw4fin
LET cp4ini = cp4fin
REM
REM
REM-----
REM
REM
PRINT USING "### "; t; counter;
PRINT USING "#.#### "; ETAA(t); EM; ETAC(t);
PRINT USING "##### "; jt; cm5(t); ct5(t); cmt5(t); cdmt5(t); cp5(t)
REM
REM
REM-----
REM
REM
END SUB
*****
*

SUB wamassbalance
REM
REM    mass balance on water in anode
REM-----
REM
REM
LET conc = cw1ini
FOR n = 1 TO 4
LET b3 = kLW * kf3 * cm1ini * conc / (kLW + kf3 * cm1ini)
LET b5 = F7 * cw7
LET b6 = F1 * conc
LET g(n) = (b5 - b6 - b3 * Aa) / Va

```

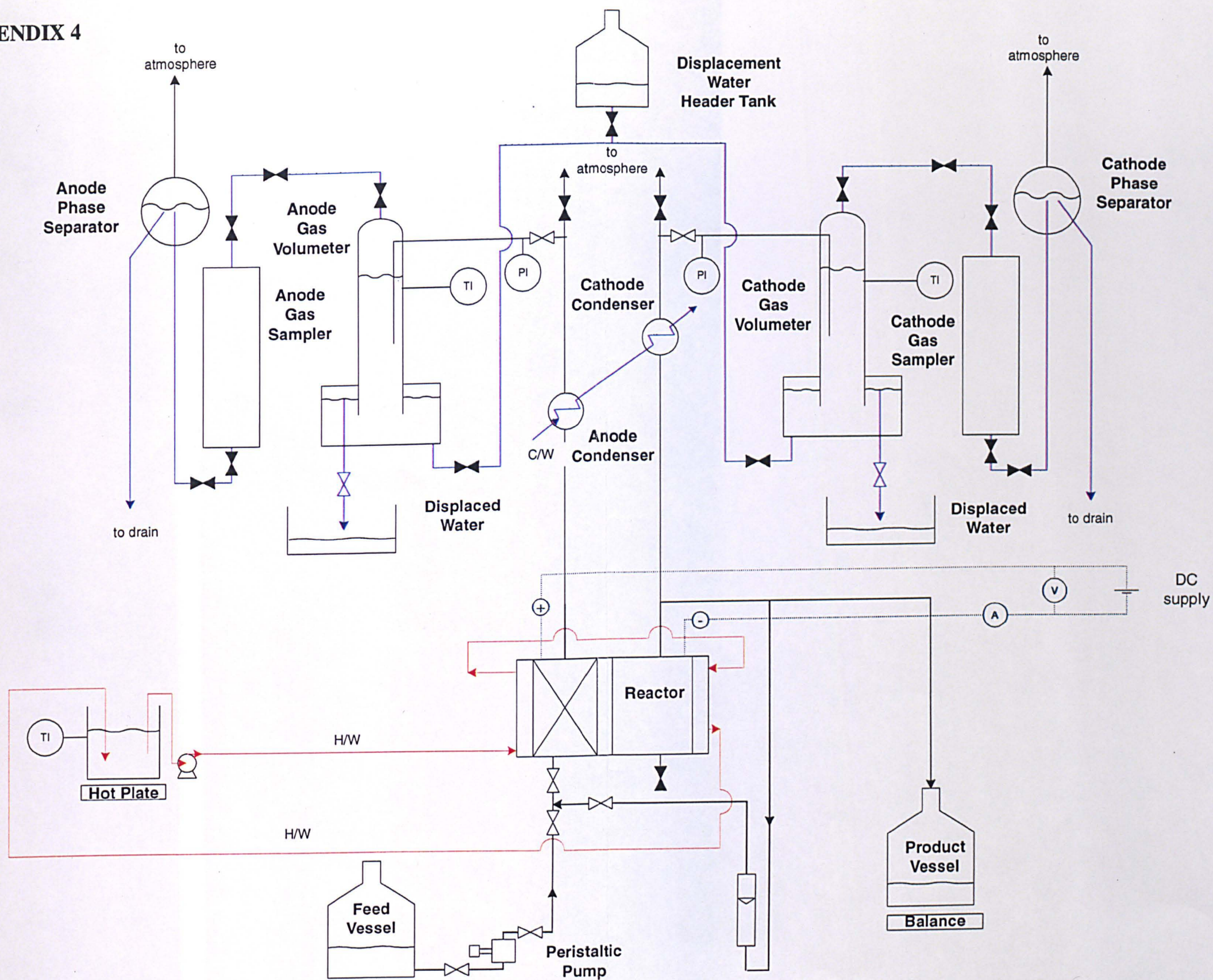
```

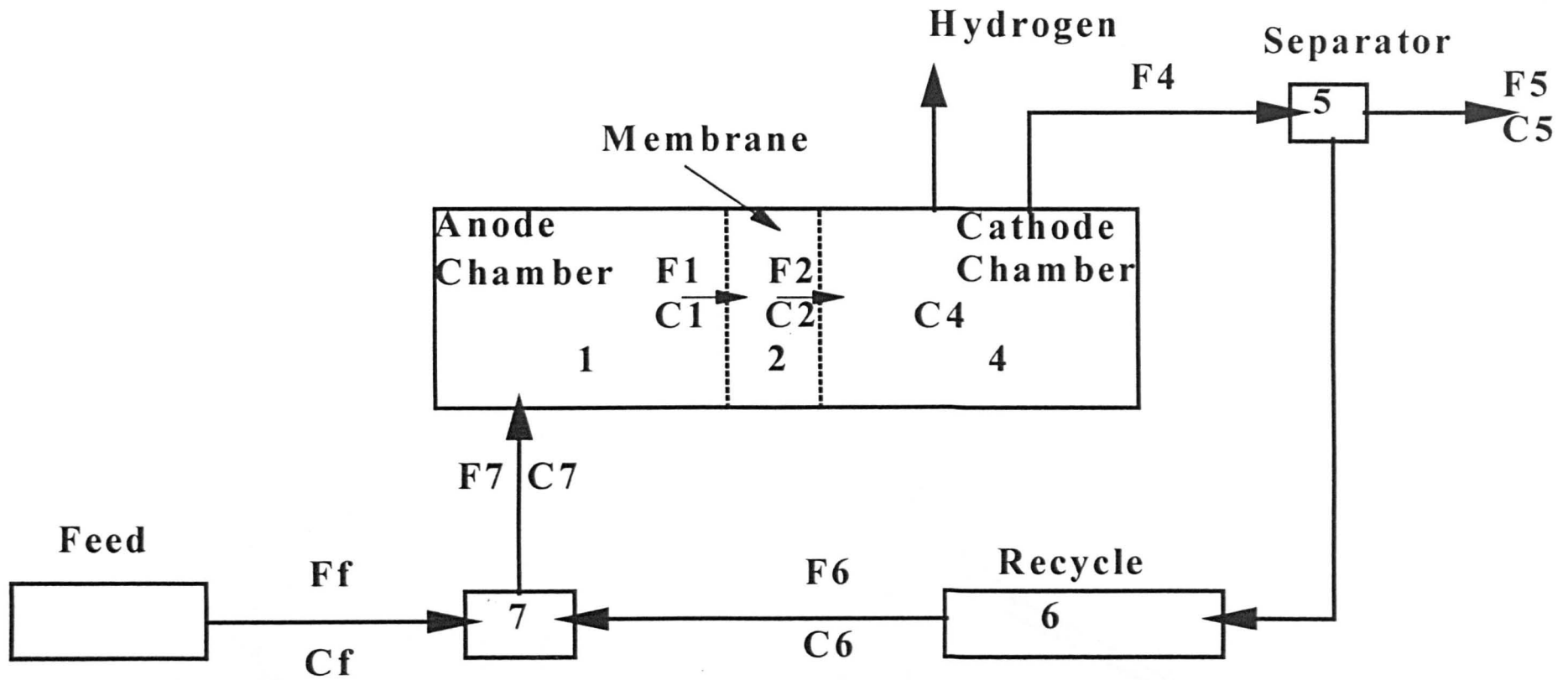
LET conc = cw1ini + n * h * g(n) / a(n)
NEXT n
LET cw1fin = cw1ini + h * (g(1) + 2 * g(2) + 2 * g(3) + g(4)) / 6
REM
REM
REM-----
REM
REM
END SUB
*****
*

SUB wcmassbalance
REM
REM  mass balance on water in cathode chamber
REM-----
REM
REM
LET conc = cw4ini
FOR n = 1 TO 4
LET b5 = F2 * CW2ini / Vc
LET b6 = F4 * conc / Vc
LET g(n) = b5 - b6
LET conc = cw4ini + n * h * g(n) / a(n)
NEXT n
LET cw4fin = cw4ini + h * (g(1) + 2 * g(2) + 2 * g(3) + g(4)) / 6
REM
REM
REM-----
REM
REM
END SUB
*****
*

```


APPENDIX 4





APPENDIX 6: MLR ASSESSMENTS

Figure A6-1: Electro-Osmotic Flow

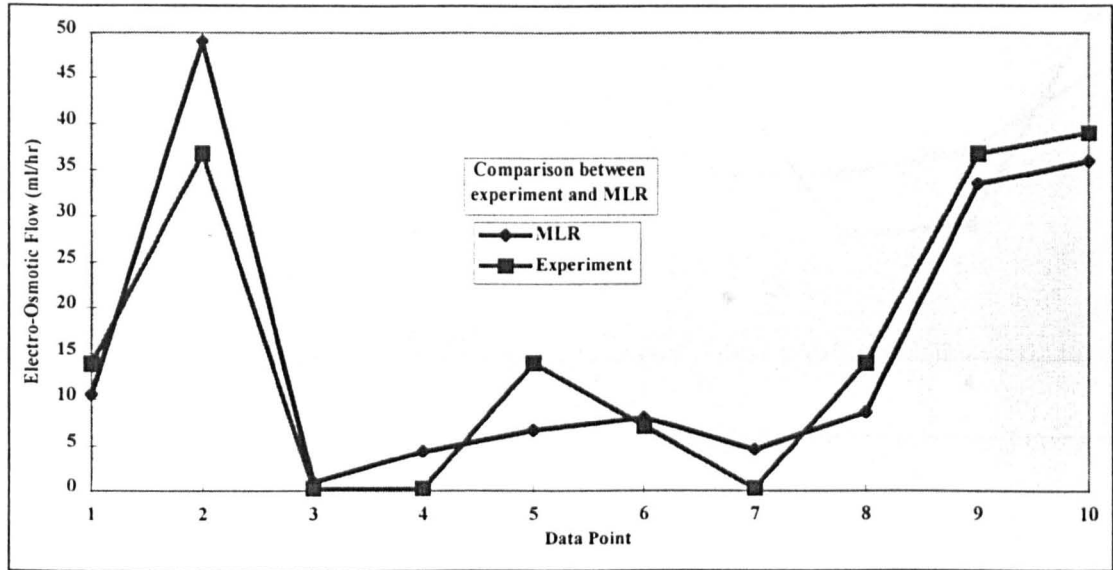


Figure A6-2: Anode Potential

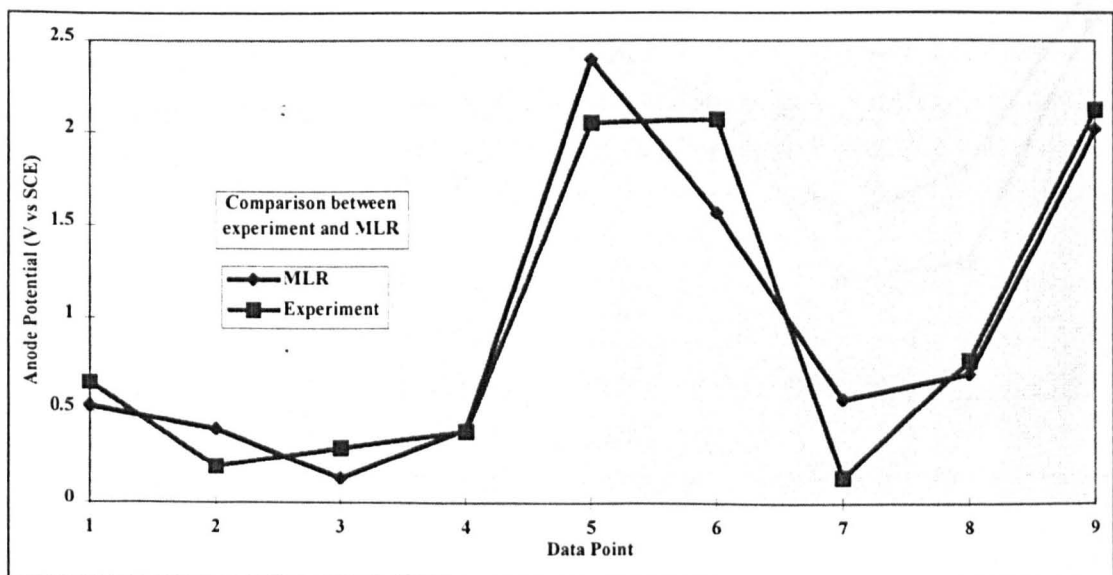


Figure A6-3: Membrane Potential

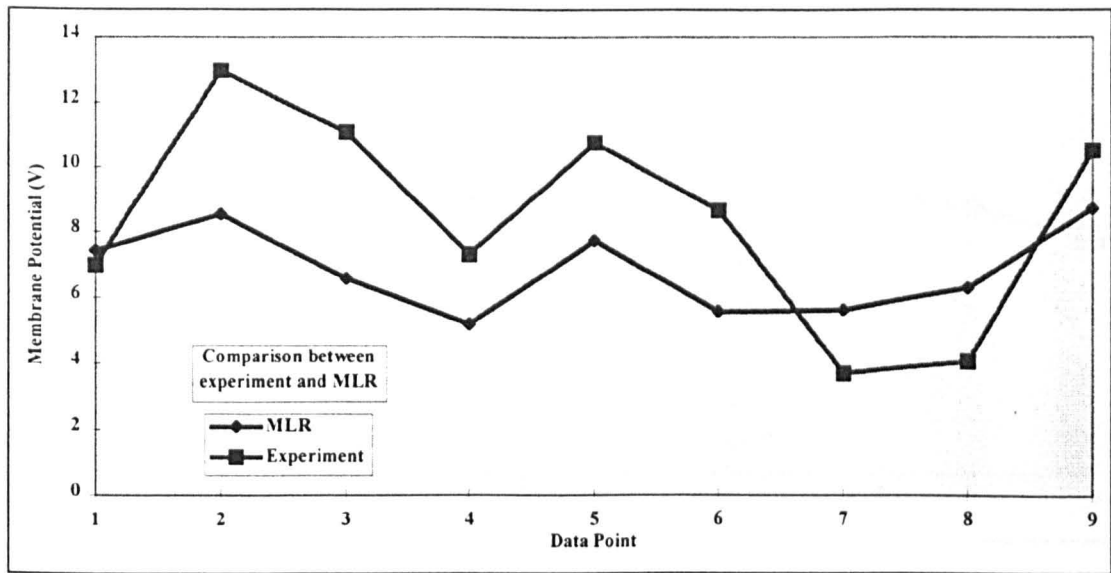


Figure A6-4: Cell Potential

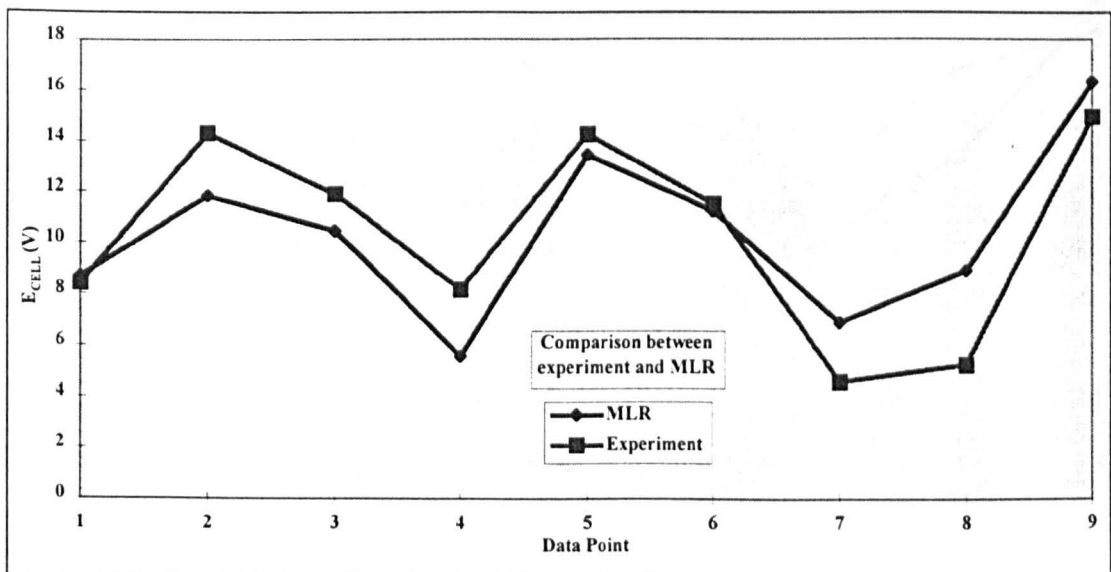


Figure A6-5: Unreacted Toluene

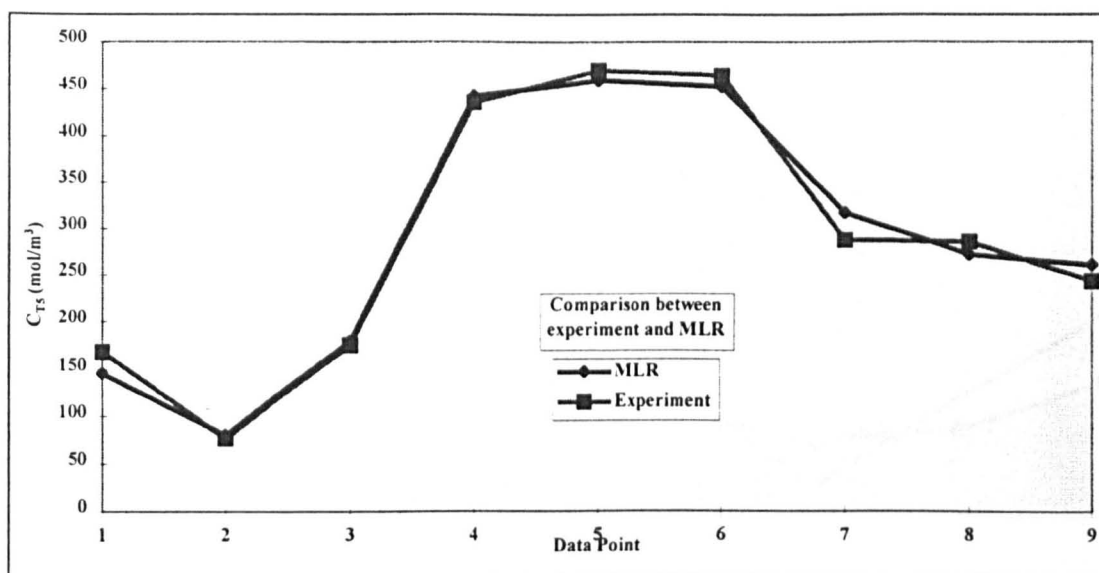
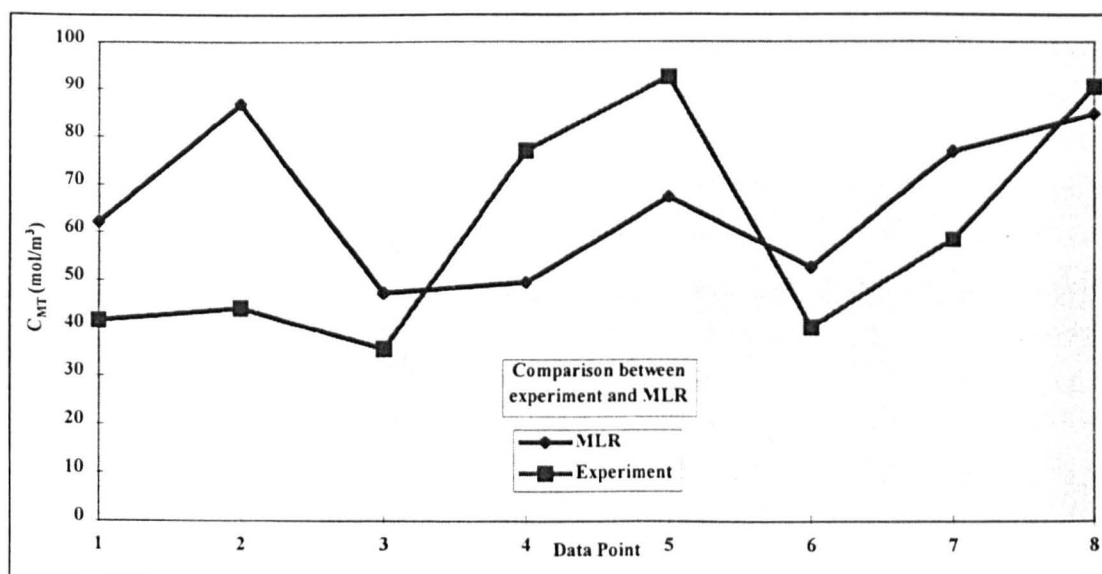
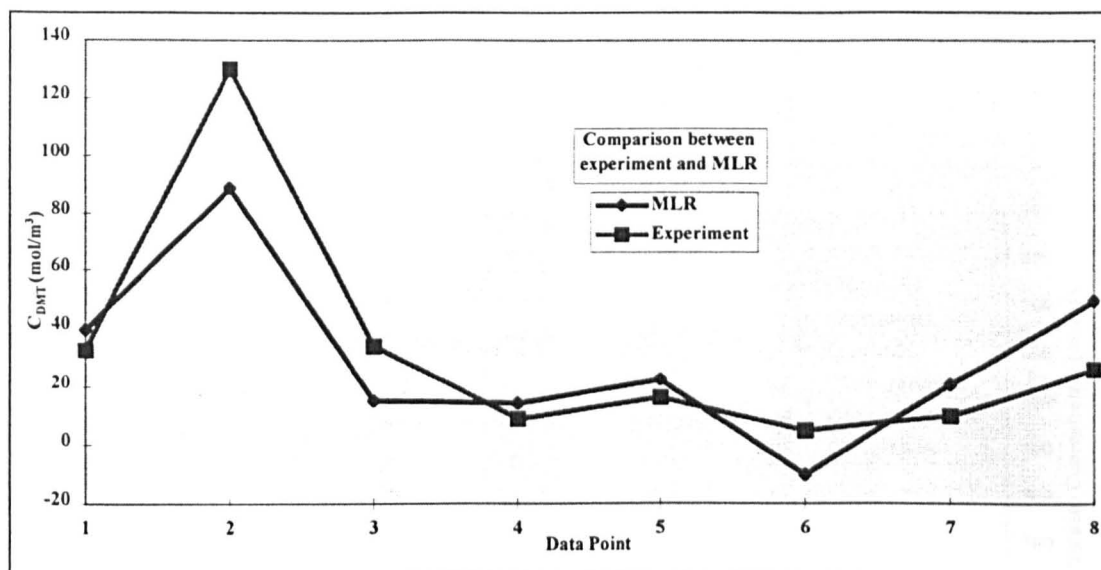
Figure A6-6: α -methoxytoluene Concentration

Figure A6-7: α,α -dimethoxytoluene Concentration

APPENDIX 7: COMPARISON

Figure A7-1: EXP547 - Final Concentrations

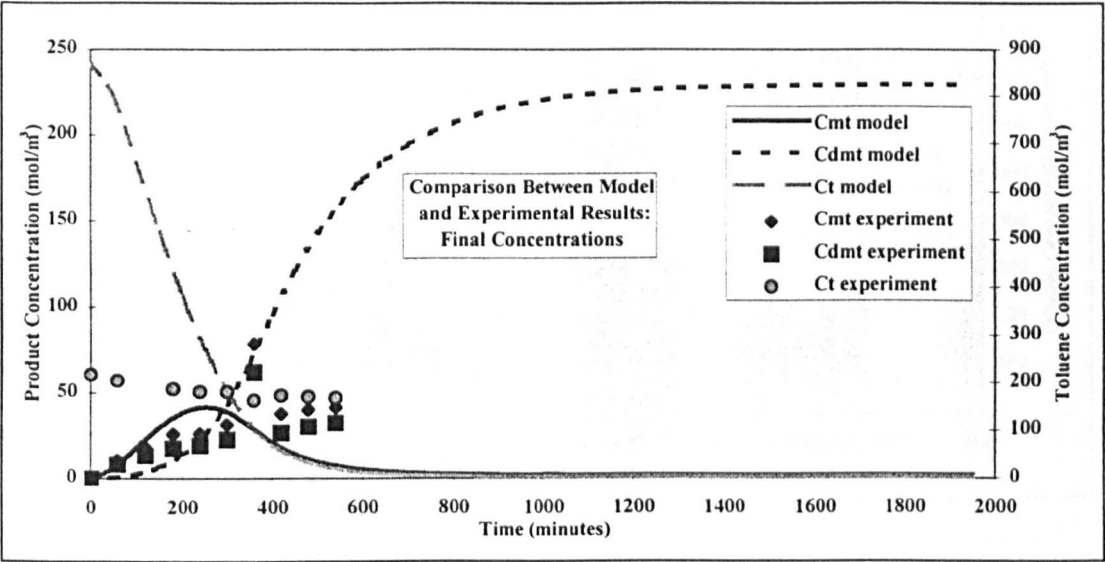


Figure A7-2: EXP547 - Potentials

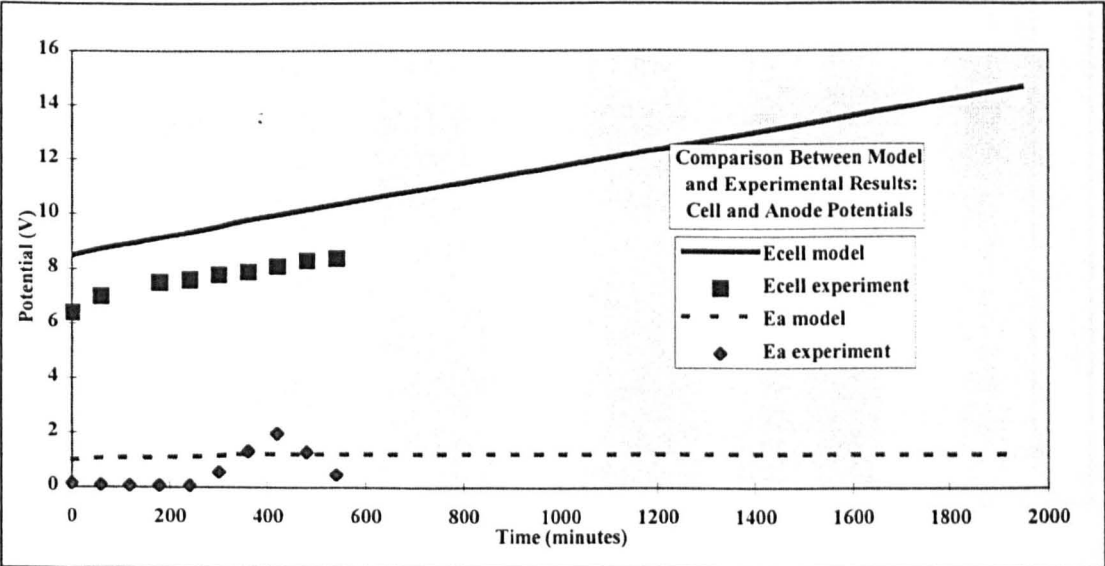


Figure A7-3: EXP548 - Final Concentrations

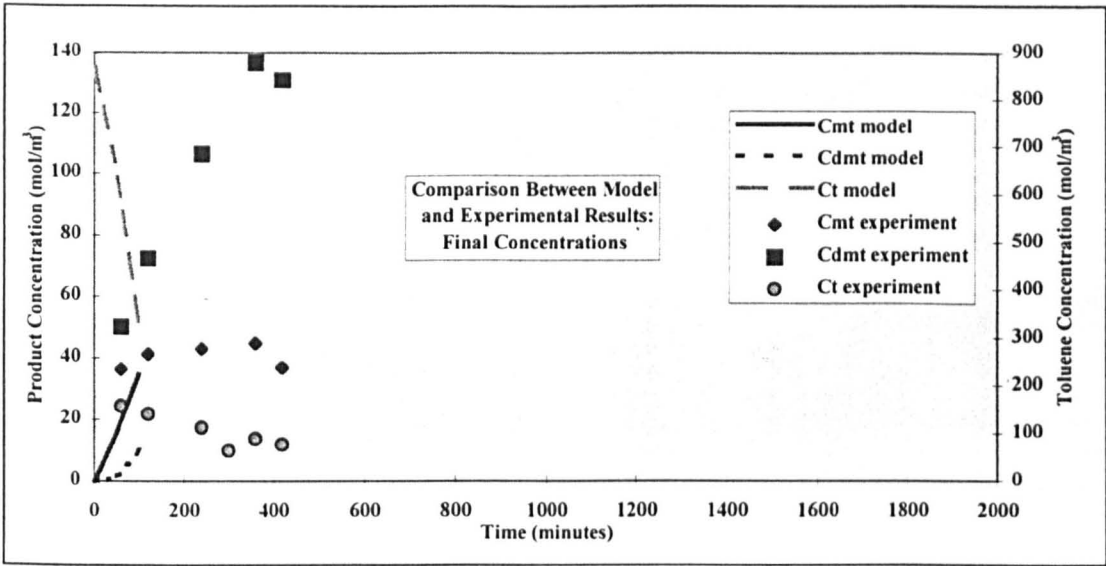


Figure A7-4: EXP548 - Potentials

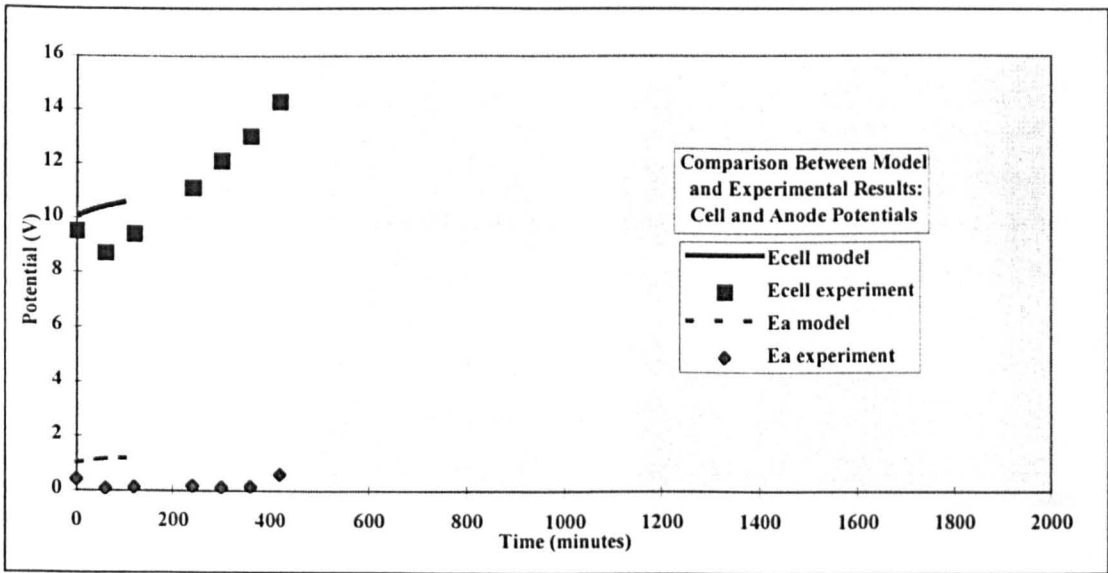


Figure A7-5: EXP549 - Final Concentrations

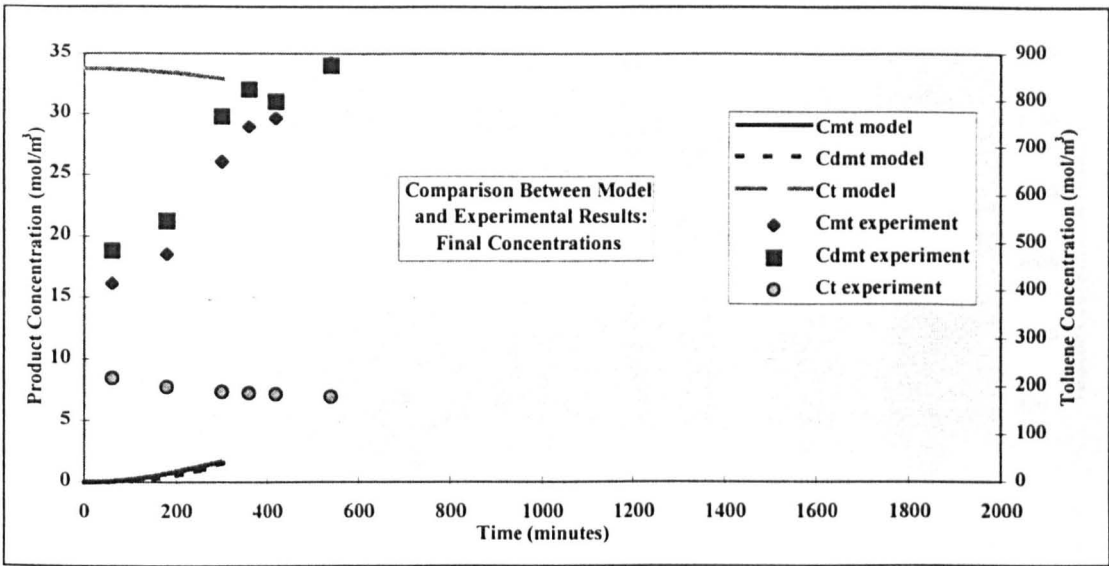


Figure A7-6: EXP549 - Potentials

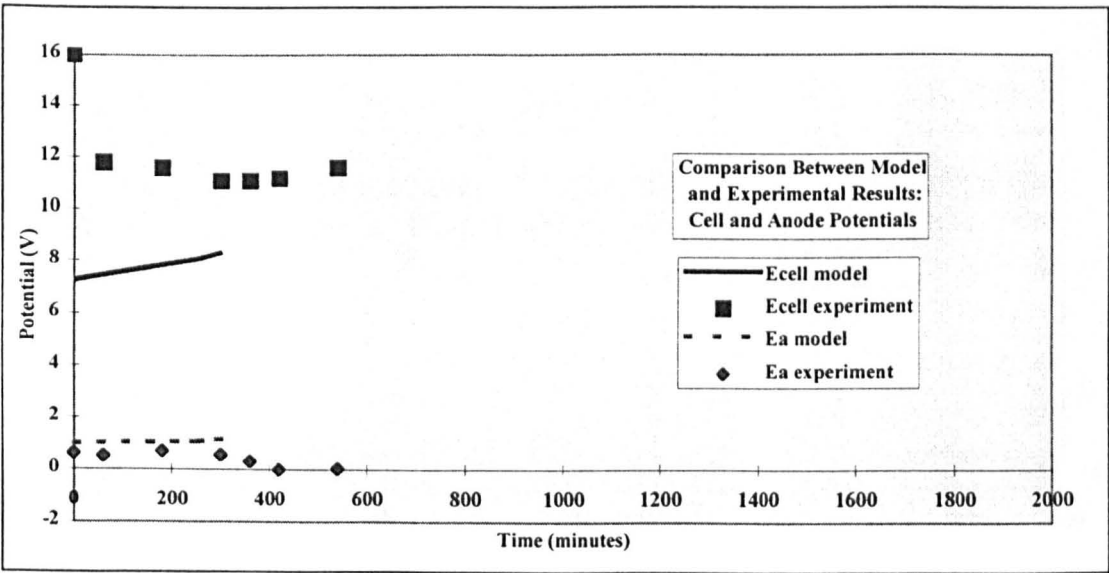


Figure A7-7: EXP552 - Final Concentrations

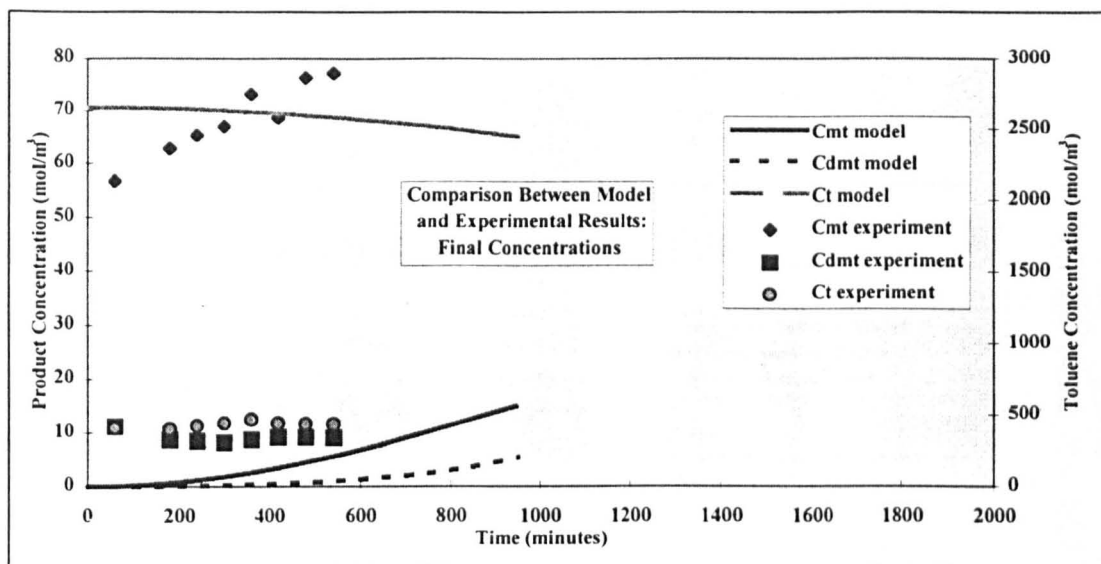


Figure A7-8: EXP552 - Potentials

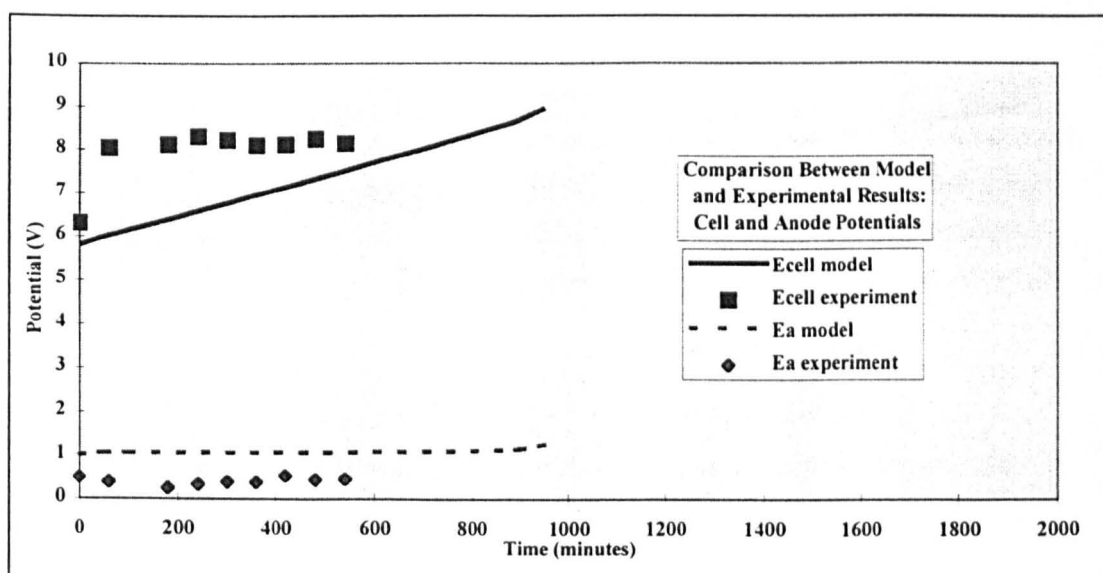


Figure A7-9: EXP553 - Final Concentrations

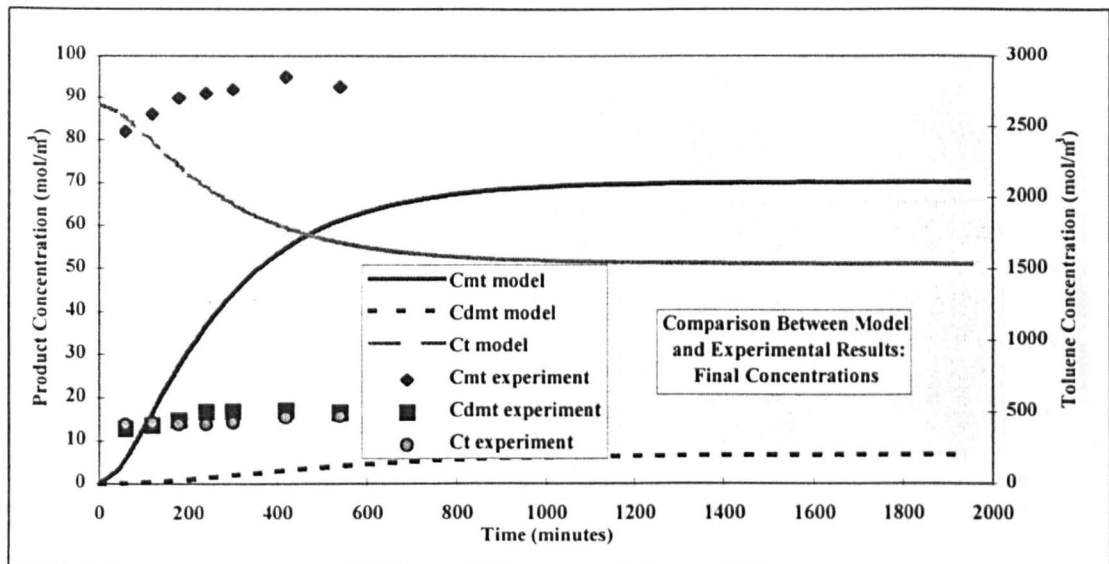


Figure A7-10: EXP553 - Potentials

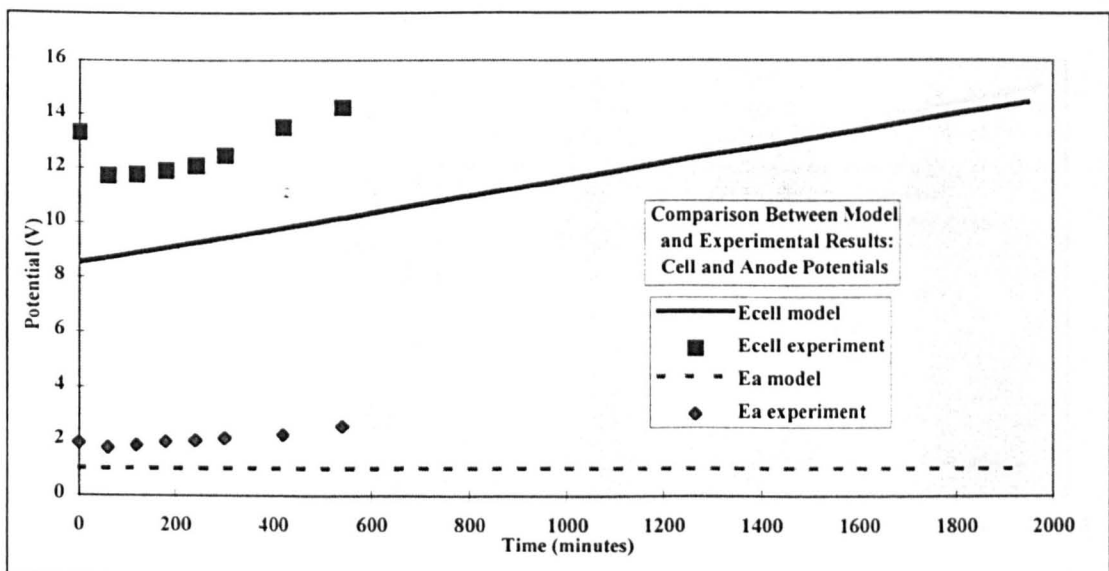


Figure A7-11: EXP554 - Final Concentrations

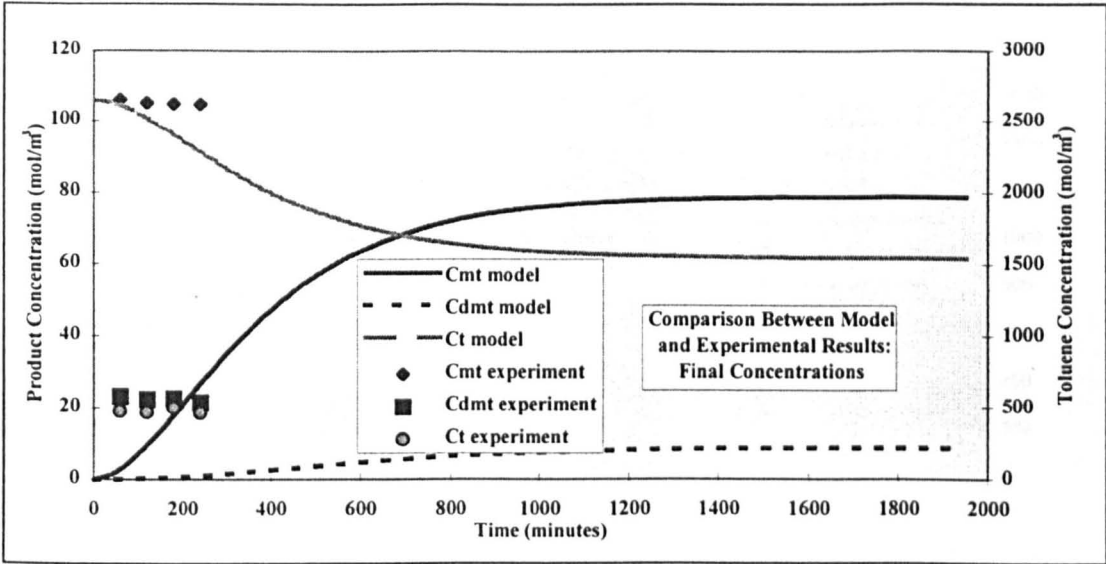


Figure A7-12: EXP554 - Potentials

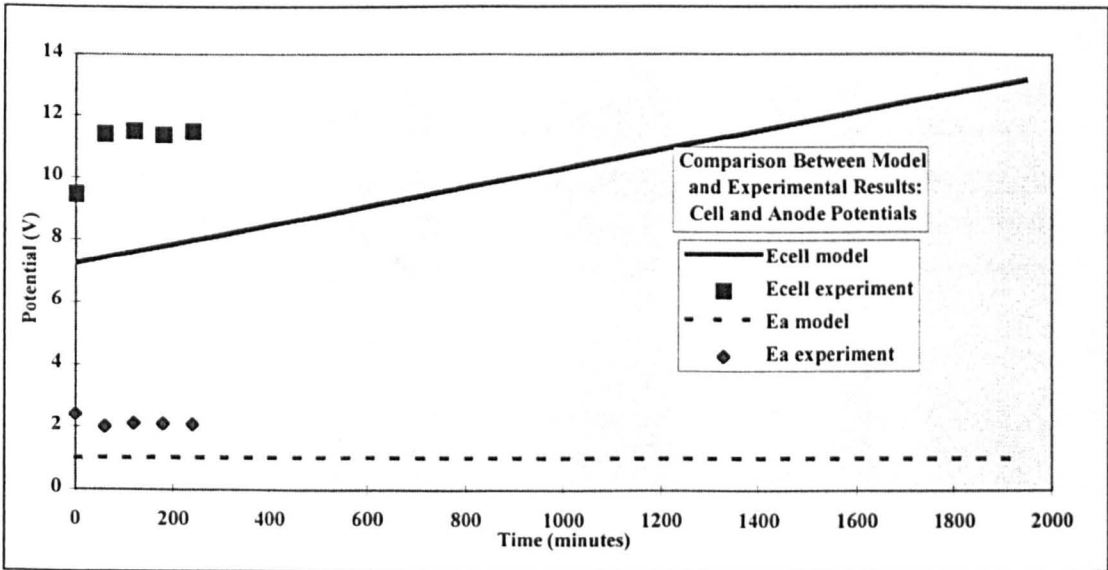


Figure A7-13: EXP557 - Final Concentrations

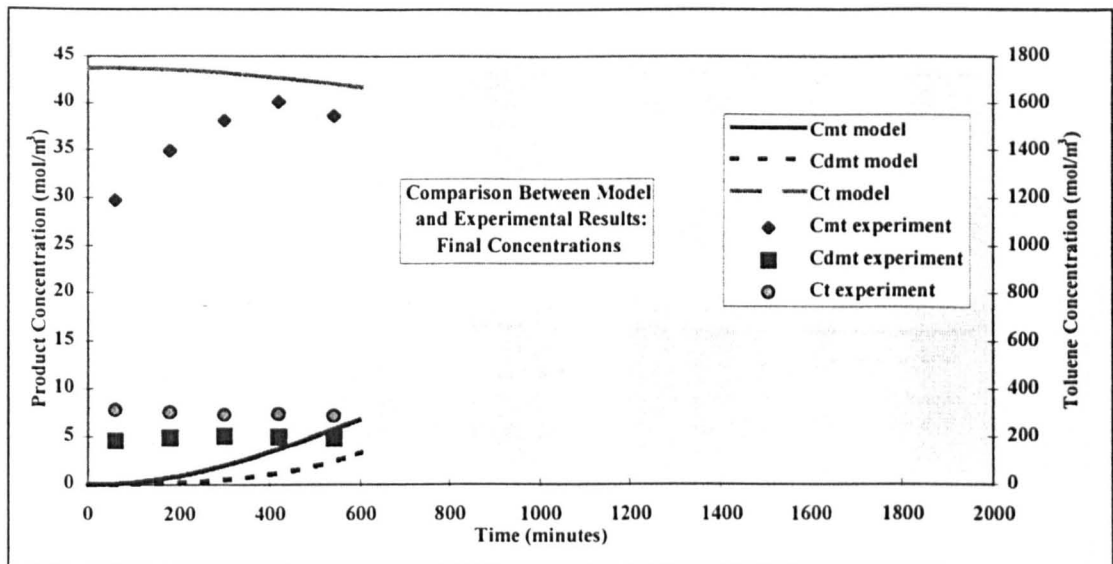


Figure A7-14: EXP557 - Potentials

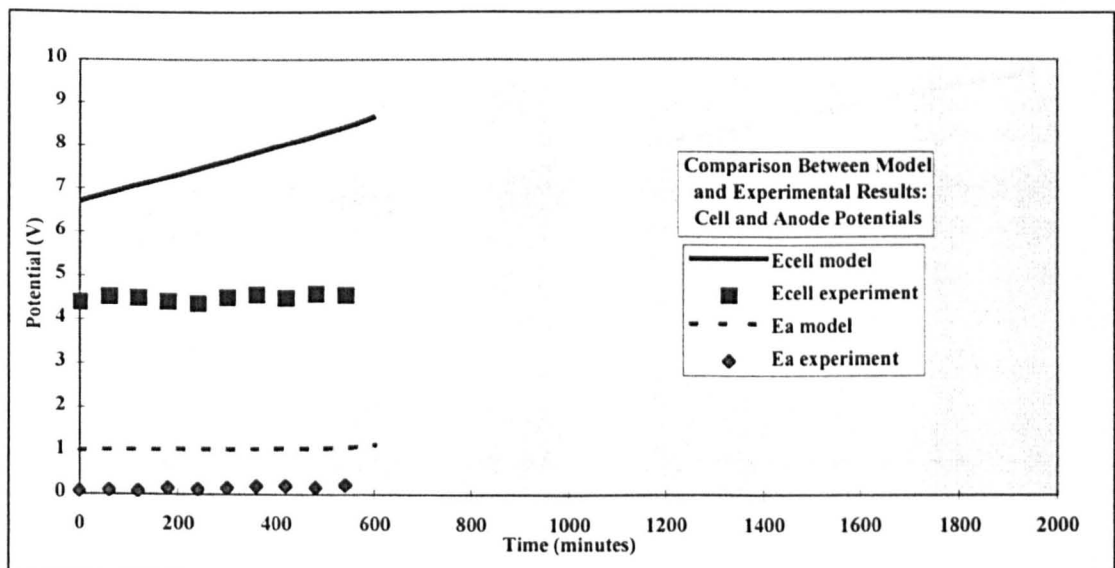


Figure A7-15: EXP558 - Final Concentrations

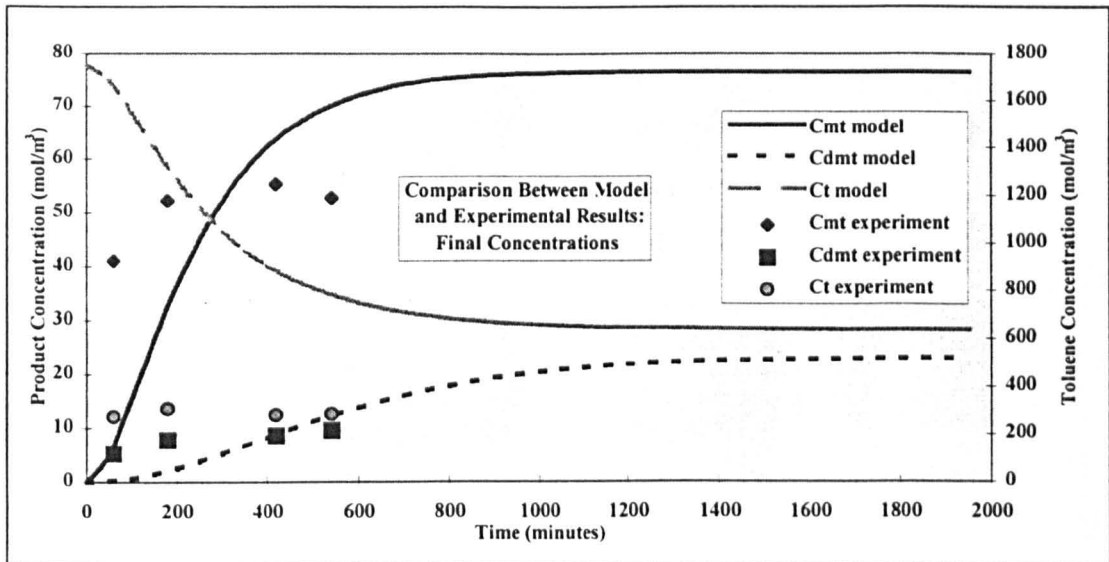


Figure A7-16: EXP558 - Potentials

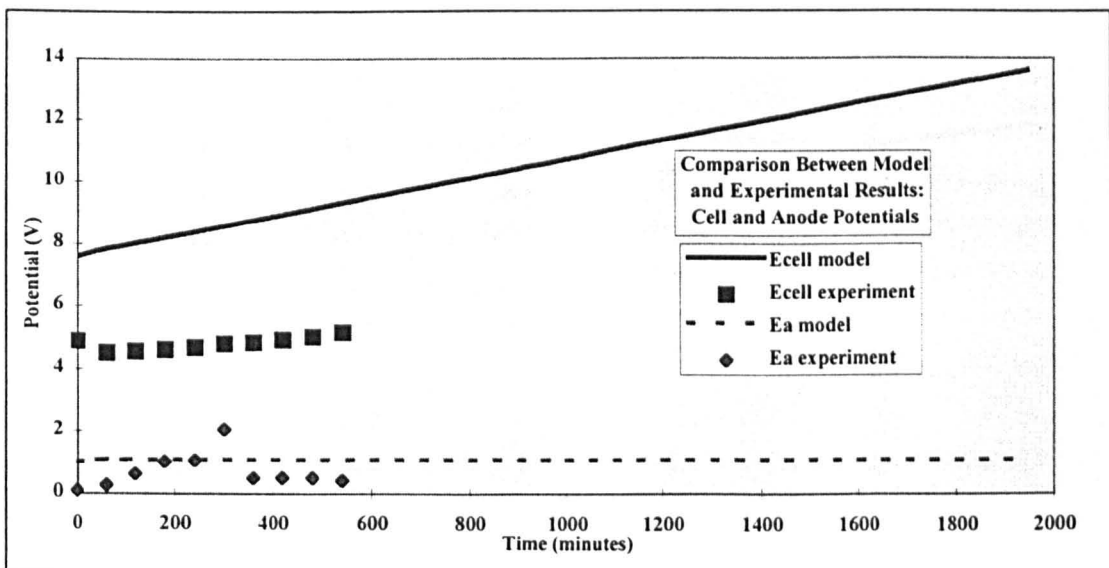


Figure A7-17: EXP559 - Final Concentrations

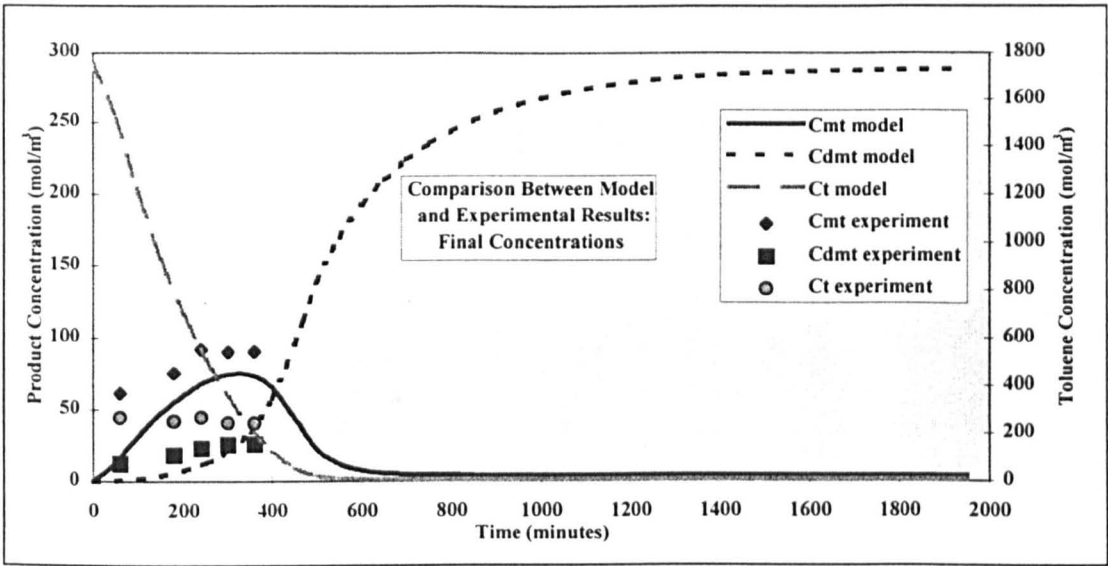


Figure A7-18: EXP559 - Potentials

